# Microbial Sulfur Oxidation in Mine Wastewaters

by

Jay Gordon

A thesis submitted in conformity with the requirements
for the degree of Doctor of Philosophy

Civil & Mineral Engineering

University of Toronto

# Microbial Sulfur Oxidation in Mine Wastewaters

Jay Gordon

Doctor of Philosophy

Civil & Mineral Engineering
University of Toronto

2025

## Abstract

Acid generation in mine wastewater is a problem wherever metal ore deposits contain sulfide mineral assemblages. This problem is due to sulfur oxidation intermediates (SOI), formed in the milling process, oxidizing in onsite tailings impoundments. The resulting acid generation must be treated before the water leaves site, or it will have negative environmental impacts. At the initiation of this thesis, SOI oxidation had been recently attributed to sulfur oxidizing bacteria (SOB) genera such as *Halothiobacillus*, *Thiomonas*, *Thiobacillus*, *Thiovirga*, and *Sulfurovum*. Although linked to SOB, these acid generating processes were not yet explained by specific enzymatic mechanisms.

In the literature, the sulfur metabolic enzymes are highly conserved. They fall into three pathways: the complete sulfur oxidation (cSOx) pathway, the incomplete sulfur oxidation (iSOx) plus reverse dissimilatory sulfur reduction (rDSR) pathway, and the tetrathionate intermediate ($S_4I$) pathway. Additionally, some sulfur enzymes do not fall neatly into these categories, and other reactions may yet be discovered. We have yet to clarify which pathways are present in mine tailings impoundments, which conditions promote them, and – most critically – how much acid results.

To fill this gap, I used field mesocosms and benchtop microcosms to explore relationships between ecological niche space, sulfur metabolism, and acid generation. First, field mesocosms were used to explore the response of microbial sulfur oxidation to environmental parameters. Here, SOB contained all three pathways in two main guilds, and proton yield varied with conditions. The next set of field mesocosms aligned three lines of evidence (16S rRNA, mRNA,

and geochemistry) to confirm that all three sulfur pathways (cSOx, $S_4I$, and iSOx + rDSR) were active. Here, the activity varied with sulfur substrate and electron acceptor concentrations, and actual proton yields were lower than theoretical. Finally, I used benchtop microcosms to closely observe the low proton yield with thiosulfate oxidation. These data revealed gaps between the theoretical stoichiometry of the cSOx and $S_4I$ pathways and the reactions observed, suggesting that unidentified sulfur pathways and corresponding enzymes exist. Together, this research identifies the crucial impact of sulfur pathway activity on the timing and mechanism of acid generation, helping to improve future modeling and prevention.

# Acknowledgments

*"Perhaps the secret of living well is not in having all the answers*
*but in pursuing unanswerable questions in good company."*

*~ Rachel Naomi Remen*

To undertake scientific discovery has been a lifelong dream, and so has working for the faithful stewardship of our planet. Thus, my efforts might in some way be directed towards the preservation of beautiful life in this world. The work put forward in this thesis would not be possible without the collective efforts of everyone who gave of their strength, knowledge and creativity to the Mine, Water and Environment research group.

To the senior members of the Mine Wastewater Solutions project: Tara Colenbrander Nelson, Dr. Kelly Whaley-Martin, and Lauren Twible — thank you for the guidance, methods, and context you provided. To the field team members — Kelly Whaley-Martin, Lauren Twible, Felicia Chen, Sarah Kumar, and Anthony Botzo, and particularly the team lead Tara Colenbrander Nelson — thank you for the careful planning, positive energy, and heavy lifting. Skilled labour is too often undervalued in the scientific community, but it is essential for projects of this scale. For their meticulous efforts in the lab, I thank Josh Crawford, In Him Lee, Sara Kumar, James Array and Sara Sugin. You were all a pleasure to work with, competent and cheerful. I wish you all the best in your future work and discoveries. For thought provoking conversations, I thank Dr. Kelly Whaley-Martin, Tara Colenbrander Nelson, Joe Radford, Heping Shen, Noel Devaere, Dr. Yunyun Yang, Yingzhe Li, and Dr. Dalal Askar. Thank you for sharing ideas and friendly debate. To the metagenomic wizard, Dr. LinXing Chen and supervisor Dr. Jillian Banfield, I admire your work, and am grateful to the strength it lends to this thesis. To Tara Penner, who I met at the end of this journey, I thank you for the careful editing, pulling clarity from my sentences; I now understand the difference between a "-", a "–", and a "—".

In addition, this work could not have been accomplished without the guidance of my supervisory committee: Dr. Lesley Warren, Dr. Simon Apte, Dr. Susan Andrews. Dr. Lesley Warren, you offered me the opportunity to pursue my dreams; Dr. Simon Apte, your patient and thoughtful coaching brought out my best work; Dr. Susan Andrews, your focused and thought-provoking

questions always hit the mark.  To my examiners Dr. Elizabeth Edwards, Dr. Bridget Bergquist and Dr. Karthik Anantharaman, your feedback was excellent and deeply appreciated.

And in my personal life, to my parents, siblings, partners and friends — it was you I leaned on for strength in the harrowing trials faced during these years. I never doubted my purpose, but sometimes I could not see the light; you lit a candle or held my hand in the dark. Nancy, Laurie, Emily, Robert, Julieta, Pedro, Amanda, Ezinneifechukwunyelu, and Ariana — thank you for the patient witness, the comfort, the care. And to all my friends at QueerSphere Grad — it's been amazing being part of the community; stay awesome!

# Table of Contents

# List of Tables

# List of Figures

# List of Appendices

# List of Abbreviations

**Terms**

| | |
|---|---|
| ARD | – acid rock drainage |
| DNA | – deoxyribonucleic acid |
| MAGs | – metagenome assembled genomes |
| mRNA | – messenger RNA |
| PCR | – polymerase chain reaction |
| RNA | – ribonucleic acid |
| rRNA | – ribosomal RNA |
| 16S rRNA | – a fragment of ribosomal RNA used to index (barcode) life |
| SOB | – sulfur oxidizing bacteria |
| SOI | – sulfur oxidation intermediates |
| SRB | – sulfate reducing bacteria |
| TEA | – terminal electron acceptor |

**Primary Pathways**

| | |
|---|---|
| cSOx | – compete sulfur oxidizing enzyme system (SoxAX, SoxYZ, SoxB, SoxCD) |
| DSR | – dissimilatory sulfur reduction enzyme system (DsrAB, DsrC, DsrEFGH, Sat, AprAB, etc.) |
| iSOx | – incomplete sulfur oxidizing enzyme system (SoxAX, SoxYZ, SoxB) |
| PSO | – partial sulfur oxidation (or the formation of ZVS globules from $HS^-$); note the acronym PSO is also sometimes used to represent the *Paracoccus* sulfur oxidation system, aka cSOx |
| rDSR | – reverse dissimilatory sulfur reduction enzyme system (DsrAB, DsrC, DsrEFGH, Sat, AprAB, etc.) |
| SOx | – sulfur oxidizing enzyme system |
| $S_4I$ | – tetrathionate intermediate enzyme system (TsdA, TetH/unknown) |
| TOMES | – Thiosulfate Oxidizing Multi-Enzyme System, aka iSOx |

**Compounds**

ADP – adenosine diphosphate
ATP – adenosine triphosphate
AMP – adenosine monophosphate
APS – adenosine 5′-phosphosulfate
DSMSA – disulfane monosulfonic acid
pH – potential of hydrogen (pH ~ $-\log[H^+]$)
PT – pentathionate
R-$SS^-$ – cysteine-bound persulfide
$S_8$ – elemental sulfur / cyclooctasulfur
$S_{react}$ – reactive sulfur
$S_nO_x^{2-}$ – thiosalts
ZVS – zero-valent sulfur

**Enzymes**

AprAB – adenosine 5′-phosphosulfate reductase
AprM – serine protease
AsrABC – anaerobic sulfite reductase
Ddd – nonorthologous dimethylsulfoniopropionate (DMSP) lyases
DmdABCD – de-methylation pathway for DMSP
DoxDA – thiosulfate:quinone oxidoreductase (TQO)
DsrABCEFHMKJOP
– dissimilatory sulfate reduction enzyme complex; dissimilatory (bi)sulfite reductase (DsrAB), co-substrate for DsrAB in sulfite reduction (DsrC), sulfurtransferase (DsrEFH), sulfite reduction complex (DsrMKJOP)
FccAB – flavocytochrome c
GplE – thiosulfate:cyanide sulfurtransferase/thiosulfate sulfurtransferase
Hyd – [NiFe]-hydrogenases
Otr – octoheme tetrathionate reductase
Pdo – persulfide dioxygenase

PhsABC – thiosulfate reductase

PsrABC – polysulfide reductase

Sat – sulfate adenylytransferase

SauUTS – sulfoacetate transporter (sauU), sulfoacetate-CoA ligase (sauT), sulfoacetaldehyde dehydrogenase (sauS)

SdoAB – sulfur dioxygenase

sHdr – sulfur-oxidizing heterodisulfide reductase-like system

SoeABC – sulfite-oxidizing enzyme

SorAB – sulfite:acceptor oxidoreductase

SOR – sulfur oxygenase/reductase

SoxAXBCDYZ – sulfur-oxidizing multienzyme complex; heme-thiolate protein (SoxAX), carrier protein (SoxYZ); thiosulfohydrolase protein (SoxB); and a sulfane dehydrogenase protein (SoxCD)

SreABC – sulfur reductase

SsuABCDE – alkane-sulfonate monooxygenase (SsuDE), alkanesulfonate-transporter (SsuABC)

Sqr – sulfide:quinone oxidoreductase

SUOX – sulfite oxidase

TdhT – thiol dehydrotransferase

TetH – tetrathionate hydrolase (aka TTH / 4THase)

TtrABC – tetrathionate reductase

TsdAB – thiosulfate dehydrogenase

Tsr/Phs – thiosulfate reductase

TST – thiosulfate:cyanide sulfur transferase

Tau – taurine transporters and processing

TusA – sulfur/thiosulfate transfer protein

# 1

# Sulfur Metabolism in Mine Wastewater Systems

*"Perplexity is the beginning of knowledge."*
*~Khalil Gibran*

## 1.1 The Challenge: Conceptualizing Sulfur Cycling in Mine Wastewaters

Many metal mines process ores that contain sulfide mineral assemblages and, therefore, produce waste tailings with high sulfur content; this waste is often disposed of sub-aqueously in tailings ponds as part of the on-site management of these materials (Herbert et al. 2005; Luther et al. 2011; Verburg et al. 2009). Sub-aqueous disposal leads to a release of sulfur oxidation intermediates (SOI), many of which are known as thiosalts ($S_nO_x^{2-}$), into mine wastewater (Table 1.1); the most important of these for acid generation are thiosulfate ($S_2O_3^{2-}$) and the polythionates that include trithionate ($S_3O_6^{2-}$), tetrathionate ($S_4O_6^{2-}$), and pentathionate [$S_5O_6^{2-}$, (Miranda-Trevino et al. 2013; Mhonde et al. 2021)]. These thiosalts originate from the milling process. Thiosalt formation from ore (primarily from pyrite, but also pyrrhotite and galena), is a complicated process; the proportion formed corresponds to the fraction of sulfide present in the ore, as well as temperature, pH, grind size, and oxidants (Kuyucak 1998). In addition, microbial oxidation contributes to the generation and processing of thiosulfate during the flotation process (Schippers, Jozsa, and Sand 1996; Bernier and Warren 2007; Miettinen et al. 2021). Once formed, temperature, pH and oxygen also affect their reactivity (Miranda-Trevino et al. 2013). Thiosulfate and tetrathionate can also affect xanthate adsorption, a method used to recover metals, during the flotation process (Mhonde et al. 2021; Kirjavainen, Schreithofer, and Heiskanen 2002), limiting the amount of water recycling that can be achieved before thiosalts must be discarded in effluent with waste tailings.

If SOI in mine wastewaters are recalcitrant to treatment and persist in waters that are discharged to receiving environments, they may subsequently oxidize. This oxidation process generates acidity (see equation 1) and so increases the solubility of toxic metals in freshwater streams and

rivers (Lopes et al. 2020; Lindsay et al. 2015; Camacho, Frazao, et al. 2020a). The proportion of acid generation to SOI oxidation can be considered in a methodical fashion by comparing the proton yield by mole of sulfur oxidized:

$$S_2O_3^{2-} + H_2O + 2\ O_2 \rightarrow 2\ SO_4^{2-} + 2\ H^+ \qquad \Delta H^+/\Delta S = 1 \qquad (1)$$

Acid generated onsite can be immediately treated with lime, raising the pH to circumneutral conditions before the water passes a compliance point. However, if acidity is generated downstream of the compliance point because of slow SOI oxidation, it can go untreated in the receiving environment (as active management and treatment occurs onsite). Similar to how acid rock drainage (ARD) from waste rock damages receiving environments, this wastewater acidity can undermine a mine's social license to operate and cause a regulatory shutdown (Hall and Jeanneret 2015; Verburg et al. 2009). To manage this risk, industry must better predict the rates of microbial SOI cycling and its impacts.

**Table 1.1** Sulfur Compound Concentrations in Canadian Metal Mine Wastewater Systems*

| | **Tailings Impoundment in Sudbury, ON (Source for this study)** | **Average in Metal Mine Wastewater** |
|---|---|---|
| Sulfate ($SO_4^{2-}$) | 0.7–9 mmol/L (average 5.0 ± 2.6 mmol/L) | 0.09–11.4 mmol/L |
| Thiosulfate ($S\text{-}S_2O_3^{2-}$) | 0.1–1.6 mmol/L (average 0.4 ± 0.5 mmol/L) | <0.003–0.8 mmol/L |
| Tetrathionate ($S\text{-}S_4O_6^{2-}$) | NA | <0.03–0.23 mmol/L |
| Sulfite ($SO_3^{2-}$) | negligible | negligible |

*table summarizes values described by Whaley-Martin (K. Whaley-Martin et al. 2020); NA = data not available

Three catabolic pathways for microbial SOI oxidation have been identified to date: the complete sulfur oxidization (cSOx) pathway, the incomplete SOx plus reverse dissimilatory sulfur reduction (iSOx + rDSR) pathway, and the tetrathionate intermediate ($S_4I$) pathway [Fig 1.1, Table 1.2, Table 1.3, (Dahl 2005; Watanabe et al. 2019; Wasmund, Mußmann, and Loy 2017a; Friedrich et al. 2001a)]. For each of these pathways, the structures of many of the catalytic enzymes have been studied in detail to provide a precise understanding of how sulfur bonds are transformed, often through interactions with water molecules (Jenner et al. 2019; Venceslau et al. 2014; Zander et al. 2011; Sauvé et al. 2009). Yet, from this foundation, two important questions arise: (i) do these metabolic processes translate to geochemical changes at the macro-scale? and (ii) can we use metagenomic characterization of communities of sulfur oxidizing bacteria (SOB)

and sulfate reducing bacteria (SRB), to predict changes in sulfur speciation or the onset of acidity generation in mine wastewater?

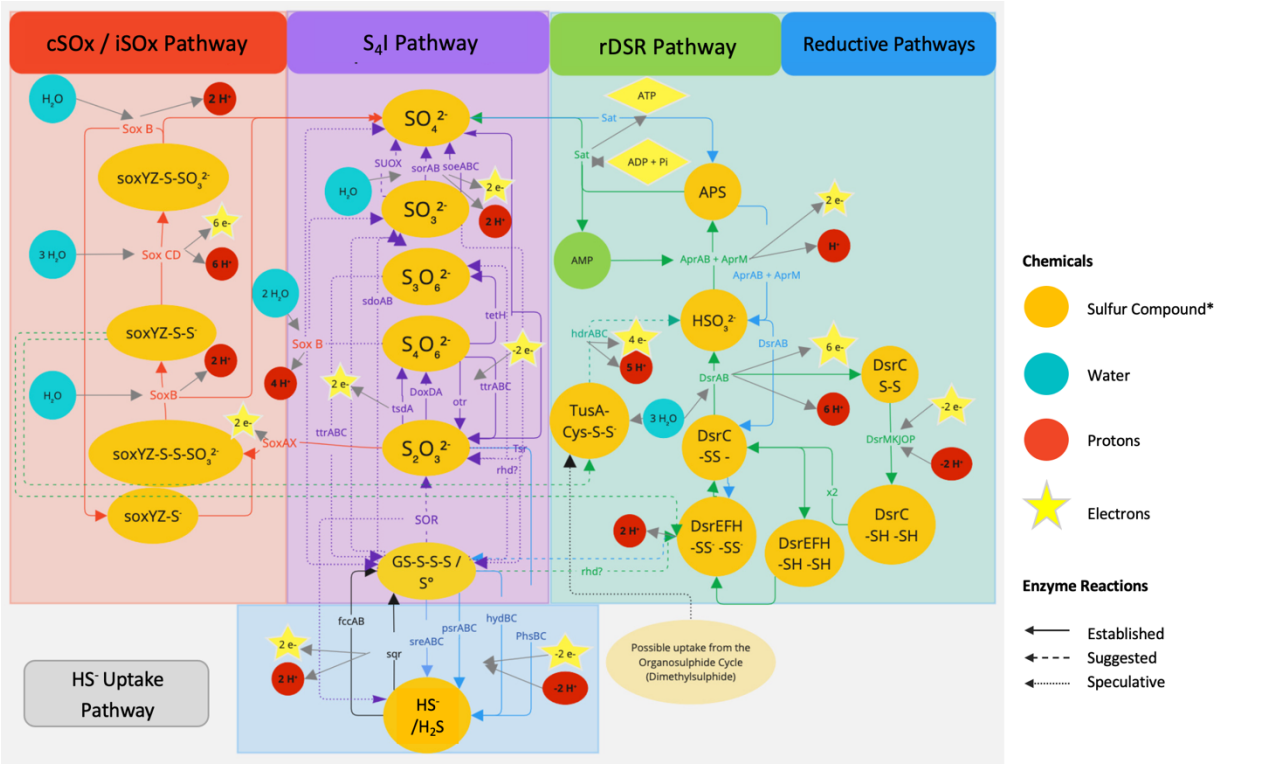


**Fig 1.1** Overview of the sulfur oxidizing pathways present across all sulfur oxidizing bacteria. The three primary pathways for thiosulfate oxidation are emphasized: SOx (red), $S_4I$ (purple), and rDSR (green). Pathways for sulfur reduction (blue) and sulfide uptake (grey) are also represented. See Table 1.2 for full names of sulfur compounds and enzymes, and Table 1.3 for stoichiometry of the sulfur half-reactions facilitated by each pathway (below). Other chemicals represented are water ($H_2O$), protons ($H^+$), electrons ($e^-$), adenosine monophosphate (AMP), adenosine diphosphate (ADP), adenosine triphosphate (ATP), and inorganic phosphate ($P_i$).

In this thesis, I hypothesize that the answer to both questions is yes, and metagenomic information can be meaningfully interpreted to predict changes in mine wastewater geochemistry at a landscape scale. Once genomes are characterized, identification of SOB and SRB communities through 16S rRNA sequencing should be a means inferring dominant sulfur processes occurring in mine wastewater. Furthermore, although not yet well constrained, I hypothesize that there will be a clear link between these sulfur processes and both the timing and magnitude of acid generation in mine wastewater.

**Table 1.2** Nomenclature for Common Sulfur Compounds and Enzymes

| Type | Name | Symbol/abbreviation |
|---|---|---|
| Compound | adenosine 5'-phosphosulfate | APS |
| Compound | cysteine-bound persulfide | R-$SS^-$ |
| Compound | disulfane monosulfonic acid | DSMSA |
| Compound | elemental sulfur / cyclooctasulfur | $S_8$ / ZVS |
| Compound | glutathione:sulfodisulfane adduct | GS–S–S–$SO_3^-$ |
| Compound | inorganic polysulfide | $^-S$-$S_n$-$S^-$ / $S_n^{2-}$ |
| Compound | thiosulfate | $S_2O_3^{2-}$ / S-$SO_3^{2-}$ |
| Compound | tetrathionate | $S_4O_6^{2-}$ / $^{2-}O_3$-S-S-S-$SO_3^{2-}$ |
| Compound | trithionate | $S_3O_3^{2-}$ /$^-$S-S-$SO_3^-$ |
| Compound | sulfide | $HS^-$ |
| Compound | sulfite | $SO_3^{2-}$ |
| Compound | sulfate | $SO_4^{2-}$ |
| Compound | | -SH |
| Group of Compounds | thiosalts | $S_nO_x^{2-}$ |
| Group of Compounds | polythionates | $S_3O_6^{2-}$, $S_4O_6^{2-}$, $S_5O_6^{2-}$ |
| Group of Compounds | sulfur oxidation intermediates (SOI) | Sulfur compounds with intermediate valance $e^-$ states (not $HS^-$ or $SO_4^{2-}$) |
| Group of Compounds | $S_{react}$ | Reactive Sulfur; not fully oxidized (excludes $SO_4^{2-}$) |
| Enzyme | adenosine 5’-phosphosulfate reductase | Apr |
| Enzyme | a type of thiosulfate:quinone oxidoreductase (TQO) | Dox |
| Enzyme | dissimilatory sulfate reduction | Dsr |
| Enzyme | flavocytochrome c | Fcc |
| Enzyme | sulfur-oxidizing heterodisulfide reductase–like system | Hdr |
| Enzyme | [NiFe]-hydrogenases | Hyd |
| Enzyme | octoheme tetrathionate reductase | Otr |
| Enzyme | persulfide dioxygenase | Pdo |
| Enzyme | thiosulfate reductase | Phs |
| Enzyme | polysulfide reductase | Psr |
| Enzyme | rhodanese-related sulfurtransferase | rhd |
| Enzyme | sulfate adenylyltransferase | Sat |
| Enzyme | sulfur dioxygenase | Sdo |
| Enzyme | sulfite-oxidizing enzyme | Soe |
| Enzyme | sulfite:cytochrome c oxidoreductase | Sor |
| Enzyme | sulfur oxygenase/reductase | SOR |
| Enzyme | sulfur-oxidizing multienzyme complex | SOx |
| Enzyme | sulfur reductase | Sre |
| Enzyme | sulfide:quinone oxidoreductase | Sqr |
| Enzyme | sulfite oxidase | SUOX |
| Enzyme | thiol dehydrotransferase | TdhT |
| Enzyme | tetrathionate hydrolase | TetH / TTH |
| Enzyme | thiosulfate:quinol oxidoreductase | TQO |
| Enzyme | thiosulfate dehydrogenase | Tsd |
| Enzyme | thiosulfate:dithioerythritol sulfurtransferase | Tsr |
| Enzyme | tetrathionate reductase | Ttr |
| Enzyme | tRNA 2-thiouridine synthesizing protein | Tus |

Pragmatically, I will define how SOB metabolisms affect the onset and magnitude of acidity generation in mine wastewater. The following chapters outline work that demonstrates connections between environmental conditions, 16S rRNA gene sequences, metagenomes, transcriptomes, and geochemical changes. I also explore the predictive relationship between environmental niche space and sulfur pathway activity. To ground the discussion of SOB pathways and geochemical changes, let us begin by reviewing the work of the scientists who have come before.

## 1.2 Discovery of the Sulfur Enzyme System

### 1.2.1 The Complete SOx Pathway: a Common Mechanism Emerges

Over 20 years ago, in their paper "Oxidation of Reduced Inorganic Sulfur Compounds by Bacteria: Emergence of a Common Mechanism?", Friedrich et al. (2001) proposed that many SOB oxidized thiosulfate to sulfate using a series of four key enzymes which comprise the complete sulfur oxidation pathway (cSOx: SoxYZ, a carrier protein; SoxAX, a heme-thiolate protein; SoxB, a thiosulfohydrolase protein; and SoxCD, a sulfane dehydrogenase protein), as found in the model organism in *Paracoccus pantotrophus* [Fig 1.1, Table 1.3 (Friedrich et al. 2001)]. Each enzyme's function in the proposed mechanism for the cSOx pathway, as a result of the configuration of its active site, has since been described in detail (Zander et al. 2011; Sauvé et al. 2009; Kilmartin et al. 2011). To begin the cSOx pathway, SoxAX attaches thiosulfate to the carrier SoxYZ via a heterodisulfide bond as shown in the half reaction described by equation 2:

$$S_2O_3^{2-} + \text{SoxYZ-S}^- \rightarrow \text{SoxYZ-S-S-SO}_3^- + 2\ e^- \quad (2)$$

The electrons ($e^-$) released in this process are captured by ferricytochrome c, reducing it the form ferrocytochrome c; this $e^-$ carrier shuttles them to an $e^-$ transport chain which maintains a proton gradient used to synthesize ATP (Kilmartin et al. 2011).

Once attached to SoxYZ, the terminal $SO_3^-$ group of thiosulfate (sulfone-sulfur) is oxidized to sulfate via a proton-generating hydrolysis reaction facilitated by $Mn^{2+}$ in the active site of SoxB (Sauvé et al. 2009), according to equation 3:

$$\text{SoxYZ-S}_3O_3^- + H_2O \rightarrow SO_4^{2-} + 2\ H^+ + \text{SoxYZ-S-S}^- \quad (3)$$

The sulfane-sulfur atom, a sulfur atom with six electrons bonded to another sulfur, is then exposed. This allows SoxCD (also written as $Sox(CD)_2$, a molybdohemo-enzyme sulfane dehydrogenase with double SoxC and SoxD subunits) to oxidize the sulfane-sulfur atom to sulfonate in a reaction releasing both protons ($H^+$) and $e^-$, which are carried to the $e^-$ transport chain by cytochrome c (Zander et al. 2011), as per equation 4:

$$SoxYZ\text{-}S\text{-}S^- + 3\ H_2O \rightarrow SoxYZ\text{-}S\text{-}SO_3^- + 6\ H^+ + 6\ e^- \quad (4)$$

The cSOx cycle is completed by a second hydrolysis reaction performed by SoxB (equation 3). This cSOx pathway, located in the cell's periplasm, has been found to be a central part of sulfur metabolism in many SOB isolated from a wide variety of habitats (Whaley-Martin1 et al. 2023; Camacho, Frazao, et al. 2020; Ghosh and Dam 2009; Kappler et al. 2001; Cai et al. 2022; Gwak et al. 2022; Luo et al. 2018; Bell et al. 2020; Magnuson et al. 2023). Although some variations in enzyme structures are present in different genera, the overall chain of reactions that form the cSOx pathway appears to be highly conserved (Kilmartin et al. 2011; Sauvé et al. 2009; Meyer, Imhoff, and Kuever 2007).

The proton yield of this pathway is dependent on the compound used as a terminal electron acceptor (TEA) and can been determined from the overall balanced equation. Assuming the use of oxygen as a TEA, the cSOx pathway generates an average of one proton for every atom of sulfur when thiosulfate is oxidized completely to sulfate (equation 1, Table 1.3).

With the role and structure of enzymes precisely clarified, studies of the cSOx system are now moving into explorations of associated pathway enzymes. For instance, SoxL has been identified as a key enzyme in sulfur transfer and trafficking when recycling SoxYZ (Welte et al. 2009). Recent studies include using mRNA to explore transcriptional regulation of pathway activation in *Thermus thermophilus HB8* by the CsoR-like enzyme TTHA1953 (Barrows and Van Dyke 2023), and in *Hyphomicrobium denitrificans* via the enzyme SoxR (J. Li et al. 2023). Other research uses proteomics to explore the up- and down-regulation of sulfur pathway expression in the photosynthetic sulfur-storing *Chlorobaculum tepidum* (Lyratzakis et al. 2023).

**Table 1.3** Summary of Enzyme-Facilitated Sulfur Reactions from Current Literature*

| Pathway | Sulfur Gene | Sulfur Substrate Half Reaction | Oxygen as TEA Half Reaction | $\Delta H^+/\Delta S$** |
|---|---|---|---|---|
| $H_2S$ Oxidation | *fccAB/ sqr* | $H_2S \rightarrow S^0 + 2\ H^+ + 2\ e^-$ | $2\ e^- + 2\ H^+ + ½\ O_2 \rightarrow H_2O$ | 0 |
| Overall | | $H_2S + ½\ O_2 \rightarrow S^0 + H_2O$ | | 0 |
| cSOx | *soxAX, soxYZ* | $S_2O_3^{2-}$ + SoxYZ-$S^-$ $\rightarrow$ SoxYZ-S-S-$SO_3^-$ + 2 $e^-$ | $2\ e^- + 2H^+ + ½\ O_2 \rightarrow H_2O$ | −1 |
| | *soxB* | SoxYZ−$S_3O_3^-$ + $H_2O$ $\rightarrow$ $SO_4^{2-}$ + 2 $H^+$ + SoxYZ-S-$S^-$ | | 1 |
| | *soxCD* | SoxYZ-S-$S^-$ + 3 $H_2O$ $\rightarrow$ SoxYZ-S-$SO_3^-$ + 6 $H^+$ + 6 $e^-$ | $6\ e^- + 6\ H^+ + 3/2\ O_2 \rightarrow 3\ H_2O$ | 0 |
| | *soxB* | SoxYZ-S-$SO_3^-$ + $H_2O$ $\rightarrow$ $SO_4^{2-}$ + 2 $H^+$ + SoxYZ-$S^-$ | | 1 |
| cSOx Overall | *soxAXBCDYZ* | $S_2O_3^{2-} + H_2O + 2\ O_2 \rightarrow 2\ SO_4^{2-} + 2\ H^+$ | | 1 |
| iSOx | *soxAX, soxYZ* | $S_2O_3^{2-}$ +SoxYZ-$S^-$ $\rightarrow$ SoxYZ-S-S-$SO_3^-$ + 2 $e^-$ | $2\ e^- + 2H^+ + ½\ O_2 \rightarrow H_2O$ | −1 |
| | *soxB* | SoxYZ-$S_3O_3^-$ + $H_2O$ $\rightarrow$ $SO_4^{2-}$ + 2 $H^+$ + SoxYZ-S-$S^-$ | | 1 |
| iSOx Overall | *soxAXZYB* | $S_2O_3^{2-} + ½\ O_2 \rightarrow SO_4^{2-} + S^0$ (attached to SoxYZ) | | 0 |
| rDSR | *?* | DsrEFH-SH $\rightarrow$ DsrEFH-S-SH | | |
| | *dsrC, dsrEFH* | DsrEFH-S-SH + DsrC(-SH)$_2$ $\rightarrow$ DsrC(-SH -SS) + $H^+$ + DsrEFH-SH | | 1 |
| | *dsrAB* | DsrC(-SH -SS) + 3 $H_2O$ $\rightarrow$ $SO_3^{2-}$ + DsrC(-$S_2$) + 7 $H^+$ + 6 $e^-$ | $4\ e^- + 4\ H^+ + O_2 \rightarrow 2\ H_2O$ | 1 |
| | *dsrMKJOP* | DsrC($S_2$) + 2 $H^+$ + 2 $e^-$ $\rightarrow$ DsrC(-SH)$_2$ | | |
| | *aprAB, aprM* | $SO_3^{2-}$ + AMP $\rightarrow$ APS + $e^-$ | $1\ e^- + 1\ H^+ + ¼\ O_2 \rightarrow ½\ H_2O$ | −1 |
| | *sat* | APS + $H_2O$ $\rightarrow$ $SO_4^{2-}$ + $e^-$ + 2 $H^+$ | $1\ e^- + 1\ H^+ + ¼\ O_2 \rightarrow ½\ H_2O$ | 1 |
| rDSR Overall | *dsrABCEFHM KJOP, aprABM, sat* | $S^0 + 3/2\ O_2 + 1\ H_2O \rightarrow SO_4^{2-} + 2\ H^+$ | | 2 |
| iSOx + rDSR | | $S_2O_3^{2-} + H_2O + 2\ O_2 \rightarrow 2\ SO_4^{2-} + 2\ H^+$ | | 1 |
| $S_4I$ –Part 1 | *doxDA/tsdA* | $2\ S_2O_3^{2-} \rightarrow S_4O_6^{2-} + 2\ e^-$ | $2\ e^- + 2\ H^+ + ½\ O \rightarrow H_2O$ | −0.5 |
| Part 1 Overall | | $2\ S_2O_3^{2-} + 2\ H^+ + ½\ O_2 \rightarrow S_4O_6^{2-} + H_2O$ | | −0.5 |
| | *Otr / ttrABC* | $S_4O_6^{2-} + 2\ e^- \rightarrow 2\ S_2O_3^{2-}$ | | |
| | *tetH* | $S_4O_6^{2-} + H_2O$ $\rightarrow$ $SO_4^{2-} + S_2O_3^{2-} + 2\ H^+$ | | |
| | *soeABC / sorAB* | $SO_3^{2-} + H_2O \rightarrow SO_4^{2-} + 2\ H^+ + 2\ e^-$ | $2\ e^- + 2\ H^+ + ½\ O_2 \rightarrow H_2O$ | |
| | *soxB* | $S_4O_6^{2-}$ + 2 $H_2O$ $\rightarrow$ 2 $SO_4^{2-}$ + 4 $H^+$ + 2 $S^0$ | | |
| Part 2 Overall | | $S_4O_6^{2-} + 3.5\ O_2 + 3\ H_2O \rightarrow 4\ SO_4^{2-} + 6\ H^+$ | | 1.5 |
| $S_4I$ Overall | | $S_2O_3^{2-} + H_2O + 2\ O_2 \rightarrow 2\ SO_4^{2-} + 2\ H^+$ | | 1 |

? indicates a gap in the literature around processes.

For full names of sulfur genes and compounds, see Table 1.2.

*Table 1.3 is based on a review of current literature; other unlisted enzymes may also play a role in $S^0$ processing: Sdo, SOR (Friedrich et al. 2001a; Thorup et al. 2017; Vigneron et al. 2021; Watanabe et al. 2019; Klatt and Polerecky 2015; Wasmund, Mußmann, and Loy 2017a; W. Li et al. 2020; Camacho, Frazao, et al. 2020a; Venceslau et al. 2014; Koch and Dahl 2018b; J. Zhang et al. 2020; Cron et al. 2020; Govil et al. 2019; Bell et al. 2020; Yuan et al. 2021; Rameez et al. 2020; R. Wang et al. 2019; Dahl et al. 2013; Buonvino, Arciero, and Melino 2022; Ray et al. 2000; Spallarossa et al. 2001; Pott and Dahl 1998; Stockdreher et al. 2012; Grein, Pereira, and Dahl 2010, Zhou et al. 2025).

**$\Delta H^+/\Delta S$ = the theoretical ratio of $H^+$ decreases (−) or increases (+) to sulfur atoms in the reaction products is calculated from combining the half reactions for each enzymatic stage of the oxidation process. For the $\Delta H^+/\Delta S$ of the enzyme-facilitated reactions with nitrate as a TEA, see Table C1.

### 1.2.2 The Incomplete SOx and rDSR Pathway: Reversing an Ancient System

In a review article published four years after clarifying the cSOx pathway mechanisms, Friedrich et al. (2005) returned to the subject, this time highlighting their insight that the pathway can function when SoxCD is missing, forming the incomplete sulfur oxidation pathway (iSOx pathway, Friedrich et al. 2005). Without SoxCD's oxidative electron transfer (equation 3), the iSOx pathway leads to storage of the terminal sulfane-sulfur atom, and an immediate yield of only two, instead of eight, $e^-$ donated by each molecule of thiosulfate processed. This mechanism, also known as the thiosulfate oxidizing multi-enzyme system (TOMES) complex or the branched *Paracoccus* sulfur oxidation (PSO) pathway, was identified as a source of extracellular sulfur globule formation (as zero-valent sulfur: ZVS or $S^0$, commonly in the form of cyclooctasulfur, $S_8$) in green sulfur bacteria (Sakurai et al. 2010). The iSOx pathway has since been linked to periplasmic sulfur globule formation in SOB genera such as *Allochromatium, Beggiatoa, Chromatiaceae, Thiothrix* and *Thiobacillus,* as well as to extracellular sulfur globule formation in genera such as *Chlorobiaceae* and *Ectothiorhodospiraceae* (Hensen et al. 2006; Meyer, Imhoff, and Kuever 2007; Cai et al. 2022). The theoretical link between the cSOx and iSOx mechanism was confirmed in a recent gene knockout experiment, demonstrating that when *soxCD* was removed from the genome of *Cupriavidus pinatubonensis JMP134*, sulfane-sulfur temporarily accumulated with thiosulfate oxidation (Xin et al. 2023).

Once ZVS is stored, SOB require a mechanism to oxidize this potential energy source. Most frequently, SOB achieve this through reversing the dissimilatory sulfate reduction (DSR) pathway (Fig 1.1, Table 1.3, equations 5 to 10):

dsrEFH: $DsrEFH\text{-}SH + S^0 \rightarrow DsrEFH\text{-}S\text{-}SH$ (5)

dsrC, dsrEFH: $DsrEFH\text{-}S\text{-}SH + DsrC(\text{-}SH)_2 \rightarrow DsrC(\text{-}SH\ \text{-}SS) + H^+ + DsrEFH\text{-}SH$ (6)

dsrAB: $DsrC(\text{-}SH\ \text{-}SS) + 3\ H_2O \rightarrow SO_3^{2-} + DsrC(\text{-}S_2) + 7\ H^+ + 6\ e^-$ (7)

dsrMKJOP: $DsrC(S_2) + 2\ H^+ + 2\ e^- \rightarrow DsrC(\text{-}SH)_2$ (8)

aprAB, aprM: $SO_3^{2-} + AMP \rightarrow APS + e^-$ (9)

sat: $APS + H_2O \rightarrow SO_4^{2-} + e^- + 2\ H^+$ (10)

In their article "Disguised as a sulfate reducer: Growth of the deltaproteobacterium *Desulfurivibrio alkaliphilus* by sulfide oxidation with nitrate," Thorup et al. (2017) first identified the reverse action of the DSR pathway by measuring changes in sulfur and nitrogen speciation endpoints ($HS^-$ and $SO_4^{2-}$; $NO_3^-$ and $NH_3$, Thorup et al. 2017). While distinguishing between the genes describing the DSR and rDSR pathway is difficult, the enzymes DsrC and DsrAB may have enough structural variation to be used as signals; additionally, DsrD and DsrT may indicate the presence of DSR pathway alone (Venceslau et al. 2014; Anantharaman et al. 2018). Although typically paired with nitrate reduction (Zhou et al. 2023), the rDSR pathway has also been recently found to function in *Desulfurivibrio* spp. coupled to Sb(V) reduction (Sun et al. 2022). In addition to the rDSR pathway, there is some evidence that an even more incomplete SOx (*soxCD* and *soxYZ* alone) pathway may be capable of oxidizing ZVS to thiosulfate and sulfate when paired with nitrate under anaerobic conditions; this incomplete pathway cannot subsequently oxidize the thiosulfate formed due to lacking *soxB* (Lahme et al. 2020; Götz et al. 2019). Alternatively, sulfur dioxygenases (SdoAB) can in some cases oxidize ZVS to sulfite (Zhang et al. 2020).

Recent research has added depth to our understanding of the iSOx + rDSR pathway. The two enzyme systems (iSOx and rDSR) are frequently found linked in genera such as *Chlorobium* and *Thiobacillus* (Gregersen, Bryant, and Frigaard 2011; K. J. Whaley-Martin et al. 2023; Beller et al. 2006). While presence of the iSOx pathway does not appear to be required for the function of the rDSR pathway, the rDSR pathway does appear to be paired to the function of iSOx vs. cSOx. This is in alignment with the observation that the presence of SoxCD (indicating the cSOx

pathway) and rDSR genes appear to be mutually exclusive, according to a survey of 127 genomes (Gregersen, Bryant, and Frigaard 2011). Beyond the core enzyme mechanisms described above, recent research has also explored how transportation of thiosulfate into the cytoplasm via SoxT1A and SoxT1B is required for function of the iSOx pathway, noting these enzymes interact with the SoxR regulator (J. Li et al. 2024).

In a similar manner to the cSOx pathway, the proton yield of the iSOx + rDSR pathway is dependent on the compound used as a TEA. If we again assume the use of oxygen as a TEA, the iSOx pathway generates no net protons for every atom of sulfur in thiosulfate that is partially oxidized, as the storage of the sulfane-sulfur atom cancels the effect of oxidizing the other to sulfate (equation 11):

$$S_2O_3^{2-} + ½\ O_2 \rightarrow SO_4^{2-} + S^0 \text{ (attached to SoxYZ)} \qquad \Delta H^+/\Delta S = 0 \qquad (11)$$

The following rDSR segment of this pathway then produces a higher ratio of protons to sulfur atoms oxidized (equation 12):

$$S^0 + 3/2\ O_2 + 1\ H_2O \rightarrow SO_4^{2-} + 2\ H^+ \qquad \Delta H^+/\Delta S = 2 \qquad (12)$$

Overall, this results in a net acid-generating ratio for the iSOx + rDSR pathway of $\Delta H^+/\Delta S\text{-}S_2O_3^{2-} = 1$, which matches that produced by the cSOx pathway. However, importantly, the iSOx + rDSR pathway process can pause at the inorganic polysulfide storage stage for an indefinite length of time, delaying acid generation.

### 1.2.3 The $S_4I$ Pathway: Discombobulating Proposed Mechanisms

While the mechanisms of the cSOx and iSOx + rDSR pathways are established in the current literature, the role of the $S_4I$ pathway is not as well understood. This may be in part due to a lack of consensus about its enzymatic stages (Fig 1.2, Table 1.4, Table 1.5). The initial stage of the $S_4I$ pathway is commonly recognized. In a reaction facilitated by thiosulfate dehydrogenase (TsdA), or occasionally thiosulfate:quinone oxidoreductase (DoxDA; Christel et al. 2016), two thiosulfate molecules are condensed to form tetrathionate in wide range of genera including *Paracoccus*, *Allochromatium*, *Shewanella*, and *Acidithiobacillus* [equation 13 (Q. Yu,

Sun, and Gao 2021; W. Li et al. 2020; Rameez et al. 2020; Brito et al. 2015; Jenner et al. 2019; Du et al. 2022; Müller et al. 2004; Denkmann et al. 2012)]:

$$\text{TsdA/DoxDA: } 2\ S_2O_3^{2-} + 2\ H^+ + \tfrac{1}{2}\ O_2 \rightarrow S_4O_6^{2-} + H_2O \qquad \Delta H^+/\Delta S = -0.5 \qquad (13)$$

Instead of generating acid, this initial stage of the $S_4I$ pathway reduces the proton concentration as thiosulfate is oxidized, resulting in a pH increase.

The lack of consensus is found regarding the second stage of the $S_4I$ pathway. TetH and SoxB are both proposed as mechanisms for the second stage of the $S_4I$ pathway, and the third stage is also unresolved (Table 1.4, Table 1.5). Whether ZVS can form via disproportionation during a later stage of the $S_4I$ pathway, and which enzymes would account for its subsequent oxidation are both open questions (Fig 1.2, Table 1.5). Some enzymes such as *sdoAB* (Table 1.4) or *pdo* (Table 1.5) might be broadly considered part of the $S_4I$ pathway or could be allocated to a pool of unclassified sulfur enzymes with no clear linkage to established pathways (Fig 1.2, Table 1.4). Additionally, several other enzyme mechanisms are speculatively used to explain sulfur cycling in the polythionate pool following tetrathionate formation (Fig 1.2, Table 1.5). Examples of the mechanisms speculated on in the literature, but which have yet to find place in the established canon, are sulfur comproportionation (Camacho, Frazao, et al. 2020) or the action of trithionate hydrolase (Meulenberg, Pronk, Frank, et al. 1992). Due to this ambiguity, it is not currently possible to calculate precise theoretical proton yields for the final stage(s) of the $S_4I$ pathway, although net acid generation would be expected (Table 1.3, Table 1.4).

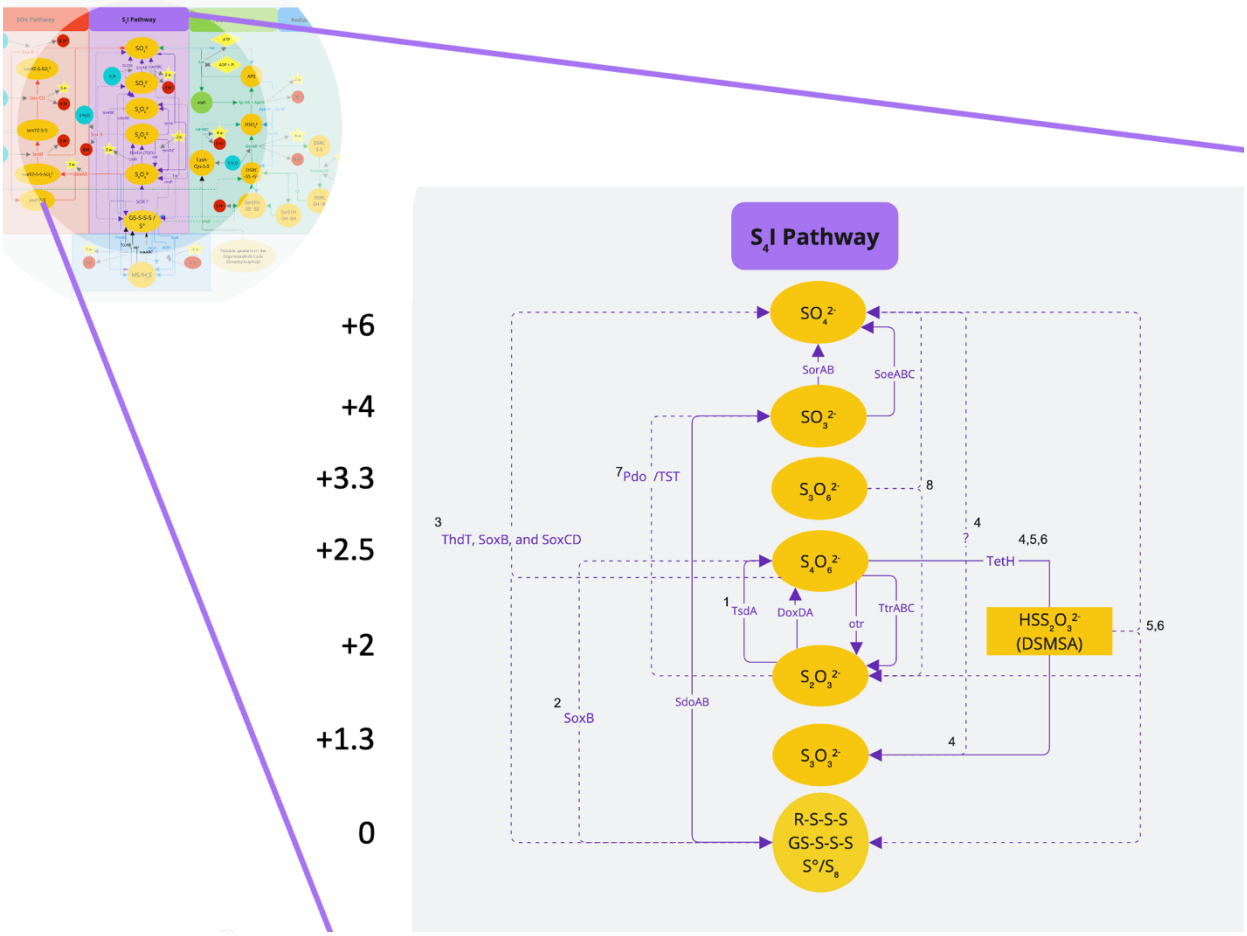


**Fig 1.2** A review of the proposed $S_4I$ pathway and other SOI cycling reactions found in the literature. This review reveals several potential enzymatic pathways that SOB might employ following the oxidation of thiosulfate to tetrathionate via TsdA. See Table 1.3 for established (solid line) and potential (dashed line) reactions. 1: TsdA (Q. Yu, Sun, and Gao 2021; W. Li et al. 2020; Rameez et al. 2020; Brito et al. 2015; Jenner et al. 2019; Du et al. 2022; Müller et al. 2004; Denkmann et al. 2012); 2: SoxB (J. Zhang et al. 2020; Cai et al. 2022b); 3: ThdT, SoxB and SoxCD (Pyne et al. 2018); 4: TetH (Dahl 2005; Beard et al. 2011a); 5/6: TetH (Kanao, Kamimura, and Sugio 2007; Meulenberg, Pronk, Hazeu, et al. 1992); 7: pdo/TST (Vigneron et al. 2021; Xin et al. 2023); 8: trithionate hydrolase (Meulenberg, Pronk, Frank, et al. 1992; Anandham et al. 2008; Lu and Kelly 1988; Pronk et al. 1990). DSMSA is disulfane monosulfonic acid. For full names of sulfur genes and compounds, see Table 1.2.

**Table 1.4** Established Enzyme-Facilitated SOx and $S_4I$ Pathway Reactions from Current Literature

| **Part A: Established S Enzyme Pathways** | | | | |
|---|---|---|---|---|
| Pathway | S Gene | Sulfur SubstrateHalf Reaction | Oxygen as TEA Half Reaction | $\Delta H^+/S$ |
| cSOx* | *soxAX, soxYZ* | $S_2O_3^{2-}$ + SoxYZ-$S^-$ → SoxYZ-S-S-$SO_3^-$ + 2 $e^-$ | 2 $e^-$ + 2$H^+$ + ½ $O_2$ → $H_2O$ | −1 |
| | *soxB* | SoxYZ-$S_3O_3^-$ + $H_2O$ → $SO_4^{2-}$ + 2 $H^+$ + SoxYZ-S-$S^-$ | NA | 1 |
| | *soxCD* | SoxYZ-S-$S^-$ + 3 $H_2O$ → SoxYZ-S-$SO_3^-$ + 6 $H^+$ + 6 $e^-$ | 6 $e^-$ + 6 $H^+$ + 3/2 $O_2$ → 3 $H_2O$ | 0 |
| | *soxB* | SoxYZ-S-$SO_3^-$ + $H_2O$ → $SO_4^{2-}$ + 2 $H^+$ + SoxYZ-$S^-$ | NA | 1 |
| **cSOx Overall** | ***soxAXBCDYZ*** | **$S_2O_3^{2-}$ + $H_2O$ + 2 $O_2$ → 2 $SO_4^{2-}$ + 2 $H^+$** | | **1** |
| iSOx | *soxAX, soxYZ* | $S_2O_3^{2-}$ + SoxYZ-$S^-$ → SoxYZ-S-S-$SO_3^-$ + 2 $e^-$ | 2 $e^-$ + 2$H^+$ + ½ $O_2$ → $H_2O$ | −1 |
| | *soxB* | SoxYZ-$S_3O_3^-$ + $H_2O$ → $SO_4^{2-}$ + 2 $H^+$ + SoxYZ-S-$S^-$ | NA | 1 |
| **iSOx Overall** | ***soxAXBYZ*** | **$S_2O_3^{2-}$ + ½ $O_2$ → $SO_4^{2-}$ + $S^0$ (attached to SoxYZ)** | | **0** |
| $S_4I$ – Part 1 | *doxDA* [1] */ tsdAB* [2] | 2 $S_2O_3^{2-}$ → $S_4O_6^{2-}$ + 2 $e^-$ | 2 $e^-$ + 2 $H^+$ + ½ $O_2$ → $H_2O$ | −0.5 |
| **P1 Overall** | | **2 $S_2O_3^{2-}$ + 2 $H^+$ + ½ $O_2$ → $S_4O_6^{2-}$ + $H_2O$** | | **−0.5** |
| $S_4I$ – Part 2 / Other SOI cycling | *tetH* [3] | $S_4O_6^{2-}$ + $H_20$ → $S_2O_3^{2-}$ + $S^0$ + $SO_4^{2-}$ +2 $H^+$ (via DSMSA) | NA | 0.5 |
| | *sdoAB* [4] | $S^0$ + 3 $H_2O$ → $SO_3^{2-}$ + 6 $H^+$ + 4 $e^-$ | 4 $e^-$ + 4 $H^+$ + $O_2$ → 2 $H_2O$ | 2 |
| | *soeABC / sorAB /abiotic/SUOX* | $SO_3^{2-}$ + $H_20$ → $SO_4^{2-}$ + 2 $H^+$ + 2 $e^-$ | 2 $e^-$ + 2 $H^+$ + ½ $O_2$ → $H_2O$ | 0 |
| | *SOR* [5] | 4 R-S-S/$S^0$ + 6 $H_2O$ → $HS^-$ + $S_2O_3^{2-}$ + $SO_3^{2-}$ + 11 $H^+$ + 6 $e^-$ | 6 $e^-$ + 6 $H^+$ + 3/2 $O_2$ → 3 $H_2O$ | 5/4 |
| S reduction | *otr/ttrABC* [6] | $S_4O_6^{2-}$ + 2 $e^-$ → 2 $S_2O_3^{2-}$ | NA, S is e− acceptor | |

*For details of the SOx cycle see *Oxidation of Reduced Inorganic Sulfur Compounds by Bacteria: Emergence of a Common Mechanism?* (Meulenberg, Pronk, Frank, et al. 1992); For full names of sulfur genes and compounds, see Table 1.2.

NA = $e^-$ acceptor not required for this reaction (example: decomposition, double replacement, disproportionation)

| Footnotes | Study |
|---|---|
| 1 | (Friedrich et al. 2001a) |
| 2 | (Müller et al. 2004) |
| 3 | (Q. Yu, Sun, and Gao 2021; W. Li et al. 2020; Rameez et al. 2020; Brito et al. 2015; Jenner et al. 2019; Du et al. 2022; Müller et al. 2004; Denkmann et al. 2012; Kanao, Kamimura, and Sugio 2007; Meulenberg, Pronk, Hazeu, et al. 1992; Tanabe and Dahl 2022b) |
| 4 | (De Jong et al. 1997a) |
| 5 | (R. Wang et al. 2019; W. Li et al. 2020) |
| 6 | (Ghosh and Dam 2009; Kletzin 1992) |

**Table 1.5** Speculative Enzyme-Facilitated SOx and $S_4I$ Pathway Reactions from Current Literature

| **Part B: Speculative S Enzyme Pathways** | | | |
|---|---|---|---|
| Pathway | S Gene | Sulfur Substrate Half Reaction | Oxygen as TEA Half Reaction |
| $S_4I$ – Part 2 / Other SOI cycling | *pdo/TST* [7] | $S_2O_3^{2-} + 3\ H_20 \rightarrow 2\ SO_3^{2-} + 6\ H^+ + 4\ e^-$ | $4\ e^- + 4\ H^+ + O_2 \rightarrow 2\ H_2O$ |
| | *tetH* [8]; *spontaneous* | $S_4O_6^{2-} + H_2O \rightarrow {}^-S\text{-}S\text{-}SO_3^- + SO_4^{2-} + 2\ H^+$;<br>${}^-S\text{-}S\text{-}SO_3^- \rightarrow S_2O_3^{2-} + S^0$ **or**<br>$2\ {}^-S\text{-}S\text{-}SO_3^- \rightarrow {}^-S\text{-}S\text{-}S\text{-}S\text{-}SO_3^- + SO_3^{2-}$<br>$2\ {}^-S\text{-}S\text{-}S\text{-}S\text{-}SO_3^- \rightarrow S_9O_3^{2-} + SO_3^{2-}$<br>$S_9O_3^{2-} \rightarrow SO_3^{2-} + S_8$ | NA<br>NA<br>NA<br>NA<br>NA |
| | *tetH* [22] | $2\ S_4O_6^{2-} + H_20 \rightarrow S_2O_3^{2-} + S_5O_6^{2-} + SO_4^{2-} + 2\ H^+$ | NA |
| | *tetH* [23] | $4\ S_4O_6^{2-} + 5\ H_20 \rightarrow 7\ S_2O_3^{2-} + 2\ SO_4^{2-} + 10\ H^+$ | NA |
| | *ThdT* [9] | $2\ S_2O_3^{2-} \rightarrow S_4O_6^{2-} + 2\ e^-$ /<br>$GSH + S_4O_6^{2-} \rightarrow GSSSSO_3^- + SO_3^{2-} + H^+$ | $2\ e^- + 2\ H^+ + ½\ O_2 \rightarrow H_2O$<br>NA |
| | *soxB*<br>*soxCD*<br>*soxB* [10] | $GSSSSO_3^- + H_20 \rightarrow GSSS^- + SO_4^{2-} + 2\ H^+$<br>$GSSS^- + 3\ H_20 \rightarrow GSSSO_3^- + 6\ H^+ + 6\ e^-$<br>$GSSSSO_3^- + H_20 \rightarrow GSSS^- + SO_4^{2-} + 2\ H^+$ | NA<br>$6\ e^- + 6\ H^+ + 3/2\ O_2 \rightarrow 3\ H_2O$<br>NA |
| | *soxB* [11] | $S_4O_6^{2-} + ??? \rightarrow SO_4^{2-}$ | ? |
| | *soxB* [12] | $S_4O_6^{2-} + 2\ H_2O \rightarrow R\text{-}SS/S^0 + 2\ SO_4^{2-} + 4\ H^+ + 2\ e^-$ | $2\ e^- + 2\ H^+ + ½\ O_2 \rightarrow H_2O$ |
| | *trithionate hydrolase* [13] | $S_3O_6^{2-} + H_2O \rightarrow S_2O_3^{2-} + SO_4^{2-} + 2\ H^+$ | NA |
| | *SOR* [14] | $7\ R\text{-}S\text{-}S/S^0 + 3\ H_2O + 8\ e– \rightarrow 6\ HS^- + SO_3^{2-}$ | NA |
| | *gplE* [15] | $S_2O_3^{2-} + CN^- \rightarrow SO_3^{2-} + SCN^-$ | NA |
| | *tetH* [20] | $S_5O_6^{2-} + H_2O \rightarrow 2S^0 + S_2O_3^{2-} + SO_4^{2-} + 2\ H^+$ | NA |
| | *Not matched to gene* [21] | $S_3O_3^{2-} + S_4O_6^{2-} \rightarrow S_2O_3^{2-} + S_5O_6^{2-}$<br>$2\ S_3O_3^{2-} + S_4O_6^{2-} \rightarrow 2\ S_2O_3^{2-} + S_6O_6^{2-}$<br>$S_3O_3^{2-} + S_5O_6^{2-} \rightarrow S_2O_3^{2-} + S_6O_6^{2-}$<br>$4\ S_3O_3^{2-} \rightarrow S_8 + 4\ SO_3^{2-}$ | NA |

**Table 1.5** cont. Speculative Enzyme-Facilitated SOx and $S_4I$ Pathway Reactions from Current Literature

| **Part B: Speculative S Enzyme Pathways** | | | |
|---|---|---|---|
| Pathway | S Gene | Sulfur Substrate Half Reaction | Oxygen as TEA Half Reaction |
| $S_4I$ – Part 2 / Other SOI cycling | *Abiotic*[16] | $S_4O_6^{2-} + SO_3^{2-} \rightarrow S_3O_6^{2-} + S_2O_3^{2-}$ | NA |
| | *Abiotic*[16] | $1/8\ S_8 + SO_3^{2-} \rightarrow S_2O_3^{2-}$ | NA |
| | *Not matched to gene*[17] | $4\ S_4O_6^{2-} + 4\ H_2O \rightarrow 6\ S_2O_3^{2-} + S_3O_6^{2-} + SO_4^{2-} + 8\ H^+$ | NA, disproportionation |
| S reduction | *ttrABC*[18] | $S_3O_6^{2-} + 2\ e^- \rightarrow S_2O_3^{2-} + SO_3^{2-}$ | NA, S is e− acceptor |

For full names of sulfur genes and compounds, see Table 1.2. In addition, the follow compounds and genes are listed in Table 1.4 and 1.5.

**Compounds:** $CN^-$ = cyanide

**S metabolism enzymes:** GplE, thiosulfate:cyanide sulfurtranserase/thiosulfate sulfurtransferase; TST, thiosulfate:cyanide sulfur transferase.

| Footnotes | Study |
|---|---|
| 7 | (Hensel et al. 1999) |
| 8 | (Vigneron et al. 2021) |
| 9 | (Dahl 2005; Gwak et al. 2022) |
| 10 | (Pyne et al. 2018) |
| 11 | (Pyne et al. 2018) |
| 12 | (Rameez et al. 2020) |
| 13 | (Meulenberg, Pronk, Frank, et al. 1992; W. Li et al. 2020; Cai et al. 2022b; Anandham et al. 2008; Lu and Kelly 1988) |
| 14 | (Pronk et al. 1990) |
| 15 | (Tanabe and Dahl 2022b) |
| 16 | (Ray et al. 2000; Spallarossa et al. 2001) |
| 17 | (Hinsley and Berks 2002) |
| 18 | (Wentzien and Sand 2004) |
| 19 | (Hinsley and Berks 2002) |
| 20 | (Haja et al. 2020; Hinsley and Berks 2002; Heinzinger et al. 1995) |
| 21 | (De Jong et al. 1997b) |
| 22 | (Wentzien and Sand 2004) |
| 23 | (Bugaytsova and Lindström 2004) |

### 1.2.4 Sulfide Oxidation, Sulfur Reduction, and the Organosulfur Cycle

In addition to the cSOx, iSOx + rDSR, and $S_4I$ pathways, there are other forms of sulfur metabolism that may function in mine wastewater systems: partial sulfur oxidation (PSO), sulfur reduction, and the organosulfur cycle. PSO is a term applied to the incomplete oxidation of $HS^-$ to $S^0$, which is then stored in sulfur globules (W. Li et al. 2020). Facilitated by flavocytochrome c sulfide dehydrogenase or sulfide:quinone oxidoreductase (enzymes coded by the genes *fcc* or *sqr*), these processes are of interest to designers of bioreactors for sulfur removal (Schwarz et al. 2020; W. Li et al. 2020; J. Wang et al. 2023; Romero, Viedma, and Cotoras 2024). Although the only pathway for sulfate reduction is DSR (Pereira et al. 2011), once SOI form, several other enzymes can play a role in the reduction of other sulfur compounds: tetrathionate reductase (TtrABC, tetrathionate to thiosulfate), thiosulfate reductase (PhsABC, thiosulfate to sulfide and sulfite), anaerobic sulfite reductase (AsrABC, sulfite to sulfide), and polysulfide reductase or sulfur reductase (PsrABC or SreABC ZVS to sulfide; Hinsley and Berks 2002; Tanabe and Dahl 2022). Finally, although generally used at much lower concentrations for cell synthesis than the catabolic processes described above, the complex organosulfur cycle (De Anda et al. 2017) involves dimethylsulfoniopropionate demethyalthion (Dmd), dimethylsulfoniopropionate lyases (Ddd), sulfur-oxidizing heterodisulfide reductase-like (sHdr), taurine transport and processing (Tau), sulfoacetate (Sau), and alkane-sulfonate (Ssu) enzyme systems, among others (Koch and Dahl 2018; Wasmund, Mußmann, and Loy 2017; Tanabe and Dahl 2023; Hirschler et al. 2021). Except in cases of extremely high increases in SOB biomass in a tailings reservoir, these anabolic rates are negligible when compared with catabolic sulfur metabolism (Cook, Smits, and Denger 2008).

## 1.3 An Ecological Niche Space Framework

By exploring where sulfur pathways succeed, in a wide variety of environments, it becomes possible to understand the importance of ecological fitness as a driver of niche space differentiation. Sulfur metabolizing bacteria thrive in environments ranging from arctic lakes (Vigneron et al. 2021), hotsprings (Magnuson et al. 2023), and glaciers (Harrold et al. 2016) to deep-sea hydrothermal vents (Cron et al. 2020; Dick 2019) and marine sediments (Wasmund, Mußmann, and Loy 2017). Across these environments, SOB communities differentiate as

community succession occurs in response to key environmental drivers such as temperature (Dick 2019; Rameez et al. 2020; Zakharyuk et al. 2019), pH (Jin and Kirk 2018a, 2018b; Y. Wang et al. 2023; Camacho, Jessen, et al. 2020), thiosulfate concentration (Liu et al. 2025), and oxygen (Meier et al. 2017; Junkins et al. 2022).

Oxygen gradients are commonly found in these systems, produced by the rate oxygen consumption exceeding the rate of replacement through diffusion or mixing. Because oxygen is the most favorable electron acceptor, these gradients affect microbial community composition. In other contexts, research shows that both shifts in microbial community composition (Ma et al. 2020) and the up- or down-regulation of sulfur cycling gene expression (Paredes et al. 2020) occur in response to changes in available TEAs and substrates. Another recent study supports the hypothesis that partitioning can be observed between the cSOx and rDSR pathways with oxygen gradients in an active mine wastewater systems (Whaley-Martin et al. 2023). Similar observations are seen in two other cases: the upregulation of rDSR in deep ocean microbes across the oxic/anoxic boundary, and the correlation of high rDSR gene abundance in sulfur-oxidizing γ-proteobacteria with the anoxic, nitrate-rich portions of the Eastern South pacific (Paredes et al. 2020; Murillo et al. 2014).

There are energetic reasons why ecological niche space parameters, such as oxygen, drive the success of functional guilds of SOB across many environments. A few universal principles, such as (a) thermodynamics and (b) kinetics, bound the possible metabolic reactions that bacteria can exploit (Jin and Kirk 2018a, 2018b). When considering thermodynamics, the cell's catabolic reactions will lead to evolutionary success when they maximize energy captured for cell growth and reproduction (Table 1.6). This may necessitate different mechanisms under different conditions. For example, in more energetically limiting suboxic waters of the hypolimnion, where nitrate is the most available TEA, higher expression of the more efficient (higher ε) but more expensive to build (due to a higher number of required enzymes) iSOx + rDSR pathway enzymes appear to be favoured (Whaley-Martin et al. 2023). The many staged reactions of the rDSR pathway may also reduce the activation energy of each step, allowing oxidation where less thermodynamic drive exists. In contrast, where oxygen is abundant, the less efficient but

metabolically inexpensive (requiring construction of only four enzymes) cSOx pathway may provide higher fitness (Whaley-Martin et al. 2023).

**Table 1.6** Gibbs Free Energy Calculations for Sulfur Pathways with Oxygen or Nitrate as the TEA*

| Sulfur Pathway | Sulfur Donor half reaction | TEA half reaction | Gibbs Free Energy (ΔG) (KJ/$e^-$) |
|---|---|---|---|
| **cSOx** | $S_2O_3^{2-} + 5\ H_2O \rightarrow$ $2\ SO_4^{2-} + 10\ H^+ + 8\ e^-$ | $8\ e^- + 8\ H^+ + 2\ O_2 \rightarrow$ $4\ H_2O$ | -102 |
| | | $8\ e^- + 8/5\ NO_3^- + 48/5\ H^+ \rightarrow$ $4/5\ N_2 + 24/5\ H_2O$ | -83 |
| | | $8\ e^- + 1\ NO_3^- + 10\ H^+ \rightarrow$ $1\ NH_4^+ + 3\ H_2O$ | -53 |
| **iSOx** | $S_2O_3^{2-} + H_2O + SoxYZ\text{-}S^- \rightarrow$ $SO_4^{2-} + 2\ H^+ + 2\ e^- + SoxYZ\text{-}S\text{-}S^-$ | $2\ e^- + 2\ H^+ + 1/2\ O_2 \rightarrow$ $H_2O$ | -116 |
| | | $2\ e^- + 2/5\ NO_3^- + 12/5\ H^+ \rightarrow$ $1/5\ N_2 + 6/5\ H_2O$ | -109 |
| | | $2\ e^- + ¼\ NO_3^- + 10/4\ H^+ \rightarrow$ $¼\ NH_4^+ + ¾\ H_2O$ | -72 |
| **rDSR** | $DsrEFH\text{-}S\text{-}SH + 4\ H_2O \rightarrow$ $SO_4^{2-} + 8\ H^+ + 6\ e^-$ | $6\ e^- + 6\ H^+ + 3/2\ O_2 \rightarrow$ $3\ H_2O$ | -105 |
| | | $6\ e^- + 6/5\ NO_3^- + 36/5\ H^+ \rightarrow$ $3/5\ N_2 + 18/5\ H_2O$ | -86 |
| | | $3\ e^- + ¾\ NO_3^- + 30/4\ H^+ \rightarrow$ $¾\ NH_4^+ + 9/4\ H_2O$ | -55 |
| **$S_4$I P1** | $2\ S_2O_3^{2-} \rightarrow S_4O_6^{2-} + 2\ e^-$ | $2\ e^- + 2\ H^+ + 1/2\ O_2 \rightarrow$ $H_2O$ | -52 |
| | | $2\ e^- + 2/5\ NO_3^- + 12/5\ H^+ \rightarrow$ $1/5\ N_2 + 6/5\ H_2O$ | -33 |
| | | $2\ e^- + ¼\ NO_3^- + 10/4\ H^+ \rightarrow$ $¼\ NH_4^+ + ¾\ H_2O$ | -2 |
| **$S_4$I P2** | $S_4O_6^{2-} + 10\ H_2O \rightarrow$ $4\ SO_4^{2-} + 20\ e^- + 20\ H^+$ | $14\ e^- + 14\ H^+ + 3.5\ O_2 \rightarrow$ $7\ H_2O$ | -112 |
| | | $14\ e^- + 14/5\ NO_3^- + 84/5\ H^+ \rightarrow$ $7/5\ N_2 + 42/5\ H_2O$ | -93 |
| | | $14\ e^- + 7/4\ NO_3^- + 35/2\ H^+ \rightarrow$ $7/4\ NH_4^+ + 21/4\ H_2O$ | -62 |

*See Appendix A, Table A1 for detailed calculations of Gibbs Free Energy under standard conditions, and a comparison calculations in a saline Black Sea environment.

In terms of kinetics, the concentration of reactants, the concentration of enzyme catalysis, and the temperature of reaction are key factors which impact reaction rates. Over a fixed period of time, quicker reactions generate more net ATP for cell growth, since total ATP production is a result of the ΔG of the reaction, concentration of reactions occurring in an instant (which can be limited by

substrate or enzyme availability), and the efficiency of energy capture. Therefore, as a shorter pathway, the cSOx pathway may also process substrate more rapidly than the rDSR pathway, providing a higher rate of energy production if reactants are not limiting; however, should TEA become scarce this fast but inefficient process would no longer be favourable. Finally, limiting nutrients also play a crucial role. For example, the selection of microbial communities that are adapted to optimize the use of key elements was explored with N and P in marine environments (Garcia et al. 2020; J. Zhou and Ning 2017; Coles et al. 2017). As a result of the kinetics and thermodynamics of these pathways, surprisingly predictable deterministic relationships between niche space and function are often observed. These relationships exist regardless of the stochastic processes of population dynamics (Jin and Kirk 2018a, 2018b; Baquero et al. 2021; J. Zhou and Ning 2017). Chemical ecologists continually seek to understand how the structure of environments drives microbial community assembly through metabolic pathway properties (Junkins et al. 2022).

## 1.4 Addressing the Knowledge Gap: Linking Sulfur Metabolism to Mine Wastewater Systems

### 1.4.1 Research Objectives

Can this understanding of sulfur metabolism in bacteria translate to the geochemical changes observed in mine wastewater systems? With so few studies in these systems, several knowledge gaps exist. First, we must determine if SOB communities present in mine wastewaters process thiosulfate through all three universal sulfur pathways (cSOx, iSOx + rDSR, and $S_4I$) or if they simply employ the widespread cSOx pathway for direct oxidation. Then, we must explore where and when these pathways are active, and if gaps between known pathway mechanisms and geochemical outcomes exist. The goal of this thesis is to develop a conceptual framework for understanding the impact of microbial sulfur oxidation in a metal mine tailings reservoir. The framework will begin to constrain biogeochemical sulfur cycling based on TEAs, sulfur substrate availability, and environmental factors. It links conditions to which SOB are most likely to be present, infers the pathways within them, and therefore can be used to predict the timing of acid generation (Fig 1.3). To develop this framework, the body chapters of this thesis address the following objectives:

1) In a series of preliminary mesocosms, survey a range of environmental niche space parameters (availability of light, oxygen, nitrate, organic carbon, and sulfur substrate concentration) to determine which of these factors influence the magnitude and timing of sulfate formation and acid generation in mine wastewater. Concurrently, identify which SOB communities are present using 16S rRNA sequencing and use this to infer which sulfur-oxidizing pathways (cSOx, iSOx + rDSR, and $S_4I$) are present in mine wastewater.

2) In a set of eight field mesocosms, identify which sulfur-oxidizing pathways (cSOx, $S_4I$, and iSOx + rDSR) are active in mine tailings by combining geochemical, DNA and RNA lines of evidence. Further, to investigate how occurrence and activity of these pathways vary in response to the concentration of environmental parameters such as TEAs ($O_2$, and $NO_3^-$), sulfur substrates ($S_2O_3^{2-}$ and $S_4O_6^{2-}$), and tailings.

3) In a series of laboratory microcosms, compare the theoretical vs. actual acid generation ratios for SOI oxidation. Use metagenomic inference from 16S rRNA data to try to explain gaps between the established sulfur enzyme reactions facilitated by the genes of key SOB from mine wastewater systems (such as *Halothiobacillus* and *Thiomonas*), and the stoichiometry of the reactions that are observed.

4) Overall, identify several key SOB genera from a Canadian tailings management system. Classifying these genera adds to our collective understanding of a mine waste microbiome that began with identifying the roles that *Halothiobacillus* (K. Whaley-Martin et al. 2019) and *Thiomonas* (Camacho, Jessen, et al. 2020a) play in acid generation (Fig 1.3).

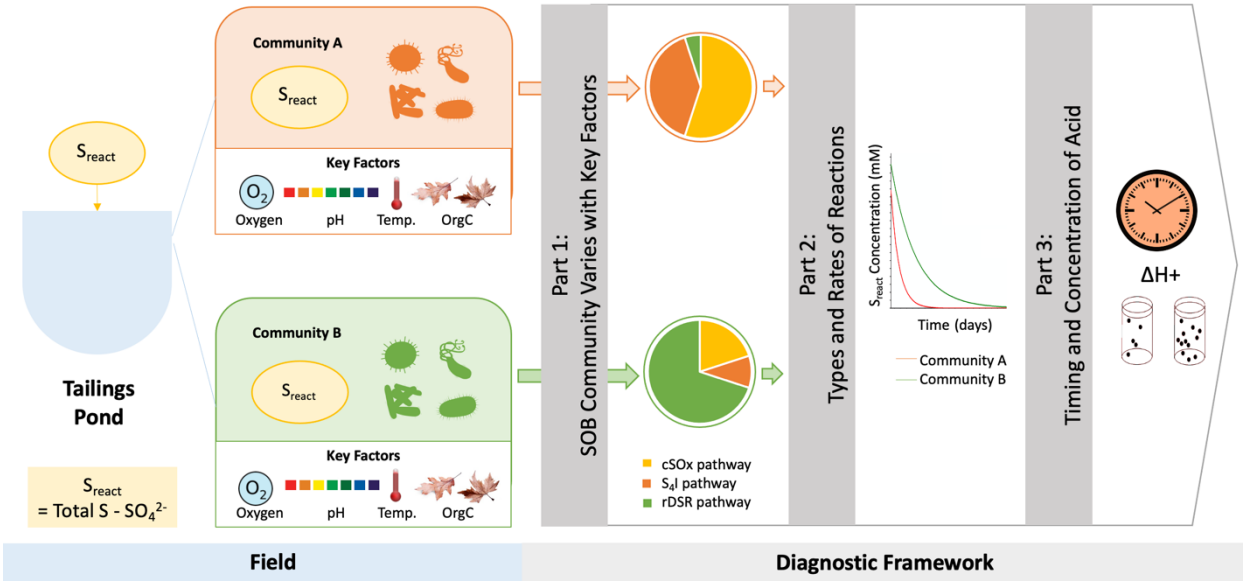


**Fig 1.3** A conceptual framework for diagnosing timing of acidity generation in the oxidation reservoir. This visual overview outlines the stages in this conceptual framework from right to left: tailings pond water containing reactive sulfur ($S_{react}$) and native SOB communities were used to fill mesocosms for onsite experiments. The conditions in these mesocosm were varied to mimic conditions found in the epilimnion or hypolimnion of the tailings impoundments (Field). The SOB communities sampled from the field mesocosms are proposed to reflect this variation in conditions by hosting different proportions of SOB pathways (Diagnostic Framework Part 1). Because they hosting different sulfur oxidation pathways, the endpoints and rates of the $S_{react}$ oxidation reactions can vary (Diagnostic Framework Part 2). This then informs the timing and magnitude of acid generation in mining wastewater (Diagnostic Framework Part 3).

### 1.4.2 Thesis Description by Chapter

Chapter 2 provides a high-level overview of the experimental design and methods used in this integrated investigation of geochemistry, microbial communities, and gene expression. Although built on established techniques, the pairing of a sulfur speciation mass balance with community abundance data (16S rRNA gene sequences) and metatranscriptomic gene expression (mRNA) is rare. The combination of these techniques allows a pairing of theory with bulk processes that is essential to the engineering application of mine wastewater treatment.

Chapter 3 describes a set of field mesocosm experiments that begin to explore the impact of environmental niche space parameters (different concentrations of light, dissolved oxygen, nitrate, and organic carbon) on SOB communities and their internal pathways. It examines when and if the functional communities of SOB (defined by genera containing the same sulfur oxidation pathway) can be deterministically predicted from the ecological niche space (as defined by sulfur substrate, pH, oxygen, and nitrate) of the community. Chapter 3 also begins to describe the impact of the type of sulfur substrate, contrasting thiosulfate and tetrathionate amendments, on the timing of acid generation.

In the field experiments described in Chapter 4, ecological niche space partitioning is again observed in response to concentrations of both nitrate and sulfur substrate (tetrathionate and thiosulfate) amendments in a series of eight 500 L mine wastewater mesocosms. Here, I explored the gaps between established enzyme pathways identified in the metagenomes of SOB from a mine tailings wastewater system, and the sulfur speciation redox reactants/products isolated in their cultures.

Chapter 5 uses a series of 16 benchtop microcosms to explore several sulfur redox reactions unexplained by our current knowledge of sulfur enzyme systems. Several gaps between experimental evidence and theoretical sulfur pathway stoichiometry were observed. This highlights the importance of future research in this field.

Finally, Chapter 6 summarizes the main results of this thesis and concludes with a few potential research directions. I propose that a direct relationship might exist between the concentrations of sulfur enzymes and the speed of the reactions they facilitate. I also ask if we can account for reactions that are not yet fully characterized or for sulfur-catabolizing proteins not yet discovered. These questions reach beyond the scope of my current work but provide possible research directions for future scientists and engineers.

## 1.5 Statement of Authorship and Publication Status

### 1.5.1 Thesis Chapter Contributions

**Chapter 3 Title:** Preliminary Mesocosms: The Influence of Ecological Niche Space on Mining Wastewater SOB Communities

**Publication Information:** Preliminary work not intended for publication.

**Authors: J. Gordon**[1]**,** K. W. Martin[1], T. C. Nelson[1], L. Twible[1] , S. Kumar[1], A. Bozzo[1], S. Marshall[3], S. Apte[2], L.A. Warren[1]

**Affiliations:** [1] Civil and Mineral Engineering, University of Toronto, Toronto, Ontario, Canada; [2] CSIRO Environment, Lucas Heights, NSW, Australia; [3] Glencore, Sudbury Integrated Nickel Operation, Sudbury, ON, Canada

**Contributions:** L.A.W., J.G, and K.W.M. designed the study. J.G., T.C.N, K.W.M., A.B, and S.K. set up field mesocosms, collected samples, and performed geochemical analyses and DNA extraction. S.M. oversaw field experiment logistics and supported field crews during mesocosm set up, sampling and take down. L.E.T. performed 16S rRNA analysis. L.A.W. secured funding, equipment and facilities. J.G. and S.A. led the writing, data interpretation, and development of results with input from all other co-authors.

**Chapter 4 Excerpted and modified from:** Microbial Sulfur Pathways and Outcomes in Tailings Impoundments: A Mesocosm Study

**Publication Information:** Published November 7, 2024. Gordon, J., Apte, S.C., Colenbrander Nelson, T.E. *et al.* Microbial Sulfur Pathways and Outcomes in Tailings Impoundments: A Mesocosm Study. *Mine Water Environ* (2024). https://doi.org/10.1007/s10230-024-01016-x

**Authors: Jay Gordon[1]**, Simon C. Apte[2], Tara E. Colenbrander Nelson[1], Kelly Whaley-Martin[1], Lauren E. Twible[1], LinXing Chen[3], Felicia Liu[1], Samantha McGarry[4], Jillian F. Banfield[3], Lesley A. Warren[1]

**Affiliations:** [1]Civil and Mineral Engineering, University of Toronto, Toronto, Ontario, Canada; [2]CSIRO Environment, Lucas Heights, NSW, Australia; [3]Earth and Planetary Sciences Department, University of California, Berkeley, CA, USA, 94720; [4]Glencore, Sudbury Integrated Nickel Operation, Sudbury, ON, Canada

**Contributions:** L.A.W., J.F.B., and S.A. designed the study. J.G., T.C.N, K.W.M., F.L., L.E.T, and S.M. set up field mesocosms, collected samples, and performed geochemical analyses and DNA extraction. S.M. oversaw field experiment logistics and supported field crews during mesocosm set up, sampling and take down. J.G. and T.C.N. performed mRNA extraction and purification. L.E.T. and J.G. performed 16S rRNA analysis. L.X.C. performed metatranscriptomic data quality control, assembly, genome binning, and curation, as well as metabolic, phylogenetic, and mRNA expression analyses. S.A. and K.W.M. developed the method for tetrathionate analysis. J.G., L.A.W., and S.A. led in the writing, data interpretation, and development of results with input from all other co-authors.

**Chapter 5: Excerpted and modified from:** Beyond SOx: Mining Sulfur Bacteria Generate Low Proton Yields due to Unidentified Enzyme Pathways

**Publication Information:** Manuscript prepared for submission to a journal.

**Authors: Jay Gordon**[1]

**Affiliations:** [1]Civil and Mineral Engineering, University of Toronto, Toronto, Ontario, Canada

**Acknowledgements:** The author would like to thank on-site mine personnel who aided in site orientation and collection of samples from which SOB communities were isolated. Thanks go to Dr. Kelly Whaley-Martin who cryopreserved the 2017 SOB cultures, isolated from an active tailings reservoir, used as inocula for these experiments. Further, I would like to thank Dr. Dalal Askar for equipment training and maintenance, analytical method improvements, and research

guidance. I would also like to thank Lauren Twible for demonstrating correct techniques for 16S analysis, ensuring QA/QC. In addition, I am very grateful to the efforts of Joshua Crawford and In Him Lee, who assisted in setting up microcosms, collecting samples, performing aqueous geochemical analyses and DNA extractions. In Him Lee also developed python script for consolidating and analysing pH and DO probe data, which aided in data analysis. Finally, many thanks go out to Dr. Simon Apte (S.A.) who provided coaching and guidance through the drafting of the manuscript and Dr. Lesley Warren (L.A.W.) for funding/facilities.

### 1.5.2 Related Work

#### Co-authored Papers

**Title:** $O_2$ Partitioning of Sulfur Oxidizing Bacteria Drives Acidity and Thiosulfate Distributions in Mining Waters.

**Publication Information:** Nature Communications, 2023. DOI: 10.1101/2021.09.16.460096.

**Authors:** Kelly J. Whaley-Martin[1,2,8], Lin-Xing Chen[3,8], Tara Colenbrander Nelson[1], **Jennifer Gordon[1]**, Rose Kantor[3], Lauren E.Twible[1], Stephanie Marshall[4,2], Sam McGarry[5], Laura Rossi[4], Benoit Bessette[6], Christian Baron[6], Simon Apte[7], Jillian F. Banfield[3] & Lesley A. Warren[1]

**Affiliations:** [1]University of Toronto, Toronto, ON, Canada; [2]Environmental Resources management (ERM), Toronto, ON, Canada. [3]Department of Earth and Planetary Science, University of California, Berkeley, CA, USA. [4]McMaster University, Hamilton, ON, Canada. [5]Glencore, Sudbury Integrated Nickel Operations, Sudbury, ON, Canada. [6]Université de Montréal, Montréal, Montréal, QC, Canada. [7]CSIRO Land and Water, Clayton, NSW, Australia. [8]These authors contributed equally: Kelly J. Whaley-Martin, Lin-Xing Chen.

**Contributions:** L.A.W. and J.F.B. designed the study. K.J.W-M., T.C.N., and L.T. collected samples, performed aqueous geochemical analyses, and undertook DNA extraction. C.B. and B.B. performed RNA extraction and purification. L.X.C. performed metagenomic data quality control, assembly, genome binning and curation, metabolic analyses, phylogenetic analyses, and RNA

expression analyses. R.K. and L.R. aided in analysis and interpretation of genomic data. S.Ma. and S.Mc. provided logistical support, field assistance, infrastructure and input. S.A's laboratory performed the total S analyses. K.J.W-M, L.X.C. and L.A.W. led in the writing, data interpretation and development of figures in the manuscript with input from all other co-authors including literature examinations by J.G. which were incorporated.

Note: JG contributions were collaborating on the sulfur enzyme literature review (clarifying the three-pathway narrative), and proposing an energetic mechanism for SOB partitioning with depth in the reservoir due to electron acceptor.

## Conference Publications

**Gordon, J.,** Colenbrander Nelson, T.C., Whaley-Martin, K., Twible, L., Kumar, S., Bozzo A., Apte, S.C. Warren, L.A. (2021) Factors which Influence Microbial Sulphur Cycling in Mine Wastewater. RemTEC. Oral and Poster Presentation.

**Gordon, J.,** Colenbrander Nelson, T.C., Whaley-Martin, K., Twible, L., Kumar, S., Bozzo A., Apte, S.C. Warren, L.A. (2020) Assessing Microbial Sulphur Oxidation Intermediates Cycling in Mine Water Mesocosms. Goldschmidt Geochemistry Meetings. Q&A Presentation.

## Educational Outreach

Microbes in Mining [video]. October 2023, 5 min. Masters of Science in Biomedical Communication, UTM. Stephen Nachtsheim. [Accessed 2024 July 10]. https://vimeo.com/935997846?share=copy

Committee members: Derek Ng (Associate Professor, Biomedical Communications), Marc Dryer (Associate Professor, Teaching Stream), **Jay Gordon** (PhD Candidate, Subject Matter Expert). Note: the "Microbes in Mining" video was circulated as a part of the Impact Assessment Agency of Canada newsletter "News @ IAAC | Nouvelles @ AEIC" on November 13, 2024.

# 2

# Methodology

*"The true method of knowledge is experiment."*
*~William Blake*

This chapter provides a high-level overview of the study site, experimental design, sampling methods and analytical techniques used in chapters 3 to 5. Specific, detailed information about equipment and sampling or analytical procedures are found in the subsequent chapters' methods sections.

## 2.1 Study Site

The wastewater and sulfur oxidizing bacteria (SOB) communities for each experiment were collected from a large tailings impoundment (19,975,000 $m^3$ average volume and ~38 m maximum depth) actively receiving tailings from an operational copper and nickel mine in Sudbury, Ontario, Canada. Tailings and milling wastewater are deposited directly into the tailings impoundment, where subaqueous disposal is intended to limit the oxidation of tailings high in sulfides. From the tailings impoundment, the wastewater flows through several checkpoints where of SOI oxidation is encouraged, then to a neutralization reservoir where liming occurs prior to release in the downstream river system. This site has been the focus of recent research into sulfur intermediate oxidation by SOB (Whaley-Martin et al. 2023; Camacho et al. 2020; Whaley-Martin et al. 2019). It was originally chosen because it experienced interesting chemical changes during a period of mill operations shutdown. Because of its situation in a northern climate, the tailings impoundment undergoes thermal stratification during winters and summers and periods of turnover during spring and fall.

## 2.2 Experimental Design: Mesocosms and Microcosms

Mesocosms refer to larger, onsite experimental vessels (500 L). Mesocosm experiments were conducted in each of two summer field seasons, as described below. Microcosms refer to laboratory benchtop experiments (6 L), which were performed in a subsequent year and a half.

### 2.2.1 Onsite Mesocosms (2019 and 2020)

In 2019 and 2020, a set of eight field mesocosms were used for a series of experiments to study SOB communities from a wastewater impoundment under partially closed conditions. The 500 L mesocosms were embedded into a peninsula protruding into the tailings impoundment (see section 2.1). The mesocosms were fitted with launch and retrieve style data loggers to monitor physio-chemical parameters (pH, $O_2$, and temperature), outboard motors to allow stirring, and vinyl tubing for sample collection. See the respective methods sections in each chapter for equipment specifics (see sections 3.2.2 and 4.2.2.).

During the summer of 2019, three sets of month-long experiments (Experiments a, b, and c) were performed to study the effects of environmental niche space parameters and SOB amendments (see details in Chapter 3, section 3.2.2) on DNA of SOB communities and, therefore, changes in sulfur speciation ($S_2O_3^{2-}$, $SO_3^{2-}$, $SO_4^{2-}$) and pH. During Experiment a, ambient sulfur compounds and SOB were exposed to variations in light and dissolved oxygen (DO) concentrations, to determine if phototrophic sulfur metabolizing bacteria were active in the systems, and whether oxygen concentrations were limiting. In Experiment b, amendments of thiosulfate, tetrathionate, organic carbon (OrgC), and nitrate were used, as a variety of other key nutrients and energy sources for the cell. In Experiment c, thiosulfate and tetrathionate amendments were again used – this time with the focus of exploring the stages of sulfur oxidation – and *Halothiobacillus*-dominated SOB community inocula were re-introduced to see if this would increase the rate at which these oxidation processes occurred.

During the summer of 2020, a six-week experiment was again performed; this experiment included measurement of several additional sulfur species (ZVS, $S_4O_6^{2-}$, Total S) and RNA expression was added to the DNA as a response variable. This experiment focused again on the impact of thiosulfate, tetrathionate, and nitrate amendments, to examine the impact of the electron

donor (thiosulfate and tetrathionate) and acceptor (oxygen – manipulated with tailings amendments - and nitrate) concentrations on sulfur pathway activity. The eight mesocosms were filled with water from the tailings impoundment in July, and but an unplanned pre-treatment period occurred over the month of August due to unavoidable COVID delays.

### 2.2.2 Benchtop Microcosms (2022)

Using the microbial inoculum of mixed culture SOB isolated and cultured from the tailing impoundment described in section 2.1, a series of three benchtop experiments (Experiments A, B, and C; using 16 microcosms) were used to isolate the acid-generating phenomenon observed in the mesocosms. The mesocosms were performed in 6 L glass flasks filled with SOB media and given amendments of thiosulfate or tetrathionate. Sulfur amendments were increased to ~ 15 - 30 x the mean concentrations detected in Canadian mine wastewater systems (11.4 mM S-$S_2O_3^{2-}$, and 8.0 mM S-$S_4O_6^{2-}$, see Table 1.1) to exaggerate the changes in sulfur speciation for analytical detection. The 8.3 mM $NO_3^-$ amendment concentration was selected to be in well in excess (at least 1.5 x) of the amount required to completely oxidize either sulfur substrate (cSOx requires 0.5 mole $NO_3^-$ per mole S-$S_2O_3^{2-}$, or 5.7 mols; $S_4$I P2 requires 0.4 mole $NO_3^-$ per mole S-$S_2O_3^{2-}$, or 3.5 mols) as the sole electron acceptor.

## 2.3 SOB Inocula

The experimental designs for the 2019 mesocosms used native mixed SOB communities, but during Experiment c these communities were augmented with *Halothiobacillus*-dominated SOB inocula (Chapter 3). These inocula were prepared from SOB communities isolated from the study site in previous years, enriched with media in the laboratory environment, cryopreserved, and then revitalized in media prior to adding them as an amendment to the field mesocosms. When the cultures were preserved, a portion of the community was DNA sequenced, so that an approximate community composition was known. Cryopreserved communities collected from two depths of the tailings impoundment in 2017 and were dominated by the genus *Halothiobacillus*, known to contain genes for both cSOx and $S_4$I P1 pathways, were used as the initial communities for the laboratory microcosm experiments performed in 6 L flasks (Chapter 5).

## 2.4 Sampling Strategy for Mesocosms and Microcosms

Mesocosms and microcosms were sampled using a syringe to draw aliquots of water through the non-reactive vinyl tubing. Samples were collected in sterile Falcon™ tubes or ion chromatography vials and refrigerated at 4 °C, or frozen at −20 ºC, prior to shipping. Samples were stored under these cooled conditions until analyzed.

### 2.4.1 Onsite 500 L Mesocosms (2019 and 2020)

Triplicate water samples were collected from each mesocosms with a sterile syringe, and filtered into vials and refrigerated until analysed on an ion chromatograph for anion and cation speciation ($S_4O_6^{2-}$, $SO_4^{2-}$, $NO_2^-$, $NO_3^-$, $NH_4^+$). Triplicate water samples (whole water and 0.2 μm filtered) were preserved with 0.02 % $HNO_3$ in flacon tubes if destined for total sulfur analysis, and refrigerated until quantified using an inductively coupled plasma optical emission spectroscope. The $S_2O_3^{2-}$ and $SO_3^-$ anions were stabilized via a monobromobimane derivatization process [the monobromobimane reacts with thiosulfate and sulfite to generate a fluorescent product which can be detected using liquid chromatography (Rethmeier et al. 1997)] in dark glass vials and then frozen for storage. When $S^o$ was analyzed (Chapter 4), whole water samples were collected in sterile 120 mL cups, frozen until a chloroform extraction was performed. Field sample blanks were prepared using Milli-Q ultrapure water transported to the field in falcon tubes and preserved in the same manner as collected samples. See sections 3.2.4, 4.2.3, and 5.2.2 for detailed descriptions of the sample collection and preservation methods.

Mesocosms were sampled for DNA and, in 2020, RNA analysis, using sterile filter towers with a 0.1 μm filter pore membrane. During 2019, the water was pumped with a Geopump™ Peristaltic Pump into the tower from two mesocosm depths (Chapter 3, section 3.2.2). Filters were excised on site and stored at −20 °C until DNA was extracted. During 2020, RNA filters were also collected from the samples taken from a 90 cm depth (Chapter 4, section 4.2.2). Once excised, the filters were stored and transported in liquid nitrogen shipping dewars to the laboratory, where they were stored at −80 °C until extraction and sequencing.

### 2.4.2 Benchtop 6 L Microcosms (2022)

Samples for sulfur speciation ($S^0$, $S_2O_3^{2-}$, $SO_3^{2-}$, $SO_4^{2-}$, and Total S) were collected using sterile tubing, syringes, and falcon tubes, as described in section 5.2.2, for a total of three experiments (Experiments A, B, and C). Samples were refrigerated immediately after collection until analysis. For Experiments A and B, when $HS^-$ concentrations were also collected, the analysis was done immediately using a portable spectrophotometer because of the volatile nature of hydrogen sulfide. DNA samples from which 16S rRNA genes were isolated and sequenced were collected using filter towers. The filter membranes coated with samples were excised immediately and stored at −80 °C until extraction. See Chapter 5, section 5.2.2, for more details.

## 2.5 Geochemical Analyses of Sulfur and Nitrogen

Geochemical analyses were performed in triplicate on stored samples. Concentrations of sulfur and nitrogen ions were measured using Thermo Scientific Dionex ICS-6000 for ion chromatography ($S_4O_6^{2-}$, $SO_4^{2-}$, $NO_2^-$, $NO_3^-$, and $NH_4^+$). $S_2O_3^{2-}$, $SO_3^{2-}$, and $S^0$ were measured using a Shimadzu LC-20AD Prominence high performance liquid chromatography, and total sulfur (TotS) using a ThermoFisher Scientific inductively coupled plasma–optical emission spectrograph (ICP-OES). See sections 3.2.5, 4.2.4, and 5.2.3 for details.

## 2.6 Proton Yield Calculations

Once of the techniques use in this thesis was to compare changes in proton and sulfur speciation concentrations to the theoretical stoichiometric ratios of enzyme facilitated reactions. To do this, it was important to calculate hydrogen ion concentrations ($[H^+]$) and their changes with time ($[\Delta H^+]$. For the purposes of this thesis, each $[H^+]$ was calculated from pH measurements collected via data loggers (above). Approximate $[H^+]$ were calculated according to the equation:

$$pH = -\log_{10}[H^+] \quad (1)$$

Since pH does not directly measure $[H^+]$, but instead detects hydrogen ion activity ($a_{H^+}$), this calculation reports values slightly below the true proton concentration. This reporting error due to an estimation of the hydrogen ion activity coefficient ($\gamma$), according to the following equation (Fujishiro, Hatae, and Kawata 1994):

$$pH = -\log_{10} a_{H^+} \quad (2)$$

$$a_{H^+} = \gamma[H^+] \quad (3)$$

sub (3) into (2):

$$pH = -\log_{10} (\gamma[H^+]) \quad (4)$$

$$[H^+] = 10^{-pH/\gamma} \quad (5)$$

The ion activity coefficient ($\gamma$) depends strongly on ion concentration (Prausnitz, Lichtenthaler, and de Azevedo 1978). At extremely low concentrations, the coefficient can be assumed to be unity, with no influence between ions (Prausnitz, Lichtenthaler, and de Azevedo 1978). At low ionic strengths, it can be determined through the Debye-Hückel equation (Prausnitz, Lichtenthaler, and de Azevedo 1978). According to the Debye-Hückel equation, a shielding effect from Coulombic forces results in decreased attraction between positively and negatively charged ions, and therefore result in an activity coefficient of less than 1:

$$\log\gamma = -0.5 \mid z_1 z_2 \mid I^{1/2} \quad (6)$$

where $\mid z_1 z_2 \mid$ is the absolute value of the product of the charges, and I is the ionic strength (Prausnitz, Lichtenthaler, and de Azevedo 1978). For solutions where $I^{1/2} < 0.1$ molal, experimental data is in good agreement with this model (Prausnitz, Lichtenthaler, and de Azevedo 1978). However, at higher concentrations, forces such as ion-ion repulsion, cause considerable deviation from this law. Therefore, in the moderately saline mine wastewater environments {$[Na^+]$~ 6 mM and 2000-2500 µS/cm (Whaley-Martin, unpublished data circa Whaley Martin et al. 2020) which is ~1/80$^{th}$ of sea water at $[Na^+]$~ 480 mM and 5000 µS/cm (Prausnitz, Lichtenthaler, and de Azevedo 1978)} without complete characterization, but from which a moderate ionic strength of $I^{1/2}$ ~ 0.2 molal can be estimated [based on $Ca^{2+}$, $Fe^{2+}$, $Na^+$ and $SO_4^{2-}$ concentrations (Ionic Strength Calculator, 2025)] a semi-empirical approximation such as the Davis equation is more suitable:

$$\log(\gamma\pm) = -0.5\, z_1 z_2 \left(\frac{\sqrt{I}}{1+\sqrt{I}} - 0.30I\right) \quad (7)$$

Where $z_1$ and $z_2$ are ion charges, and I is ionic strength, and 0.5 is the temperature dependant constant (A) at 25ºC (Stumm and Morgan 1995). Therefore, if we estimate an ionic strength of 0.04 molal ($I^{1/2} \sim 0.22$, therefore $I \sim 0.048$), the activity coefficient for monovalent $H^+$ ($z_1 = 1$) is found to equal:

$$\log(\gamma\pm) = -0.5\, z_1\, z_2 \left(\frac{\sqrt{0.048}}{1+\sqrt{0.048}} - 0.30(0.048)\right)$$

$$\log10(\gamma) \approx -0.084$$

$$\gamma \approx 0.8$$

Therefore, the factoring in ion activity, a more accurate $[H^+]$ can be calculated for a solution at pH 4 as:

$$[H^+] = \frac{10\text{^}-\text{pH}}{\gamma} = \frac{10\text{^}-4}{0.8}$$

$$\approx 0.000125 \text{ mol/L}$$

Therefore, the ion activity constant is within the range of 0.8-1.0, and so calculating $[H^+]$ from pH directly as suitable for comparisons between ratios with different orders of magnitude.

Further, in each of the body chapters, $\Delta H^+$ were calculated. In this case there was some variation in the technique. For the field based mesocosms (Chapters 3 and 4), the $\Delta H^+$ values were simply determined using:

$$\Delta H^+ = [H^+] \text{ at } t_{end} - [H^+] \text{ at } t_0 \qquad (8)$$

In these field systems, neither abiotic controls, nor controls without SOIs were possible since the wastewater was drawn from the oxidation reservoir. In these systems, $\Delta H^+$ calculations (see section 3.2.6, 4.2.2) demonstrated observed acid generation, but assume that systems without SOI or SOB would not vary in pH.

However, in Chapter 5, where laboratory microcosms allowed more precision, abiotic controls were established. The controls demonstrated that extreme acid production was a unique property of SOB metabolism. The minor pH changes observed in the abiotic controls ($[\Delta H^+]_{abiotic}$) were subtracted from the $\Delta H^+$ calculations, as follows:

$$\Delta H^+ = [H^+] \text{ at } t_{end} - [H^+] \text{ at } t_0 - [\Delta H^+]_{abiotic} \qquad (9)$$

where $[\Delta H^+]_{abiotic}$ is accounts for the changes in pH observed in the abiotic controls. Yet, due to the logarithmic nature of the pH scale, this subtraction of abiotic controls (pH decreases from ~7.8 – 7.0, $\Delta H^+ < -0.0001$ mM) did not impact to $[H^+]$ reported to 0.01 mM concentration. From this we can infer that the simplified equation 6, used in Chapters 3 and 4 was reasonable. For the influence of tailings alkalinity of the pH of field mesocosms, which was found to be negligible, see Chapter 4, section 4.2.2.

## 2.7 Genomic DNA and mRNA Extraction, Quantification, and Sequencing, Reads Processing, and Assembly

The community genomic DNA was extracted using the manufacturer's protocols for the DNeasy PowerWater DNA Isolation Kit (Qiagen), and the RNA was extracted using RNeasy PowerWater Kit (Qiagen). The DNA samples isolated for each of the experiments were sequenced at the McMaster Genomics Facility according to standard Earth Microbiome protocols [with primers 515F:GTGCCAGCMGCCGCGGTAA, and 806R:GGACTACHVGGGTWTCTAAT (Caporaso et al. 2012)**]**. Samples underwent a PCR reaction, gel electrophoresis, and Illumina MiSeq. Post-sequencing analysis was performed with DADA2 and Cutadapt, with taxonomy assigned using the SILVA database. See sections 3.2.7–8, 4.2.5–6, and 5.2.4 for details.

Isolated RNA was also sequenced at the McMaster Genomics Facility. Sequencing was performed with an Agilent Bioanalyser 2100, NEBNext® rRNA Depletion Kit, NEBNext Ultra II Directional RNA LP Kit for Illumina, Agilent Tapestation D1000, and Ampure bead clean-up kit. See Chapter 4, section 4.2.6 and 4.2.7 for more details.

Next, the RNA Illumina sequences were filtered using BBTools and Sickle to remove low quality bases. The contigs were then assembled *de novo* (Peng et al, 2013) with Prodigal used to predict protein coding genes, and reads mapped to assembled gene sequences using Bowtie2. The reads per kilobase of transcript (RPKM) represent the transcriptional activity of the gene. See Chapter 4, section 4.2.7 for more details including kit numbers.

## 2.8 Metagenomic Inference from 16S rRNA

A new approach was developed to infer the metagenomic capacity of the sulfur metabolizing genera (SOB and SRB) identified in the tailing impoundment or isolated and used as inocula for the benchtop laboratory experiments. First, the 16S rRNA .fastq files were processed according to the DADA2 pipeline described above, with taxonomy according to the latest version of the SILVA database. This produced datafiles listing the total read counts of all genera (assigned through matching operational taxonomic units; OTUs) detected by sample. To identify the dominant members of the community, relative abundances of each genus by sample were then calculated from the total counts (Total Read Counts per Genus/ ∑Read Counts in entire sample × 100 %), and data was subsequently filtered to select genera with >1% relative abundance. In some cases, where key SOB genera (*Halothiobacillus*, *Thiobacillus*, or *Thiomonas*) fell below the 1% threshold but were over the 0.01% threshold, these genera were also carried forward to the next step in the analysis. For stepwise processing of 16S rRNA data post taxonomic assignment, see http://128.100.14.155:8088/share.cgi?ssid=204a2ab4254d4911874cd20953dfb1ed.

Once a list of bacterial genera present in the community was identified, the genera were then filtered to identify key sulfur metabolizers. To identify which genera contained sulfur metabolic pathways, the classification (genera, species) identified via 16S rRNA sequence data was compared to the taxonomic assignments of Metagenome Assembled Genomes (MAGs) sequenced from a series of environmental samples collected from the tailings impoundment between 2015 and 2019 (Appendix A). These MAGs are available at https://ggkbase.berkeley.edu/mine_tailing_impoundment_time_series/organisms, with raw data for several of the genera also available with the National Centre for Biotechnology Information at https://www.ncbi.nlm.nih.gov/bioproject/?term=PRJNA379596. Data on the number of gene copies available for each MAG from each MAG from each of the 30 samples sequenced (Appendix A) was provided as direct correspondence from LinXing Chen with the Banfield lab at the University of Berkeley (data not publicly available). To determine the likelihood of the presence of a specific sulfur gene (such as *soxCD*) in a species belonging to each of these genera, the frequency of the gene's presence (at least one copy) across all MAGs sequenced for the genus was calculated as a value between 0 and 1 (see Table C4, Table D4). Where metagenomic

information was not available for a SOB genus, a literature review was performed to identify other relevant metagenomic data (such as for *Pandoraea*).

In the metagenomic summaries presented in Fig 3.8, Table C4, and Table D4, pathway presence was inferred for a genus when the sequence for the sulfur enzyme was detected in >70% of all MAGs. To produce several of the sulfur metabolising community abundance tables and figures, the 16S rRNA data was filtered to identify only the relevant SOB and SRB.

## 2.9 Statistical and Data Analysis

Statistical analyses were performed on triplicate samples in R using vegan, indicspecies, and complex heat map packages, and displayed using Ggplot. Zeros replaced "Less than detection limit" data for statistical analysis. Due to feasibility limits of biological experimentation, biological treatments were frequently performed in duplicate. Although low replicate sizes limit the strength of statistical analysis, a duplication of trends in sulfur speciation or pH changes provided some reassurance that observed phenomena were a result or treatments and not random variability. See sections 3.2.9, 4.2.8, and 5.2.6 for details.

# 3

# Preliminary Mesocosms: The Influence of Ecological Niche Space on Mining Wastewater and SOB Communities

*"In one drop of water are found the secrets of all the oceans."*
*~ Kahlil Gibran*

Three sets of preliminary field studies were performed in mesocosms onsite during the summer of 2019. Several challenges arose during this ambitious field season; some samples were lost in transportation, sample preservation techniques were improved throughout the season, and some compounds important to a sulfur mass balance were not measured. Nonetheless, the following chapter describes interesting findings. Using lessons learned from this season, these findings were explored in more detail in future studies.

## 3.1 Introduction

The link between the oxidation of sulfur oxidation intermediates (SOIs) and acidity generation in mine wastewaters is an important risk management concern in the metal mining industry (Schmidt and Conn 1969; K. Whaley-Martin et al. 2020). Extensive research investigates microbial sulfur cycling of acid rock drainage (ARD) communities (Pakostova et al. 2020; Hua et al. 2015; Ullrich et al. 2016; Denef, Mueller, and Banfield 2010; Nancucheo et al. 2017; Skousen et al. 2017), but there is limited characterization of sulfur-oxidizing bacteria (SOB) in actively managed tailings impoundments (K. Whaley-Martin et al. 2019; Twible et al. 2024; K. Whaley-Martin et al. 2023; Camacho, Jessen, et al. 2020; Miettinen et al. 2021). A significant challenge in this field is the complexity of the systems, which includes a dynamic water balance that obscures the stoichiometry of biogeochemical changes.

To see through the variability in such data due to a range of external factors, a strong conceptual framework is required. A tailings impoundment can be understood as a series of zones, where differentiated SOB communities are sustained because of variations in ecological niche space drivers such as light, dissolved oxygen (DO), nitrate, organic carbon (OrgC), and sulfur substrate availability (Lester, Adams, and Farmer 1988; Gao et al. 2022; Huang et al. 2022; Meier et al. 2017). Mesocosm experiments allow segments of these systems to be mimicked in isolation, so the fluxes of thiosulfate and acidity in semi-closed systems can be determined. This initial, exploratory study occurred over three sets of month-long experiments performed in 500 L mesocosms filled with water from an active tailings impoundment. The purpose of this study was to provide an early exploration of microbial sulfur cycling in the upper, oxic portion of a constrained mine wastewater system. It aimed to identify key environmental niche space parameters (light, DO, nitrate, OrgC, thiosulfate, and tetrathionate amendments) that constrain variations in SOB communities and the sulfur cycling pathways they contain, so that the key parameters could be studied in greater depth in future work.

## 3.2 Methods

During the summer of 2019, a set of onsite mesocosms were used to explore the effects of ecological niche space parameters on SOB communities. The following sections describe the study site, experimental design, sampling strategy, as well as the geochemical and microbial analyses performed.

### 3.2.1 Study Site

The wastewater for each of the experiments was collected from a large tailings impoundment at an operational nickel mine in Sudbury, Ontario, Canada that is actively receiving tailings (section 2.1). The water column of the tailings impoundment experiences both winter and summer thermal stratification, interspersed with mixing periods during spring and fall. For additional study site details, see Whaley-Martin et al. (2023). A few days before the initiation of each mesocosm experiment, approximately 4000 L of wastewater was collected from ~1 m depth and transferred by a water truck to the mesocosms on site (the transfer occurred within 2 h, as the collection site was ~0.5 km from the impoundment). While baseline geochemistry of the initial wastewater was not quantified, its composition was likely similar to mean values detected in this tailings impoundment over during previous studies spanning from 2014-2021 (Table 3.1).

**Table 3.1** Sulfur Compound Concentrations in the Tailings Impoundment May - September

| | **Tailings Impoundment in Sudbury, ON** |
|---|---|
| pH | 6.6 |
| Sulfate ($SO_4^{2-}$) | average 4.5 ± 0.3 mmol/L |
| Thiosulfate ($S\text{-}S_2O_3^{2-}$) | average 0.7 ± 0.1 mmol/L |
| Tetrathionate ($S\text{-}S_4O_6^{2-}$) | NA |
| Sulfite ($SO_3^{2-}$) | average 0.1 ± 0.0 mmol/L |

*table summarizes additional unpublished data collected between 2014-2021 along with values described by Whaley-Martin (K. Whaley-Martin et al. 2020) and (K. J. Whaley-Martin et al. 2023); NA = data not available

### 3.2.2 Experimental Design: Onsite 500 L Mesocosms

Three sets of experiments (a, b, and c) were performed to study the impacts of light, oxygen, nitrate, OrgC, and sulfur substrate concentrations on the SOB communities. Each experiment built on the previous one, repeating treatments which were found to have an effect, omitting those where no significant effect was observed, and including other factors which appeared likely to impact microbial sulfur oxidation.

The set of eight 500 L field mesocosms were initially set up in June 2019. Eight high density linear polyethylene (HDLPE, 47.5″ height × 30″ diameter, or 121 cm × 76 cm; ACO container systems manufactured to ASTM-D-1988 Standard) tanks were buried ~80 cm into the ground, leaving ~40 cm remaining above ground level, in coarse fill forming a peninsula protruding into an active tailings impoundment on the study site (Fig 3.1). At the end of June 2019, these mesocosms were filled with wastewater from the epilimnion of mine site's tailings impoundment. Mesocosms were allowed to equilibrate with ground temperature and environmental conditions for four days before experimental manipulations were undertaken (Fig 3.1). The experiment ran for ~4 weeks under varied treatments of light exposure and DO (Table 3.2). It was a $2^2$–factorial experiment, with two levels of light exposure (daily maxima of 250–858 lum/ft² were detected in the mesocosms with translucent polyethylene lids, while the low daily maxima of 5–20 lum/ft² were detected in mesocosms with foil-covered lids) and DO input (stirred vs. unstirred). Two replicates of each of the combinations of light and DO levels were used (Fig 3.1). Four of the mesocosms were fitted with automated outboard electric motors (connected to a solar panel array) to allow continuous stirring, which increased the concentration of DO; the other four mesocosms were allowed to stratify. Light levels were adjusted by covering four of the mesocosms with opaque reflective foil and four with translucent polyethylene lids (allowing 40-60% of light to be transmitted (Van Aardt et al. 2001)).

(a)

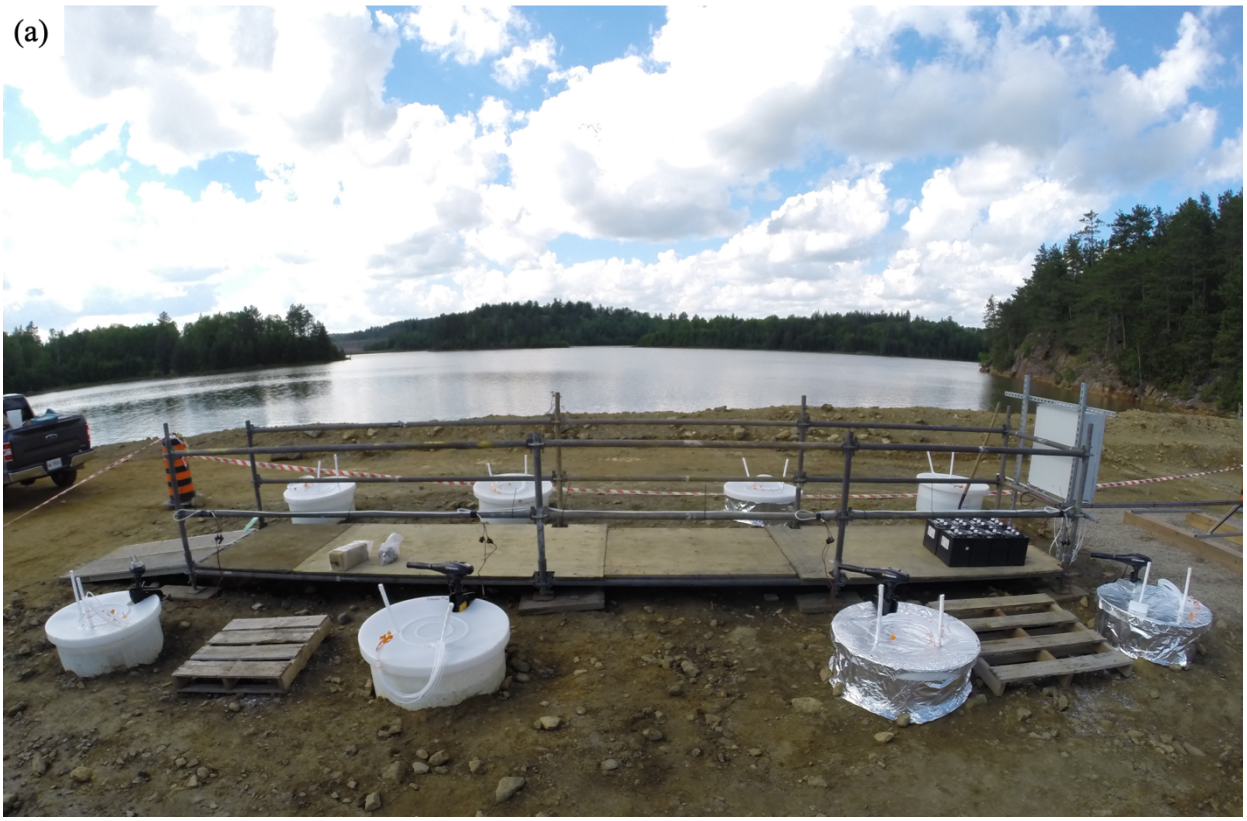

(b)

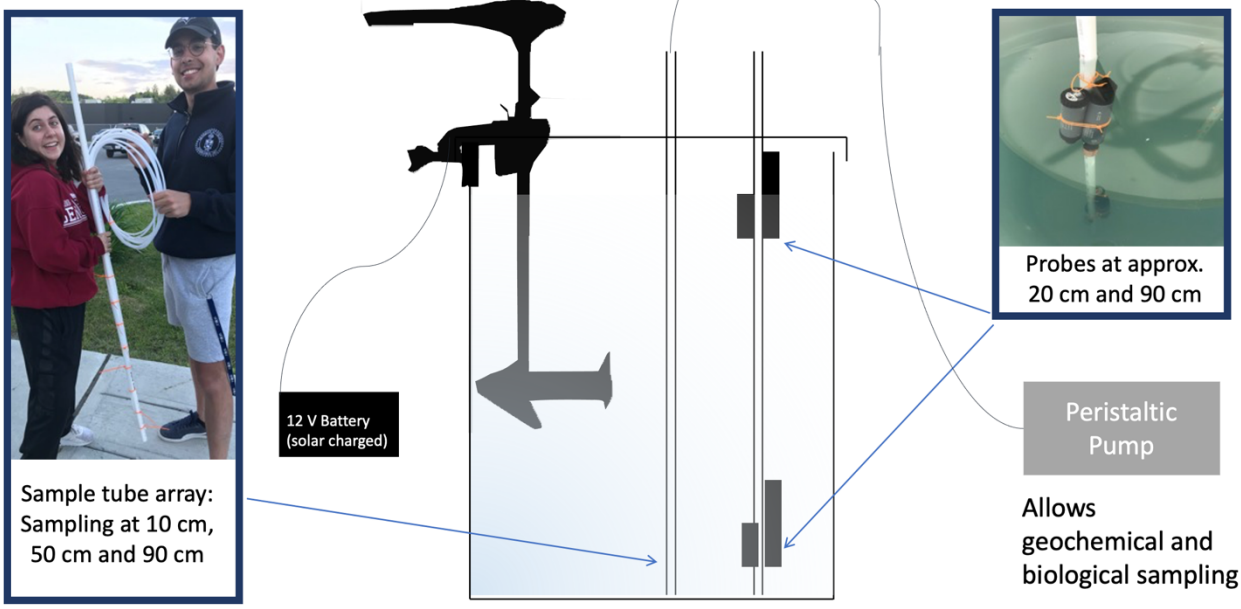
Sample tube array: Sampling at 10 cm, 50 cm and 90 cm
12 V Battery (solar charged)
Probes at approx. 20 cm and 90 cm
Peristaltic Pump
Allows geochemical and biological sampling

(c)

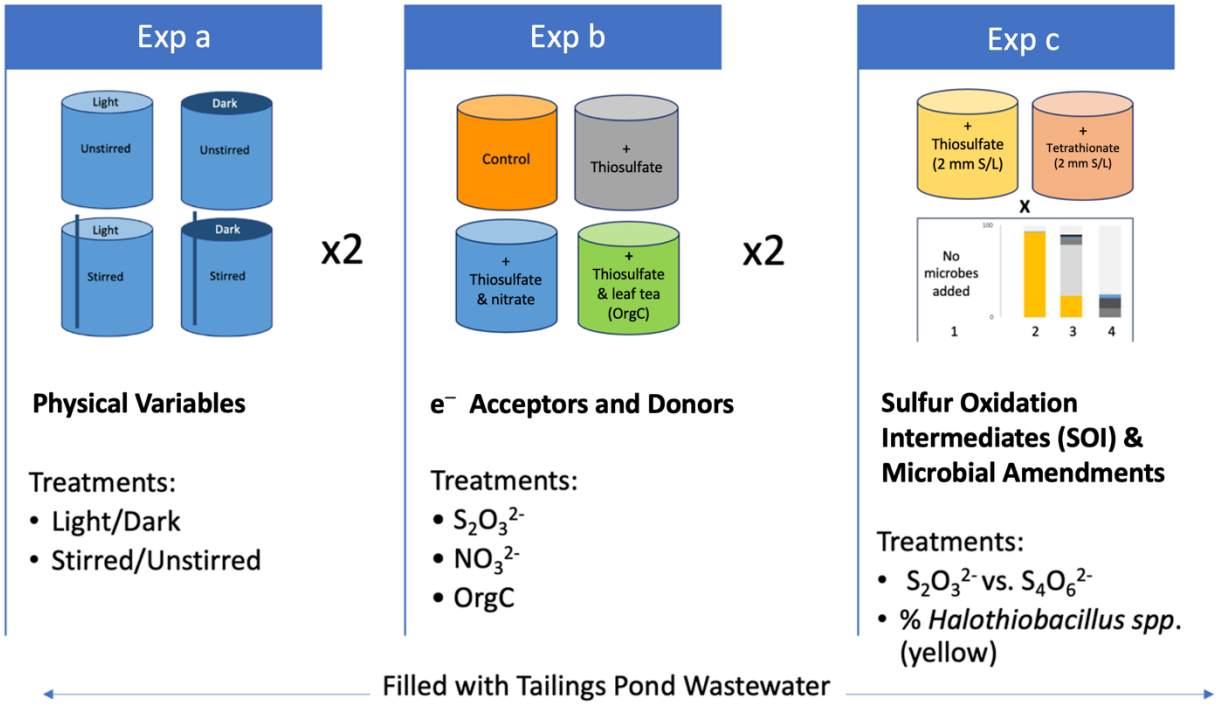


**Fig 3.1** Experimental design of the mesocosm experiments in the summer of 2019. (a) For each experiment, 8 mesocosms were filled with water from an active tailings impoundment, placed under different initial conditions, and the microbial community and geochemistry were monitored weekly over 4–6 weeks. (b) The probes, sampling assembly, and outboard motors used in Experiment a are displayed. (c) Experiment a, which occurred in July 2019, explored the effects of stirring (to increase oxygen availability) and light. Experiment b, performed in August 2019, measured the effects of thiosulfate, nitrate, and OrgC treatments. Experiment c, performed in October 2019, explored the impact of the oxidation state of the sulfur intermediates and amendment with inocula containing different fractions of *Halothiobacillus* spp. Treatments in experiments a and b were performed in duplicate to examine replicability.

Mesocosms were fitted with Hobo data logger probes (DO: HOBO® U26-001, and pH: HOBO® MX2501, 25 cm and 95 cm from the surface) to monitor physio-chemical parameters (pH, $O_2$, and temperature) at 30-minute intervals, sampled for sulfur speciation weekly, and sampled for 16S rRNA sequence analysis at $day_0$ (when initial samples were collected following the period of equilibration) and $day_{end}$.

After the experiment in July 2019, the mesocosms were emptied and rinsed twice with bleach (>1% sodium hypochlorite concentration) to sterilize. Once clean, mesocosms were rinsed with wastewater taken from the epilimnion (0.5 m depth) of the oxidation reservoir by water truck from

a location ~0.5 km from the experimental site. The wastewater was collected at the beginning of August, and after rinsing the mesocosms refilled with water from the same water truck for the subsequent experiment. For Experiment b, this water used to fill the mesocosms already hosted microbial SOB communities present in the oxidation reservoir. The communities were then exposed to treatments which explored impacts of thiosulfate as an electron donor, electron acceptor, and carbon source. The mesocosm were treated with two replicates of four different conditions: (i) no amendment, (ii) 2.0 mM thiosulfate, (iii) 2.0 mM thiosulfate + 0.2 mM nitrate, and (iv) 2.0 mM thiosulfate + OrgC (see Fig 3.1). The OrgC amendment was created by soaking a mixture of deciduous and coniferous twigs and leaves from the site in water from the oxidation reservoir to create a solution high in organic material. Amendments were added directly to the mesocosms, and mesocosms were stirred to allow even distribution. Thiosulfate and OrgC amendments were performed at $day_0$, while nitrate amendments were added at $day_9$, once oxygen levels were partially depleted.

**Table 3.2** Experimental Factors for 500 L Mesocosms from 2019

| | **Factor 1** | **Factor 2** | **Factor 3** |
|---|---|---|---|
| **Experiment a** | Light (0–800 lum/ft$^{2*}$) /Dark (<20 lum/ft$^{2*}$) *varies with time of day | Stirred/Unstirred | |
| **Experiment b** | 2.0 mM S-$S_2O_3^{2-}$ | 200 µM $NO_3^-$ | Leaf Tea (OrgC) |
| **Experiment c** | 2.0 mM S-$S_2O_3^{2-}$ | 2.0 mM S-$S_4O_6^{2-}$ | SOB inocula |

Samples were collected over the course of six weeks (refrigerated or frozen by the end of the field day) and Hobo data loggers were used to measure DO concentrations (HOBO® U26-001) and pH (HOBO® MX2501) at 30-min intervals. Mesocosms were emptied and double rinsed with 1% hypochlorite after the experiment concluded in early September 2019.

In mid-September 2019, mesocosms were refilled with water from the epilimnion of the oxidation reservoir, as the system was cooling and entering fall turnover. For Experiment c, treatments focused on the different impacts of thiosulfate vs. tetrathionate as sulfur substrates, and also explored the influence of addition SOB communities. The amendments were applied in the following combinations: 2.0 mM thiosulfate + no SOB, 2.0 mM thiosulfate + Community 1, 2.0 mM thiosulfate + Community 2, 2.0 mM thiosulfate + Community 3, 2.0 mM tetrathionate + no SOB, 2.0 mM tetrathionate + Community 1, 2.0 mM tetrathionate + 25% Community 2, 2.0 mM tetrathionate + Community 3 (see section 3.2.3 for details of SOB communities). As with the

August experiment, samples for sulfur speciation and 16S rRNA gene sequencing were collected on site and refrigerated or frozen by the end of the day, and pH and DO values were logged (sampling and measurements only occurred at $day_0$ and $day_{end}$).

### 3.2.3 SOB Inocula

During Experiment c, native microbial SOB communities were augmented with *Halothiobacillus*-dominated SOB inocula. The microbial SOB cultures used as inocula were isolated from the same oxidation reservoir in 2017, enriched with media in a laboratory and then cryopreserved in glycol at -80°C. Two weeks before the experiment, these communities were revitalized in media containing thiosulfate prior to adding them as an amendment to the field mesocosms. The 16S rRNA genes from the regrown communities were sequenced to determine the percentage of *Halothiobacillus* in the inocula, and three SOB communities were developed: Community 1 (<1% *Halothiobacillus* abundance), Community 2 (25% *Halothiobacillus* abundance), and Community 3 (98% *Halothiobacillus* abundance).

### 3.2.4 Sampling Strategy

Mesocosms were sampled for 16S rRNA gene sequence and geochemical analyses by drawing water up through non-reactive vinyl tubing (Crack-Rst Polyethylene-Lined EVA tubing for Food & Beverage; ¼″, 0.635 cm). Between 1.5-2 L of water was collected, via peristaltic pump, for 16S rRNA analysis, as the standardized 2 L volume was sometimes not achieved due to heavy biomass. About 200 mL of water was collected using a sampling syringe that was thoroughly rinsed with water drawn from the vinyl tubing prior to sample collection for all geochemical analysis. For all experiments, triplicate water samples were collected from each mesocosm for quantification of anion concentrations ($SO_4^{2-}$ and $NO_3^-$), filtered with a Pall Acrodisc® 25 mm 0.2-µm filter into Falcon™ tubes, and stored at 4 °C until analyzed. Concentrations of $S_2O_3^{2-}$ and $SO_3^{2-}$ anions, by contrast, were stabilized from unfiltered samples via a monobromobimane derivatization process (Rethmeier et al. 1997). To describe the monobromobimane derivatization briefly, 100 µL whole water was pipetted into a 2-mL glass amber vial containing 100 µL acetonitrile, 100 µL HEPES/EDTA buffer (50 mmol/L HEPES [4-{2-hydroxyethyl} piperazine-1-ethanesulfonic acid], ≥99.5%, Sigma; 5 mmol/L EDTA buffer [ethylenediaminetetraacetic acid], 99.4–100.6%, Sigma Aldrich). The sample was then adjusted to pH 8.0 with NaOH) and 20 µL 48 mmol/L monobromobimane (>97%, Sigma Aldrich, in acetonitrile, stored at -20°C) to

cause sample fluorescence. After the sample reacted with reagents for 30 min, the reaction was stopped with 200 µL methanesulfonic acid (~100 mmol; ≥99.5%, Sigma Aldrich). Following derivatization, samples were immediately frozen, transported on ice, and stored in a -20 ºC freezer until processed. Sample analysis was performed on an in-house Shimadzu LC-20AD Prominence high performance liquid chromatography (HPLC) following published protocols (K. Whaley-Martin et al. 2020; Rethmeier et al. 1997).

Mesocosms were sampled for 16S rRNA gene analysis at $day_0$ using a 0.1-µm filter towers (Thermo Scientific™ Nalgene™ Rapid-Flow™ Sterile Disposable Filter Units with CN Membrane) from a 50 cm depth, and at $day_{end}$ using 0.1-µm filter towers from a 90 cm depth. Filtered volumes varied between 1.5–2.0 L, as filtering was performed until sufficient biomass was collected to cause the filters to slow. Excised filters were stored at −20 °C until DNA was extracted for 16S rRNA gene analysis of the 100 samples.

### 3.2.5 Geochemical Analyses of Sulfur and Nitrogen

Detailed methods for geochemical analysis of all ions, except for tetrathionate and ammonia, are described in Whaley-Martin et al. (2019). Briefly, dissolved $SO_4^{2-}$, $NO_2^-$, and $NO_3^-$ concentrations were determined by ion chromatography (Thermo Scientific Dionex™ ICS-6000) in triplicate from filtered (0.2 µm) samples. Anion samples were analyzed on a Thermo Scientific Dionex™ ICS-6000 HPIC™ (high pressure ion chromatography) System using EPA Methods 300.0 and 300.1. Anions samples were calibrated with curves prepared by dilution of liquid 1000 ppm standards. The samples were then eluted onto a Dionex IonPac™ AS18-FASTAS18 anion exchange column (7.5 µm × 150 mm, Thermo Scientific™ eluted with 23 mM KOH at 30 °C and a flow rate of 1 mL/min). Elution times were approximately 3.2 min for $NO_2^-$, 4.9 min for $NO_3^-$, and 5.8 min for $SO_4^{2-}$.

Quantification of $S_2O_3^{2-}$and $SO_3^{2-}$ was performed in triplicate by HPLC (Prominence, Shimadzu). $S_2O_3^{2-}$ and $SO_3^{2-}$ concentrations were determined using a UV/VIS detector and a Alltima™ HP C18 reversed phase column (150 mm × 4.6 mm × 5 µm, Grace™) at 35 °C (Rethmeier et al. 1997). Samples were eluted with an isocratic mobile phase of 35:65 methanol to 0.25% acetic acid v/v (pH 3.5 adjusted with NaOH). The column flow rate was set to 0.5 mL/min, with a total run time of 12 min, excitation wavelength 380 nm, emission wavelength of 478 nm, and elution times of approximately 5.1 min for $SO_3^{2-}$ and 5.5 min for thiosulfate. The detection peaks were

calibrated against curves prepared from solid standards of sodium sulfite and sodium thiosulfate (Sigma Aldrich, ≥98% purity and 99% purity respectively; data is reported as sulfur molarity [i.e., $S\text{-}S_2O_3^{2-}$]).

### 3.2.6 Proton Yield Calculations

Hydrogen ion concentrations ($[H^+]$) and their changes with time [$\Delta H^+$], were calculated according to equations 1 and 2.

$$pH = -\log_{10}[H^+] \quad (1)$$

$$\Delta H^+ = [H^+] \text{ at } t_{end} - [H^+] \text{ at } t_0 \quad (2)$$

Although this results in an underestimation of free protons due omitting the ion activity coefficient ($\gamma \sim 0.8$), this conversion allowed for a stoichiometric exploration of $H^+$ - S ratios, accurate for order of magnitude comparisons. For these studies, it would also have been valuable to quantify potential influence of alkalinity in the field mesocosms. Nonetheless, the high variability in pH values over time (large increases and decreases in $[H^+]$ were observed) suggests that the alkalinity was negligible. This omission was corrected by characterizing both wastewater and tailings buffering via acid titration curves in the following year (see section 4.2.4 and 4.4.2), where its influence was minor.

### 3.2.7 Genomic DNA Extraction

The genomic DNA from the mesocosm communities was extracted using the manufacturer's protocols for the DNeasy PowerWater DNA Isolation Kit (Qiagen). Once extracted, samples were stored at −20 °C. The DNA concentrations were quantified at the McMaster facility using qPCR, and quality-assessed via agarose gel electrophoresis.

### 3.2.8 DNA Gene Amplicon Sequencing and Analyses

Isolated DNA samples were prepared and sequenced at the McMaster Genomics Facility as described in Whaley-Martin et al. 2019. The V4 region of the 16S rRNA gene was amplified by PCR using primer set 515F/806R using standard Earth Microbiome Project protocols (Caporaso et al. 2012) with added Illumina dual-index adapters. In short, for each PCR reaction, 5 pM of each primer was added to 50 ng of template strand, along with 1U of Taq DNA polymerase (Invitrogen™), BSA (0.4 mg/mL), $MgCl_2$ (1.5 mM), dNTPs (0.2 mM), and buffer. The PCR

reaction cycle was 5 min at 98 °C followed by 35 cycles (98 °C for 30 s, 50 °C for 30 s and 72 °C for 30 s), and a final extension time of 10 min at 72 °C. Gel electrophoresis was used to check the quality of amplified products prior to sequencing. For sequencing, all amplicons were normalized using SequalPrep (ThermoFisher #A1051001) to 1.25 ng/μL and then sequenced using Illumina MiSeq platform with paired-ends of 250 bp. More than 70% of reads exceeded "Q30" average quality control parameter for all runs. DADA2 (version 1.6.0) was used to detect and exclude bimeras and chloroplast and mitochondrial sequences, and Cutadapt was used to filter sequences to a minimum quality score of 30 and trim them to a minimum read length of 100 bp (Martin 2011). Taxonomy was assigned using SILVA database version 138.1.

### 3.2.9 Statistical and Data Analysis

Non-metric dimensional scaling (NMDS), canonical analysis, indicator species tests, and ANOVA/ACNOVA tests were carried out in R version 4.4.4, utilizing the Vegan package version 2.6.4 and indicspecies package 1.1.7 7 (De Cáceres et al. 2012). Statistical analyses were carried out on triplicate samples for geochemistry, unless noted, with standard deviation calculated on mean analytical data from triplicate injections. "Less than detection limit" chemical or biological data were treated as zero for statistical analyses. Thiosulfate loss rates were calculated using log scale mean ($\mu$) and variance ($\sigma^2$), from the arithmetic mean ($x$) and standard deviation ($s_x$) of the original data by assuming log-normal distribution. Data were displayed using the Ggplot package in R.

## 3.3 Results

### 3.3.1 Experiment a: Light and Oxygen Exposure

Experiment a, which occurred over 30 days in July 2019, explored the impacts of variation in light and DO levels on thiosulfate loss and subsequent acidity generation. It was a $2^2$–factorial experiment, with two levels of light exposure (high daily maxima of 250–858 lum/ft², and low daily maxima of 5–20 lum/ft²) and DO input (stirred vs. unstirred). Treatments were performed in duplicate. A summary of the geochemical data is provided in Table 3.3; for complete geochemistry and SOB community data, see Table B1 and Table B2.

## Geochemistry: Thiosulfate Loss and Acidity Trends

During Experiment a, the ambient thiosulfate concentration ($[S_2O_3^{2-}]_0$ = 0.2 mM S) decreased by an average of 0.008 +/- 0.003 mM S/day (Fig B1) under both light (daily maxima of 250–858 lum/ft², see Fig B2) and dark conditions (daily maxima of 5–20 lum/ft²), and under both medium (0 < DO < 0.30 mM, decreasing with time) or high (DO ~0.25 mM) oxygen concentrations (Fig 3.2, Table B1). The pH also changed, but not simultaneously with thiosulfate loss. Instead, the pH across all systems remained circumneutral until at least $day_{14}$ (pH = 6.4 ± 0.4), decreasing rapidly after $day_{22}$ (pH = 5.2 ± 0.8) to acidic conditions by $day_{29}$ (pH = 4.6 ± 0.7) for most experiments.

Despite no direct correlation between thiosulfate loss and acidity generation, increases in proton concentrations ($[H^+]$) were observed in all but one of the treatments (Fig 3.2). These increases occurred when thiosulfate concentrations decreased below the 0.01 mM threshold and where oxygen was readily available (both light and dark stirred treatments, and the dark unstirred treatments, see Fig 3.2). A relationship between thiosulfate loss and proton concentration was determined by assuming smooth curves for the thiosulfate concentration and interpolating that a $[S\text{-}S_2O_3^{2-}]$ < 0.01 mM was reached between $day_{20}$ and $day_{22}$ ($S\text{-}S_2O_3^{2-}$ is thiosulfate as sulfur), as > 0.19 mM $S\text{-}S_2O_3^{2-}$ was converted to a different sulfur compound by the SOB community (Fig 3.2). The exception to this pattern occurred in the light unstirred mesocosms, where the systems became suboxic. In these exceptional mesocosms, increases in $[H^+]$ concentrations began on $day_{13}$ and $day_{18}$ when DO concentrations dropped below 0.025 mM, and suboxic conditions were reached (Fig 3.2).

A two-way ANOVA was performed to examine the statistical effects of light levels and DO on $[H^+]$ at $day_{29}$; however, neither the main effects of light levels ($F_{1,3}$ = 3.39, $p$ > 0.05), stirring ($F_{1,3}$ = 0.40, ns), nor the interaction effect between the two ($F_{1,3}$ = 0.09, ns) were statistically significant. Instead, the ratio between $[S\text{-}S_2O_3^{2-}]$:[DO] appears to link to the onset of acid generation, because when either sulfur substrate or oxygen became limited, $[H^+]$ increased. Although the magnitude of the Δ[H+] increases varied between replicates, and was quite low in one of the dark, unstirred replicates, this trend was visible across all treatments. Where acid generation began prior to thiosulfate limitation (the light, unstirred treatments), oxygen levels dropped below 0.05 mM, see Table 3.4).

**Table 3.3** Summary of Geochemical Data from Experiment a Mesocosms

| Exp | Treatment | Rep | Mesocosm | Day | pH (Bottom) | DO (mg/L) | DO (mM) | $NO_3^-$ (mM) | Std Dev $NO_3^-$ (mM) | $S\text{-}S_2O_3^{2-}$ (mM) | St Dev $S\text{-}S_2O_3^{2-}$ (mM) |
|---|---|---|---|---|---|---|---|---|---|---|---|
| (a) | Dark, Unstirred | R1 | M01 | 0 | - | 9.58 | 0.30 | 0.01 | 0.02 | 0.18 | 0.01 |
| (a) | Dark, Unstirred | R1 | M01 | 8 | 7.58 | 7.52 | 0.24 | - | - | 0.13 | 0.03 |
| (a) | Dark, Unstirred | R1 | M01 | 29 | 4.75 | 0.24 | 0.01 | 0.03 | 0.00 | nd | nd |
| (a) | Dark, Stirred | R1 | M02 | 0 | - | 8.06 | 0.25 | 0.02 | 0.02 | 0.16 | 0.00 |
| (a) | Dark, Stirred | R1 | M02 | 8 | 7.14 | 7.08 | 0.22 | - | - | 0.04 | 0.01 |
| (a) | Dark, Stirred | R1 | M02 | 29 | 4.26 | 7.14 | 0.22 | - | - | nd | nd |
| (a) | Dark, Unstirred | R2 | M03 | 0 | - | 7.84 | 0.25 | 0.00 | 0.00 | 0.17 | 0.01 |
| (a) | Dark, Unstirred | R2 | M03 | 8 | 7.58 | 7.05 | 0.22 | - | - | 0.11 | 0.01 |
| (a) | Dark, Unstirred | R2 | M03 | 29 | 6.09 | 2.92 | 0.09 | 0.05 | 0.00 | nd | nd |
| (a) | Dark, Stirred | R2 | M04 | 0 | - | 7.48 | 0.23 | 0.01 | 0.02 | 0.17 | 0.00 |
| (a) | Dark, Stirred | R2 | M04 | 8 | 7.18 | 7.04 | 0.22 | - | - | 0.08 | 0.01 |
| (a) | Dark, Stirred | R2 | M04 | 29 | 4.80 | 2.62 | 0.08 | 0.04 | 0.00 | nd | nd |
| (a) | Light, Unstirred | R1 | M05 | 0 | - | 7.63 | 0.24 | 0.01 | 0.01 | 0.18 | 0.01 |
| (a) | Light, Unstirred | R1 | M05 | 8 | 7.45 | 6.06 | 0.19 | - | - | 0.11 | 0.02 |
| (a) | Light, Unstirred | R1 | M05 | 29 | 4.48 | 0.17 | 0.01 | - | - | nd | nd |
| (a) | Light, Stirred | R1 | M06 | 0 | - | 9.22 | 0.29 | 0.00 | 0.00 | 0.17 | 0.01 |
| (a) | Light, Stirred | R1 | M06 | 8 | 7.20 | 7.08 | 0.22 | - | - | 0.09 | 0.01 |
| (a) | Light, Stirred | R1 | M06 | 29 | 4.31 | 2.64 | 0.08 | 0.04 | 0.00 | nd | nd |
| (a) | Light, Unstirred | R2 | M07 | 0 | - | 9.24 | 0.29 | 0.03 | 0.00 | 0.18 | 0.01 |
| (a) | Light, Unstirred | R2 | M07 | 8 | 7.30 | 6.68 | 0.21 | - | - | 0.19 | 0.05 |
| (a) | Light, Unstirred | R2 | M07 | 29 | 3.97 | 1.37 | 0.04 | 0.01 | 0.03 | nd | nd |
| (a) | Light, Stirred | R2 | M08 | 0 | - | 7.48 | 0.23 | 0.03 | 0.00 | 0.18 | 0.01 |
| (a) | Light, Stirred | R2 | M08 | 8 | 7.13 | 6.84 | 0.21 | - | - | 0.13 | 0.03 |
| (a) | Light, Stirred | R2 | M08 | 29 | 3.96 | 2.86 | 0.09 | 0.04 | 0.04 | nd | nd |

Notes: Sulfite ($SO_3^{2-}$) was non-detectable throughout all experiments and timepoints; $Day_0$ DO data inferred from June 26, 2019. All samples were collected from 50 cm depth.

(-) indicates no value available; gap in data; sulfate ($SO_4^{2-}$) data was not available for Experiment a, and several timepoints for nitrogen species measured by ion chromatography are also missing due to vials breaking during transportation.

nd = non-detectable, below limit of detection; conservative LOD for analysis were as follows: 0.04 mM S for thiosulfate, 0.013 mM N for nitrate.

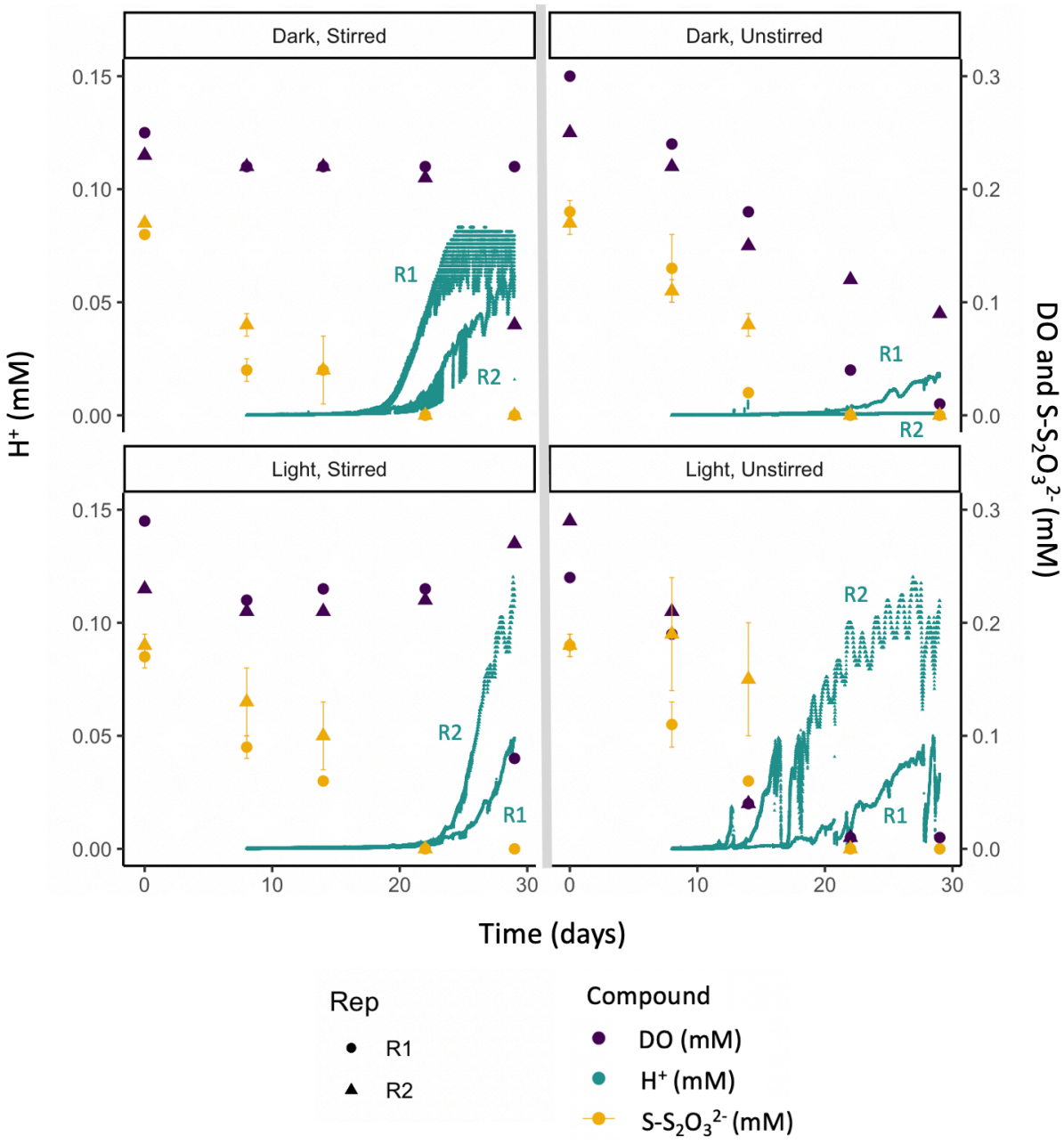


**Fig 3.2** Chemical concentration profiles over 29 days in Experiment a. The $[H^+]$ was calculated from pH detected via a data logger to allow stoichiometric comparison; $[H^+] = -\log(pH)$ – see section 3.2.5 (turquoise symbols, two replicates). Concentrations for [DO] (purple symbols, two replicates), and $[S\text{-}S_2O_3^{2-}]$ (gold symbols, two replicates) are displayed. Replicates 1 (circles) and 2 (triangles) of the four treatments demonstrate similar responses to the variations in light levels and stirring (increasing DO availability). Sulfate samples were not available for analysis from Experiment a because of sample loss due to the vials breaking during transportation.

## Bacteria: Sulfur Metabolizing Community Trends (DNA)

By examining the 16S rRNA gene sequences extracted from $day_0$ and $day_{end}$, dominant members of the microbial community could be identified and the changes in response to the different treatments could be tracked (Fig 3.3). Similar responses to the different abiotic conditions were observed in both replicates in all treatments. In Experiment a, six SOB genera were identified (via metagenomic inference, see section 2.8). At $day_0$, the relative abundances of the three most abundant were: *Sediminibacterium* (37.3 ± 3.7%), *Acidovorax* (17.2 ± 4.2%), *Halothiobacillus* (0.6 ± 0.8%), while the remaining genera (*Brevundimonas*, *Thiobacillus*, and *Thiomonas*) composed <0.05 % of the initial communities. The initial communities were also composed of non-sulfur catabolizing genera such as *Polynucleobacter* (25.6 ± 12.9%), *Xanthobacter* (13.9 ± 5.6%), *Bradyrhizobium* (4.4 ± 6.6%), *Sphingobium* (2.1 ± 1.4%), and *Sphingomonas* (1.4 ± 1.4%). Although present at <1% relative abundance at $day_0$, *Halothiobacillus* increased to 25–43% abundance by $day_{end}$ in the light stirred treatments, where oxygen was abundant. The second replicate light stirred treatment, which had a high proportion of *Halothiobacillus* present (43 %, Fig 3.3a), also experienced the largest increase in proton concentration (Fig 3.2). *Halothiobacillus* also was detected in the communities in the dark stirred (0–8 %), light unstirred treatments (5–13 %), and slightly in the first replicate of the dark, unstirred treatment (3 %), where proton increases were observed (Fig 3.2, 3.3a). At $day_{end}$, the highest proportion of *Brevundimonas* appeared in the dark unstirred treatments (18–50 %); no proton increase was observed in the second replicate where *Brevundimonas* composed 50 % of the community. The highest proportion of *Thiobacillus* appeared in the light stirred treatments (7–19%).

A canonical analysis with a posteriori projection of the environmental variables pH, DO, temperature (°C), and [S-$S_2O_3^{2-}$], shows no clear dominance of any of these environmental factors when explaining variation in the relative abundance of SOB genera, although [DO], pH, or [S-$S_2O_3^{2-}$] appear to be counter-correlated to dominance of *Thiobacillus*. Likewise, an NMDS performed on all 16S rRNA gene sequence data from Experiments a and b showed no clustering by depth or treatment (Fig B3).

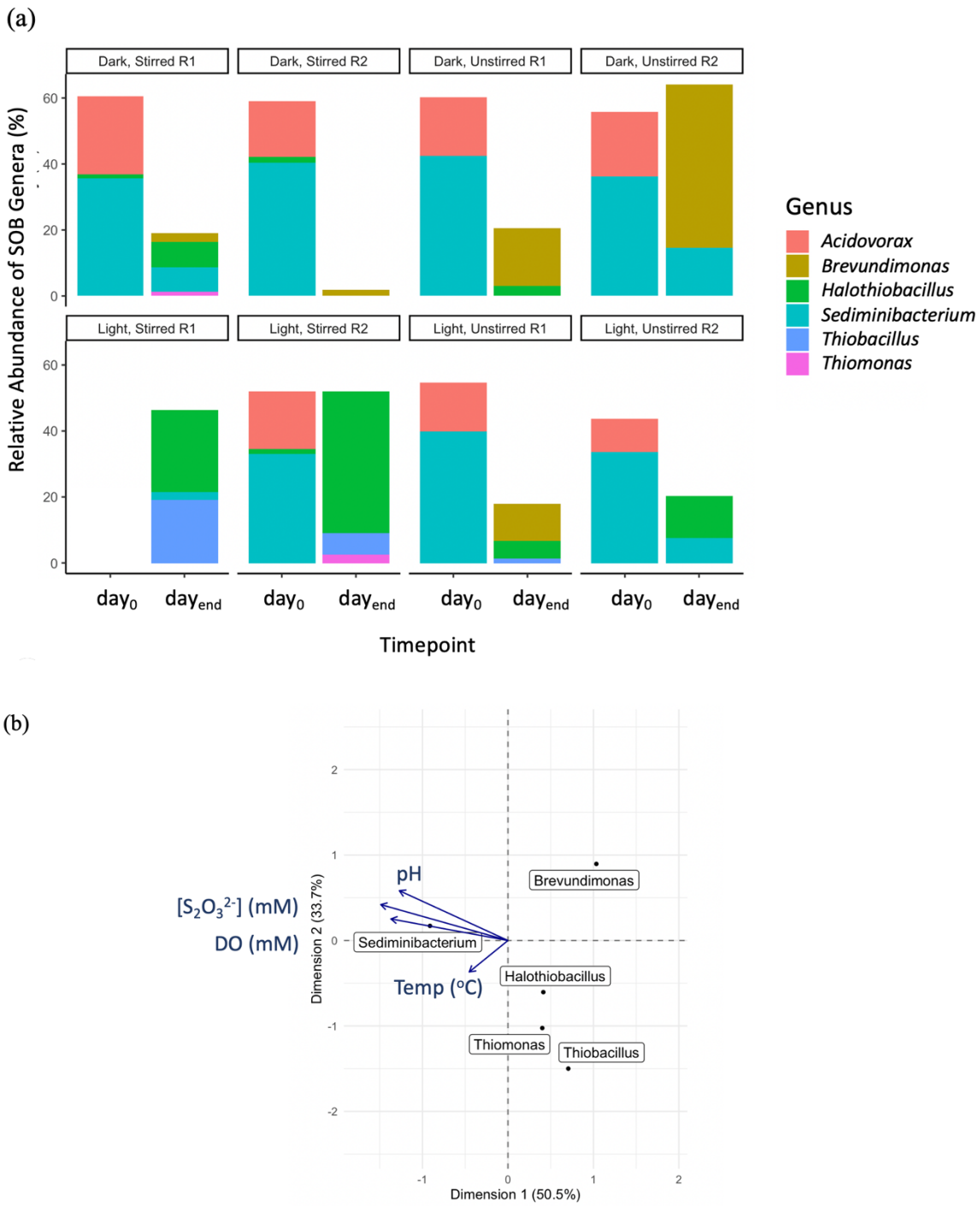


**Fig 3.3** SOB and their response to environmental variables in Experiment a. (a) The relative abundance of sulfur-oxidizing bacteria (SOB), as a proportion of the overall bacterial community is displayed from samples collected at $day_0$ and $day_{end}$ in each of the two replicates across the four treatments of light and oxygen levels. (Note: $day_{end} = day_{29}$ for all mesocosms except for the dark unstirred replicate 2, which was collected on $day_{28}$.) Sequence data for $day_0$ from the light stirred replicate 1 was not available. (b) A canonical analysis was used to explore potential relationships between environmental variables and the dominance of different SOB genera.

### 3.3.2 Experiment b: Variations in Thiosulfate, Nitrate, and Organic Carbon Concentrations

Experiment b, which occurred over 22 days in August 2019, explored the impacts of variation in thiosulfate, nitrate, and OrgC amendments on thiosulfate loss and subsequent acidity generation. The experiment was performed in duplicate with the following treatments: controls (no amendments), 2.0 mM S-$S_2O_3^{2-}$ (on $day_0$), 2.0 mM S-$S_2O_3^{2-}$ (on $day_0$) + 0.2 mM $NO_3^-$ (on $day_9$), 2.0 mM S-$S_2O_3^{2-}$ + OrgC from leaf tea (on $day_0$). A summary of the geochemical data is provided in Table 3.4; for complete geochemistry and SOB community data, see Table B1 and Table B2 cont.

#### Geochemistry: Thiosulfate Loss and Acidity Trends

During Experiment b, where mesocosms were amended with 2.0 mM S-$S_2O_3^{2-}$ (10× the ambient thiosulfate concentration), thiosulfate decreased according to a pseudo-first order reaction, where the rate constant was $k = \sim 0.20 \pm 0.03\ d^{-1}$ (Fig 3.4b). In the control treatments, ambient thiosulfate concentrations were below detection, so no loss rate could be calculated. The thiosulfate loss rates observed in the amended mesocosms of Experiment b indicate that, although not statically significant, the half-life of thiosulfate may have been longer in the mesocosms with nitrate amendments (9.9 d) than without (3.5 d), or than when OrgC was also available (6.3 d).

During the 6 days prior to initial amendments, the pH in each mesocosm decreased from circumneutral (6.1 ± 0.7) to acidic (4.6 ± 0.7). During this period, the $[H^+]$ increases occurred rapidly, without thiosulfate loss (Fig 3.4a). However, upon amendment with thiosulfate, all treated mesocosms rapidly returned to circumneutral conditions, and maintained these until thiosulfate concentrations were depleted under oxic conditions (as in Experiment a). The initial thiosulfate concentration (2.5 mM) dropped to <0.1 mM by day 21 for the 2.0 mM S-$S_2O_3^{2-}$ treatments (with or without OrgC), after which the $[H^+]$ of the mesocosms again began to increase under oxic conditions. This conversion of 2.4 mM S into another sulfur compound(s) was not accounted for by equivalent increases in sulfate concentration (Table 3.4). Rather, where data was available between $day_{13}$ and $day_{27}$, no sulfate increase was observed (8.7 ± 0.8 at $day_{13}$ to 8.2 ± 1.1 at $day_{27}$, Table B1). As was observed in Experiment a, in Experiment b the acidity generation began when the [S-$S_2O_3^{2-}$] dropped to less than 1/20 of its original concentration, and sulfur was cycled into other forms (not sulfate) in the aqueous solution.

**Table 3.3** Summary of Geochemical Data from Experiment b Mesocosms

| Exp | Treat-ment | Rep | Meso-cosm | Day | pH (Bottom) | DO (mg/L) | DO (mM) | $NO_3^-$ (mM) | Std Dev $NO_3^-$ (mM) | $S\text{-}S_2O_3^{2-}$ (mM) | St Dev $S\text{-}S_2O_3^{2-}$ (mM) | $SO_4^{2-}$ (mM) | St Dev $SO_4^{2-}$ (mM) |
|---|---|---|---|---|---|---|---|---|---|---|---|---|---|
| (b) | Control | R1 | M09 | -6 | 6.56 | 8.25 | 0.26 | - | - | - | - | - | - |
| (b) | Control | R1 | M09 | 0 | 3.91 | 4.73 | 0.15 | 0.11 | 0.00 | nd | nd | - | - |
| (b) | Control | R1 | M09 | 27 | 3.95 | 7.67 | 0.24 | 0.07 | 0.00 | nd | nd | 7.7 | 0.5 |
| (b) | Control | R2 | M10 | -6 | 6.16 | 8.38 | 0.26 | - | - | - | - | - | - |
| (b) | Control | R2 | M10 | 0 | 3.99 | 4.02 | 0.13 | 0.12 | 0.00 | nd | nd | - | - |
| (b) | Control | R2 | M10 | 27 | 4.03 | 7.75 | 0.24 | 0.07 | 0.00 | nd | nd | 8.0 | 0.3 |
| (b) | 2.0 mM $S\text{-}S_2O_3^{2-}$ | R1 | M11 | -6 | 5.99 | 8.68 | 0.27 | 0.12 | 0.00 | - | - | 8.2 | 0.1 |
| (b) | 2.0 mM $S\text{-}S_2O_3^{2-}$ | R1 | M11 | 0 | 4.38 | 4.39 | 0.14 | 0.12 | 0.00 | 2.23 | 0.04 | - | - |
| (b) | 2.0 mM $S\text{-}S_2O_3^{2-}$ | R1 | M11 | 27 | 4.39 | 4.11 | 0.13 | 0.07 | 0.00 | 1.12 | 0.15 | 8.9 | 0.0 |
| (b) | 2.0 mM $S\text{-}S_2O_3^{2-}$ | R2 | M12 | -6 | 6.36 | 7.82 | 0.24 | 0.21 | 0.01 | - | - | 8.1 | 0.2 |
| (b) | 2.0 mM $S\text{-}S_2O_3^{2-}$ | R2 | M12 | 0 | 4.15 | 4.92 | 0.15 | 0.12 | 0.00 | 1.76 | 0.16 | - | - |
| (b) | 2.0 mM $S\text{-}S_2O_3^{2-}$ and 0.2 mM $NO_3^-$ | R1 | M13 | -6 | 6.53 | 8.5 | 0.27 | 0.22 | 0.00 | - | - | 8.4 | 0.1 |
| (b) | 2.0 mM $S\text{-}S_2O_3^{2-}$ and 0.2 mM $NO_3^-$ | R1 | M13 | 0 | 5.50 | 4.26 | 0.13 | 0.10 | 0.03 | 2.14 | 0.06 | - | - |
| (b) | 2.0 mM $S\text{-}S_2O_3^{2-}$ and 0.2 mM $NO_3^-$ | R1 | M13 | 27 | 5.96 | 2.77 | 0.09 | 0.04 | 0.00 | 0.84 | 0.02 | 8.6 | 0.1 |
| (b) | 2.0 mM $S\text{-}S_2O_3^{2-}$ and 0.2 mM $NO_3^-$ | R2 | M14 | -6 | 5.94 | 8.31 | 0.26 | 0.17 | 0.00 | - | - | 8.5 | 0.6 |
| (b) | 2.0 mM $S\text{-}S_2O_3^{2-}$ and 0.2 mM $NO_3^-$ | R2 | M14 | 0 | 4.28 | 4.42 | 0.14 | 0.12 | 0.00 | 1.68 | 0.02 | - | - |
| (b) | 2.0 mM $S\text{-}S_2O_3^{2-}$ and 0.2 mM $NO_3^-$ | R2 | M14 | 27 | 5.74 | 2.36 | 0.07 | 0.04 | 0.00 | nd | nd | 8.7 | 0.3 |
| (b) | 2.0 mM $S\text{-}S_2O_3^{2-}$ and OrgC | R1 | M15 | -6 | 6.51 | 6.19 | 0.19 | - | - | - | - | - | - |
| (b) | 2.0 mM $S\text{-}S_2O_3^{2-}$ and OrgC | R1 | M15 | 0 | 4.49 | 3.6 | 0.11 | 0.12 | 0.00 | 0.12 | 0.00 | - | - |
| (b) | 2.0 mM $S\text{-}S_2O_3^{2-}$ and OrgC | R1 | M15 | 27 | 3.59 | 0.13 | 0.00 | 0.08 | 0.00 | 1.09 | 0.09 | 9.0 | 0.7 |
| (b) | 2.0 mM $S\text{-}S_2O_3^{2-}$ and OrgC | R2 | M16 | -6 | 4.59 | 6.94 | 0.22 | - | - | - | - | - | - |
| (b) | 2.0 mM $S\text{-}S_2O_3^{2-}$ and OrgC | R2 | M16 | 0 | 5.69 | 3.7 | 0.12 | 0.10 | 0.03 | 3.07 | 0.03 | - | - |
| (b) | 2.0 mM $S\text{-}S_2O_3^{2-}$ and OrgC | R2 | M16 | 27 | 3.65 | 0.37 | 0.01 | 0.09 | 0.00 | 0.89 | 0.03 | 5.7 | 0.3 |

Notes: Sulfite ($SO_3^{2-}$) was non-detectable throughout all experiments and timepoints; All samples were collected from 90 cm depth.

(-) indicates no value available; gap in data; nd = non-detect, below limit of detection; a conservative LOD for analysis were as follows: 0.04 mM S for thiosulfate, 0.013 mM S for sulfate, 0.013 mM N for nitrate. All sulfate values were calculated using a 10× dilution technique.

(a)

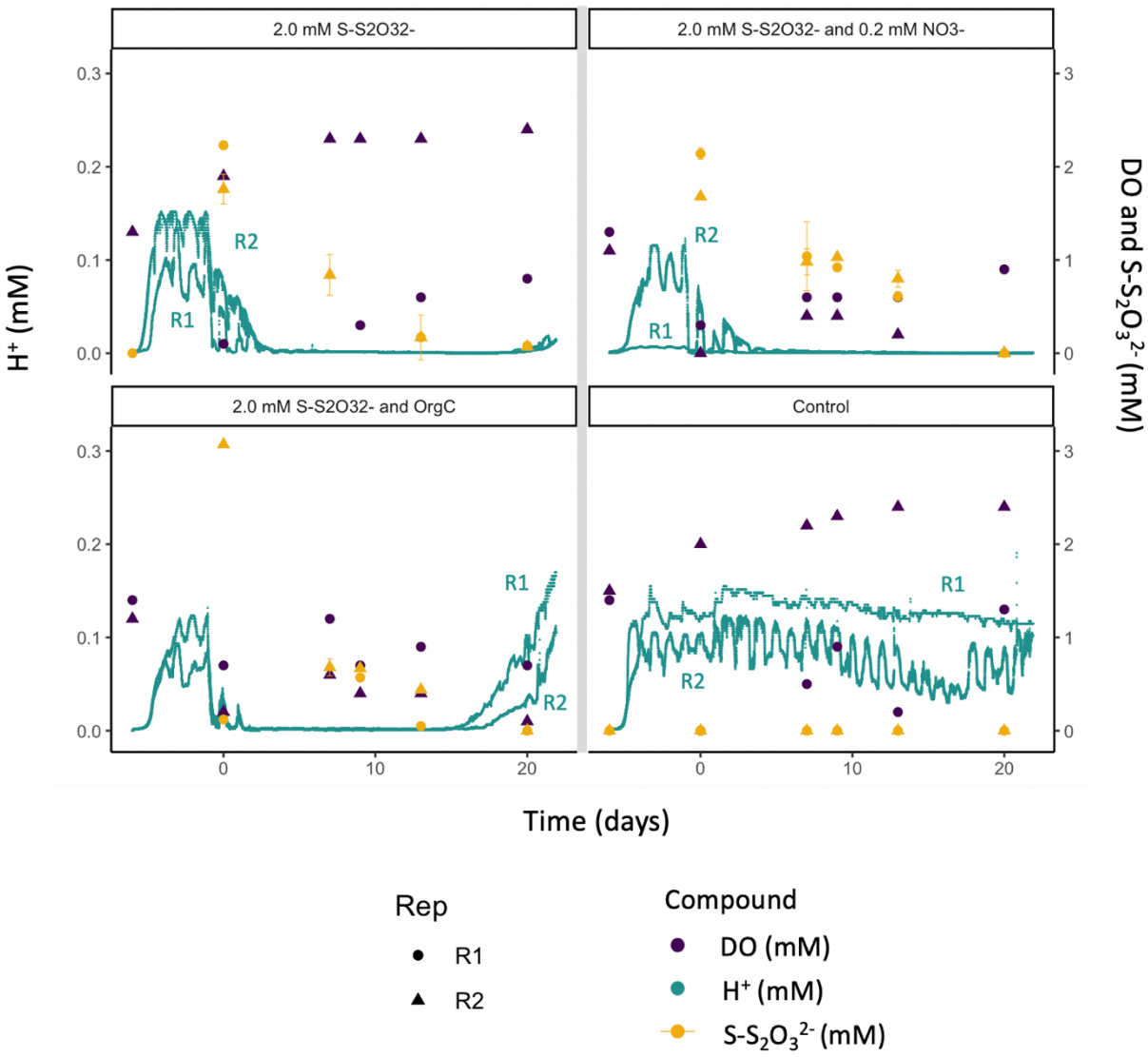
2.0 mM S-S2O32-
2.0 mM S-S2O32- and 0.2 mM NO3-
2.0 mM S-S2O32- and OrgC
Control
R1
R2
H+ (mM)
DO and S-S2O32- (mM)
Time (days)
Rep
R1
R2
Compound
DO (mM)
H+ (mM)
S-S2O32- (mM)

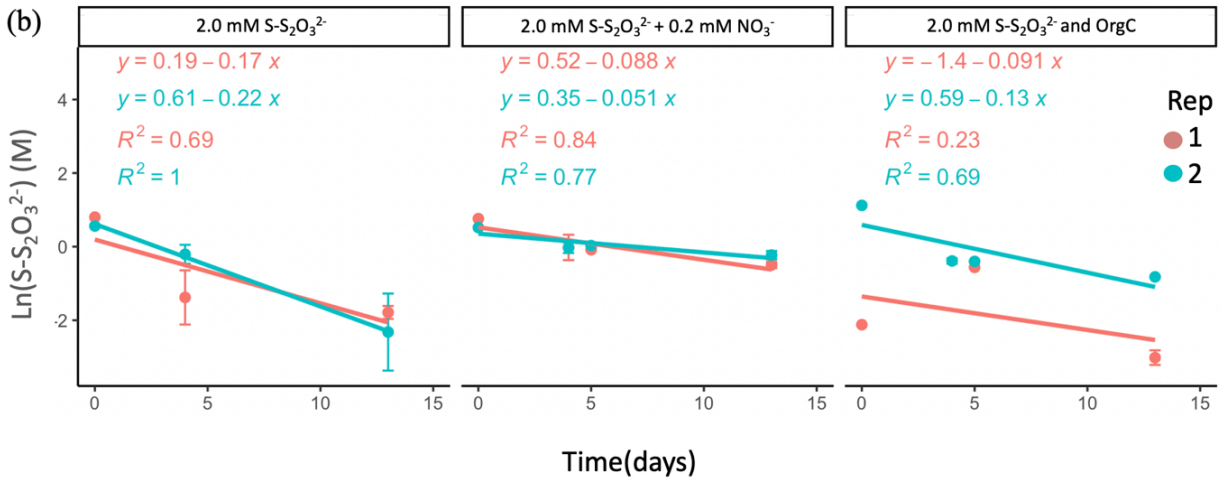


| Amendment | Mean thiosulfate loss rate, k ($days^{-1}$) | Half life (days) |
|---|---|---|
| 2.0 mM $S\text{-}S_2O_3^{2-}$ | 0.20 +/- 0.03 | 3.47 |
| 2.0 mM $S\text{-}S_2O_3^{2-}$ + 0.2 mM $NO_3^-$ | 0.07 +/- 0.02 | 9.90 |
| 2.0 mM $S\text{-}S_2O_3^{2-}$ + OrgC | 0.11 +/- 0.02 | 6.30 |

**Fig 3.4** Chemical concentration profiles and thiosulfate loss rates over 22 days in Experiment b. (a) The $[H^+]$ (turquoise, two replicates), [DO] (purple, two replicates) and $[S\text{-}S_2O_3^{2-}]$ (gold, two replicates) are displayed for replicates 1 (circles) and 2 (triangles) of the four treatments with variations in thiosulfate, nitrate, and OrgC. (b) Assuming a pseudo-first order reaction, the thiosulfate loss rates observed in Experiment b demonstrate that the half-life of thiosulfate was longer (9.9 d) in the mesocosms with nitrate amendments than without (3.9 d), or when OrgC was also available (6.3 d). However, an ANCOVA model indicated that with the small dataset, these differences in rate are not statically significant (p-value = 0.72).

## Bacteria: Sulfur Metabolizing Community Trends (16S rRNA)

The 16S rRNA gene sequences obtained in Experiment b identified five of the same six SOB genera that were present in Experiment a. The relative abundances of these genera in water used to fill the mesocosms (six days prior to the initiation of the experiment, i.e., $day_{-6}$) were as follows: *Halothiobacillus* (44.3), *Thiomonas* (10.0%), *Acidovorax* (8.0%), *Brevundimonas* (0.0%), and *Thiobacillus* (0.0%, note: standard deviation for these relative abundance was not available as a single sample was collected at $day_{-6}$). However, the genera *Sediminibacterium*, highly abundant in Experiment a, was not found to be present during Experiment b (Fig 3.5a). Similar trends were

observed in both replicates of each abiotic treatment, although variability in the relative abundance of all genera occurred, particularly for *Brevundimonas*.

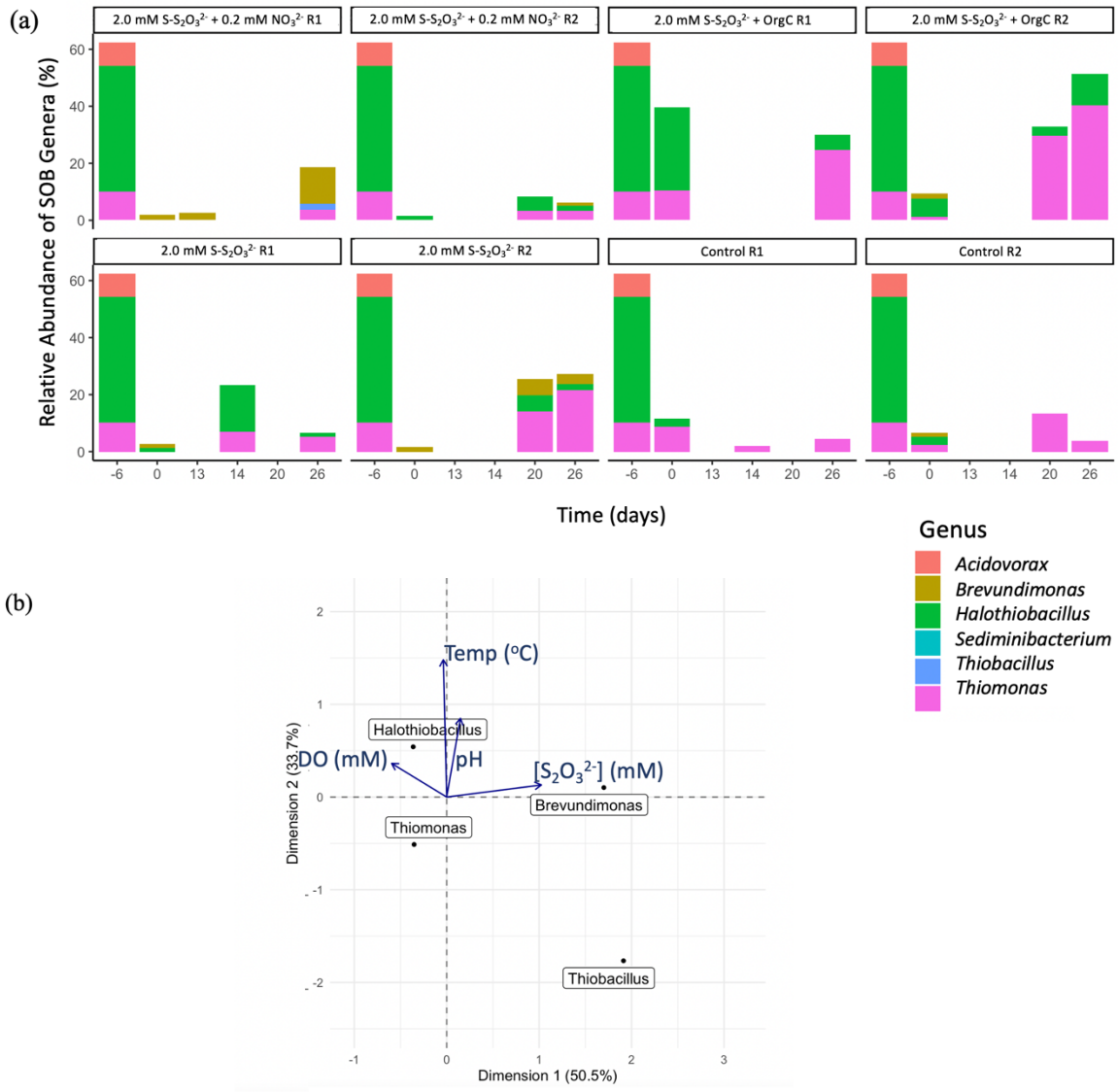


**Fig 3.5** SOB and their response to environmental variables in Experiment b. (a) The relative abundances of sulfur-oxidizing bacteria (SOB), as a fraction of the overall bacteria community, in Experiment b are displayed from samples collected at several timepoints ($day_{-6}$, $day_0$, $day_{13/14}$, $day_{20}$ and $day_{26}$) in each of the two replicates across the four treatments of light and oxygen levels. Similar changes in relative abundance of SOB genera are observed in both replicates. (b) A canonical analysis of the relative abundance of SOB genera, with an a posteriori projection of abiotic conditions (DO, pH, temp, and thiosulfate concentration) was used to explore potential relationships between environmental variables and the dominance of different genera during Experiment b.

In Experiment b, *Halothiobacillus* and *Thiomonas* were present in much higher initial abundances than in Experiment a; however, both genera decreased in abundance throughout the experiments. The largest relative abundance of these two genera persisted in mesocosms with thiosulfate amendments in the presence of oxygen, both without OrgC ($day_{26}$ mean concentrations of 1.8 ± 0.6% and 13.4 ± 11.5% respectively) — and in particular, with OrgC ($day_{26}$ mean concentrations of 8.2 ± 4.0% and 32.4 ± 11.0% respectively, Fig 3.5). It is worth noting that following a return to circumneutral conditions post thiosulfate amendments (Fig 3.4), the highest $[H^+]$ occurred in the 2.0 mM S-$S_2O_3^{2-}$ and OrgC- amended mesocosms. In these mesocosms, *Halothiobacillus* and *Thiomonas* were most abundant. The second highest $[H^+]$ occurred in the thiosulfate-amended mesocosms where *Halothiobacillus* and *Thiomonas* were also present. The change in $[H^+]$ was < $10^{-3}$ mM in the thiosulfate- and nitrate-amended mesocosms. In these experiments, the relative abundances of *Thiobacillus* and *Brevundimonas sp.* exhibited opposite trends to *Halothiobacillus* and *Thiomonas*; both increased from below detection limit to their highest concentrations in the first replicate of mesocosms amended with thiosulfate and nitrate ($day_{26}$ concentrations of 2.0 % and 12.9 %), and *Brevundimonas sp.* also increase in concentration in the second replicate with thiosulfate and nitrate (to $day_{26}$ concentrations of 1.0 %), although *Thiobacillus* was not detected in this replicate.

Limited statistical associations could be discerned from the SOB community responses to geochemical drivers. A multilevel pattern analysis, run using IndicSpecies package for Experiment b, revealed a moderately strong statistically significant relationship between the relative abundance of *Thiomonas* and 2.0 mM S-$S_2O_3^{2-}$, 2.0 mM S-$S_2O_3^{2-}$+ OrgC, and the Control treatments (stat = 0.66, p = 0.038, $\alpha = 0.05$). A canonical analysis with an a posteriori projection of the environmental variables pH, DO (mM), temperature (°C), and [S-$S_2O_3^{2-}$] (mM) also shows no clear dominance of any of these environmental factors when explaining variation in the relative abundance of the SOB genera, although the relative abundance of *Thiobacillus* appears to be counter-correlated to dissolved oxygen concentration.

### 3.3.3 Experiment c: Thiosulfate, Tetrathionate, and SOB Amendments

Experiment c, which occurred over 20 days in late September to early October 2019, explored the impacts of thiosulfate, tetrathionate, and amendments of *Halothiobacillus*-dominated SOB inocula on thiosulfate loss and subsequent acidity generation. The experiment was performed using tailings impoundment wastewater amended with 2.0 mM S-$S_2O_3^{2-}$ or S-$S_4O_6^{2-}$ and with four levels of *Halothiobacillus* enrichments (fraction in mesocosms at $day_0$: Community 1 = 22%, Community 2 = 19%, Community 3 = 11%, Control = 5%). Each combination of treatments was run as a single replicate, and samples were collected from $day_0$ and $day_{end}$. A summary of the geochemical data is provided in Table 3.5; for complete geochemistry and SOB community data, see Table B1 and B2.

#### 3.3.3.1 Geochemistry: Thiosulfate Loss and Acidity Trends

Irrespective of the initial concentration of *Halothiobacillus*, very little acidity (<0.1 mM $H^+$) was generated in the mesocosms amended with 2.0 mM S-$S_2O_3^{2-}$ over the 20-day experiment (Fig 3.6). In contrast, over the same period, mesocosms amended with *Halothiobacillus* enrichments (11%, 19%, or 22% initial populations) and 2.0 mM S-$S_4O_6^{2-}$ generated relatively high net acidity (0.48–0.93 mM $H^+$, Fig 3.6). However, there was no correlation between the proportion of *Halothiobacillus* in the enrichment inoculum and the concentration of $H^+$ generated. During the course of the Experiment c, sulfate concentrations in the thiosulfate-amended mesocosms remained stable (8.8 ± 0.0 mM at $day_0$ and 8.8 ± 0.5 mM at $day_{20}$), and the tetrathionate-amended mesocosms experienced a slight decrease (9.2 ± 0.4 mM at $day_0$ and 8.8 ± 0.3 mM at $day_{20}$, Table 3.5). This suggests that the acidity generated by *Halothiobacillus* was linked to the oxidation of tetrathionate, but not directly to the oxidation of thiosulfate, and that the end product(s) were sulfur species other than sulfate.

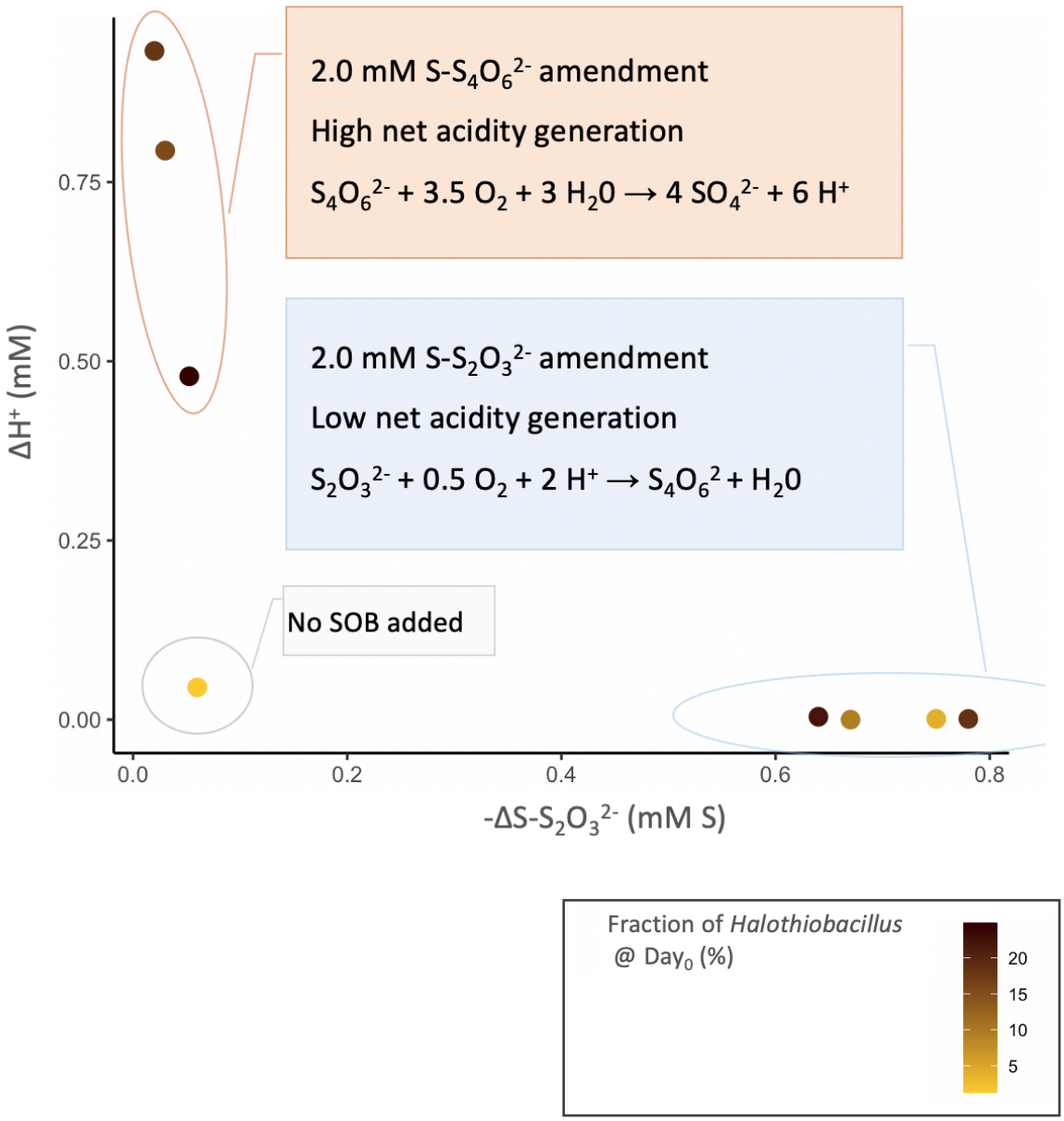


**Fig 3.6** A comparison of proton yield to thiosulfate loss in Experiment c**.** High acid generation linked to low thiosulfate loss from the mesocosm amended with *Halothiobacillus*. In contrast, large negative changes in thiosulfate did not correspond with acid generation over 20 days in Experiment c.

**Table 3.4** Summary of Geochemical Data from Experiment c Mesocosms

| Exp | Treatment | Mesocosm | Day | pH (Bottom) | S-$S_2O_3^{2-}$ (mM) | St Dev S-$S_2O_3^{2-}$ (mM) | $SO_4^{2-}$ (mM) | St Dev $SO_4^{2-}$ (mM) |
|---|---|---|---|---|---|---|---|---|
| (c) | SOB Community 1 + 2.0 mM S-$S_4O_6^{2-}$ | M17 | 0 | 7.2 | 0.05 | 0.00 | 9.0 | 0.7 |
| (c) | SOB Community 1 + 2.0 mM S-$S_4O_6^{2-}$ | M17 | 20 | 3.3 | nd | nd | 9.2 | 0.4 |
| (c) | Control: 2.0 mM S-$S_4O_6^{2-}$+ No SOB | M18 | 0 | 7.2 | 0.06 | 0.01 | 9.5 | 1.0 |
| (c) | Control: 2.0 mM S-$S_4O_6^{2-}$+ No SOB | M18 | 20 | 4.4 | nd | nd | 8.7 | 1.0 |
| (c) | SOB Community 1 + S-$S_2O_3^{2-}$ | M19 | 0 | 7.2 | 1.76 | 0.03 | 8.5 | 0.3 |
| (c) | SOB Community 1 + S-$S_2O_3^{2-}$ | M19 | 20 | 6.1 | 0.98 | 0.01 | 8.7 | 1.0 |
| (c) | Control: 2.0 mM S-S2O32- + No SOB | M20 | 0 | 7.2 | 1.74 | 0.12 | 9.0 | 0.4 |
| (c) | Control: 2.0 mM S-S2O32- + No SOB | M20 | 20 | 7.3 | 1.07 | 0.02 | 8.7 | 1.0 |
| (c) | SOB Community 2 + 2.0 mM S-$S_4O_6^{2-}$ | M21 | 0 | 7.2 | 0.03 | 0.00 | 9.6 | 1.0 |
| (c) | SOB Community 2 + 2.0 mM S-$S_4O_6^{2-}$ | M21 | 20 | 3.1 | nd | nd | 9.0 | 1.0 |
| (c) | SOB Community 3 + 2.0 mM S-$S_4O_6^{2-}$ | M22 | 0 | 7.2 | 0.02 | 0.00 | 8.9 | 0.3 |
| (c) | SOB Community 3 + 2.0 mM S-$S_4O_6^{2-}$ | M22 | 20 | 3.0 | nd | nd | 8.4 | 1.0 |
| (c) | SOB Community 2 + 2.0 mM S-$S_2O_3^{2-}$ | M23 | 20 | 5.4 | 1.03 | 0.01 | 8.3 | 0.3 |
| (c) | SOB Community 2 + 2.0 mM S-$S_2O_3^{2-}$ | M23* | 0 | 7.2 | 1.67 | 0.25 | 8.3 | 0.3 |
| (c) | SOB Community 3 + 2.0 mM S-$S_2O_3^{2-}$ | M23 | 20 | 5.4 | 1.03 | 0.01 | 8.1 | 0.2 |
| (c) | SOB Community 3 + 2.0 mM S-$S_2O_3^{2-}$ | M24 | 0 | 7.2 | 1.87 | 0.22 | 9.7 | 0.2 |
| (c) | SOB Community 2 + 2.0 mM S-$S_2O_3^{2-}$ | M24 | 20 | 6.2 | 1.12 | 0.01 | 9.5 | 0.3 |

*Thiosulfate concentration from 10 cm depth used to substituted for missing data at $day_0$; all other samples were collected from 90 cm depth.

Sulfate concentration error at $day_{end}$ was estimated for Experiment c samples where none was recorded.
Note: Sulfite ($SO_3^{2-}$) was not detected throughout all experiments and timepoints
(-) indicates no value available; gap in data
nd = non-detectable, below limit of detection; a conservative LOD for analysis were as follows: 0.04 mM S for thiosulfate, 0.013 mM S for sulfate. All sulfate values were calculated using a 10× dilution technique.

## Bacteria: Sulfur Metabolizing Community Trends (16S rRNA)

Although *Thiomonas* was not present in Experiment c, the other five SOB genera from Experiments a and b were detected, with mean initial relative abundances of: *Halothiobacillus* (14.2 ± 8.5%), *Acidovorax* (8.9 ± 4.7%), *Thiobacillus* (5.6 ± 3.1%), *Sediminibacterium* (2.7 ± 2.0%), and *Brevundimonas* (0.0 ± 0.0%). By $day_{end}$, *Halothiobacillus* persisted in all mesocosms, although its relative abundance had decreased to 5.0 ± 3.9%, while the acidophile *Acidovorax* increased in relative abundance to 11.8 ± 11.1%, with no discernable pattern between treatments.

*Thiobacillus* also persisted in several mesocosms at lower relative abundances (mean 0.9 ± 0.8%), while *Sediminibacterium* fell below the reporting threshold (>1% relative abundance) in all microcosms except for the thiosulfate-amended control (3.9%; Fig 7).

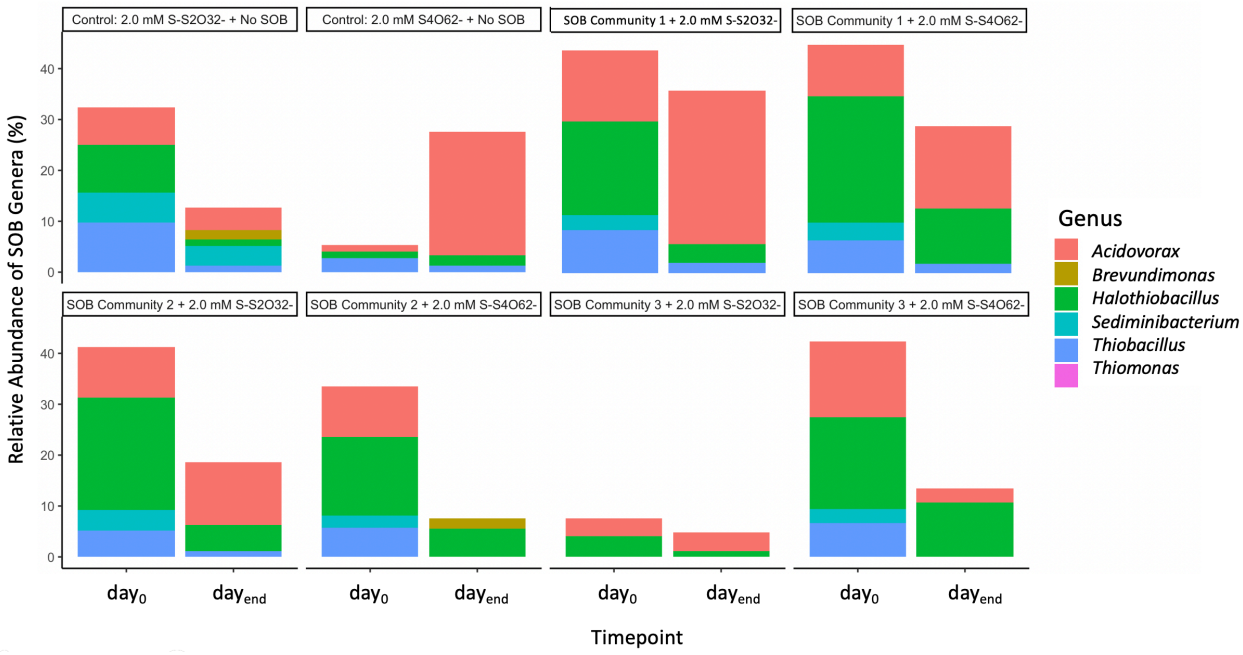


**Fig 3.7** Relative abundance SOB communities in Exp c. The samples were collected at $day_0$ and $day_{end}$ in for each treatment combination of 2.0 mM S-$S_4O_6^{2-}$, or S-$S_2O_3^{2-}$, and SOB Community 1, 2, or 3. Treatments combinations in Experiment c were run without replicates. (Note: $day_{end}$ = $day_{21}$ for all mesocosms except SOB Community 3 + 2.0 mM S-$S_4O_6^{2-}$ and SOB Community 2 + 2.0 mM S-$S_2O_3^{2-}$, which were collected on $day_{20}$, and SOB Community 2 + 2.0 mM S-$S_4O_6^{2-}$, which was collected on $day_{22}$.)

### 3.3.4 Metagenomic Inference: Sulfur Metabolizing Pathways

The genera present in the oxidation reservoir appear to fall into two distinct guilds. Guild A, containing *Halothiobacillus*, *Thiomonas*, and possibly *Acidovorax*, processes thiosulfate while generating acidity. However, there appears to be an intermediate step where thiosulfate loss is not accompanied by acidity generation (perhaps because of the formation of tetrathionate); members Guild A also are able to process tetrathionate. Within Guild A, *Halothiobacillus* spp. are most abundant in circumneutral conditions, while *Thiomonas* spp. appears as the pH decreases (such as the end of Experiment B). Guild B, containing *Thiobacillus,* appears to be inversely correlated

with DO availability and is most prevalent when nitrate is available. These changes highlight the interactive importance of aqueous chemistry and the microbial community in determining sulfur cycling and acidity generation in mining wastewater contexts.

Intriguingly, these two guilds can be distinguished not only by behaviour and growth conditions, but also by the distinct sulfur pathways present within their genomes for the cycling of sulfur (Fig 3.8). The frequency of sulfur-oxidizing genes in each microbial genus can be identified by referencing a metagenomic analysis performed on the bacteria within the tailings impoundment water used to fill the mesocosms for this study (see section 2.8 and Appendix A).

Microbes belonging to Guild A (*Halothiobacillus* and *Thiomonas)* contain genes that, when expressed, form the complete sulfur oxidation enzymatic pathway (cSOx, *soxXYZABCD*) and the first stage of the $S_4I$ pathway (*tsdA*); however, these microbes lack the genes required for the reverse dissimilatory sulfur reduction pathway (rDSR, *dsrABCEFHMKJOP*, *sat*, *aprAB*, and *qmoABC*). In contrast, members of Guild B contain all the genes for the incomplete sulfur oxidation pathway (iSOx, *soxXYZAB*), the first stage of the $S_4I$ pathway (*tsdA*), and the genes required to oxidize thiosulfate to sulfate through the rDSR pathway. *Acidovorax*, *Brevundimonas,* and *Sediminibacterium* appear to have a more limited sulfur oxidation capacity, including the oxidation of zero-valent sulfur (ZVS) to sulfite (*sdo*). *Sediminibacterium* also contains genes for converting thiosulfate to tetrathionate via the first stage of the $S_4I$ pathway (*tsdA*). These important distinctions indicate which stages of thiosulfate oxidation are likely to occur depending on what microbes are present: the cSOx pathway directly oxidizes thiosulfate to sulfate, the iSOx pathway hydrolyses thiosulfate to sulfate and ZVS, and the first stage of the $S_4I$ pathway converts thiosulfate to tetrathionate (a higher order SOI).

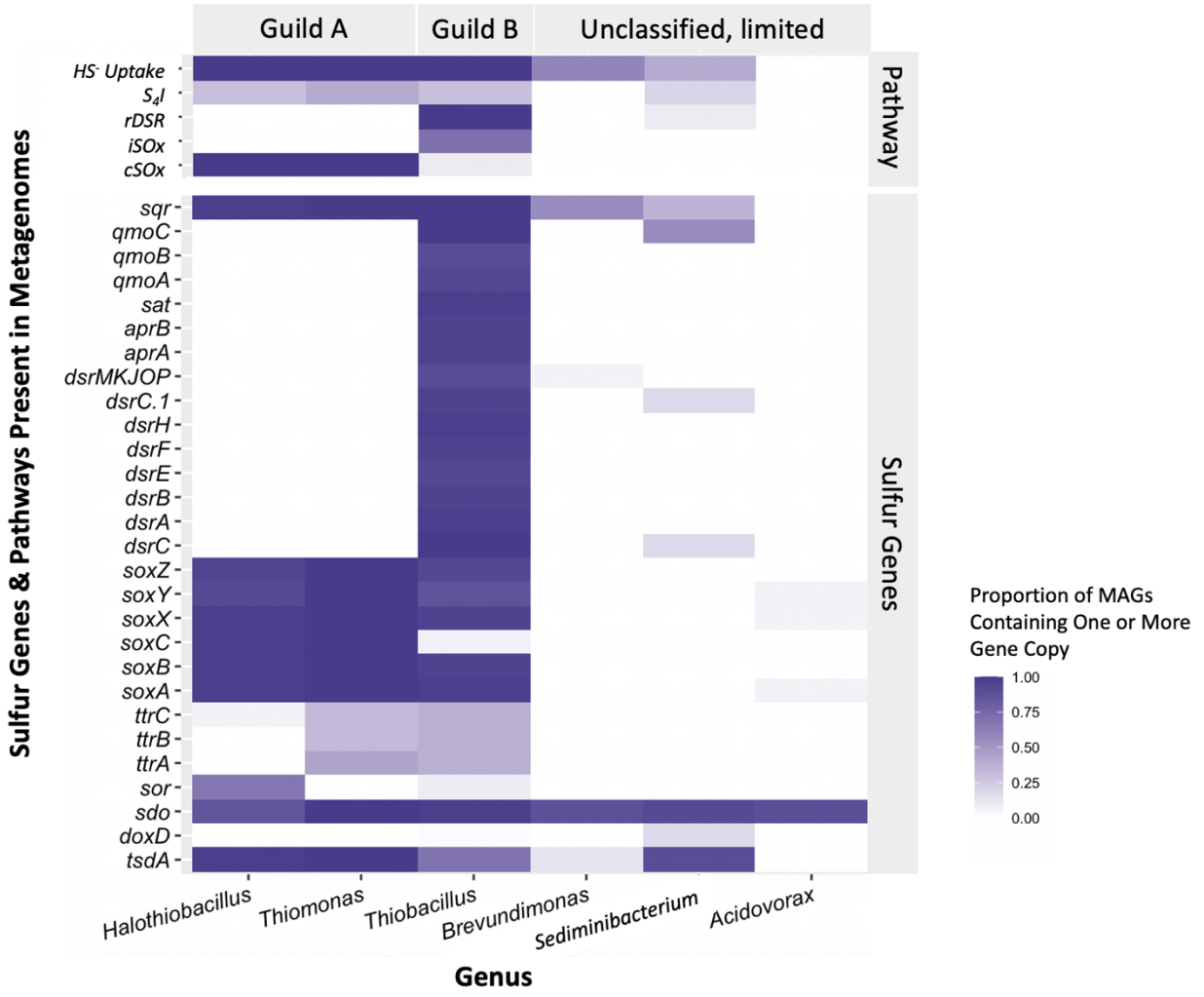


**Fig 3.8** Metagenomic inference of key sulfur pathways from sulfur-oxidizing bacteria (SOB). The metagenomic capacity of six sulfur-oxidizing bacteria identified in the mine wastewater communities of the mine tailings impoundment, can be divided into guilds using genes inferred from metagenome assembled genomes sequenced by the Banfield Lab, Berkeley, for a previous study (K. Whaley-Martin et al. 2023). The gene frequency is calculated as the number of sequenced MAGs containing one or more copy of each sulfur oxidation gene (see methods section 2.8). The five lines at the top of the figure summarize gene presence in the rows below into sulfide uptake ($HS^- \rightarrow S^0$) and three thiosulfate oxidation ($S_4I$, iSOx + rDSR, cSOx) pathways.

## 3.4 Discussion

### 3.4.1 Thiosulfate as a Preferred SOI Substrate and Delayed Acidity

All three experiments demonstrated that acid generation did not coincide with thiosulfate processing by SOB. In Experiments a and b, onset of acid generation was observed only after thiosulfate decreased to < 1/20$^{th}$ of original concentrations under oxic conditions. Acid generation was also observed when SOB from Guild A were provided tetrathionate (Experiment c), or when they entered suboxic conditions (Experiment a). Taken together, this suggests that the dominant sulfur metabolism in these systems may be a two-stage thiosulfate oxidation to sulfate processes, according to the $S_4I$ pathway:

$$\text{TsdA: } 2\ S_2O_3^{2-} + 2\ H^+ + ½\ O_2 \rightarrow S_4O_6^{2-} + H_2O \qquad \Delta H^+/\Delta S = -0.5 \quad (1)$$

$$\text{enzymes unidentified: } S_4O_6^{2-} + 3.5\ O_2 + 3\ H_2O \rightarrow 4\ SO_4^{2-} + 6\ H^+ \qquad \Delta H^+/\ \Delta S = 1.5 \quad (2)$$

In this oxidation process, which contains at least two stages (the intermediate between tetrathionate and sulfate being unknown), the first phase consumes protons before the second phase generates them. (Note: $\Delta H^+$ were calculated from pH values using $[H^+] = 10^{-pH}$ , assuming that the ion activity coefficient is 1. Ion activity coefficients were found to vary from 0.8-1 based on experimental data, see methods section 2.6. Therefore, assuming an ion activity coefficient of 1 produces a slight underestimation of $\Delta H^+$ concentrations). If thiosulfate is the preferred sulfur substrate, there will be a delay in the onset of acidity generation by several days. However, no changes in sulfate concentration were detected in mesocosms amended with tetrathionate in Experiment c, suggesting that this second stage may be more complicated than direct tetrathionate oxidation to sulfate.

These findings contrast with Whaley-Martin et al. (2023), which identified the cSOx pathway as the primary pathway for sulfur oxidation under oxic conditions in the epilimnion and metalimnion. Metagenomic analysis of *Halothiobacillus* across various mine waters (including the active tailings impoundment waters investigated in Whaley-Martin et al., 2019, 2023) confirmed the consistent presence of cSOx genes in all *Halothiobacillus* studies and an absence of nitrate reductase genes; however, the role and reactions of the $S_4I$ pathway need to be further

explored. The metagenomes sequenced from the tailings impoundment in this study suggest that *Acidovorax* [typically classified as a nitrate-dependant sulfur oxidizer, (Pantke et al. 2012)], *Brevundimonas* (capable of carbon or thiosulfate oxidation (Smirnov, Kiprianova, and Babich 2001)), and *Sediminibacterium* (heterotrophic strict or facultative anaerobes (Song et al. 2017)) may contribute to this tetrathionate oxidation via unestablished mechanisms or play secondary roles in sulfur oxidation, as their few sulfur-metabolizing genes did not fall into either or the assigned guilds.

### 3.4.2 Environmental Niche Space as a Driver of SOB Community

These three sets of experiments reveal that thiosulfate loss occurred in all systems, and the rate of thiosulfate loss may vary due to presence of different abiotic niche space drivers (i.e., slower rates with nitrate amendments, but were not statistically significant as indicated in Fig 3.4; no effect was observed with changes in light availability, see section 3.3.1). Although not statistically significant, this possible variance with TEA corresponded with changes in the proportion of bacteria from a dominance of Guild A (cSOx and $S_4I$, found in *Halothiobacillus* or *Thiomonas*) under oxic conditions to prevalence of Guild B (iSOx and rDSR, found in *Thiobacillus*, see 3.8, Fig 3.3, and Fig 3.5) when nitrate amendments were available. Likewise, in Experiment b, *Thiomonas* was identified as a statistically significant indicator of thiosulfate treatments without nitrate, while *Thiobacillus* appeared to differentiate from *Halothiobacillus* or *Thiomonas* depending on oxygen availability, and was more abundant under lower oxygen conditions (Fig 3.5). These findings align with previous SOB studies in this active tailings impoundment where the genus *Halothiobacillus* grew to dominated communities enriched with thiosulfate under oxic conditions and reduce the pH from circumneutral to ~4 (K. Whaley-Martin et al. 2019). This separation of guilds also aligns with a study of the stratified layers of the oxidation reservoir (during 2016 and 2017), in which *Halothiobacillus* appeared to be correlated with the onset of acidity generation, while mRNA profiles demonstrated that rDSR and nitrate reduction genes were only expressed in the suboxic hypolimnion (K. Whaley-Martin et al. 2023).

The lack of acid production observed in the thiosulfate- and nitrate- amended mesocosms aligns with the use of nitrate as a terminal electron acceptor (TEA), often observed in connection with

the iSOx + rDSR pathway in *Thiobacillus* in both mine wastewater (K. J. Whaley-Martin et al. 2023) and extremophile (Harrold et al. 2016) studies:

$$S_2O_3^{2-} + 2\ H_2O + NO_3^- \rightarrow 2\ SO_4^{2-} + NH_4^+ \qquad \Delta H^+/\ \Delta S = 0 \quad (3)$$

In the deep subsurface, rDSR/nitrate coupling was also found in *Rhodocyclaceae* (Harrold et al. 2016). Use of energetically limiting nitrate as an alternate TEA also highlights a competitive advantage of the iSOx + rDSR pathway: ATP formation is twice as efficient (ε = 22% vs. 10%) than when cSOx is employed (Klatt and Polerecky 2015). Here, I propose that pathway activation is controlled by a trade-off between the efficiency of energy capture ($\varepsilon_{rDSR} = 2\ x\ \varepsilon_{SOx}$) and the energetic cost to activate it (the cSOx pathway only requires the assembly of four enzymes, while the iSOx + rDSR pathway requires more than nine). As well, under low TEA:S conditions, the iSOx + rDSR pathway may provide SOB with a competitive advantage for two reasons: (i) sulfur storage, and (ii) uneven electron distribution. Since no statically significant change in sulfate was detected in these systems, nitrate pairing appears to have been paired with a more complex sulfur oxidation process than direct sulfate formation, such as the storage of ZVS.

Beyond sulfur substrate and electron acceptor availability, only OrgC was found to possibly influence acidity generation, although the impact was not statistically significant (Fig 3.4). The increase in $[H^+]$ with OrgC amendment is aligned with previous studies showing that amendments of acetate, glucose, or ethanol increase rates of $S^0$ generation from $HS^-$ removal (Gao et al. 2022), and also increase rates of sulfate reduction (Anantharaman et al. 2018b). However, further investigation is required to determine if the impact of OrgC is significant in this system. The lack of response to light availability (Fig 3.2) suggests that photolithotrophic purple and green sulfur bacteria, such as *Allochromatium vinosum*, are not active in the tailings impoundment (Frigaard and Dahl 2008); photolithotrophic sulfur metabolizing bacteria genera were not found through DNA sequencing (Fig 3.8).

Given the response of SOB communities to sulfur substrate and terminal electron acceptor, a framework to predict the timing (as a result of sulfur substrate conversions) and magnitude (due to concentrations of sulfur substrate and TEA) of acid generation can be built from an understanding of SOB fitness under each condition. The predictive capacity of the ecological

niche space observed here is slightly surprising since several stochastic processes (i.e., replication, death, immigration and emigration, spatiotemporal variation, order of colonization) should also produce more random shifts in the microbial populations (Balci et al. 2012). However, the deterministic pattern of pathway responses to ecological niche space (as defined by sulfur substrate and TEA) appears here to be an effective simplification, perhaps because the critical nature of energy metabolisms decreases the relative effect of these stochastic processes.

## 3.5 Conclusion

In these experiments on oxic metal mine wastewater, acidity generation signatures suggest that thiosulfate is oxidized through a process of at least two steps. The initial low rates of acid formation, followed by higher rates once thiosulfate is consumed (suggesting a $S_2O_3^{2-}$: $S_4O_6^{2-}$ < 1:10), is aligned with a two-stage $S_4I$ pathway mechanism. However, sulfate concentrations did not increase in alignment with the conversion of tetrathionate to sulfate, indicating that other steps must be present in this process. In addition, nitrate amendments were found to possibly slow the rate at which acid generation occurred from thiosulfate oxidation (after the initial lag period).

This oxidation of thiosulfate and tetrathionate requires the presence of sulfur-metabolising enzymes hosted in the SOB communities. There appears to be a distinction between the success of SOB in Guild A (cSOx and $S_4I$, found in *Halothiobacillus* or *Thiomonas*) and Guild B (iSOx + rDSR, found in *Thiobacillus*) that corresponds to the availability of the electron acceptors oxygen and nitrate. When Guild A was dominant in circumneutral wastewater, direct thiosulfate oxidation through the cSOx pathway appeared to play a smaller role than the $S_4I$ pathway. Although thiosulfate concentrations were depleted when either guild was present, the function of iSOx + rDSR genes (Guild B) resulted in considerably less net acidity production over 22 days in nitrate-treated systems. The key ecological niche space parameters identified here (thiosulfate, tetrathionate, oxygen, nitrate), and guild differentiation (cSOx + $S_4I$ vs. iSOx + rDSR) provide guidance for framing the research directions presented in Chapters 4 and 5.

# 4

# Microbial Sulfur Pathways and Outcomes in Tailings Impoundments: A Mesocosm Study

*"What we observe is not nature itself, but nature exposed to our method of questioning."*
*~ Werner Heisenberg*

## Abstract

In mine wastewaters, three microbial sulfur oxidation pathways have the potential to cause different water quality outcomes. These outcomes can differ from abiotic models of sulfate and acidity predictions currently used to monitor potential sulfur risks. However, studies integrating microbiology and geochemistry in active mine tailings impoundments are very limited. Here, we developed a novel diagnostic approach to detect microbially driven sulfur pathways. Within this 28-day study, eight on-site, 500 L mesocosms were filled with water extracted directly from the water cap of an active Ni/Cu mine tailings impoundment. Diverse combinations of tailings, sulfur compounds, and nitrate amendments were added to the mesocosms simulating common operational variations experienced by active tailings impoundments. Mesocosm results linked complete SOx, $S_4I$, and incomplete SOx + rDSR pathway occurrence (metagenomes, inferred from the identity, i.e. 16S rRNA) and activity (mRNA) to physiochemistry and sulfur geochemistry. By integrating the three lines of evidence, the diagnostic approach was able to identify which sulfur pathways were active under varying physiochemical conditions and how geochemical outcomes were affected. A relationship emerged between acid generation and *soxCD* expression (*soxCD* expression indicates the complete SOx pathway activity). However, observed proton yields and sulfate concentrations were less than those predicted by complete SOx pathway activity alone. This indicates other sulfur pathways, e.g. the partial $S_4I$ pathway (within *Thiomonas* and *Halothiobacillus*), and/or activity of the incomplete SOx pathway (within

*Thiobacillus* and *Desulfurivibrio*) when either not coupled to rDSR, or paired with use of nitrate, influenced overall sulfur outcomes along with the complete SOx pathway.

## 4.1 Introduction

Wastewaters associated with base metal mining commonly contain higher concentrations of reduced sulfide ($HS^-$), sulfur oxidation intermediate compounds (SOI, e.g. thiosulfate [$S_2O_3^{2-}$], tetrathionate [$S_4O_6^{2-}$], zero valent sulfur [ZVS; $S^0$]), and metals than most freshwater and marine systems and consistently contain moderate levels of nitrate (Miettinen et al. 2021; Skousen et al. 2017; Whaley-Martin et al. 2019, 2020). These high sulfur concentrations result from storage of tailings in wastewater impoundments that are managed on site. Wastewater systems are maintained at circumneutral pH values, unlike systems where acid rock drainage (ARD) conditions exist and iron-metabolizing genera such as *Ferrovum* and *Acidithiobacillus* link sulfur metabolism with iron oxidation that keep the pH low (Grettenberger et al. 2020; Wang et al. 2019). The oxidation of sulfur compounds by sulfur-oxidizing bacteria (SOB), such as *Halothiobacillus*, *Thiomonas*, *Thiobacillus*, and *Thiovirga*, in circumneutral wastewater can lead to water quality concerns, including surface water acidification approaching ARD conditions, oxygen consumption, and metal mobilization (Camacho et al. 2020; Miettinen et al. 2021; Nancucheo et al. 2017; Skousen et al. 2017; Verburg et al. 2009). Across all studied contexts, SOB communities demonstrate the ability to catalyze sulfur oxidation through three known biochemical pathways: (1) complete sulfur oxidation (cSOx), (2) tetrathionate intermediate ($S_4I$), and (3) incomplete sulfur oxidation (iSOx, lacking the sulfur cycling enzyme SoxCD) coupled with reverse dissimilatory sulfate reduction [rDSR, see Table 1.3 and Table B1, (Dahl 2005; Watanabe et al. 2019; Wasmund, Mußmann, and Loy 2017)]. Although the gene expression profiles of sulfur pathways are extensively studied in the deep terrestrial subsurface and deep sea hydrothermal vents, little is known about how geochemical conditions affect the occurrence or activity of sulfur-oxidizing pathways in mining contexts (Bell et al. 2020; Cron et al. 2020).

If driven to completion, these three sulfur pathways produce equivalent net proton yields, dependent on the terminal electron acceptor (TEA): $\Delta H^+/\Delta S\text{-}S_2O_3^{2-} = 1$ with $O_2$ as a TEA and $\Delta H^+/\Delta S\text{-}S_2O_3^{2-} = 0$ with $NO_3^-$ as a TEA (Table 1.3 and Table C1). However, the inclusion of sub-steps in each pathway introduces complexity to the proton balance. Specifically, the cSOx

pathway catalyzes the direct oxidation of $S_2O_3^{2-}$ to $SO_4^{2-}$, generating acidity (Friedrich et al. 2005):

$$S_2O_3^{2-} + H_2O + 2\ O_2 \rightarrow 2\ SO_4^{2-} + 2\ H^+ \quad (1)$$

In contrast, the S4I pathway begins with oxidative condensation of thiosulfate to tetrathionate ($S_4O_6^{2-}$) via the enzyme TsdA, or infrequently via DoxDA, resulting in a net decrease in acidity (Rameez et al. 2020; J. Zhang et al. 2020; Beard et al. 2011):

$$2\ S_2O_3^{2-} + 2\ H^+ + \tfrac{1}{2}\ O_2 \rightarrow S_4O_6^{2-} + H_2O \quad (2)$$

The subsequent processing of tetrathionate is highly debated, indicating a knowledge gap, and this processing does not necessarily occur immediately following its production (Dam et al. 2007; Kappler et al. 2001; Rameez et al. 2020; Wei et al. 2023). Some studies suggest that the second stage of the S4I pathway (catalyzed by TetH or other enzymes) results in intracellular ZVS storage (Kanao et al. 2007; Meulenberg et al. 1992), which delays the release of additional protons yielded by its oxidation (for the potential role of other S4I pathway enzymes, see Table 1.4 and Table 1.5). Finally, the iSOx + rDSR pathway oxidizes $S_2O_3^{2-}$ to $SO_4^{2-}$ via several reaction steps. This begins with pH-neutral $S_2O_3^{2-}$ hydrolysis and intracellular storage of ZVS via the iSOx pathway:

$$S_2O_3^{2-} + \tfrac{1}{2}\ O_2 \rightarrow SO_4^{2-} + S^0 \text{ (attached to SoxYZ)} \quad (3)$$

This ZVS is thought to represent a dynamic sulfur sink, and is oxidized only when other aqueous sulfur substrates are scarce (Hensen et al. 2006), suggesting that the acidity produced by the subsequent rDSR pathway could also be delayed (Table 1.3 and Table C1). ZVS and other SOI compounds may also be processed through metabolic pathways that have yet to be identified.

In summary, proton yield can be affected by the reactions involved in sulfur oxidation through each of the three sulfur pathways presented here, and also by pairing with TEAs such as oxygen or nitrate residues originating from mine blasting. Whaley-Martin et al. (2023) recently identified differential sulfur oxidation pathway expression based on $O_2$ and $NO_3^-$ concentrations. In that study, cSOx pathway abundance and activity were linked to oxygen availability (*Halothiobacillus*

and *Thiomonas*), while the iSOx + rDSR pathway (*Thiobacillus*) dominated under anoxic conditions in the summer-stratified water column of a tailings impoundment. Under low pH conditions, these systems move into a state where iron becomes an important $e^-$ donor or acceptor, but iron does not play a major role at circumneutral pH when nitrate is available (Grettenberger et al. 2019; Jin and Kirk 2018; Warren et al. 2008).

The objective of this study was to explore how the occurrence and activity of cSOx, $S_4I$, and iSOx + rDSR pathways varied in response to available TEAs ($O_2$, and $NO_3^-$), sulfur substrates ($S_2O_3^{2-}$ and $S_4O_6^{2-}$), and tailings additions under the ambient environmental conditions experienced by an active tailings impoundment. Field-based mesocosm experiments offered the opportunity to mimic the water cap of a tailings impoundment system under site conditions and at a greater scale than laboratory mesocosms, using wastewaters drawn directly from the adjacent tailings impoundment. Geochemical and biological responses were measured after experimental amendments of tailings with thiosulfate or tetrathionate and with or without nitrate. Over the course of 28 days, these mesocosms were examined through complementary methods measuring bacterial community composition (16S rRNA gene sequences), functional repertoires (metagenomes), gene expression (mRNA), sulfur compounds ($S_2O_3^{2-}$, $S_4O_6^{2-}$, $S^0$, $SO_4^{2-}$), N species ($NO_3^-$, $NO_2^-$, $NH_4^+$), and oxygen concentrations and pH; samples for these parameters were collected at different frequencies. A new diagnostic approach was developed to combine these lines of evidence (geochemical, community composition linked to functional repertoires, and gene expression) and generate a more holistic understanding of microbial sulfur oxidation and outcomes in this mine tailings impoundment. Through this approach, parallel sulfur pathway activation and TEA switching (from oxygen to nitrate) were discernible.

## 4.2 Methods

### 4.2.1 Study Site

The mesocosm experiments in 2020 were established on the same peninsula as in 2019, with tanks which had been sterilized and stored over the winter, and then embedded into the ground at the same depth. For a detailed description of the tailings impoundment, see sections 2.1 and 3.2.1.

### 4.2.2 Experimental Design: Onsite 500 L Mesocosms

In July 2020, eight experimental mesocosms were set up using 500 L polyethylene containers (47.5″ height × 30″ diameter, or 121 cm × 76 cm; ACO Container Systems), embedded ~100 cm into the ground to minimize temperature fluctuations, and filled on July 23, 2020, to ~100 cm with tailings impoundment water collected from the epilimnetic region at a depth of ~0.5 m (Fig 4.1). The mesocosms were sterilized with bleach (rinsed twice with >1% sodium hypochlorite solution) prior to use.

During August and September 2020, the mesocosms were preconditioned ($P_x$) with treatments of either tailings and/or $S_2O_3^{2-}$ ($P_1$-$P_4$; tailings addition, $P_1$, $P_3$, $P_5$, $S_2O_3^{2-}$ addition; Fig 4.1b) which resulted in mesocosms with unique communities at the start of the experimental ($E_x$) phase in September 2020 (Table 4.1). Because these experiments were designed to explore the impact of tailings on the SOB communities, the tailings used as amendments were a combination of low-sulfur mill waste and high-sulfur pyrrhotite. On August 18, 2020, tailings treatments of either 6.8 L tailings ($P_1T_{6.8}$/$P_2T_{6.8}$) or 13.6 L tailings ($P_3T_{13.6}$/$P_4T_{13.6}$) were added to four mesocosms (Fig 4.1b), leading to a decrease in oxygen in these systems. Tailings amendments to preconditioned and experimental ($E_x$) treatment phases were composed of 50:50 (by volume) mill waste (low sulfur) tailings and pyrrhotite (high sulfur) tailings. Tailings were received in August 2020, stored in the shade on site, and allowed to settle for two weeks before being resuspended by stirring and sub-aqueously added to the mesocosms. Preconditioning treatments of 2.6 mM $S_2O_3^{2-}$ (as $Na_2S_2O_3^{2-}$) were added one week after tailings amendments to three of the mesocosms, one of each of the two tailings preconditioning treatments ($P_1T_{6.8}S_{2(2.6)}$, $P_3T_{13.6}S_{2(2.6)}$), and one that had not received a tailings amendment ($P_5S_{2(2.6)}$). Throughout this section, $day_0$ refers to the initial sampling that began on September 22, 2020, in the "E" experimental phase, after one month's exposure to tailings and/or thiosulfate preconditioning amendments (Fig 4.1b).

**Table 4.1** Experimental Treatments for 500 L Mesocosms from 2020

| Mesocosm | Tailings Amendment | Sulfur Substrate Amendment | Nitrate Amendment | Treatment Code |
|---|---|---|---|---|
| $E_1$ | 12 L | 2.0 mM S-$S_4O_6^{2-}$ | - | $T_{12}S_{4(2.0)}$ |
| $E_2$ | 12 L | 2.0 mM S-$S_4O_6^{2-}$ | 2.0 mM $NO_3^-$ | $T_{12}S_{4(2.0)}N_{2.0}$ |
| $E_3$ | 12 L | 2.0 mM S-$S_2O_3^{2-}$ | - | $T_{12}S_{2(2.0)}$ |
| $E_4$ | 12 L | 2.0 mM S-$S_2O_3^{2-}$ | 2.0 mM $NO_3^-$ | $T_{12}S_{2(2.0)}N_{2.0}$ |
| $E_5$ | - | 2.0 mM S-$S_2O_3^{2-}$ | - | $S_{2(2.0)}$ |
| $E_6$ | - | 2.0 mM S-$S_2O_3^{2-}$ | 2.0 mM $NO_3^-$ | $S_{2(2.0)}N_{2.0}$ |
| $E_7$ | 12 L | - | - | $T_{12}$ |
| $E_8$ | 12 L | - | 2.0 mM $NO_3^-$ | $T_{12}N_{2.0}$ |

(-) indicates no amendment of this type added to the mesocosm.

On September 22, 2020, the eight experimental mesocosms filled with ~470 L of tailings wastewater on July 23, 2020 were sampled at $day_0$ (mesocosms experienced varied preconditioning amendments and thus varied microbial communities associated with eight weeks of possible community succession) to characterize initial communities and geochemical conditions before additional experimental manipulation (Fig 4.1). All mesocosms were then treated with varying combinations of 12 L tailings, a mix of equal volumes of low-sulfur mill waste and high-sulfur pyrrhotite tailings ($T_{12}$), 2.0 mM S sulfur substrate ($K_2S_4O_6$: $S_{4(2.0)}$ or $Na_2S_2O_3$: $S_{2(2.0)}$), and 2.0 mM nitrate ($NaNO_3$: $N_{2.0}$) amendments, creating eight unique experimental treatments outlined in Table 4.1 and Fig 4.1b.

Mesocosms $E_1$−$E_4$, $E_7$, and $E_8$ received tailings amendments to decrease oxygen concentrations through oxidative processes to investigate possible impacts of the hypoxic-anoxic condition on SOB communities, sulfur-oxidizing pathway activity, and acidity generation. Data loggers were deployed in each mesocosm at the initiation of the experiment (at depths of 20 cm and 50 cm in each mesocosm) to monitor dissolved oxygen (DO) concentrations (HOBO® U26-001) and pH (HOBO® MX2501, accurate to ± 0.10 pH units). The loggers, initiated at $day_0$, collected data at 30 min intervals over the 28 days of the experiment.

(a)

(b)

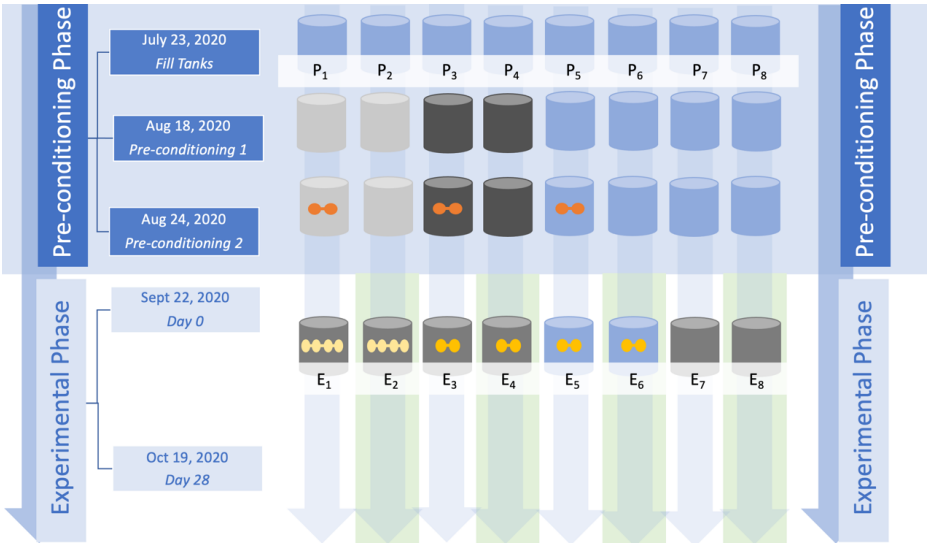


**MESOCOSM LEGEND**

$P_x$ = Pre-conditioning Phase (Mesocosm #)

*Water was initially filled to 100 cm depth. During the preconditioning phase ~136 L were removed, so that by the beginning of experimental phase the water level was at 70 cm depth, and 330 L remained.*

$E_x$ = Experimental Phase (Mesocosm #)

| Tailings Amendments | Sulfur Amendments | Nitrate Amendments |
|---|---|---|
| 6.8 L Tailings<br>13.6 L Tailings<br>12 L Tailings | 2.6 mM S-$S_2O_3^{2-}$ (as $Na_2S_2O_3$)<br>2.0 mM S-$S_2O_3^{2-}$ (as $Na_2S_2O_3$)<br>2.0 mM S-$S_4O_6^{2-}$ (as $K_2S_4O_6$) | 2.0 mM $NO_3^-$ (as $NaNO_3$) |

Sample collection timeline (right).
Sample collected from 50 cm depth.
(See Table 1 for list of treatments by mesocosm.)

| Date | Day | Geochem | DNA | RNA |
|---|---|---|---|---|
| Sept 22 | 0 | o | o | o |
| Sept 23 | 1.25 | o | | |
| Sept 24 | 2 | o | | o |
| Sept 25 | 3 | o | | o |
| Oct 7 | 16 | o | o | |
| Oct 19 | 28 | o | o | o |

**Fig 4.1** Field study design from the summer of 2020. (a) The 500 L mesocosms were embedded in the ground and filled onsite with tailings impoundment wastewater in late July 2020, and were preconditioned prior to experimentation. (b) At $day_0$ (September 22, 2020), several sulfur, nitrate, and tailings amendments were added to the mesocosms for the experimental phase (indicated to the left) and sampled at several timepoints until $day_{28}$ on October 19, 2020 (right).

Prior to the experimental phase, mesocosms were preconditioned with tailing and/or thiosulfate treatments (Fig. 4.1) and remained at pH 4 but returned to circumneutral following tailings amendments made at $day_0$. The composition of tailings from the mine have previously been characterised and reported (Duffy et al. 2015). The nickel-rich tailings are composed primarily of pyrrhotite (60%) with associated silica gangue phases (e.g. quartz and albite) comprising around 30% of total mass. Minor mineral components include chalcopyrite, pentlandite and magnetite.

Total alkalinity measurements (Lipps et al. 2023) indicated mean total alkalinity values of 530 mg $CaCO_3$/L, or 10.6 meq/L for the undiluted mine tailings slurry. Note that total alkalinity also includes protonation reactions involving mineral phases as well as carbonate equilibria. Alkalinity measurements from the waters of the mesocosms were negligible throughout the experiment (< LOD by $day_3$).

These experiments explored the effects of $S_2O_3^{2-}$, $S_4O_6^{2-}$, $O_2$, and $NO_3^-$ concentrations ($E_1$–$E_8$, Fig 4.1b) on the sulfur metabolizing microbial community composition, abundance, and presence/activity of sulfur oxidation pathways (cSOx, iSOx + rDSR, and $S_4I$) of SOB communities that were presumed to be differentiated by the effects of the varied preconditioning amendments. Tailings impoundments are dynamically exposed to operational changes in tailings discharges in addition to seasonal and spatial biogeochemical and environmental variability; therefore, these experiments provided new insights into how microbial communities may change in response to such geochemical and physicochemical changes and, in turn, how they may influence water chemistry outcomes.

### 4.2.3 Sample Collection in Onsite 500 L Mesocosms

Mesocosms were sampled for 16S rRNA gene sequence, mRNA and geochemical analyses by drawing water up through non-reactive the vinyl tubing (Crack-Rst Polyethylene-Lined EVA tubing for Food & Beverage; ¼ inch, 0.635 cm). Geochemical samples were collected using a sampling syringe that was thoroughly rinsed prior to sample collection, and biological samples were collected with the aid of peristaltic pump (2 L for 16S rRNA and 1 L for mRNA). Triplicate water samples were collected with from each mesocosm for geochemical analyses, filtered with

a Pall Acrodisc® 25 mm 0.2 μm filters for anions ($SO_4^{2-}$, $NO_2^-$, $NO_3^-$) into Falcon™ tubes, and stored at 4 °C until analyzed. Using unfiltered samples, $S_2O_3^{2-}$ and $SO_3^-$ anions were stabilized via a monobromobimane derivatization process [(Rethmeier et al. 1997), see section 2.5)]. Following derivatization, unfiltered samples were stored frozen (in a freezer onsite, and transported in coolers), until analyzed on a Shimadzu LC-20AD Prominence high performance liquid chromatography (HPLC) following published protocols (K. Whaley-Martin et al. 2020; Rethmeier et al. 1997).

For 16S rRNA and mRNA isolation, samples of water were collected (2 L for 16S rRNA and 1 L for mRNA) from 90 cm depth in each mesocosm using a Geopump™ Peristaltic Pump, filtered through sterile, 0.1 μm, Polyethersulfone (PES) membrane filters (ThermoScientific™ Nalgene™ Rapid-Flow™ Sterile Disposable Filter Units). Filters were excised immediately after sampling and flash frozen in liquid nitrogen for transportation and stored in -80°C before extraction in the laboratory. Geochemical and metatranscriptomic (mRNA) samples were collected, (i) at $day_0$ on Sept 22nd, before experimental amendments, (ii) twice daily for the first 3 days of the experiment, and (iii) weekly until $day_{28}$ from 50 cm below the water surface in each mesocosm. Community composition (via 16S rRNA) samples were collected at three points during the experiment ($day_0$, $day_{16}$, and $day_{28}$, Fig. 4.1b).

### 4.2.4 Geochemical Analyses of Sulfur and Nitrogen

Detailed methods for geochemical analysis of all ions, except for tetrathionate and ammonia, are described in Whaley-Martin et al. (2019). Briefly, dissolved $S_4O_6^{2-}$, $SO_4^{2-}$, $NO_2^-$, $NO_3^-$, and $NH_4^+$ concentrations were determined by ion chromatography (Thermo Scientific Dionex™ ICS-6000) in triplicate, filtered (0.2 μm) samples. Excluding, tetrathionate, anion and cation samples were analyzed on a Thermo Scientific Dionex™ ICS-6000 HPIC™ (high pressure ion chromatography) System using EPA Methods 300.0 and 300.1, respectively. Anion samples were calibrated with curves prepared by dilution of liquid 1000 ppm standards. Anion samples were eluted onto a Dionex IonPac™ AS18-FASTAS18 anion exchange column (7.5 μm × 150 mm, Thermo Scientific™ eluted with 23 mM KOH at 30 $^0$C and a flow rate of 1 mL/min). Elution times were approximately 3.2 min for $NO_2^-$, 4.9 min for $NO_3^-$, and 5.8 min for $SO_4^{2-}$). Tetrathionate anions were processed separately using a Dionex IonPac™ AS32-Fast-4 μm

Column (run time of 25 min and 1 mL/min flow rate, at 30 °C with gradient elution as follows: 4 mM KOH from 0−4 min ramped up to 25 mM KOH from 10–17 min, 17–25 min 4 mM KOH returned to 4 mM to equilibrate; elution time approximately: 10.1 min; see product manual for details). Ammonium was processed using an isocratic 4.0 mM ECG 500 methanesulfonic acid (MSA) eluent with a flow rate of 0.64 mL/min on a Shodex IC YS-50 column (temperature 40 °C, run time 35 min, elution time approximately 10 min)**.**

Quantification of $S_2O_3^{2-}$, $SO_3^{2-}$ and $S^0$ was performed in triplicate by HPLC (high performance liquid chromatography; Prominence, Shimadzu). $S_2O_3^{2-}$ and $SO_3^{2-}$ concentrations were determined using a UV/VIS detector and a Alltima™ HP C18 reversed phase column (150 mm x 4.6 mm x 5 µm, Grace™) at 35°C (Rethmeier et al. 1997). Samples were eluted with an isocratic mobile phase of 35 % methanol and 65 % of 0.25 % acetic acid v/v (pH 3.5 adjusted with NaOH). The flow rate for the HPLC analysis was 0.5 mL/min, the total run time 12 min., the excitation wavelength 380 nm, the emission wavelength of 478 nm, and the elution times approx. 5.1 min for $SO_3^{2-}$ and 5.5 min for $S_2O_3^{2-}$. Peaks were calibrated against curves prepared from solid standards of sodium sulfite and sodium thiosulfate (Sigma Aldrich, ≥98 % purity and 99 % purity respectively), data is reported as sulfur molarity (i.e., S-$S_2O_3^{2-}$)). $S^0$ extraction was performed on previously frozen samples, using chloroform extraction and concentrated using $N_2$ gas (15 ml sample extracted and redissolved in a final volume of 0.3 ml chloroform), as described by Whaley-Martin et al. (2020) and Yan et al (2022). Samples were analyzed using a HPLC–UV/VIS system (with the same Alltima™ HP C18 reversed phase column) flow rate 1 mL/min , mobile phase 95 % HPLC grade methanol and 5 % 18.2 MΩ cm deionised water (v/v) isocratic mobile phase, and 263 nm absorbance wavelength (Rethmeier et al. 1997).

Total S detection was performed in triplicate using an Inductively Coupled Plasma - Optical Emission Spectrograph (ICP-OES, iCAP 7000 Series, Thermo Scientific™). The radial emission from wavelength 180.731 selected for standard curve calibration and S concentration calculations according to methods described in Yan et al. 2022.

### 4.2.5 DNA and RNA Extraction

The community genomic DNA was extracted using the manufacturer's protocols for the DNeasy PowerWater DNA Isolation Kit (Qiagen). Extracted DNA concentrations were quantified using qPCR and quality-assessed via agarose gel electrophoresis. For RNA, frozen extraction filters were thawed and then RNA was isolated using the manufacturer's protocols for the RNeasy PowerWater Kit (Qiagen). Isolated RNA concentrations were quantified by Nanodrop at the McMaster Genomics Facility and quality-assessed via agarose gel electrophoresis.

### 4.2.6 DNA Gene Amplicon Sequencing and Analyses

Isolated DNA samples were prepared and sequenced at the McMaster Genomics Facility for preparation and sequencing as described in Whaley-Martin et al. 2019, and section 3.2.6 above. Briefly, the 16S rRNA amplicon sequencing was performed on the V4 region by PCR, according to standard Earth Microbiome Project protocols (Caporaso et al. 2012). Gel electrophoresis was used for quality control prior to sequencing, for which the Illumina MiSeq platform was used with paired-ends of 100 bp. DADA2 (version 1.6.0) was used to exclude bimeras, chloroplasts, and mitochondrial sequences, after which Cutadapt was used to filter and trim sequences (Martin 2011). The taxonomy was assigned using version 138.1 of the SILVA database. (For workflow from raw 16S gene sequencing data with operational taxonomic units (OTUs) listed, see "Chapter 4 Supplementary 16S rRNA data (curation steps)" at the following link: http://128.100.14.155:8088/share.cgi?ssid=204a2ab4254d4911874cd20953dfb1ed).

### 4.2.7 Metatranscriptomic Sequencing, Reads Processing and Assembly

At the McMaster Genomics Facility, isolated RNA was subjected to quality control using an Agilent Bioanalyzer 2100 using the RNA Pico chip assay, and then rRNA depletion (using the NEBNext® rRNA Depletion Kit [Bacteria], catalog #E7850X) to remove the bacterial rRNA. The remaining RNA was converted to cDNA libraries using the NEBNext Ultra II Directional RNA LP Kit for Illumina (catalog #E7760L). The size and quality of each of the 20 libraries were then assessed using Agilent Tapestation D1000 tape and undergoing qPCR (in triplicate). Because the initial input RNA was low, some libraries had visible adapter-dimers after library preparation (quality control on the pooled libraries was performed with a HSDNA chip on an Agilent

Bioanalyzer 2100). To remove the adapter-dimers, library pool clean-up was performed with a 0.9× Ampure bead clean-up. Sequencing of the RNAseq libraries was performed using an Illumina HiSeq PE run with on-board cluster generation at McMaster University (Hamilton, Ontario, Canada) and the demultiplexed data were uploaded to BaseSpace.

Following sequencing, the raw Illumina reads were filtered to remove Illumina sequencing adapters, PhiX and other Illumina trace contaminants were removed using BBTools (Bushnell 2018), and the low-quality bases and reads were removed using Sickle (v. 1.33). The remaining paired-end reads were used for subsequent *de novo* assembly idba_tran (Peng et al. 2013), with the parameters as of --mink = 20, --max = 120, --step = 20 and "--pre_correction." The protein-coding genes were predicted from the assembled contigs using Prodigal (Hyatt et al. 2010) (parameters: -m -p meta). To calculate the reads per kilobase of transcript (RPKM, per million mapped reads) of each protein-coding gene, the corresponding quality reads were mapped to all the assembled gene sequences from a given sample using Bowtie2 with default parameters (Longmead and Salzberg 2012). The generated .sam files were converted to .bam format and sorted using samtools (Li et al. 2009). The RPKM of a protein-coding gene was calculated using [a/(b/1,000 × c/1,000,000)], where "a" is the number of reads mapped to the gene sequence, "b" is the length of the gene, and "c" is the total number of reads of the corresponding sample. The RPKM value of a gene was used as the transcriptional activity of the gene, and represented as unmodified values in figure 4.4 below.

### 4.2.8 Statistical and Data Analysis

Non-metric dimensional scaling (NMDS), Bray-Curtis dissimilarity clustering, and Pearson R correlation matrices were carried out in R version (3.6.2 in 2020, 4.4.4 in 2022) utilizing the Vegan package version (2.5-7 in 2020 and 2.6.4 in 2022) and indicspecies package 1.1.7 7 (De Cáceres et al. 2012). Statistical analyses were carried out on triplicate samples for geochemistry, unless noted, with standard deviation calculated on mean analytical data from triplicate injections. "Less than detection limit" chemical or biological data were treated as zero for statistical analyses. Data were displayed using the complex heatmap package in R (Gu, Eils, and Schlesner 2016), and y-axis graph break using Ggbreak (Xu et al. 2021).

## 4.3 Results: Mesocosm Study

In the mesocosm study, mine water taken from the tailings impoundment was exposed to different experimental amendments of $NO_3^-$ (a compound often found in mine wastewaters from blasting residues), sulfur substrates ($S_2O_3^{2-}$ and $S_4O_6^{2-}$), and tailings. Over the course of 28 days, the mesocosms were sampled for standard chemistry parameters (pH; [$O_2$]; temperature, °C), sulfur speciation and concentration, and 16S rRNA gene sequencing and mRNA analyses.

### 4.3.1 Geochemistry: Alkalinity and Acidity Trends

Over the 28-day experiment, five mesocosms ($E_1$, $E_2$, $E_3$, $E_5$, and $E_8$) experienced pH decreases and net acidity generation (Table C2). The water contained in mesocosms $E_1$ (tetrathionate, tailings, and nitrate) and $E_2$ (tetrathionate, tailings, no nitrate) experienced a pH decrease from 6.5 to 5.2 ($\Delta H^+$ = 0.0056 mM) and 6.2 to 5.6 ($\Delta H^+$ = 0.0011 mM), respectively. Water in mesocosms $E_3$ (thiosulfate, tailings) and $E_5$ (thiosulfate, no tailings) decreased in pH from 7.4 to 6.1 ($\Delta H^+$ = 0.0008 mM) and 6.1 to 5.8 ($\Delta H^+$ = 0.0013 mM), respectively. Mesocosm $E_8$ (tailings, nitrate) experienced a pH decrease from 7.0 to 6.0 ($\Delta H^+$ = 0.0008 mM).

Over the same timeframe, the remaining three mesocosms ($E_4$, $E_6$, and $E_7$) experienced pH increases, indicating proton-consuming reactions were dominant (Table C2). Mesocosms $E_4$ (thiosulfate, nitrate, tailings) and $E_6$ (thiosulfate, nitrate, no tailings) experienced a pH increase from 5.6 to 6.5 ($\Delta H^+$ = −0.0019 mM), and 4.0 to 7.1 ($\Delta H^+$ = −0.0954 mM), respectively. The lowest change in proton concentration was observed in mesocosm $E_7$ (tailings), where the pH increased from 6.5 to 6.7 ($\Delta H^+$ = −0.0001 mM).

Acid neutralization calculations that accounted for the alkalinity of the added tailings slurry (530 mg $CaCO_3$/L, or 10.6 meq/L) indicated that following the initial upward pH adjustment, the added tailings alkalinity had only a slight moderating effect on solution pH. The potential effect of the tailings alkalinity on reducing acidity generation was assessed by calculating the proton equilibria using a spreadsheet model based on that of Nhantumbo et al. (2018). During development of the spreadsheet model, test calculations were validated against predictions obtained from the geochemical model PHREEQC. The total alkalinity measured in the mesocosms was also negligible throughout the experiment (below limit of detection by $day_3$).

Calculations indicated that the low acid generation observed in the mesocosms could not be accounted for by neutralisation with the small concentration of total alkalinity from the tailings. For instance, in mesocosm $E_3$, the decrease in thiosulfate concentration over the duration of the experiment was 0.55 mM. If this amount of thiosulfate was oxidised via the cSOx pathway, it would be predicted to generate a pH of 2.7. However, a final pH of 6.1 was observed. Including the alkalinity effect modeled from the tailings would, at most, account for a shift in pH from 2.7 to 2.9, far less than the effect observed. Thus, it is reasonable to exclude tailings alkalinity from proton yield calculations. This supports the assumption that net $\Delta H^+$ ($\Delta H^+ = 10^{-pH}$ at $day_{28} - 10^{-pH}$ at $day_0$) represents actual acidity produced by microbial processes.

### 4.3.2 Geochemistry: Sulfur Speciation Trends

Although baseline sulfate concentrations in the wastewater were high (~7.6 mM) prior to the experimental phase, all eight mesocosms showed increases in sulfate over the 28 days (Fig 4.2, (Table C2). Mesocosms $E_1$–$E_4$ had an average $\Delta SO_4^{2-}$ of 1.6 ± 0.3 mM, and mesocosms $E_5$–$E_8$ had an average $\Delta SO_4^{2-}$ of 0.6 ± 0.2. mM. The thiosulfate concentration decreased in all mesocosms, following a pseudo–first order reaction (calculated according to equation 4):

$$\left[S_2O_3{}^{2-}\right] = \left[S_2O_3{}^{2-}\right]_0 e^{-k\prime t} \qquad (4)$$

where t is time and k' is the first derivative of the rate constant for a first-order reaction (Table C3). This thiosulfate loss indicates processing via any of the three pathways (equations 1–3).

Low concentrations of $S^0$ (0.01–0.48 mM, $[S^0]_{median}$ = 0.05 mM) were detected in all mesocosms over the duration of the experiment. The lowest $S^0$ concentrations were found in the tailings-only treatments ($E_7$ and $E_8$, Fig , Table C2), indicating tailings were not a substantial $S^0$ source.

In the tetrathionate-amended mesocosm, a large tetrathionate loss over the course of the experiment ($\Delta S\text{-}S_4O_6^{2-}$ = −0.39 mM) occurred in mesocosm $E_1$, but not in tetrathionate- and nitrate-amended $E_2$ ($\Delta S\text{-}S_4O_6^{2-}$ = 0.02 mM). Similarly, a small tetrathionate loss ($\Delta S\text{-}S_4O_6^{2-}$ = −0.06 mM) was measured in the thiosulfate amended mesocosm ($E_3$), but not the thiosulfate- and tailings-amended $E_4$ ($\Delta S\text{-}S_4O_6^{2-}$ = 0.03 mM). However, these data are only semi-quantitative. The 0.2 μm–filtered samples had high standard deviations, perhaps because of sampling variation or

the >1-year storage of samples prior to analysis. The detection of tetrathionate concentrations greater than the background level of 0.1 mM also occurred in the tailings-only control mesocosms ($E_7$ and $E_8$) and in the thiosulfate-amended mesocosms where no tetrathionate was added ($E_3$ – $E_6$; see Fig 4.2, Table C2).

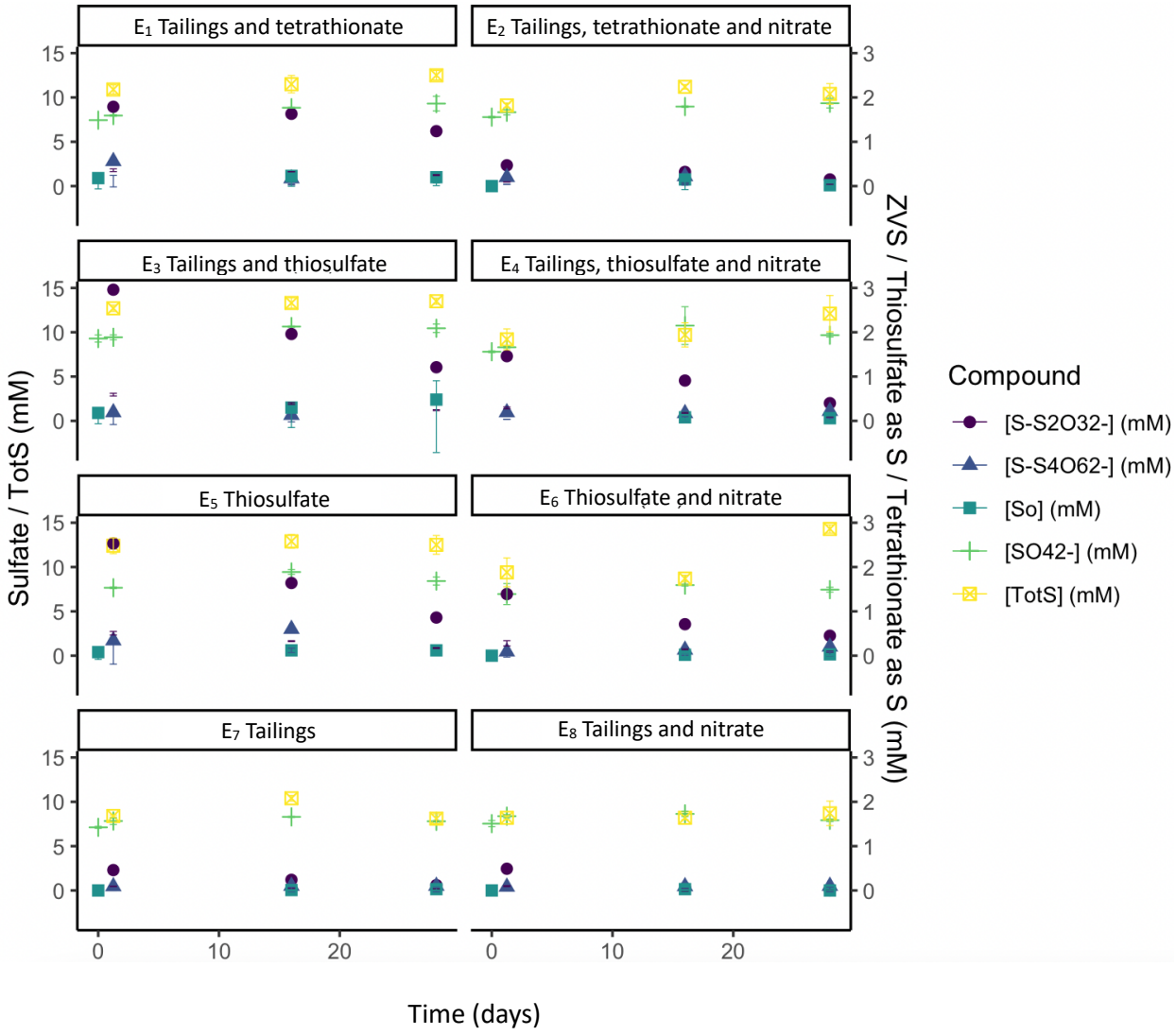


**Fig 4.2** Changes in sulfur speciation trends across the eight mesocosms. Sulfite concentrations ($[SO_3^{2-}]$), were non-detectable in all systems and timepoints. (Where standard deviation values for sulfur speciation data were not available [n=3], the mean values of 0.05 mM for S-$S_4O_6^{2-}$ and 0.1 mM for $S^0$ are presented.); (-) indicates no amendment of that type was added to the respective mesocosm.

In most mesocosms, the measured sulfur species accounted for over 90% of the total sulfur present (Fig 4.2, Table C2). However, larger gaps in the sulfur mass balance occurred at $day_{28}$ (Total S − ∑ measured sulfur species) for the two thiosulfate- and tailings-amended mesocosms: $E_5$ (75% of TotS) and $E_6$ (57% of TotS). This indicates the formation of other unidentified SOI species. In mesocosms $E_3$, $E_5$, $E_7$, and $E_8$, not all the thiosulfate loss could be accounted for by increases in sulfate ($\Delta[SO_4^{2-}] < -\Delta[S_2O_3^{2-}]$), also suggesting the formation of SOIs such as polythionates. Alternately, gaps in the S mass balance may be partially accounted for by $S^0$ formation and subsequent sedimentation through excretion or cell death.

### 4.3.3 Geochemistry: Oxygen and Nitrate Availability for Sulfur Compound Oxidation

Published experimental evidence suggests that nitrate and oxygen are used concurrently by SOB when the oxygen concentration is below 0.3 mg/L $O_2$, and that a decrease in nitrate use occurs above that threshold $O_2$ concentration (X. Wang et al. 2016; R.-C. Zhang et al. 2019). Therefore, we conservatively estimated 0.5 mg/L (0.016 mM) to be the threshold above which oxygen is used exclusively.

DO concentrations varied with time, depth, and mesocosm (Table C2, Fig C1). Yet, except for $E_6$, all mesocosms experienced some periods of oxygen depletion to levels below the assigned threshold value (<0.016 mM, Table 4.2), often during the first 10 days. Nitrate was detected at all timepoints (Table C2) suggesting that SOB had the opportunity to use nitrate as an alternate TEA to oxygen. However, the simultaneous increases in nitrate and ammonia observed in all tanks over the experimental period were consistent with activity of both N-reducing and N-oxidizing microorganisms.

Nitrate amendments increased thiosulfate oxidation rates in the mesocosms containing tailings. Thiosulfate oxidation rates increased by 1.7-fold in the mesocosms amended with tailings and thiosulfate ($E_4$ and $E_3$) when amended with nitrate (the half-life was 13.9 d for $E_4$ [with nitrate], and 21.3 d for $E_3$ [without nitrate]). This was also observed when comparing the tailings-only treatments, which had a 2.8-fold increase in thiosulfate oxidation with nitrate. The half-life of thiosulfate was 4.95 d for $E_8$ [with nitrate] and 13.9 d for $E_7$ [without nitrate] (see Table C3). In

addition, the nitrate-amended treatments ($E_2$, $E_4$, $E_6$) had lower [$S^0$] than their nitrate-free equivalents, and [$S^0$] generally decreased over the latter half of the experiment (Table C2).

**Table 4.2** Estimated Proportion of Time that Nitrate could be the Terminal Electron Acceptor based on Observed [$O_2$]*

| Mesocosm | Treatment | Code | Sum of all periods DO below 0.5 mg/L (days) | Fraction of 28-day experiment with DO below 0.5 mg/L (%) |
|---|---|---|---|---|
| $E_1$ | Tailings and tetrathionate | $T_{12}S_{4(2.0)}$ | 5.4 | 19 |
| $E_2$ | Tailings, tetrathionate and nitrate | $T_{12}S_{4(2.0)}N_{2.0}$ | 4.2 | 15 |
| $E_3$ | Tailings, thiosulfate and nitrate | $T_{12}S_{2(2.0)}$ | 16.5 | 59 |
| $E_4$ | Tailings, thiosulfate and nitrate | $T_{12}S_{2(2.0)}N_{2.0}$ | 8.8 | 31 |
| $E_5$ | Thiosulfate | $S_{2(2.0)}$ | 6.9 | 25 |
| $E_6$ | Thiosulfate and nitrate | $S_{2(2.0)}N_{2.0}$ | 0 | 0 |
| $E_7$ | Tailings | $T_{12}$ | 3.5 | 13 |
| $E_8$ | Tailings and nitrate | $T_{12}N_{2.0}$ | 8.1 | 30 |

*[$NO_3^-$] > 0.04 mM throughout entire time course in all mesocosms.

### 4.3.4 Bacteria: Sulfur Metabolizing Community Trends (16S rRNA)

Six SOB genera (*Halothiobacillus, Thiomonas, Sediminibacterium, Thiovirga, Acidovorax,* and *Sulfurovum*) and one sulfate-reducing bacteria that is also able to oxidize sulfur (*Desulfurivibrio*; Melton et al. 2016; Sun et al. 2022; Thorup et al. 2017) were identified through 16S rRNA gene sequencing (Fig 4.3b, Table C4). An additional nitrate-dependent iron oxidizing (NDFO) genus (*Acidovorax*) was found to also have tetrathionate-reducing genes (Fig 4.3b, Table C4).

The six SOB genera detected catalyze different pathways: two genera contained genes for cSOx alone (*Thiovirga* and *Sulfurovum*), one $S_4I$ alone (*Sediminibacterium,* as indicated by *tsdA*), and two had both cSOx and $S_4I$ (*Halothiobacillus* and *Thiomonas*) pathways (Fig 4.3b). Genes for the iSOx and rDSR pathways were only present in the genus *Thiobacillus,* where they were accompanied by genes for the $S_4I$ pathway, although genes for the rDSR pathway segment were also hosted by *Desulfurivibrio* (Fig 4.3b). The NDFO genera *Acidovorax* possessed the gene *ttrABC* that codes for tetrathionate reductase ($S_4O_6^{2-}$), an enzyme that reduces tetrathionate to thiosulfate, along with traces of the rDSR pathway system (Fig 4.3b). The metagenomic

inferences for these eight sulfur-metabolizing genera were based on previous whole-genome characterization of SOB from this tailings impoundment (Whaley-Martin et al. 2023).

During the experimental phase (28 days, September, 22, 2020 to October 19, 2020; Fig 4.3b), sulfur-metabolizing bacteria comprised 0.1–21.9% of the mesocosm communities, with a median abundance of sulfur-metabolizing bacteria of 1.6% (Fig 4.3a). The varied tailings and thiosulfate pre-treatments resulted in divergent initial communities at $day_0$, with a higher mean total abundance of sulfur-metabolizing bacteria occurring in mesocosms pre-treated with thiosulfate prior to the experimental phase (4.6% for mesocosms $E_1$–$E_5$) than in those that received no pre-treatment (0.3% for mesocosms $E_6$–$E_8$; Fig 4.3a). At the beginning of the experimental stage ($day_0$), *Thiomonas* was dominant in six of the mesocosms (>50% of the sulfur community in $E_2$ and $E_4$–$E_8$; Fig 4.3a, Table C5). The sulfur-metabolizing communities in the eight mesocosms diverged with time, with only mesocosm $E_5$ remaining dominated by *Thiomonas* on $day_{28}$ (>97% of sulfur metabolizing bacteria), indicating that communities changed independently (Fig 4.3a).

Mesocosms $E_5$ and $E_6$ (two of the thiosulfate-amended mesocosms) were dominated by *Thiomonas* (cSOx and $S_4I$ pathways) making up >50% of the SOB population throughout the course of the experiment. However, when nitrate was added in addition to thiosulfate ($E_6$), this resulted in an increase in *Sediminibacterium* ($S_4I$ pathway) abundance from <1% at $day_0$ to 42% by $day_{16}$, and *Acidovorax* (*ttrABC*) abundance from <1% $day_0$ to 34% by $day_{24}$ (Fig 4.3). Mesocosms $E_2$ (tailings, tetrathionate, nitrate) and $E_4$ (tailings, thiosulfate, nitrate) transitioned from *Thiomonas*-dominated communities (cSOx and $S_4I$) to communities dominated by *Thiobacillus* (iSOx + rDSR, and $S_4I$).

Mesocosms $E_1$ (tailings, tetrathionate, nitrate) and $E_3$ (tailings, thiosulfate, no nitrate) became dominated by *Desulfurivibrio* (rDSR) as the most abundant sulfur-cycling genus. Although time series data are missing for $E_3$, the abundance of *Desulfurivibrio* in $E_1$ increased as a proportion of both the sulfur-metabolizing and total microbial community (Fig 4.3; Table C5).

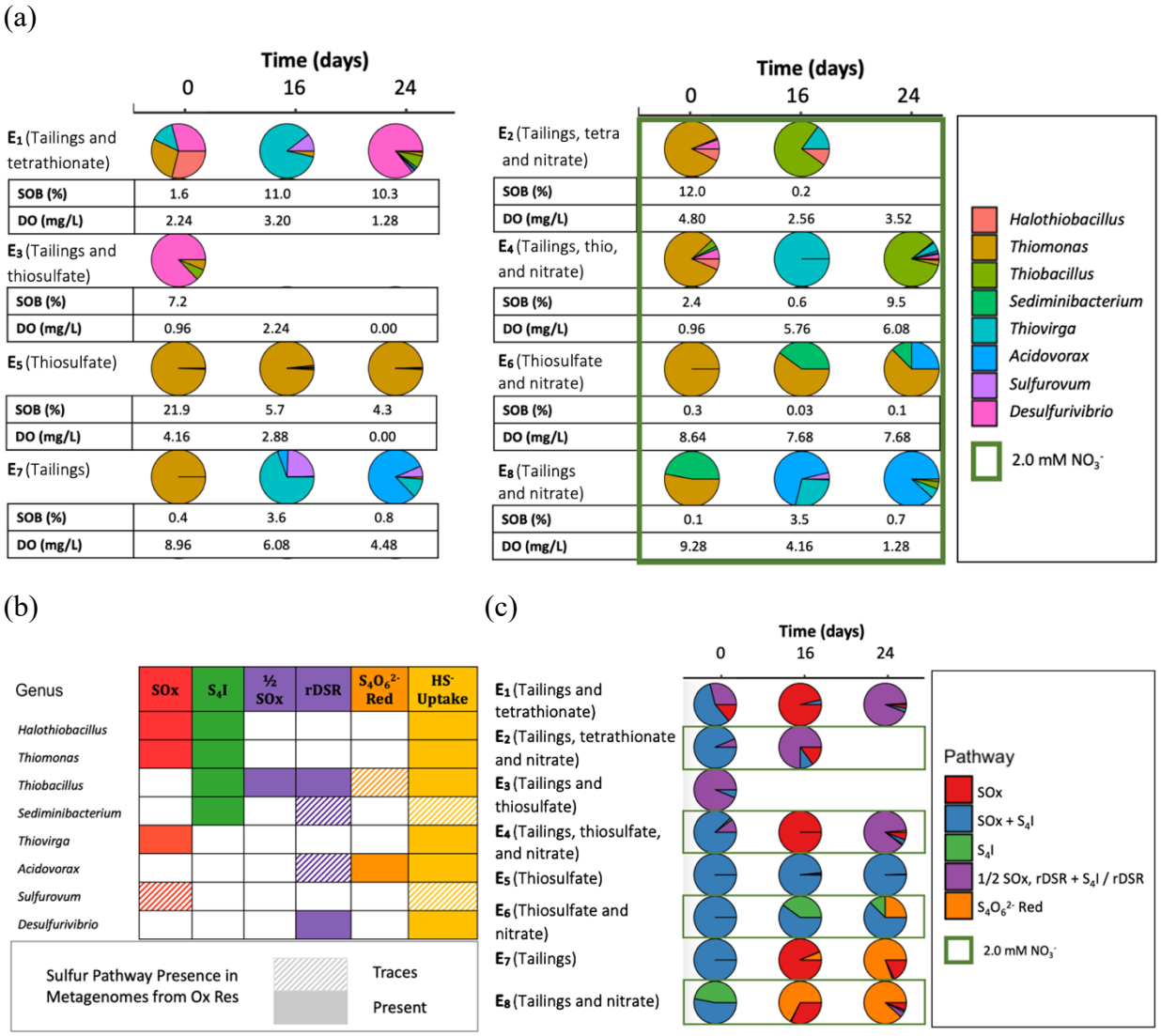


**Fig 4.3** SOB communities in the mesocosms and metagenomic inference of sulfur pathways. (a) Relative abundance of the sulfur-metabolizing bacteria in the 8 mesocosms at up to three timepoints. Reported oxygen concentrations observed at the lowest mesocosm water depth (90 cm) and the relative abundance of sulfur-oxidizing bacteria in the total community are provided for each sampling timepoint available. (b) The sulfur pathways detected in sulfur-metabolizing bacteria. Diagonal hatching (traces) indicates <50% of the metagenomes sequenced contained one or more gene from the incomplete pathway, while solid colours indicate the complete sulfur pathway was present in most (>70%) of all metagenomes sequenced; white squares indicate no genes associated with the pathway were detected (see Table C4). (c) The relative abundance of the sulfur-metabolizing genera that contain each pathway in their metagenomes. When more than one pathway is listed, sulfur-metabolizing bacteria present within the community have the capacity to activate either or all (i.e., cSOx + $S_4I$; iSOx + rDSR + $S_4I$ or rDSR) pathways, and all have the capacity to uptake $HS^-$.

The SOB communities in mesocosms $E_7$ and $E_8$ (tailings only) shifted from *Thiomonas* (cSOx and $S_4I$) dominance to a community where, by $day_{16}$, *Thiovirga* and *Sulfurovum* (cSOx) were dominant ($E_7$) or present ($E_8$). These communities then became dominated by *Acidovorax* (81% in $E_7$ and 88% in $E_8$) by $day_{24}$, indicating a potential shift from thiosulfate oxidation to tetrathionate reduction as thiosulfate concentrations were depleted (Fig 4.3c).

### 4.3.5 Gene Expression: Sulfur Enzyme Trends (mRNA)

Pathway expression, as characterized by mRNA expression in RPKM, varied among the treatments (Fig 4.4). Several trends emerged that were consistent with those identified in the 16S rRNA gene sequence data (Fig 4.3). The highest levels of cSOx pathway expression along with low $S_4I$ pathway activity (*tsdA* expression in RPKM < 20) were detected in the mesocosm that received only an amendment of thiosulfate ($E_5$), consistent with the pathways inferred from 16S rRNA analysis (Fig 4.3). In mesocosm $E_6$, the presence of the $S_4I$ pathway was suggested by the 16S rRNA analysis (*Thiomonas* and *Sediminibacterium*; Fig 4.3), and the highest frequency of expression for the $S_4I$ Pathway Part 1 (*tsdA*) was detected (Fig 4.3). In mesocosm $E_4$, where *Thiobacillus* appeared to be a dominant species based on 16S rRNA gene sequence data (Fig 4.4), mRNA for the iSOx pathway was also observed, although only traces of the rDSR pathway were expressed (Fig 4.4). The mRNA signal for $E_2$ at $day_{24}$ was faint but did not clearly indicate iSOx or rDSR, instead suggesting the cSOx pathway.

In mesocosms $E_1$ and $E_3$, where *Desulfurivibrio* indicated the presence of the rDSR pathway, mRNA expression also indicated that several rDSR genes were active along with the tetrathionate reductase *ttrABC* ($S_4O_6^{2-}$ reduction) and the cSOx pathway (Fig 4.4). Finally, mesocosms $E_7$ and $E_8$, which had capacity for cSOx, $S_4I$, and tetrathionate reduction (*ttrABC*), also displayed partial expression of the pathways — although *ttrABC* expression was only detected in $E_8$ (Fig 4.4).

(a)

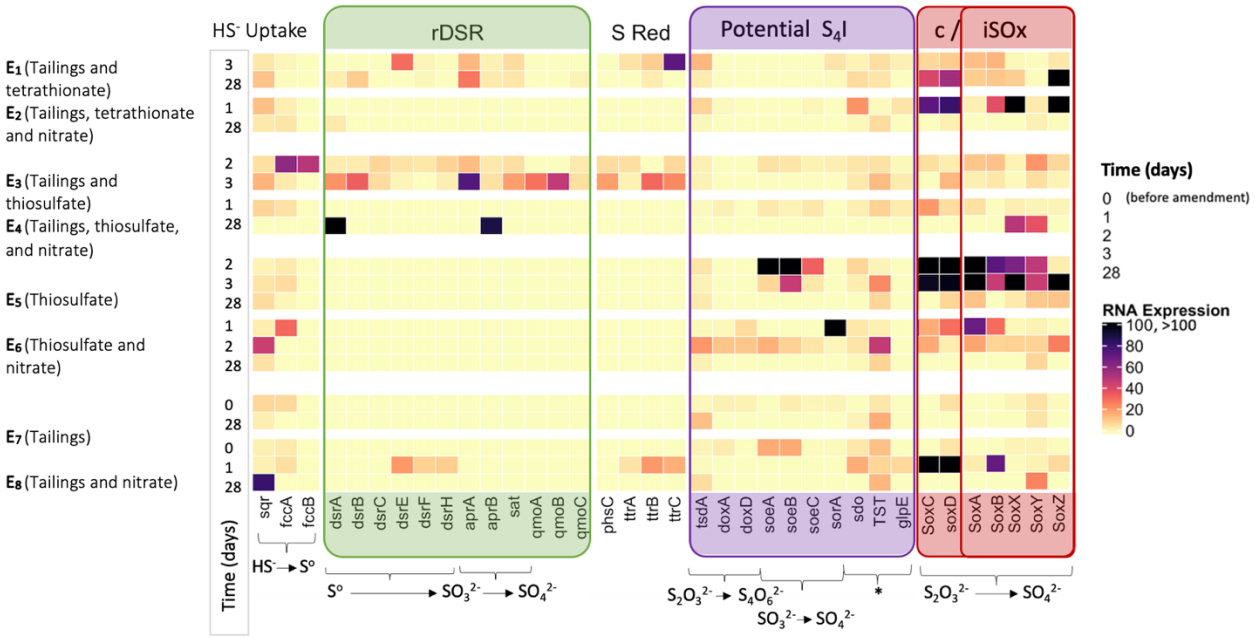


(b)

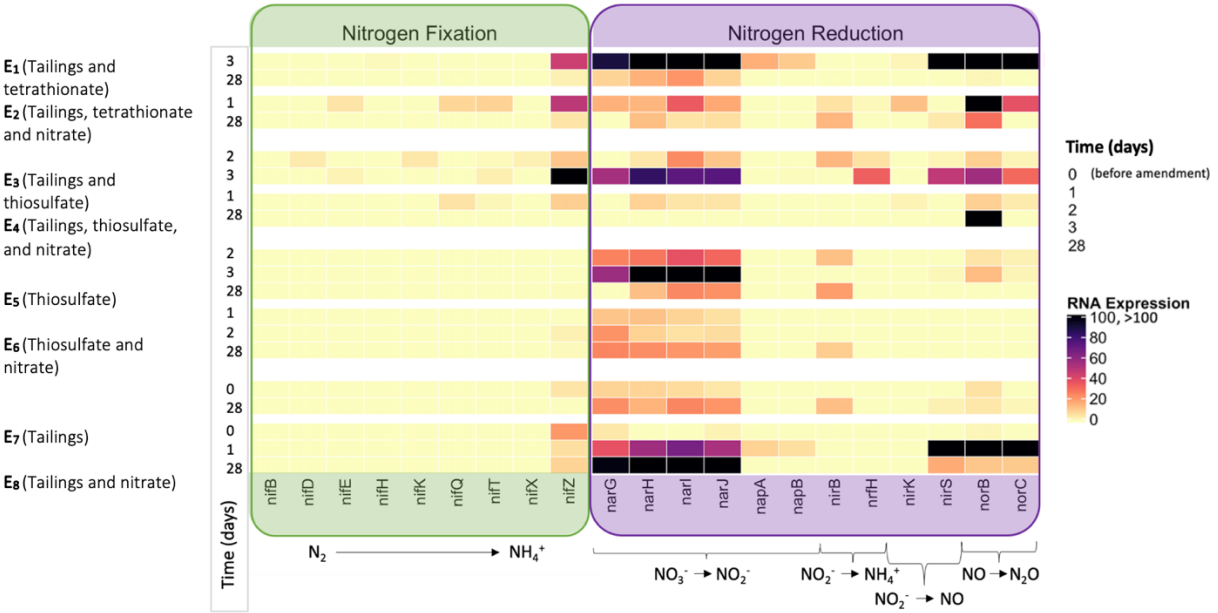


**Fig 4.4** A heat map of mRNA expression profiles based on metatranscriptomic analysis. The values (in reads per kilobase million of transcript [RPKM] indicating transcriptional activity (see methods 4.2.7); darker squares indicate greater expression) were grouped by (a) sulfur-cycling enzyme system (sulfide uptake, rDSR, sulfur reduction, potential $S_4I$, cSOx) and (b) nitrogen metabolism grouped by enzyme system. Additional variables including time (days) and treatments

(colour legend on right) were paired to treatment parameters (without and with 2.0 mM nitrate [green bar] in addition to the sulfur and tailings amendments). (*) functions of Sdo, TST, and GplE remain to be clarified but may facilitate the following transformations: Sdo ($S^0 \rightarrow SO_3^{2-}$), TST ($S_2O_3^{2-} \rightarrow SO_3^{2-}$), and GplE (sulfurtransferase, $S_2O_3^{2-} \rightarrow SO_3^{2-}$, Table 1.2, Table C1). Gene expression data for *tetH* ($S_4$I Part 2) and *nosZ* were not available.

### 4.3.6 Gene Expression: Nitrogen Enzyme Trends (mRNA)

Expression of nitrogen-processing genes provides some insight into the potential role of nitrate as a TEA (Fig 4.4b). Genes for enzymes that reduce nitrate to nitrite (*narIGH* or *napAB* are required for dissimilatory nitrate reduction) were expressed in all mesocosms, with the lowest expression in the mesocosm amended with thiosulfate, tailings, and nitrate ($E_4$), and highest in the mesocosm treated with tailings and nitrate but not sulfur ($E_8$). The mRNA data does not clearly link nitrate reduction with sulfur pathway expression. The *nar* gene expression was high (>100) at the timepoints in $E_1$ and $E_3$ where rDSR pathway expression was detected, but it was also high in $E_5$, where the rDSR pathway was not (Fig 4.4b). Expression of the *nirB* gene in $E_2$–$E_7$ may suggest further conversion of nitrite to ammonia, while *nir* and *nor* expression in $E_1$, $E_2$, $E_3$, and $E_8$ may indicate that nitrous oxide was also produced; however, no information was available on the expression frequency of *nosZ*, which would further convert the nitrous oxide to $N_{2(g)}$ (Fig 4.4b). Nitrogen fixation in the mesocosms was not supported, with only low and fragmented expression of the *nif* genes (Fig 4.4b).

## 4.4 Discussion

### 4.4.1 Diagnostic Assessment Approach to Constrain the Active Sulfur Pathway(s)

To identify trends in sulfur pathway use, the three lines of evidence (geochemical, 16S rRNA gene sequences linked to metagenomes, and mRNA results) were summarized in binary form (i.e., yes/no; Table 4.3).

This new diagnostic approach draws from an extensive literature review summarizing the reactions catalyzed by each of the three known sulfur pathways (Table 1.1 and Table C1). Here, we identified six individual segments of those pathways (constrained genes with known geochemical outcomes) as key units of pathway occurrence (cSOx, iSOx, $S_4I$ Part 1, $S_4I$ Part 2, ttrABC, and rDSR). As the field of sulfur enzyme literature grows, this approach can be refined through the addition of other constrained sulfur enzyme systems.

By applying this approach to the mesocosm study, we could discern trends in sulfur pathway activity. Results of the independent assessment for each mesocosm using the binary approach are shown in Table 4.3. The strength of this approach is apparent when considering the observed inconsistencies and ambiguities that arose when each line of evidence was considered separately. These may reflect the presence of "uncharacterised" sulfur-metabolizing bacteria, possible degradation of mRNA and 16S rRNA samples, and/or the loss or transformation of sulfur species prior to quantification. Here, alignment of these independent lines of evidence clarifies which pathway(s) occur, even in the presence of data gaps.

**Table 4.3** Lines of Evidence Supporting Sulfur-Metabolizing Pathways and Nitrate as a Terminal Electron Acceptor

| **Pathway** | | **Mesocosms** | | | | | | | |
|---|---|---|---|---|---|---|---|---|---|
| | Indicators | $E_1$ | $E_2$ | $E_3$ | $E_4$ | $E_5$ | $E_6$ | $E_7$ | $E_8$ |
| **Complete SOx ($S_2O_3^{2-} \rightarrow 2\ SO_4^{2-}$)** | | | | | | | | | |
| | pH decrease* | ✓ | ✓ | ✓ | | ✓ | | | ✓ |
| | cSOx pathway containing bacteria (*Thiomonas*, *Halothiobacillus*, *Thiovirga*, *Sulfurovum*) >10% sulfur-metabolizing community | ✓ | ✓ | | ✓ | ✓ | ✓ | ✓ | ✓ |
| | *soxCD* genes expressed in mRNA | ✓ | ✓ | ✓ | | ✓ | | ✓ | ✓ |
| **Incomplete SOx ($S_2O_3^{2-} \rightarrow SO_4^{2-} + S^0$)** | | | | | | | | | |
| | pH stable* | | | | ✓ | | | ✓ | |
| | iSOx pathway containing bacteria (*Thiobacillus*) >10 % sulfur-metabolizing community | <10 % | ✓ | <10 % | ✓ | | | | |
| | SOx genes expressed but *soxCD* absent (mRNA) | | | | ✓ | | ✓ | ✓ | |
| | [$S^0$] increase * | ✓ | ✓ | ✓ | ✓ | ✓ | ✓ | ✓ | ✓ |
| **$S_4I$ Part 1 (2 $S_2O_3^{2-} \rightarrow S_4O_6^{2-}$)** | | | | | | | | | |
| | pH increase or stable* | | | | ✓ | | ✓ | ✓ | |
| | $S_4I$ pathway containing bacteria *(Halothiobacillus*, *Thiomonas*, *Thiobacillus* and/or *Sediminibacterium*) >10 % sulfur metabolizing community | ✓ | ✓ | | ✓ | ✓ | ✓ | ✓ | ✓ |
| | *tsdA* or *doxDA* expressed in mRNA | ✓ | ✓ | ✓ | ✓ | ✓ | ✓ | ✓ | ✓ |
| | [$S_4O_6^{2-}$] increase | | | ✓ | ✓ | ✓ | ✓ | ✓ | ✓ |

✓ Indicates condition met

✓ Indicates traces of the indicator present

* Some signals, such as pH change or increases in $SO_4^{2-}$ or $S^0$ concentrations, are not uniquely associated with a single pathway. E.g., $S^0$ increases may result from the incomplete SOx pathway and/or the $S_4I$ pathway P2.

Note: all pathways require thiosulfate depletion, which was observed in all mesocosms; see reaction rates (Table C3).

**Table 4.3** cont. Lines of evidence supporting sulfur-metabolizing pathways and nitrate as a TEA

| **Pathway** Indicators | Mesocosms $E_1$ | $E_2$ | $E_3$ | $E_4$ | $E_5$ | $E_6$ | $E_7$ | $E_8$ |
|---|---|---|---|---|---|---|---|---|
| **S4I Part 2 ($S_4O_6^{2-} \rightarrow 4\ SO_4^{2-}$)** | | | | | | | | |
| [$S_4O_6^{2-}$] decrease* | ✓ | | ✓ | | | | | |
| *tetH* containing bacteria (*Thiobacillus*) >10% of the sulfur-metabolizing community | | ✓ | | ✓ | | | | |
| **ttrABC ($S_4O_6^{2-} \rightarrow 2\ S_2O_3^{2-}$)** | | | | | | | | |
| pH decrease* | ✓ | ✓ | ✓ | | ✓ | | | ✓ |
| *ttrABC* containing bacteria (*Thiobacillus, Acidovorax*) >10% of the sulfur-metabolizing community | ✓ | ✓ | ✓ | ✓ | | ✓ | ✓ | ✓ |
| *ttrABC* genes expressed in mRNA | ✓ | | ✓ | | | | | ✓ |
| [$S_4O_6^{2-}$] decrease* | ✓ | | ✓ | | | | | |
| **rDSR ($S^0 \rightarrow SO_4^{2-}$)** | | | | | | | | |
| pH decrease* | ✓ | ✓ | ✓ | | ✓ | | | ✓ |
| *Thiobacillus, Desulfurvibrio* abundance >10% of the sulfur-metabolizing community | ✓ | ✓ | ✓ | ✓ | | | | |
| rDSR genes expressed in mRNA | ✓ | ✓ | ✓ | ✓ | | | | ✓ |
| [$S^0$] decrease | ✓ | ✓ | | ✓ | | | | ✓ |
| **Nitrate as a TEA** | | | | | | | | |
| *Acidovorax* or *Desulfurivibrio* (obligate anaerobes) >10% of the sulfur-metabolizing community | ✓ | | ✓ | | | ✓ | ✓ | ✓ |
| Low oxygen concentrations (<0.5 mg/L) 10–60 % of time | ✓ | ✓ | ✓ | ✓ | ✓ | | ✓ | ✓ |
| Nitrate present (i.e., >0.04 mM) | ✓ | ✓ | ✓ | ✓ | ✓ | ✓ | ✓ | ✓ |
| Nitrate high (i.e., >1.0 mM) | | ✓ | | ✓ | | ✓ | | ✓ |
| *nar* / *nap* genes expressed in mRNA | ✓ | ✓ | ✓ | ✓ | ✓ | ✓ | ✓ | ✓ |

✓ Indicates Condition Met
✓ Indicates Traces of the Indicator Present
* Some signals are not uniquely associated with a single pathway.

The thiosulfate-amended mesocosm, $E_5$, displayed all indicators (16S rRNA, mRNA, and geochemical) of the cSOx pathway (hosted by *Halothiobacillus*, *Thiomonas, Thiovirga*, and *Sulfurovum*) and the highest levels of cSOx mRNA expression. Here, thiosulfate amendments appear to promote dominance of the cSOx pathway under conditions that are mostly, but not exclusively, oxic (Table C1). However, because the proton yield in these mesocosms did not match that predicted by the complete cSOx pathway, and *tsdA* expression was detected, it seems that the $S_4I$ Part 1 pathway — while not dominant — was active as a secondary metabolism (hosted by *Halothiobacillus*, *Thiomonas*, *Thiobacillus, Thiovirga*, *Acidovorax,* and/or *Sediminibacterium*).

Mesocosm $E_6$ exhibited both the highest frequency of *tsdA* expression and largest $-\Delta H^+$, consistent with $S_4I$ Part 1 pathway dominance (Table 4.3). The mesocosm also exhibited an increase in the genus *Sediminibacterium*, which hosts the $S_4I$ pathway but not the cSOx pathway. Here, dominance of the $S_4I$ pathway appears to be a response to the availability of thiosulfate, oxygen, and possibly nitrate ($E_6$ began with 1.39 mM $S_2O_3^{2-}$ and 1.77 mM $NO_3^{2-}$, Table 4.3). Because overall SOB populations constituted a lower fraction of the overall population with nitrate amendments (Fig 3.3), nitrate amendments may have stimulated competition from N-metabolising parts of the community and cause competition for resources with bacteria hosting the cSOx pathway.

In addition to $E_5$, three other mesocosms displayed all indicators of the cSOx pathway activity ($E_1$, $E_2$, and $E_8$), while $E_3$ displayed some indicators of the cSOx pathway except for an abundant host genus (see Table 4.3). Two other mesocosms also contained all indicators for activity of the first stage of the $S_4I$ pathway ($E_4$ and $E_7$; Table 4.3). Notably, unambiguous indicators of the $S_4I$ pathway Part 2 remain to be identified (Tanabe and Dahl 2022; Zhang et al. 2020).

In addition to indicators for activity of other pathways, only mesocosm $E_4$ (tailings, thiosulfate, and nitrate), displayed all indicators of the iSOx pathway, found in *Thiobacillus*, along with traces of the rDSR pathway in the mRNA analysis. The remaining mesocosms ($E_1$ and $E_3$: tailings; tetrathionate or thiosulfate, respectively; no nitrate) had indicators for the tetrathionate reductase *ttrABC*, and had most ($E_3$) or all ($E_1$) of the indicators for the rDSR pathway (Table 4.3).

Finally, mesocosms $E_7$ and $E_8$, which contained microbes with the capacity for cSOx and $S_4I$, were found to express all indicators of cSOx for $E_8$, and of $S_4I$ for $E_7$ as described above. The potential for the community in $E_8$ to facilitate tetrathionate reduction (*ttrABC* presence and expression) was not matched by a geochemical signal (tetrathionate loss), and so remains ambiguous.

### 4.4.2 Sulfur-Driven Acidity: Theoretical vs. Observed

To examine the effectiveness of the diagnostic strategy proposed above to identify possible sulfur pathways operating (Table 4.3), acidity generation relative to *soxCD* expression (required for the cSOx pathway, producing $H^+$ and sulfate) was evaluated (Fig 4.5). Consistent with immediate acid generation associated with the cSOx pathway, a positive relationship between *soxCD* activity (mRNA expression frequency) and proton yield ($\Delta H^+$) occurred in five of the eight mesocosms. Mesocosms $E_4$, $E_6$, and $E_7$, by contrast, developed a negative proton yield ($-\Delta H^+$) consistent with activation of the first portion of the $S_4I$ pathway (*tsdA*; see Table C6). In particular, $E_6$ displayed the largest $-\Delta H^+$ and the highest frequency of *tsdA* expression. Here, we assumed that expression frequencies of <25 were not significantly different from zero (i.e., background noise or contamination). Further work may better define a robust cut-off point to discriminate minimum *soxCD* expression and other pathway genes.

Because *soxCD* genes were active in five of the eight mesocosms, we compared the theoretical proton yields that would arise from thiosulfate oxidation by the cSOx pathway (i.e., 1 mole of $H^+$ generated from 1 mole of per mole of $S\text{-}S_2O_3^{2-}$; equation 1; Friedrich et al. 2001) with the actual proton yields calculated from the change in pH between $day_{1.25}$ and $day_{28}$ (Table 4.4). Actual proton yields were found to be much lower than theoretical across all mesocosms (Table 4.4). The relationship between $\Delta H^+$ and $\Delta SO_4^{2-}$ across all treatments was also extremely poor (Pearson r = 0.066, P = 0.88; Fig C2). Indeed, the observed acid generation could be accounted for by oxidation of only 0.1–1% of the thiosulfate to sulfate via the cSOx pathway, a scenario deemed unlikely (Table C6), and alkalinity did not account for the discrepancies (see section 4.2.2).

**Table 4.4** Theoretical vs. Actual Proton Yield from Amendment ($day_{1.25}$) to End ($day_{28}$)

| Mesocosm | $\Delta S\text{-}S_2O_3^{2-}$ (µM) | Predicted $\Delta H^+$ (µM) if cSOx* | Actual $\Delta H^+$ (µM) |
|---|---|---|---|
| $E_1$ | -550 | 550 | 5.6 |
| $E_2$ | -320 | 320 | 1.1 |
| $E_3$ | -1750 | 1750 | 0.8 |
| $E_4$ | -1060 | 1060 | -5.7 |
| $E_5$ | -1670 | 1670 | 1.3 |
| $E_6$ | -940 | 940 | -7.9 |
| $E_7$ | -340 | 340 | 0.0 |
| $E_8$ | -490 | 490 | 0.8 |

*When the calculations of protons released were reduced by the number of moles of S converted to either tetrathionate ($S_4I$ pathway) or elemental sulfur (iSOx or $S_4I$ pathway), and the proton sink of thiosulfate to tetrathionate conversions was accounted for, the predicted $\Delta H^+$ remained in the same order of magnitude as cSOx predictions (above), so were insufficient to explain the actual $\Delta H^+$.

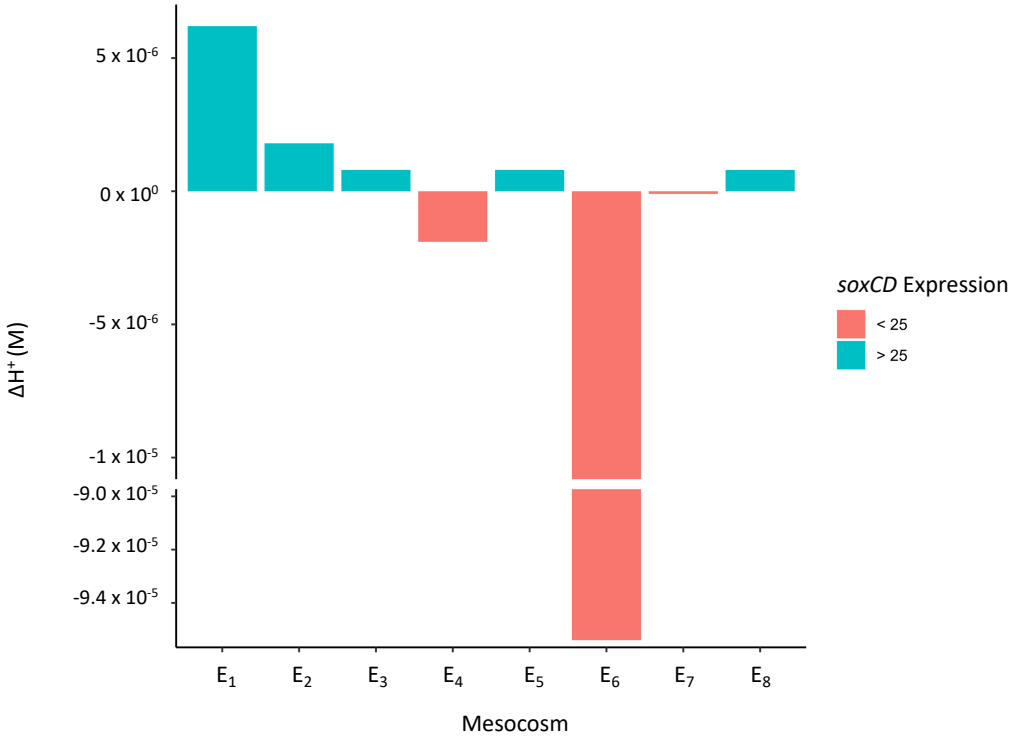


**Fig 4.5** The net proton yield vs. expression of *soxCD*. For the 8 mesocosms, the $\Delta H^+$ was calculated over the course of the experiment versus the gene expression of *soxCD* (>25 mean mRNA frequency detected at least once during the experiment), indicating the use of the cSOx vs. iSOx pathway. Note the y-axis break between $1.0\times10^{-5}$ M to $9.0\times10^{-5}$ M.

To account for the discrepancies in proton yield, it was reasoned that there must be one or more proton sink reaction(s) co-occurring with the acid generated via the cSOx pathway. While acidity generation was clearly linked to sulfur oxidation in the mesocosms, it is also possible that other independent cellular processes acted as proton sinks. These processes, for example, could include cell synthesis (equation 5), nitrogen fixation (equation 6), or nitrate reduction (equation 7) (Rittmann and McCarty 2001):

$$\tfrac{1}{2}\ CO_2 + 1/20\ NH_4^+ + 1/20\ HCO_3^- + H^+ + e^- \rightarrow 1/20\ C_5H_7O_2N + 9/20\ H_2O \quad (5)$$

$$N_2 + 8\ H^+ + 8\ e^- + 16\ ATP \rightarrow 2\ NH_3 + H_2 + 16\ ADP + 16\ P_i \quad (6)$$

$$5\ C_6H_{12}O_6 + 24\ NO_3^- + 24\ H^+ \rightarrow 30\ CO_2 + 42\ H_2O + 12\ N_2 \quad (7)$$

However, if we assume that proton-consuming reactions, in the same way as proton-generating ones, are linked to sulfur metabolism, the low rates of acid production suggest that proton-consuming and -producing sulfur-oxidizing reaction(s) may have approximately neutralized each other. Proton-consuming sulfur reactions are known to be used by SOB, such as the $S_4I$ Part 1 pathway (*tsdA*) paired with oxygen (facilitated, for example, by *Thiomonas* or *Halothiobacillus*), or the iSOx pathway (lacking SoxCD) paired with nitrate (facilitated by *Thiobacillus*, see Table C1).

### 4.4.3 Simultaneous Thiosulfate Oxidation Through Multiple Pathways

Simultaneous activity of proton-generating and -consuming reactions would minimize pH changes in the cytoplasm, thereby reducing the energetic cost to maintain homeostasis. Potential matching of proton-generating and -consuming processes could include cSOx + $S_4I$ Part 1, or $S_4I$ Part 1 + $S_4I$ Part 2 (Table 1.2, Table C1). To explore if simultaneous pathway activation could account for the observed proton yields, eight acid generation scenarios were simulated (Table C6). Each scenario consisted of different proportions of thiosulfate oxidation through cSOx, $S_4I$, and iSOx pathways (for simplicity, consistent fractions were assumed over the 28 days of the experiment, see Table C6). Theoretical sulfur oxidation scenarios that best fitted the measured $\Delta H^+$ included combinations such as 34% cSOx + 66% $S_4I$ (matching potential pathways detected

in $E_5$ and $E_6$, see Fig ) or 17% cSOx + 33% $S_4I$ + 50% iSOx (pathways detected in mesocosms $E_1$-$E_4$, see Fig 4.5), further suggesting simultaneous activity of the cSOx and $S_4I$ pathways.

Indeed, concurrent activation of the cSOx and $S_4I$ pathways was previously observed. *Paracoccus thiocyanatus SST* was observed to activate both pathways simultaneously (Rameez et al. 2020), although in that study, pH changes were not balanced between the two (10% cSOx, 90% $S_4I$ Part 1 led to net pH increase). Similarly, enzymes suggesting the parallel activation of the cSOx and potential later steps of the $S_4I$ pathway (*sorAB*) were also observed in the SOB bacterium *Starkeya novella* (formerly known as *Thiobacillus novellus*) when fed 40 mM thiosulfate (Kappler et al. 2001). Further, thiosulfate oxidation by the iSOx pathway (lacking SoxCD) and the rDSR pathway, occurring at the same time as the $S_4I$ pathway, was possible in *Allochromatium vinosum*; here, thiosulfate led to concurrent generation of sulfate (formed by upregulation of both iSOx and rDSR pathways) and tetrathionate (via the $S_4I$ pathway Part 1; Hensen et al. 2006). Together, these studies suggest that simultaneous pathway activation is possible, or even common, in SOB. However, little research exists to suggest when these pathways are activated together, and if their parallel use by specific SOB is employed as a strategy to minimize pH changes in their cytoplasm or aquatic environment.

However, when the proton-consuming side reactions accounting for the [$S^0$] and [$S_4O_6^{2-}$] measured in the mesocosms were added to the theoretical acid-yield model, they did not appreciably reduce predicted proton yields (Table 4.4). This could be caused by an underestimation of proton uptake by *tsdA*, because the actual [$S_4O_6^{2-}$] may have been greater than what was measured because of losses during prolonged sample storage (>1 year) or an underestimation of $S^0$ formation if excreted extracellular sulfur globules settled to the bottom of the mesocosms. Alternately, the proportion of the $S_4I$ pathway may also have been underestimated if $S_4O_6^{2-}$, once formed, continued to be oxidized via an acid-neutral or proton-consuming second stage of the $S_4I$ pathway (generating undetected SOIs), or reduced to thiosulfate via *ttrABC*. Unaccounted-for S could have contributed up to ~43.2% of the sulfur mass balance, indicating that additional unidentified SOI compounds were present.

The enzymes facilitating the latter half of the $S_4I$ pathway remain unclear (Rameez et al. 2020), and may occur in one or more stages (equation 8):

$$S_4O_6^{2-} + 3.5\ O_2 + 3\ H_2O \rightarrow 4\ SO_4^{2-} + 6\ H^+ \quad (8)$$

Some research suggests that $S_4O_6^{2-}$ disproportionation occurs as part of the $S_4I$ pathway, leading to $S^0$ formation (Table 1.3, Table 1.4, Table C1). This mechanism is sometimes attributed to *tetH* or *TTH*, genes detected in the metagenomes of *Thiobacillus* spp. found in the tailings impoundment used in this study (Camacho, Frazao, et al. 2020a; Beard et al. 2011). Alternately, research on the SOB *Erythrobacter flavus* suggests that in this species, genes *tsdA* and *soxB* play a role in $S^0$ formation via the $S_4I$ pathway (J. Zhang et al. 2020). Future research is required to determine whether tetrathionate oxidation occurs in a single enzyme-facilitated step, or over two or more steps. A multi-step process would allow the formation of other sulfur intermediates (pH neutral) before the onset of rapid acid generation, a phenomenon observed in preliminary mesocosm studies onsite in 2019 (Chapter 3).

### 4.4.4 Nitrate as a Possible Alternative to Oxygen for Sulfur Oxidation

Over the course of this experiment, oxygen fell below the conservative estimated lower limit where oxygen is exclusively used (0.5 mg/L, or 0.0156 mM) for approximately one-third of the experimental period in all mesocosms except for $E_6$. Nitrate, which was always present in all mesocosms at >0.04 mM, is also abundant in the tailings impoundment onsite (0.017–0.156 mM; Whaley-Martin et al. 2023).

When nitrate is used as the TEA, the theoretical $H^+$ yield is considerably lower. This impacts the $\Delta H^+$:$\Delta S$-$S_2O_3^{2-}$ ratio for any of the cSOx, complete $S_4I$, or iSOx and rDSR pathways (Table 1.2, Table C1). For example, with oxygen, the net proton yield of each is 1 mole of $H^+$ generated from 1 mole of S-$S_2O_3^{2-}$ oxidation (equation 1), while with nitrate, the net proton yield is 0 mole $H^+$ generated from 1 mole S-$S_2O_3^{2-}$ oxidation (equation 9):

$$S_2O_3^{2-} + 1\ H_2O + 2\ O_2 \rightarrow 2\ SO_4^{2-} + 2\ H^+ \qquad \Delta H^+/\ \Delta S = 1 \quad (1)$$

$$S_2O_3^{2-} + 2\ H_2O + NO_3^- \rightarrow 2\ SO_4^{2-} + NH_4^+ \qquad \Delta H^+/\ \Delta S = 0 \quad (9)$$

As a result, low oxygen conditions that favour nitrate pairing reduce the proton yield as reactive sulfur compounds are oxidized. Periods of low oxygen concentrations were detected in seven of the eight mesocosms, and $E_8$ displayed all indicators of $NO_3^-$ reduction (Table 4.3). Yet, in this mesocosm, observed $NO_3^-$ loss was not equal to the increase in $NH_4^+$. This ambiguity may be explained by heterotrophic activity (e.g., ammonia uptake), denitrification (conversion of nitrate to $N_{2(g)}$), and possibly autotrophic nitrogen fixation (although this was not supported by the mRNA analysis, as the *nif* gene activity was not detected).

Signals of nitrate use from the sulfur-metabolizing community (16S rRNA and mRNA) are more suggestive. Reports in the literature list *Halothiobacillus* (cSOx and $S_4I$), *Thiovirga* (cSOx), *Thiomonas* (cSOx and $S_4I$), and *Sediminibacterium* as strictly aerobic (Arsène-Ploetze et al. 2010; Chen et al. 2004; Kang et al. 2014; Kim et al. 2016; Sievert et al. 2000; Song et al. 2017; Wood et al. 2005); *Acidovorax* ($S_4O_6^{2-}$ reduction) and *Desulfurivibrio* (rDSR) as strictly anaerobic (Pantke et al. 2012; Carlson et al. 2013; Thorup et al. 2017; Sun et al. 2022); and *Thiobacillus* (iSOx, rDSR, and $S_4I$) and *Sulfurovum* (cSOx) as facultative anaerobes [(Beller et al. 2006; Ghosh and Dam 2009; Inagaki et al. 2004; Jong et al. 1997; Meier et al. 2017; Mori et al. 2018) Table C7)]. These categorizations are suggestive of nitrate use, although exceptions exist. Whaley-Martin et al. (2023) classified *Halothiobacillus*, collected from the same tailings impoundment as this study, as a strict aerobe; however, some species contained partial *nir* and *nor* genes associated with nitrite reduction, a function also recently reported (Magnuson et al. 2023). Likewise, one species of *Thiomonas* was reported to host a nitrate reductase gene, suggesting that facultative anaerobic respiration may be available to some species in the genus (Arsène-Ploetze et al. 2010).

Strictly anaerobic *Acidovorax* ($S_4O_6^{2-}$ reduction) and *Desulfurivibrio* (rDSR) were detected in several mesocosms, and gene expression indicating nitrate use (*nap* and *nar* genes) was detected in all mesocosms. $E_8$ had particularly high gene expression towards the end of the experiment. In addition, the abundance of the facultative anaerobe *Thiobacillus* (containing the iSOx + rDSR pathway) appears to be linked to low oxygen availability and may indicate a pairing of nitrate with the rDSR pathway, as recently proposed (K. J. Whaley-Martin et al. 2023). Thermodynamic theory supports the pairing of nitrate with the iSOx + rDSR pathway (Klatt and Polerecky 2015). Other studies have discussed the presence of nitrate-dependant thiosulfate oxidation in

*Thiobacillus denitrificans*, noting that this species stores elemental sulfur globules because ZVS formation is generally much more rapid than its subsequent oxidation (Jiang et al. 2009; Schedel and Trüper 1980; Zhang et al. 2019). In addition, *nap* and *nar* genes were found to be expressed in the microbial communities from all mesocosms, which further indicates nitrate reduction. Whether used by strict or facultative anaerobes, nitrate pairing has the potential to reduce acidity if anoxic conditions are maintained; however, if the ZVS discharged is produced under anoxic conditions, exposure of ZVS-containing SOB to oxic conditions could result in acidity generation.

## 4.5 Conclusions

This study demonstrates how a new diagnostic approach integrating three lines of evidence collected at different frequencies (physiochemistry/geochemistry, 16S rRNA gene sequences linked to metagenomes, and gene expression) enabled the identification of which microbial sulfur oxidation pathways were operating under varying environmental conditions and their influences on S geochemical outcomes. All three known sulfur biochemical pathways: cSOx, $S_4I$, and iSOx (lacking SoxCD) followed by rDSR occurred in the study of eight experimental mine wastewater mesocosms. This integrated assessment approach identified parallel pathway operation, which resulted in lower acid-sulfate ratios than those theoretically predicted. This approach offers a more complete understanding of tailings impoundment S geochemistry and the potential risks that it causes, as well as the factors associated with pathway dominance. Here, variations in conditions within concentration ranges commonly observed in an active base metal mine tailings impoundment led to cSOx pathway expression and parallel use of $S_4I$ and/or iSOx pathways. Results linking the mRNA analysis and $\Delta H^+$ from these experiments also indicate that SoxCD is a potential indicator for direct oxidation and acid generation via the cSOx pathway, although the proton balance is moderated by other factors, such as multiple pathway activities and the use of nitrate by some sulfur-oxidizing bacteria under low oxygen conditions.

# 5

# Beyond SOx: Mining Sulfur Bacteria Produce Low Proton Yields due to Unidentified Enzyme Pathways

*"But nature is an intricate jigsaw puzzle, and every piece matters."*

*~ Shannon Messenger*

## Abstract

When thiosulfate is abundant, recent research indicates that the complete Sulfur Oxidation (cSOx) pathway is prevalent in oxic wastewater, while the incomplete Sulfur Oxidation and reverse Dissimilarity Sulfur Reduction (iSOx + rDSR) pathway has been found to be active under suboxic conditions, paired with nitrate reduction. However, both (i) the activity of $S_4I$ or other enzyme systems and (ii) the suboxic sulfur reactions which occur when the rDSR pathway is not present in an SOB community remain unexplored. During this study, a series of 6 L benchtop microcosms were inoculated with *Halothiobacillus spp.*-dominated (containing cSOx and $S_4I$ pathways) sulfur oxidizing bacterial (SOB) communities preserved from an active tailing reservoir. The 16 microcosms were provided with high concentrations of the sulfur oxidation intermediate (SOI) compounds thiosulfate or tetrathionate under oxic and suboxic conditions to amplify the acid generating processes. The study identifies *Halothiobacillus*, *Thiomonas,* and *Pandoraea*, as the key SOB genera processing SOI. These microcosms demonstrate that the protons yields resulting from thiosulfate oxidation by SOB are less than half of those predicted for complete thiosulfate oxidation. Despite adjustments for ion activity and $PO_4^{2-}$ buffering, this difference is indicative of mechanisms beyond cSOx. Further, when offered tetrathionate under oxic conditions, undescribed reactions unmatched to known sulfur enzymes were likely employed, since disproportionation is insufficient to explain observations. Meanwhile, suboxic depletion of thiosulfate, without changes in nitrate or nitrite concentrations sufficient to indicate their use as TEA requires further investigation.

## 5.1 Introduction

Mine wastewater systems contain communities of sulfur-oxidizing bacteria (SOB) that influence the fate of sulfur oxidation intermediates (SOI) and resulting acidity [(K. J. Whaley-Martin et al. 2023b; K. Whaley-Martin et al. 2019; Miettinen et al. 2021; Lopes et al. 2020; Twible et al. 2024), Chapter 4]. Thiosalts ($S_nO_x^{2-}$, common forms of SOI compounds containing combinations of sulfur and oxygen) are generated during milling processes and are a water quality concern for metal mines (Musuku et al. 2023; Miranda-Trevino et al. 2013). However, other than the field research mentioned above, few studies link a metagenomic understanding of sulfur oxidation with metal mine wastewater systems (Table D1). Instead, most genetic studies consider acidophilic genera and their contributions to acid rock drainage (ARD) or applications for bioleaching (Camacho, Jessen, et al. 2020; R. Wang et al. 2019; Watling et al. 2014; X.-G. Chen et al. 2004; Bugaytsova and Lindström 2004; Opara et al. 2023; Pakostova et al. 2022; Denef, Mueller, and Banfield 2010; Grettenberger, Havig, and Hamilton 2019; Hua et al. 2015; L. Chen et al. 2015).

The SOB communities identified in circumneutral wastewater from metal mines processing sulfidic ores include key genera such as *Halothiobacillus, Thiomonas, Thiobacillus, Thiovirga, Sulfuricurvum, Sulfurovum,* and *Desulfurivibrio* [(K. Whaley-Martin et al. 2023, 2019; Miettinen et al. 2021; Lopes et al. 2020), Chapter 4]. These genera metabolically oxidize SOI via three sulfur oxidation pathways: the complete sulfur oxidation (cSOx), the incomplete SOx and reverse dissimilatory sulfur reduction (iSOx + rDSR), or the tetrathionate intermediate ($S_4I$) [Chapter 4, (Friedrich et al. 2001; Ghosh and Dam 2009; Wasmund, Mußmann, and Loy 2017; Watanabe et al. 2019; K. Whaley-Martin et al. 2023)]. The cSOx pathway is common in mine systems where thiosulfate is ubiquitous in processed tailings from sulfidic ore (equation 1):

$$\text{cSOx: } S_2O_3^{2-} + H_2O + 2\ O_2 \rightarrow 2\ SO_4^{2-} + 2\ H^+ \qquad \Delta H^+ : \Delta SO_4^{2-} = 1:1 \quad (1)$$

Geochemical studies focusing on sulfur oxidation in mine wastewater communities suggest that the cSOx pathway is dominant in the oxic epilimnion of mine wastewater systems where the community also lacks the enzymes required to couple thiosulfate oxidation with nitrate reduction (K. Whaley-Martin et al. 2023; Twible et al. 2024). Yet, as thiosulfate is consumed by *Halothiobacillus* and *Acidithiobacillus* in these systems, it fails to produce an observed $\Delta H^+$: $\Delta SO_4^{2-}$ of 1:1 which would be expected from activity of the cSOx pathway [(K. Whaley-Martin

et al. 2019; Bernier and Warren 2007; Camacho, Jessen, et al. 2020; Warren, Norlund, and Bernier 2008), Chapter 4]. Whaley-Martin et al. (2019) isolated and cryopreserved communities from an active tailings impoundment which comprised ~76–100% *Halothiobacillus*. Because the flasks were open to the atmosphere, the SOB reactions were assumed to occur under oxic conditions, yet the $\Delta H^+$: $\Delta SO_4^{2-}$ fell well below the theoretical cSOx ratio [(K. Whaley-Martin et al. 2019)]. These SOB communities were used as inocula for this study to explore the phenomenon, perhaps due to $S_4I$ pathway activity, further.

While the detailed mechanisms of the cSOx pathway are well established, there is a lack of consensus about the enzymatic stages of the $S_4I$ pathway (Table 1.5). Only the first stage of the $S_4I$ pathway is universally agreed upon: the oxidative condensation of two thiosulfate molecules into tetrathionate facilitated by thiosulfate dehydrogenase (TsdA), or occasionally DoxDA, in wide range of genera such as *Paracoccus thiocyanatus*, *Allochromatium vinosum*, *Campylobacter jejuni*, *Erythrobacter flavus*, and *Acidithiobacillus ferrooxidans*, see equation 2 (Müller et al. 2004; Brito et al. 2015; Jenner et al. 2019; Rameez et al. 2020; J. Zhang et al. 2020; Q. Yu, Sun, and Gao 2021; Du et al. 2022):

$$\text{TsdA/DoxDA: } 2\ S_2O_3^{2-} + 2\ H^+ + ½\ O_2 \rightarrow S_4O_6^{2-} + H_2O \quad (2)$$

The widespread occurrence of *tsdA* across SOB genera, including *Halothiobacillus,* suggests that the $S_4I$ pathway often occurs in mine wastewater systems in both Canada and Spain, a mechanism that has been previously overlooked [(Miettinen et al. 2021; K. Whaley-Martin et al. 2023) Chapter 4]. Following tetrathionate formation by TsdA, TetH and SoxB have both been proposed as mechanisms for the second stage, and it is an open question whether zero valent sulfur (ZVS) can form during the $S_4I$ pathway {Table D2 (Pyne et al. 2018; Cai et al. 2022)}.

This study used a series of 16 benchtop laboratory microcosms inoculated with SOB communities that had been cryogenically preserved from two depths of an active mine tailings impoundment (Whaley-Martin et al. 2019). The microcosms — grown with high density SOB populations, offered high concentrations of thiosulfate or tetrathionate, and monitored for changes in sulfur speciation and acidity generation — were designed to isolate and amplify the acid-generating phenomenon observed on site in field and mesocosm experiments (K. Whaley-Martin et al. 2023)

(Chapter 4). The experiments then explored (i) if acid and sulfate generation aligned with theoretical ratios for SOI oxidation, (ii) the roles of oxygen and nitrate as electron acceptors for sulfur oxidation, and (iii) if communities initially dominated by *Halothiobacillus* spp. have sulfur enzymes (a tetrathionate amendment targeted the $S_4I$ pathway) that function alongside or instead of the cSOx pathway. By exploring aspects of microbial sulfur oxidation, this research seeks to understand how sulfur metabolism affects acidity generation in mine site wastewaters and to provide a theoretical basis for proactive management. To the best of our knowledge, only two other studies explores a metagenomic understanding of sulfur metabolism of SOB communities isolated from circumneutral mine wastewaters, considering both their capacity for thiosalt oxidation and the geochemical products of their sulfur pathways (Twible et al. 2024; Liu et al. 2025).

## 5.2 Methods

The following section describes the experimental design, sampling, analysis and calculations performed on mixed SOB cultures. The isolated SOB cultures were from the oxidation reservoir of an active tailings impoundment, cryopreserved, and regrown in benchtop microcosms.

### 5.2.1 Experimental Design Benchtop 6 L Microcosms

A series of 16 benchtop microcosms were used to explore the $S_4I$ pathway reactions (under oxic and suboxic conditions) in *Halothiobacillus*- and *Thiomonas*- dominated communities using pH, sulfur speciation and 16S rRNA gene expression data. The microcosms were staged over three experiments (Experiments A, B, and C) for feasibility, and high concentrations of sulfur amendments were employed to exaggerate the acid-generating phenomenon observed on site. Experiments A, B, and C were performed on the laboratory benchtop in 6 L glass Erlenmeyer flasks (6000 mL Pyrex No. 1980), autoclaved for sterility, and filled to capacity with 6 L of SOB medium (0.1-µm filtered for sterility using ThermoScientific™ Nalgene™ Rapid-Flow™ Sterile Disposable Filter Units with PES membrane) containing 2.0 mM $MgSO_4$, 0.2 mM $NH_4Cl$, 1.4 mM $K_2HPO_4$, 8.3 mM $NaNO_3$, and a trace element solution (Camacho, Jessen, et al. 2020) in all experiments (Fig 5.1). Microcosms were then inoculated with 2 or 10 m SOB communities, and fitted with HOBO data logger probes (sterilized with 70% vol/vol ethanol) for continuous DO and

pH measurements (DO: HOBO® U26-001, and pH: HOBO® MX2501, Fig 5.1). Note, the pH loggers were used to log data every 60 seconds throughout all experiments. However, the dissolved oxygen (DO) data loggers were used to collect oxygen concentrations at $t_0$ and $t_{end}$ of Experiments A and B; in Experiment C, methodology was improved to allow DO-logging at 60-s intervals. Sample tubing (Crack-Rst Polyethylene-Lined EVA tubing for Food & Beverage, sterilized in 70% vol/vol ethanol) was then placed in the microcosms, and the tops were sealed with ethanol-sterilized Parafilm ® M P 7793.

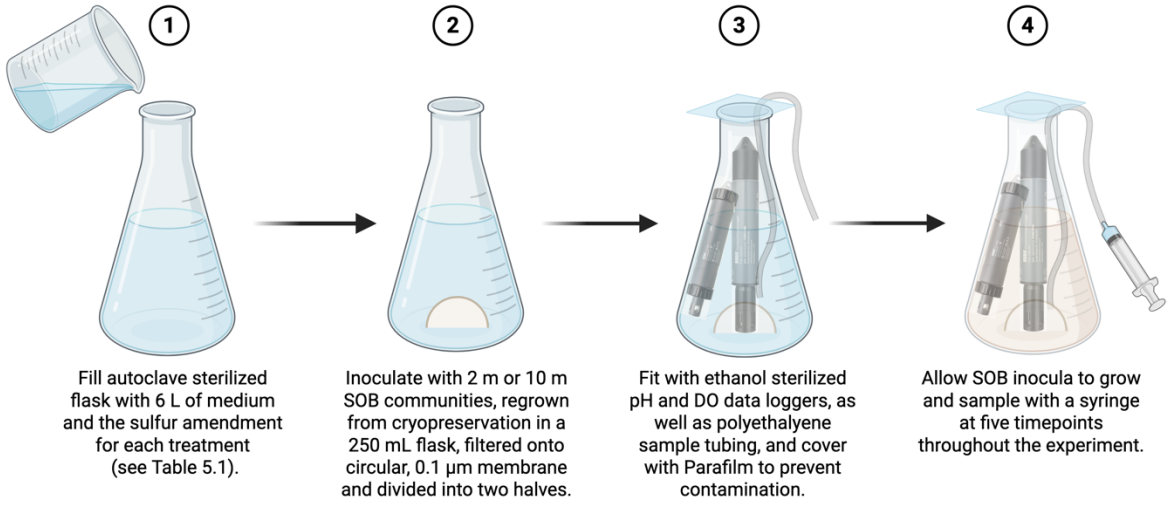


Fig 5.1 Microcosm setup for Experiments A, B, and C. The diagram above indicates the steps taken to assemble the probes, sample tubes and inocula in each of the 16 experimental microcosms. The HOBO DO data loggers were used to collect oxygen concentrations at $t_0$ and $t_{end}$ of Experiments A and B; in Experiment C, methodology was improved to allow DO-logging at 60-s intervals.

Sulfur amendments, which varied by experiment, were dissolved in Milli-Q ultrapure filtered water. Sulfur amendments were 8.0 mM S-$S_4O_6^{2-}$ (as $K_2S_4O_6$) in Experiments A and B and 11.4 mM S-$S_2O_3^{2-}$ (as $Na_2S_2O_3$) in Experiment C (Table 5.1). Microcosms were then inoculated with *Halothiobacillus*-dominated SOB communities collected from two depths of an oxidation reservoir on an active mine site in September 2017 (2 m and 10 m), cryopreserved, and regrown in similar media, resulting in treatments described in (Table 5.1).

Table 5.1 Experimental Treatments for 16 Microcosms from 2022

| Experiment | Treatment | [SOI] (mM) | [$NO_3^-$] (mM) | Rep |
|---|---|---|---|---|
| A | Abiotic Control (no SOI) | - | 8.3 | - |
| A | Abiotic Control + Tetrathionate | 8.0 S-$S_4O_6^{2-}$ | 8.3 | - |
| A | 2 m SOB (No SOI) | - | 8.3 | R1 |
| A | 2 m SOB (No SOI) | - | 8.3 | R2 |
| A | 2 m SOB + Tetrathionate | 8.0 S-$S_4O_6^{2-}$ | 8.3 | R1 |
| A | 2 m SOB + Tetrathionate | 8.0 S-$S_4O_6^{2-}$ | 8.3 | R2 |
| B | 10 m SOB (No SOI) | - | 8.3 | R1 |
| B | 10 m SOB (No SOI) | - | 8.3 | R2 |
| B | 10 m SOB + Tetrathionate | 8.0 S-$S_4O_6^{2-}$ | 8.3 | R1 |
| B | 10 m SOB + Tetrathionate | 8.0 S-$S_4O_6^{2-}$ | 8.3 | R2 |
| C | 2 m SOB + Thiosulfate | 11.4 S-$S_2O_3^{2-}$ | 8.3 | R1 |
| C | 2 m SOB + Thiosulfate | 11.4 S-$S_2O_3^{2-}$ | 8.3 | R2 |
| C | 10 m SOB + Thiosulfate | 11.4 S-$S_2O_3^{2-}$ | 8.3 | R1 |
| C | 10 m SOB + Thiosulfate | 11.4 S-$S_2O_3^{2-}$ | 8.3 | R2 |
| C | Abiotic Control + Thiosulfate | 11.4 S-$S_2O_3^{2-}$ | 8.3 | R1 |
| C | Abiotic Control + Thiosulfate | 11.4 S-$S_2O_3^{2-}$ | 8.3 | R2 |

(-) indicates no amendment of this type added to the mesocosm.

These *Halothiobacillus*-dominated communities were similar to those used to inoculate the 500 L mesocosms, but were collected from the tailings impoundment and cryopreserved the previous year. A few days prior to the initiation of each experiment, the cryopreserved SOB community was resuscitated by thawing and placing it into a 500 mL, autoclave-sterilized glass flask filled with 500 mL of medium (recipe above, amended with either thiosulfate or tetrathionate to match the experimental treatment). To inoculate the microcosms with these communities, cultures were filtered onto 0.1-µm paper filters using sterile filter columns (ThermoScientific™ Nalgene™, see above). The filter paper with microbial biofilm was cut in two, and one semi-circle was transferred into each of the two replicates of the sterile microcosms using tweezers (sterilized in 70% vol/vol ethanol for two minutes) inside a biological safety cabinet.

In Experiment C, where suboxic conditions were encountered, two additional tests for DO diffusion into the microcosms were performed. First, a replicate of the 6 L flask was filled with 5 L of thiosulfate-amended medium and inoculated with an SOB community. Once suboxic conditions were reached at the normal probe depth (10 cm from the base of the 6 L flask), DO concentrations were measured at 20 cm from the base and <1 cm below the surface of the media to ensure that probe readings at these depths were also suboxic. Second, a sterile flask filled with

MilliQ water was sparged with $N_2$ (g) for 25 min to achieve suboxia, and a DO data logger was used to check for oxygen ingress from atmospheric diffusion over 24 h (compared against a control of open water).

### 5.2.2 Sampling Strategy

Samples for sulfur speciation ($S^0$, $S_2O_3^{2-}$, $SO_3^{2-}$, $SO_4^{2-}$, and Total S) were collected for five timepoints ($t_0$, $t_1$, $t_2$, $t_3$, $t_4$, and $t_{end}$) in all Experiments (A, B, and C); samples for $HS^-$ concentrations were collected for all timepoints in Experiments A and B, but could not be measured in Experiment C because of the high biomass. Sampling frequency was decreased in Experiment C as acid generation occurred less rapidly. Samples for nitrogen speciation ($NO_2^-$, $NO_3^-$, and $NH_4^+$) were taken at the timepoints in Experiment C where suboxic conditions were established.

### 5.2.3 Geochemical Analysis of Sulfur and Nitrogen

In all benchtop experiments, samples were collected using a syringe (Fisherbrand 60 mL plastic syringe, rinsed with water from the mesocosm prior to sampling) to draw water from the microcosms via silicon tubing (Crack-Rst Polyethylene-Lined EVA tubing for Food & Beverage, ¼″). Samples were filtered, when necessary, with a 0.2-µm tip and immediately preserved in the fridge or freezer; ion chromatograph samples were 0.2-µm filtered; ICP-OES samples were unfiltered and acid preserved (0.02% $HNO_3$); HPLC samples were frozen unfiltered. Concentrations of sulfate, nitrate, nitrite, and ammonia, were measured in 0.2-µm filtered samples using Thermo Scientific Dionex ICS-6000 for ion chromatography (see sections 2.5 and 5.2.3). Shimadzu LC-20AD Prominence high performance liquid chromatography was used to measure thiosulfate and sulfite {monobromobimane derivatization method (Rethmeier et al. 1997)} and elemental sulfur (chloroform extraction method); and a ThermoFisher Scientific inductively coupled plasma–optical emission spectrograph (ICP-OES) was employed for total sulfur analyses on unfiltered samples, using detection wavelength of 180.731 nm (radial view). Samples for $S^0$ analysis for Experiments A and B were performed according to the methods outlined in Whaley Martin et al (2020) and Yan et al (2022). However, after processing the first replicate of $S^0$ samples from Experiment C, HPLC performance was improved by adding a 20-min sonication step, following redissolving the extracted $S^0$ in chloroform, prior to filtering through 0.2-µm PTFE

tips. This resulted in a method that was only semi-quantitative. Sulfide samples were quantified using a HACH spectrophotometer using the Methylene Blue Method 8131.

### 5.2.4 DNA Extraction, Gene Amplicon Sequencing and Analyses

DNA was collected by filtering 0.5 L of water from the microcosms through 0.1-µm filters using sterile filter columns (Thermo Scientific™ Nalgene™ Rapid-Flow™ Sterile Disposable Filter Units with CN Membrane) and immediately excising and freezing the filter paper. Water was transferred into filter columns using a syphon, and DNA extractions were performed in a UV-sterilized biological safety cabinet using the Qiagen's DNeasy PowerWater DNA Isolation Kit using the standard protocol.

Illumina MiSeq region V4 amplicon sequencing was performed at McMaster University's Metagenomics Facility (Hamilton, Ontario) as described in section 3.2.8 above. Once extracted, the DNA were quantified and the 515F/806R primer set was used to amplify the 16S V4 region and dual-indexed Illumina adapters were added to the amplicons. The amplicons were then quality-assessed via agarose gel electrophoresis before being normalized using a SequelPrep normalization kit. The resulting sequences were filtered and trimmed using Cutadapt (with a minimum "Q30" Phred quality score, indicating that likelihood of an incorrect base call is less than 1/1000). Fastq read files were filtered to a trimmed length (240 bp in the forward direction and 160 bp in the reverse direction) and processed according to the DADA2 pipeline (version 3.1.6) to remove bimeras and chloroplast or mitochondrial sequences. Taxonomy was then assigned using to SILVA database (version 138.1) and R (version 4.4.4) in RStudio (version 1.2).

### 5.2.5 Proton Yield Calculations

Hydrogen ion concentrations ($[H^+]$) and their changes with time $[\Delta H^+]$, were calculated according to equations 3:

$$pH = -\log_{10}[H^+] \quad (3)$$

This simplification is accurate within the range of 80 - 100 %, as:

$$[H^+] = 10^{-pH/\gamma} \quad (4)$$

The ion activity coefficient ($\gamma\pm$) was estimated for the solution with a low ionic strength (I <0.1 M) of I ~ 0.03-0.05 molal (given a media of 2.0 mM $MgSO_4$, 0.2 mM $NH_4Cl$, 1.4 mM $K_2HPO_4$, 8.3 mM $NaNO_3$, and 2.0 mM $S_4O_6^{2-}$ or 5.7 mM $S_2O_3^{2-}$), according to the Davis equation, equation 5:

$$\log(\gamma\pm) = -0.5\ z_1\ z_2\ \left(\frac{\sqrt{I}}{1+\sqrt{I}} - 0.30I\right) \quad (5)$$

Where $z_1$ and $z_2$ are ion charges, and I is ionic strength, and 0.5 is the temperature dependant coefficient (A) at 25°C (Stumm and Morgan 1995). This produces an activity coefficient of ~0.82-0.85. The range of 80 - 100 % is represented as field of potential concentrations in figure 5.3.

As a result, the conversion allows for a stoichiometric exploration of $H^+$ - S ratios, accurate within the range of 80 - 100 %, as per equation 6.

$$\Delta[H^+] = [H^+] \text{ at } t_{end} - [H^+] \text{ at } t_0 \quad (6)$$

To account for the magnitude of phosphate and carbonate buffering in the biotic systems, the buffering capacity was calculated. Based on an initial concentration of 1.4 mM $K_2HPO_4$ in the media at pH ~7, and the $[HPO_4^{2-}] / [H_2PO_4^-] = 1.38$ ratio (from the pKa = 6.86), the concentrations of the acid ($H_2PO_4^-$) would theoretically be 0.6 mM, and the conjugate base ($HPO_4^{2-}$) would be 0.8 mM at the beginning of the microcosm experiments. Since 1 mole of $HPO_4^{2-}$ can neutralize 1 mole $H^+$, this would mean that 0.8 mM $H^+$ could be neutralized in the media before the buffer is fully exhausted. When incorporating similar calculations for carbonate buffering, the total buffering capacity ($\beta$) of the media ranged from $\beta$ = 0.01 - 2.8 (VMinteq version 4.1 calcs, Dr. Simon Apte, personal correspondence):

$$\Delta pH = \Delta n / \beta \quad (7)$$

Where $\Delta n$ is the number of moles of an acid added to solution; $\beta$ is buffer capacity; $\Delta pH$ is the difference between the initial pH of the buffer and the pH of the buffer after the addition.

The VMinteq modeling was performed in version 4.1 by assuming a gas equilibrium with atmospheric $CO_2$ (a function under the menu "gases") and calculating buffering via a mass balance at 22°C (in correspondence with Simon Apte). The resulting calculations for buffering in

the media indicated that this buffering would produce gradual pH changes above pH 6.8 (when $[HPO_4^{2-}] / [H_2PO_4^-] = 1$) would be expected, accelerating slightly to 5.5 (Fig D1). After this point the buffer should be fully exhausted, and the pH can be expected to drop sharply if acid generation continues (Fig D1).

Therefore, the $\Delta[H^+]$ value used in figure 5.4 was calculated using VMinteq outputs as a single value. This VMinteq output would be equal to approximately (equation 8):

$$\text{VMinteq output} = \Delta[H^+] = [H^+] \text{ at } t_{end} - [H^+] \text{ at } t_0 + H^+ \text{ consumed by buffer} \quad (8)$$

The $\Delta[H^+]$ was then used to calculate a proton yield by mole of sulfate produced through SOI oxidation ( $\Delta H^+ : \Delta SO_4^{2-}$ ).

### 5.2.6 Statistical Analyses

Statistical analyses were carried out in R version 4.4.4, utilizing the Vegan package version 2.6.4. The analyses were carried out on triplicate samples for geochemistry, unless noted, with standard deviation calculated on mean analytical data from triplicate injections. “Less than detection limit” chemical or biological data were treated as zero for statistical analyses. Data were displayed using Ggplot, and the methods figure was created in BioRender.

Treatments were frequently performed in duplicate. Although low replicate sizes limit the strength of statistical analysis, a duplication of trends in sulfur speciation or pH changes provided some reassurance that observed phenomena were a result or treatments and not random variability. Where replicates showed a unique behaviour (example: Fig 5.3, Experiment C), this was interpreted as due to differences in the dominate microbial community.

## 5.3 Results

A summary of the geochemical data can be found in Table 5.2, and the complete dataset (sulfur speciation, nitrogen speciation, oxygen and pH) in Table D2. Table 5.2 summarizes $t_0$ and $t_{end}$ data from the 16 microcosms, with a sulfur mass balance calculated from the sulfur species quantified: [$HS^-$], [$S^0$], [$S\text{-}S_2O_3^{2-}$], [$SO_3^{2-}$], and [$SO_4^{2-}$]. The standard error from the tetrathionate ($S_4O_6^{2-}$) analysis was too high for reliable reporting; therefore, these data were omitted from the geochemical dataset. Although this limits the exploration of the later stages of the $S_4I$ pathway, changes in the remaining sulfur species nonetheless produced some interesting findings, described below.

### 5.3.1 Sulfur Speciation Patterns

In the four tetrathionate-amended microcosms with SOB (Experiments A and B), sulfate concentrations increased consistently (mean $\Delta SO_4^{2-}{}_{2m} = 1.55 \pm 0.29$ mM; mean $\Delta SO_4^{2-}{}_{10m} = 1.14 \pm 0.55$ mM on filtered samples, Fig 5.2, Table D2). There was some variability between reps in the speed of sulfate formation, with an early spike in sulfate concentration detected in one of the 10 m SOB communities. Yet, the overall increases of [$SO_4^{2-}$] were in the same order of magnitude across replicates, accounting for <20% of the 8.0 mM $\Delta S\text{-}S_4O_6^{2-}$ amendment (Fig 5.2, Table D2). This suggests either tetrathionate ($S_4O_6^{2-}$) remained unmetabolized, or other polythionates (e.g., $S_3O_6^{2-}$, $S_5O_6^{2-}$) formed during tetrathionate oxidation. In addition to sulfate formation, small increases in thiosulfate were measured at the midpoints of the tetrathionate-amended microcosms from both depths (mean $\Delta S\text{-}S_2O_3^{2-}{}_{2m} = 0.24 \pm 0.01$ mM; mean $\Delta S\text{-}S_2O_3^{2-}{}_{10m} = 0.28 \pm 0.01$ mM, Fig 5.2). Yet, at its highest concentrations, molar $S\text{-}S_2O_3^{2-}$ evolution accounted for <0.04% of the 8.0 mM $S\text{-}S_4O_6^{2-}$ amendments, not substantially change the fraction of detected sulfur species. Tetrathionate data was of too low quality to be included in the analysis.

**Table 5.2** Summary of Geochemical Data from 16 Microcosms*

| Exp | Treatment | Hours | pH | DO (mM) | $S^0$ (mM) | $S\text{-}S_2O_3^{2-}$ (mM) | $SO_3^{2-}$ (mM) | $SO_4^{2-}$ (mM) | Σ S (mM) | Total S (mM) | % S Unidentified |
|---|---|---|---|---|---|---|---|---|---|---|---|
| A | Abiotic Control (No SOI) | 0 | 7.73 | 0.28 | 0.14 | nd | nd | 1.54 | 1.67 | 2.1 | 20 |
| | | 74 | 7.00 | 0.20 | nd | nd | nd | 1.93 | 1.93 | 2.1 | 8 |
| A | Abiotic Control + 8.0 mM $S\text{-}S_4O_6^{2-}$ | 0 | 7.84 | 0.27 | 0.01 | nd | nd | 1.11 | 1.12 | 9.4 | 88 |
| | | 74 | 7.00 | 0.23 | nd | nd | nd | 1.74 | 1.74 | 9.0 | 80 |
| A | 2 m SOB (No SOI) Rep 1 | 0 | 7.68 | 0.27 | 0.01 | nd | nd | 1.88 | 1.89 | 2.2 | 14 |
| | | 74 | 7.34 | 0.06 | nd | nd | 0.02 | 2.08 | 2.10 | 2.3 | 8 |
| A | 2 m SOB (No SOI) Rep 2 | 0 | 7.91 | 0.28 | nd | nd | nd | 1.53 | 1.53 | 2.0 | 23 |
| | | 74 | 7.00 | 0.04 | nd | nd | nd | 1.86 | 1.86 | 2.0 | 6 |
| A | 2 m SOB + 8.0 mM $S\text{-}S_4O_6^{2-}$Rep 1 | 0 | 7.91 | 0.26 | nd | nd | nd | 1.33 | 1.33 | 9.7 | 86 |
| | | 74 | 3.29 | 0.08 | nd | nd | nd | 3.00 | 3.00 | 9.7 | 69 |
| A | 2 m SOB + 8.0 mM $S\text{-}S_4O_6^{2-}$Rep 2 | 0 | 7.92 | 0.27 | nd | nd | nd | 1.97 | 1.97 | 10.0 | 80 |
| | | 74 | 3.29 | 0.09 | nd | nd | 0.02 | 3.41 | 3.42 | 10.1 | 66 |
| B | 10 m SOB (No SOI) Rep 1 | 0 | 7.93 | 0.25 | nd | nd | nd | 1.61 | 1.61 | 1.7 | 7 |
| | | 70.5 | 7.06** | 0.08 | nd | nd | nd | 1.79 | 1.79 | 2.4 | 23 |
| B | 10 m SOB (No SOI) Rep 2 | 0 | 7.92 | 0.26 | nd | nd | nd | 1.69 | 1.69 | 2.3 | 27 |
| | | 70.5 | 7.00** | 0.06 | nd | nd | nd | 1.56 | 1.56 | 2.2 | 30 |
| B | 10 m SOB + 8.0 mM $S\text{-}S_4O_6^{2-}$Rep 1 | 0 | 7.92 | 0.25 | nd | nd | nd | 1.76 | 1.76 | 10.2 | 82 |
| | | 70.5 | 3.12** | 0.10 | nd | nd | nd | 3.03 | 3.03 | 10.0 | 69 |
| B | 10 m SOB + 8.0 mM $S\text{-}S_4O_6^{2-}$Rep 2 | 0 | 7.78 | 0.27 | nd | nd | nd | 1.56 | 1.56 | 10.2 | 85 |
| | | 70.5 | 3.23** | 0.10 | nd | nd | nd | 2.56 | 2.56 | 10.4 | 75 |

nd = non-detect

$[HS^-]$ was below detection limit in experiments (A) and (B), NA for exp C). TotS values on unfiltered samples showed no decrease between $t_0$ and $t_{end}$ in all microcosms.

Note: the value for Σ S = Σ $[S^0]$ + $[S\text{-}S_2O_3^{2-}]$ + $[SO_3^{2-}]$ + $[SO_4^{2-}]$, and % S Unidentified = (Total S - Σ S)/Tot S * 100 %

*For complete geochemistry, including standard deviation values, see Table D2.

** For this summary, values from 68 h were used as an approximation, as $t_{end}$ data (70.5 hours) was not available. Initial estimated pH of 7.9 for 10 m SOB + Tetra Rep 2 was estimated from the value measured 1 h after $t_0$, as $t_0$ data was missing.

**Table 5.2 cont.** Geochemical Summary from 16 Microcosms*

| Exp | Treatment | Hours | pH | DO (mM) | $S^0$ (mM) | $S\text{-}S_2O_3^{2-}$ (mM) | $SO_3^{2-}$ (mM) | $SO_4^{2-}$ (mM) | Σ S (mM) | Total S (mM) | % S Unidentified |
|---|---|---|---|---|---|---|---|---|---|---|---|
| C | 2 m SOB + 11.4 mM $S\text{-}S_2O_3^{2-}$ Rep 1 | 0 | 8.11 | 0.28 | 0.07 | 13.42 | nd | 1.56 | 15.05 | 13.5 | -12 |
| | | 192 | 4.98 | nd | 0.02 | 0.89 | nd | 6.91 | 7.81 | 14.5 | 46 |
| C | 2 m SOB + 11.4 mM $S\text{-}S_2O_3^{2-}$ Rep 2 | 0 | *** | 0.28 | 0.01 | 14.21 | nd | 1.74 | 15.96 | 12.9 | -24 |
| | | 192 | *** | nd | 0.24 | 4.24 | nd | 6.16 | 10.64 | 14.3 | 26 |
| C | 10 m SOB + 11.4 mM $S\text{-}S_2O_3^{2-}$ Rep 1 | 0 | 7.42 | 0.28 | 0.05 | 13.51 | nd | 1.78 | 15.34 | 11.7 | -31 |
| | | 192 | 6.17 | nd | 0.07 | 1.93 | nd | 5.73 | 7.72 | 14.2 | 46 |
| C | 10 m SOB + 11.4 mM $S\text{-}S_2O_3^{2-}$ Rep 2 | 0 | 7.81 | 0.28 | 0.06 | 13.46 | nd | 1.81 | 15.34 | 12.4 | -24 |
| | | 192 | 4.90 | nd | 0.15 | 0.30 | nd | 8.89 | 9.33 | 14.5 | 36 |
| C | Abiotic Control + 11.4 mM $S\text{-}S_2O_3^{2-}$ Rep 1 | 0 | 7.72 | 0.28 | 0.03 | 12.46 | nd | 1.45 | 13.94 | 11.2 | -24 |
| | | 192 | 7.80 | nd | 0.03 | 12.09 | nd | 1.83 | 13.94 | 13.3 | -5 |
| C | Abiotic Control T + 11.4 mM $S\text{-}S_2O_3^{2-}$ Rep 2 | 0 | 7.68 | 0.28 | 0.01 | 11.68 | nd | 1.51 | 13.20 | 11.2 | -18 |
| | | 192 | 6.98 | 0.00 | 0.11 | 12.09 | nd | 1.83 | 14.02 | 10.8 | -30 |

nd = non-detect

$[HS^-]$ was below detection limit in experiments (A) and (B), NA for exp (C). TotS values on unfiltered samples showed no decrease between $t_0$ and $t_{end}$ in all microcosms.

Note: the value for Σ S = Σ $[S^0]$ + $[S\text{-}S_2O_3^{2-}]$ + $[SO_3^{2-}]$ + $[SO_4^{2-}]$, and % S Unidentified = (Total S - Σ S)/Tot S * 100 %

*For complete geochemistry, including standard deviation values, see Table D2.

*** data omitted due to error in probe calibration.

A sulfur mass balance {[TotS] – Σ([$HS^-$], [$S^0$], [S-$S_2O_3^{2-}$], [$SO_3^{2-}$], [$SO_4^{2-}$]); mM} demonstrated that >50% of the S remained unaccounted for in both biotic and abiotic tetrathionate-amended microcosms (Experiments A and B; Table , Table D2). No substantial [$HS^-$], [$S^0$], or [$SO_3^{2-}$] were detected. Concentrations for the mass balance were collected from unfiltered samples, with the exception of sulfate. Since sulfate is an ion it is reasonable to assume that the filtered concentration equaled unfiltered. This gap in the S mass balance suggests that other reactive sulfur compounds {$S_{react}$, (K. Whaley-Martin et al. 2020)} were present, likely as tetrathionate ($S_4O_6^{2-}$) and possibly as other polythionates (e.g., $S_3O_6^{2-}$, $S_5O_6^{2-}$).

In the thiosulfate-amended microcosms with SOB in Experiment C, sulfate increases occurred at a consistent rate of ~0.03 mM/h under both oxic (mean $\Delta SO_4^{2-}{}_{2m}$ = 0.8 ± 0.4 mM and mean $\Delta SO_4^{2-}{}_{10m}$ = 0.6 ± 0.3 mM between hours 0–24) and suboxic (mean $\Delta SO_4^{2-}{}_{2m}$ = 3.8 ± 0.5 mM; mean $\Delta SO_4^{2-}{}_{10m}$ = 4.3 ± 0.7 mM between hours 74–192) conditions (Fig 5.2, Table D2). In sharp contrast to the tetrathionate-amended microcosms, the thiosulfate concentrations in the thiosulfate-amended microcosms decreased by 11.2 ± 1.2 mM S-$S_2O_3^{2-}$ (2 m SOB) and 12.4 ± 0.2 mM S-$S_2O_3^{2-}$ (10 m SOB) over the course of the experiment, accelerating from 0.02 mM/h under oxic conditions to a mean rate of 0.09 mM/h after the systems became suboxic (Fig 5.2). While the microcosm were under oxic conditions (between 0–24 hours), thiosulfate depletion may have been equal to the rate of sulfate formation (mean $-\Delta S_2O_3^{2-}{}_{2m}$ = 0.6 ± 0.9 mM and mean $-\Delta S_2O_3^{2-}{}_{10m}$ = 0.4 ± 0.4 mM, Table D2). However, once suboxic conditions were reached, only 30–40% of the thiosulfate loss could be accounted for by sulfate formation, and the difference was not accounted for by ZVS formation.

For the thiosulfate-amended treatments (Experiment C), the sulfur mass balance {[TotS] = Σ ([$S^0$], [S-$S_2O_3^{2-}$], [$SO_3^{2-}$], [$SO_4^{2-}$]); as [$HS^-$] was not quantifiable due to high biomass} indicates that all S could initially be accounted for (112–130% of TotS accounted for at $t_0$ on unfiltered sample) as the measured sulfur species. During both the oxic and anoxic portions of Experiment C, low [$S^0$] was detected in all microcosms (semi-quantitative measurements, Table D1). No $SO_3^{2-}$ was detected in any of the systems. However, as the experiments progressed, a gap in the accounted-for S developed (24–75% S was not accounted for at $t_{end}$), likely due to the formation of polythionates. A comparison of [TotS] at $t_0$ and $t_{end}$ indicates that no sulfur left the solution as gaseous $H_2S$.

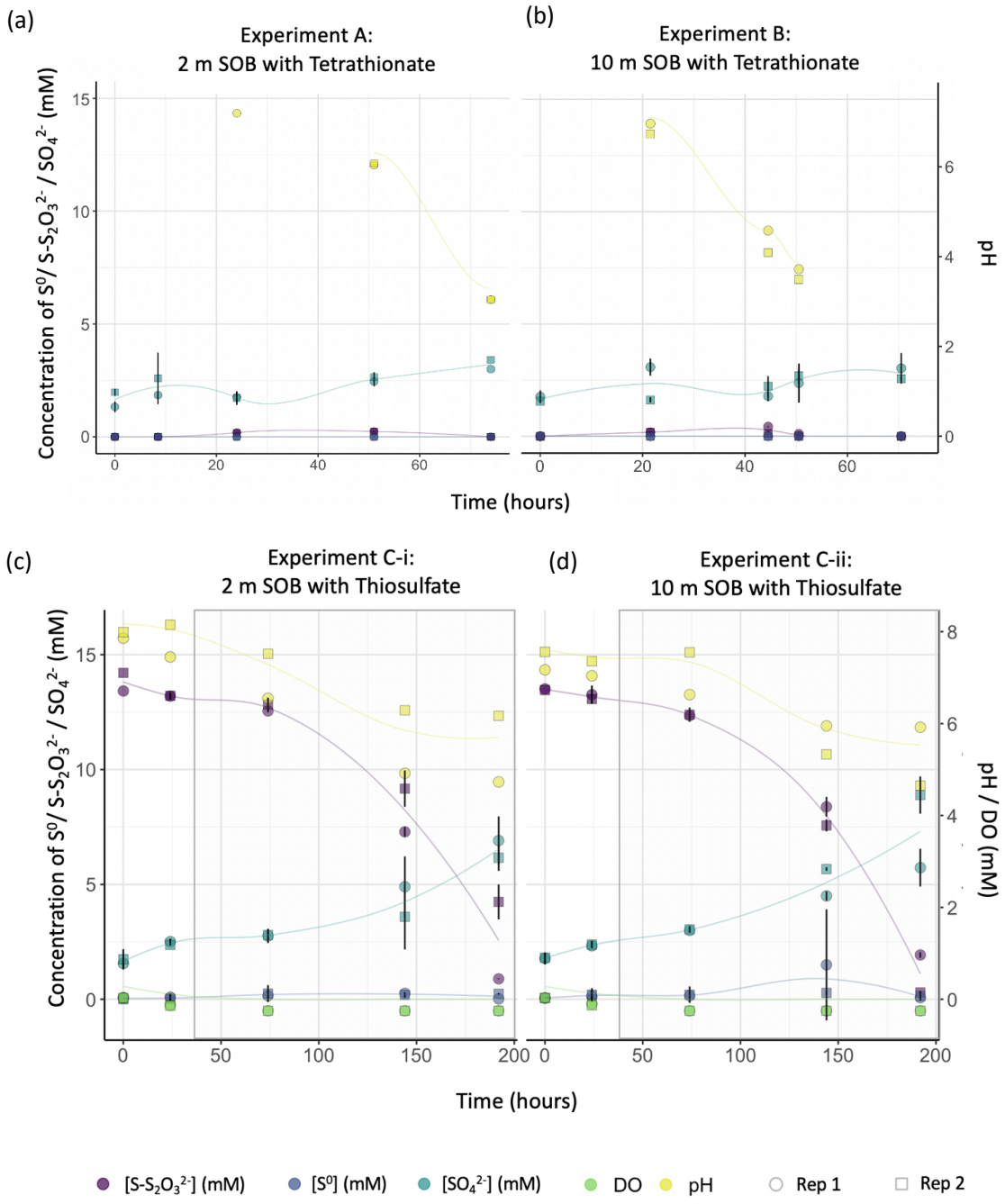


**Fig 5.2** Changes in sulfur speciation ($S^0$, $S\text{-}S_2O_3^{2-}$, $SO_4^{2-}$) in the 8 microcosms amended with either tetrathionate (top panels; Experiments A and B) or thiosulfate (bottom panels; Experiment C) sulfur-oxidizing bacterial (SOB) communities from two depths (2m and 10m). Samples were collected from two replicates (circles and squares; some circles not visible due to overlap) of each of the following treatments: (a) 2 m SOB treated with 8.0 mM $S\text{-}S_4O_6^{2-}$, (b) 10 m SOB treated with 8.0 mM $S\text{-}S_4O_6^{2-}$, (c) 2 m SOB treated with 11.4 mM $S\text{-}S_2O_3^{2-}$ and (d) 10 m SOB treated with 11.4 mM $S\text{-}S_2O_3^{2-}$. Grey rectangles indicate the suboxic portions of Experiment C. The $[SO_3^{2-}]$ < limit of detection (LoD) for all experiments. The $[HS^-]$ < LoD when samples were collected (Experiments A and B).

No statistically significant changes in sulfate concentration occurred in the abiotic controls amended with thiosulfate in Experiment C, nor in the biotic controls lacking SOI amendments (Table 5.2, Table D2). However, small increases in [$SO_4^{2-}$] were detected in the tetrathionate-amended abiotic controls in Experiment A ($\Delta SO_4^{2-}{}_{M2}$ = 0.6 ± 0.4 mM, Table ). These increases in [$SO_4^{2-}$] may be attributed to tetrathionate instability above pH 7, as the abiotic tetrathionate control remained between pH 7.7 and 7 over the course of the experiment; above pH 7, tetrathionate degrades abiotically into tri- and penta-thionate, and eventually to thiosulfate and sulfate (Varga and Horváth 2007).

### 5.3.2 pH Changes and Proton Yield from Sulfur Oxidation

Considering the pH data alone, different responses clearly arose from the combinations of SOB and sulfur substrate present each treatment. In the first two tetrathionate-amended experiments (A and B), acidity generation resulted from tetrathionate metabolism by the SOB community (pH decreased from 7.9 to 3.1–3.3, Fig 5.3). The trajectory of acid generation was similar between 2 and 10 m communities, although slightly more rapid in the microcosms inoculated with SOB from the greater depth (Experiment B, Fig 5.3). In contrast, in both biotic and abiotic controls exhibited only slight pH decreases (<1 pH unit; Fig 5.3), which can be accounted for by the acid-forming processes of the carbonate buffering system (Stumm and Morgan 1995), although slightly depressed by the phosphate buffering present (see methods).

In the thiosulfate-amended Experiment C, acidity generation also clearly resulted from thiosulfate metabolism. The pH decreased from 7.4–8.1 to 5.0–6.2 in the microcosms which received both thiosulfate and SOB amendments, with most acid generated under suboxic conditions (Fig 5.3). Again, all controls only exhibited slight pH decreases due to carbonate buffering. However, in suboxic portion of this experiment, variation was observed in one of the 10 m SOB replicates. Unlike the other two microcosms, the pH in this community experienced a point of inflection at 100 h, when the system (at a pH of 5.6) switched from acidity-generating to -consuming, suggesting a shift in thiosulfate oxidation processes (Fig 5.3c).

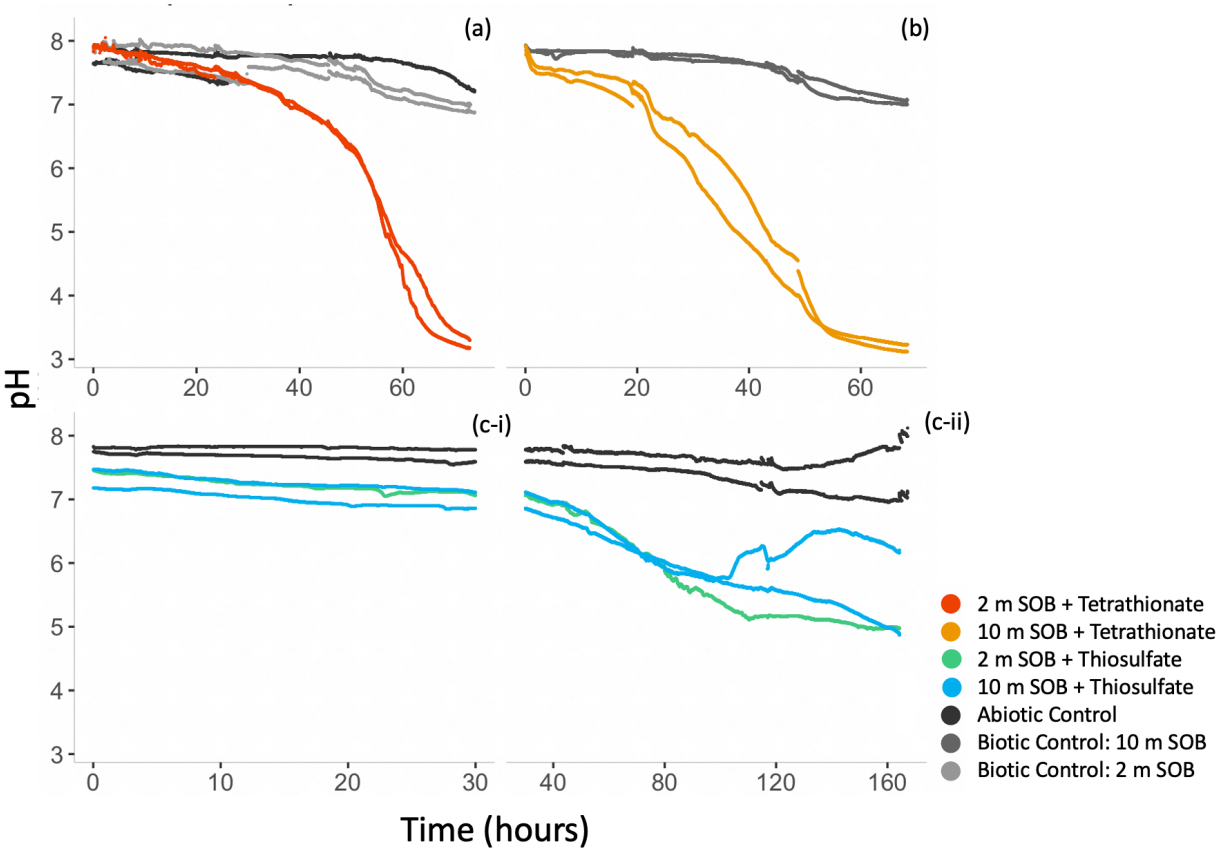


**Fig 5.3** Acid generation by sulfur-oxidizing communities in (a) Ox Res 2 m SOB community with tetrathionate amendments (oxic) over 70 h, (b) Ox Res 10 m SOB community with tetrathionate amendments (oxic) over 70 h, and (c-i) oxic or (c-ii) suboxic portions of the experiment with 2 m and 10 m SOB communities from a tailings reservoir with thiosulfate amendments over 180 h. (Note: pH readings from 2 m SOB + Thiosulfate Replicate 2 were omitted because of a calibration error; however, a pH decrease was also observed in that microcosm.)

Along with acid generation ($[H^+]$ increases), sulfate concentrations ($[SO_4^{2-}]$) also increased in the in the SOI-amended microcosms inoculated with SOB. In the tetrathionate-amended microcosms, the $\Delta H^+ : \Delta SO_4^{2-}$ between $t_0$ and $t_{end}$ (0.86:1 for 2 m SOB, and 1.19:1 for 10 m SOB, see methods section 5.2.5 for details of the calculation incorporating phosphate buffering) was slightly below a theoretical 3:2 ratio for direct tetrathionate oxidation with oxygen (equation 9, blue dashed line in Fig 5.4):

$$S_4O_6^{2-} + 3.5\ O_2 + 3\ H_2O \rightarrow 4\ SO_4^{2-} + 6\ H^+ \quad \Delta H^+ : \Delta SO_4^{2-} = 3:2 \qquad (9)$$

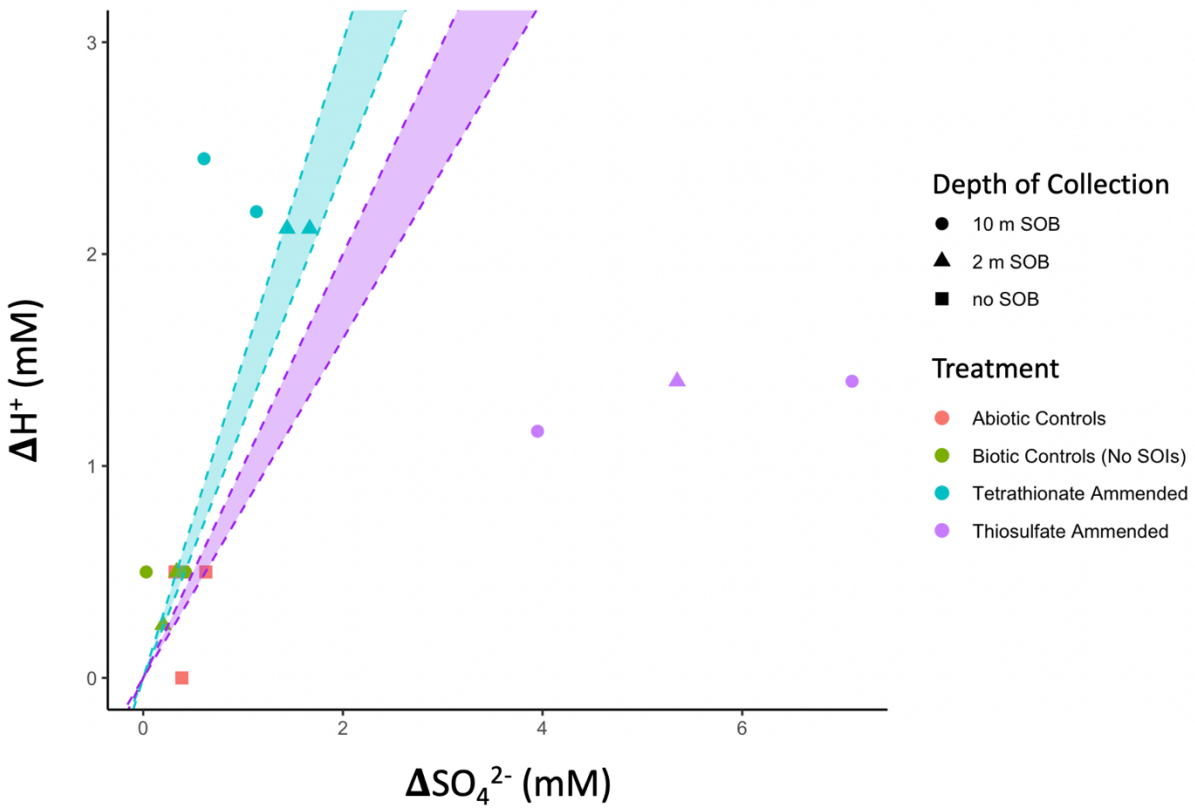


**Fig 5.4** The actual $\Delta H^+ : \Delta SO_4^{2-}$ ratio across both tetrathionate- (blue dots) and thiosulfate- (purple dots) amended experiments fall below the 3:2 theoretical ratio predicted from direct tetrathionate oxidation to sulfate (blue dashed lines and zone represent the ratio determined from the following equation, according to $S_4O_6^{2-} + 3.5\ O_2 + 3\ H_2O \rightarrow 4\ SO_4^{2-} + 6\ H^+$, with an ion activity coefficient range of 0.8-1.0 for $H^+$) or the 1:1 ratio predicted for direct thiosulfate oxidation to sulfate via cSOx (purple dashed line zone represent the ratio determined from the following equation, according to cSOx: $S_2O_3^{2-} + H_2O + 2\ O_2 \rightarrow 2\ SO_4^{2-} + 2\ H^+$, with an ion activity constant range of 0.8-1.0 for $H^+$). Actual $\Delta H^+$ for SOB- and SOI-amended systems was calculated as ($\Delta H^+ = [H^+]$ at $t_{end} - [H^+]$ at $t_0 + H^+$ consumed by buffer. See 5.2.5 for detailed calculations).

Even given the potential 20 % underestimation of $[H^+]$ resulting from the ion activity coefficient when converting pH data to directly proton concentration (coefficient range of 0.8-1 represented as fields in Fig 5.4, see methods), the detected $[H^+]$ calculated from pH are low. In the tetrathionate amended systems, this difference can be accounted for by the carbonate and phosphate buffering in the system; when accounted for the in the $[H^+]$ calculations (see methods), the $\Delta H^+ : \Delta SO_4^{2-}$ is found to be within (for 2 m SOB), or slightly above (for 10 m SOB) the expected range for direct tetrathionate oxidation to sulfate (Fig 5.4).

However, in the thiosulfate-amended microcosms, the discrepancy between theoretical and actual proton yields was pronounced. Here, the $\Delta H^+ : \Delta SO_4^{2-}$ between $t_0$ and $t_{end}$ was less than half the 1:1 theoretically predicted by direct thiosulfate oxidation to sulfate (equation 1, see Fig 5.4), even accounting for proton neutralization due to buffering. At less than half of the $\Delta H^+$ that would be expected via complete thiosulfate oxidation to sulfate, this observation cannot be explained by the stoichiometry of the cSOx pathway.

### 5.3.3 Microbial Community Signals

At the beginning of each experiment ($t_0$), biotic treatments were inoculated with communities isolated from either 2 m or 10 m depth from the tailings impoundment. Three key SOB genera were identified in these communities by referencing metagenomes previously sequenced from the oxidation reservoir and the current literature: *Halothiobacillus, Pandoraea,* and *Thiomonas* (Fig 5.4, Table D3, Table D4).

The proportion of genera in these communities shifted over the course of the experiments. At $t_0$, the inocula for Experiments A and B (both 2 and 10 m communities) were dominated by *Pandoraea* (12–74% of the total microbial community), while *Halothiobacillus* (<1%) and *Thiomonas* (<1%) were also present. For Experiment C, the 2 m and 10 m inoculum were dominated by *Halothiobacillus* (94–97%), while *Thiomonas* (2–3%) and *Pandoraea* (<1%) were also present (Fig 5.5a, Table D4). By $t_{end}$, the SOB communities became (for experiments A and B) or remained (for Experiment C) dominant in all but one of the SOI-amended microcosms (median proportion of SOB in SOI treated $t_{end}$ = 87%, Fig 5.5a), indicating that SOI compounds were an energy source. The remaining microcosm, where SOB genera at $t_{end}$ = 7%, instead contained a high abundance of *Pseudomonas*, explaining the point of inflection in pH, switching from acidity-generating to -consuming that occurred only in this system (section 5.3.1, Fig D1). In contrast to microcosms which received sulfur substrate, where the abundance of SOB was high, only two of the microcosms which did not receive sulfur substrate contained a large fraction of *Halothiobacillus* at $t_{end}$ (78–89%, Fig 5.5a); in the other two SOI-free treatments, *Halothiobacillus* concentrations at $t_{end}$ decreased to <1% (with no pattern with depth or substrate, Fig5.5a). In these microcosms without sulfur substrate, *Pandoraea* — the most abundant SOB — only comprised

9–12% of the total microbial community. Most of the remaining community in these biotic controls was composed of the heterotrophic genera *Delftia* and *Pseudomonas* (Fig D1, Table D3).

Metagenomes from both *Halothiobacillus* and *Thiomonas* (originally sequenced by Whaley-Martin et al, 2023) indicate that these genera can process thiosulfate via two pathways: the cSOx pathway (*soxAX*, *soxYZ*, *soxCD*, and *soxB*) or the first stage of the $S_4I$ pathway (*tsdA*, Fig 5.5b). While *Pandoraea* metagenomes from this study site were not available, metagenomes sequenced from a different mine site, combined with a review of 64 metagenomes, indicate that this genus contains cSOx but not TsdA (Fig 5.5b). In addition, both *Pandoraea* and *Halothiobacillus* from the 2 m and 10 m communities also contain the genes for *sdo* ($S^0 \rightarrow SO_3^{2-}$), although only the 10 m community contained *sor* ($SO_3^{2-} \rightarrow SO_4^{2-}$). It is also worth noting that *Halothiobacillus* and *Pandoraea* cells can reduce nitrite to ammonia (*nirB*) but lack the capacity to reduce nitrate to nitrite (*narGHIJ* / *napAB*, see Table D4). Bacteria belonging to the genus *Thiomonas* have the complimentary capacity to reduce nitrate to nitrite (*narGHIJ*) but lack the genes for nitrite reductase (*nirB, nirSK*).

(a)

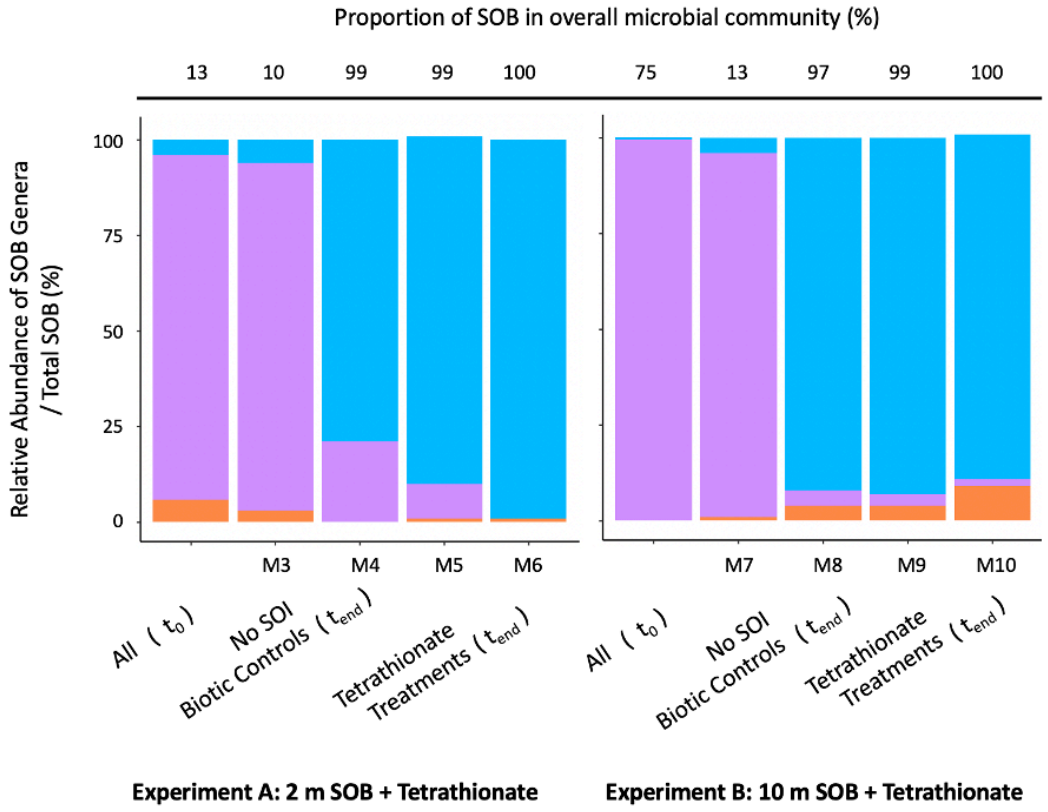
Proportion of SOB in overall microbial community (%)
13
10
99
99
100
75
13
97
99
100
Relative Abundance of SOB Genera / Total SOB (%)
100
75
50
25
0
M3
M4
M5
M6
M7
M8
M9
M10
All ( $t_0$ )
No SOI Biotic Controls ( $t_{end}$ )
Tetrathionate Treatments ( $t_{end}$ )
All ( $t_0$ )
No SOI Biotic Controls ( $t_{end}$ )
Tetrathionate Treatments ( $t_{end}$ )
Experiment A: 2 m SOB + Tetrathionate
Experiment B: 10 m SOB + Tetrathionate

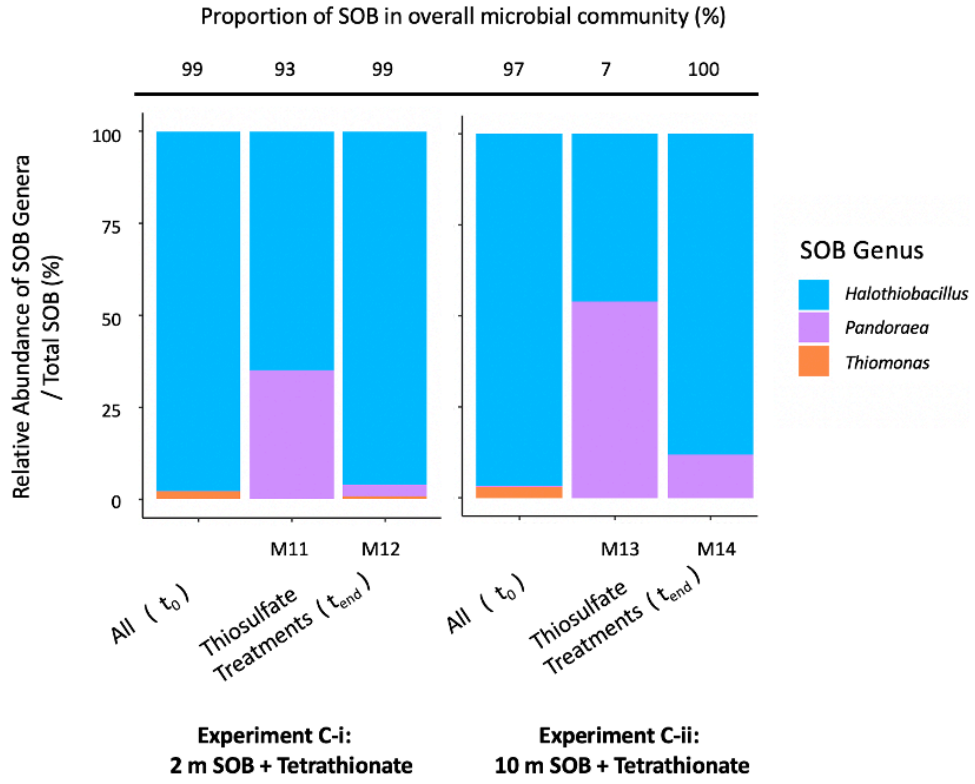
Proportion of SOB in overall microbial community (%)
99
93
99
97
7
100
Relative Abundance of SOB Genera / Total SOB (%)
100
75
50
25
0
M11
M12
M13
M14
All ( $t_0$ )
Thiosulfate Treatments ( $t_{end}$ )
All ( $t_0$ )
Thiosulfate Treatments ( $t_{end}$ )
SOB Genus
Halothiobacillus
Pandoraea
Thiomonas
Experiment C-i: 2 m SOB + Tetrathionate
Experiment C-ii: 10 m SOB + Tetrathionate

(b)

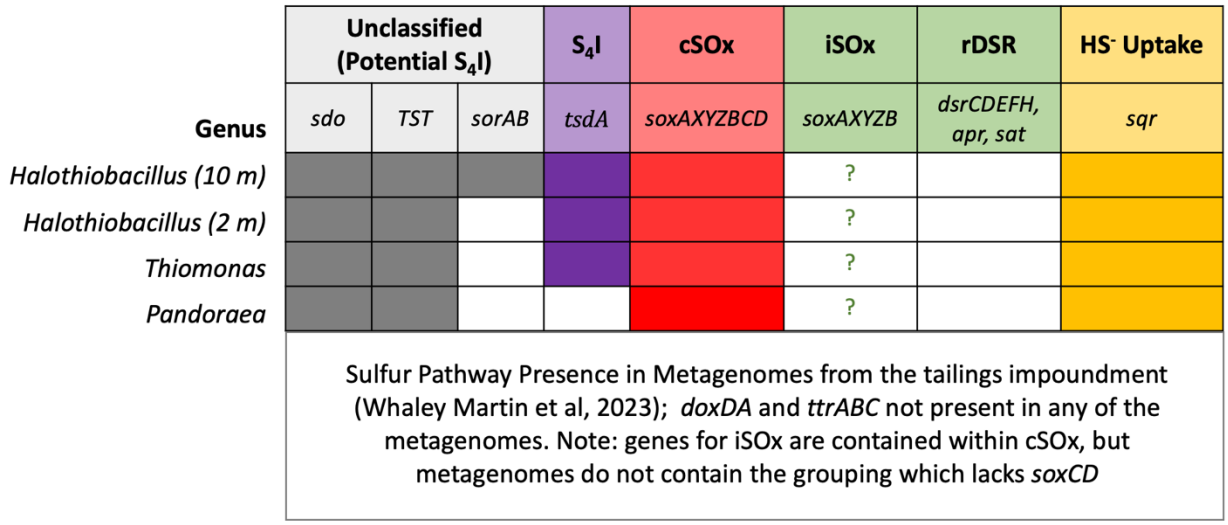


**Fig 5.5** The SOB community and metagenomic inference in the microcosms. (a) The SOB community was composed of *Halothiobacillus*, *Pandoraea*, and *Thiomonas,* isolated from samples taken from either 2 m or 10 m depths of the tailings impoundment, and forming the bulk of the communities at $t_0$ and $t_{end}$. Initial communities ($t_0$) varied due to shifts which occurred after the inocula were revitalized from cryogenic preservation. Regardless of whether *Halothiobacillus* was dominant in the initial communities, the genus comprised the largest proportion of the SOB population in microcosms that received amendments of thiosulfate or tetrathionate, although *Pandoraea* comprised a large fraction in one of the thiosulfate-amended microcosms. (b) MAG data for *Halothiobacillus*, *Thiomonas* and *Pandoraea* communities indicates that all three genera contain genes for the cSOx pathway (*soxAX, soxYZ, soxCD* and *soxB*), and therefore contain the genes required for iSOx (*soxAX, soxYZ,* and *soxB*). However, the iSOx pathway formed of *soxAX, soxYZ,* and *soxB* but lacking *soxCD* was not detected. *Halothiobacillus* and *Thiomonas* genera also contain the first stage of the $S_4I$ pathway (*tsdA*), although *Pandoraea* did not. They also contained genes for sulfide oxidation (*sqr*), and potentially the oxidation of zero valence sulfur to sulfite (*sdo*). MAGs from 10 m communities indicate they can form sulfate from sulfite (*sor*), see Table D4.

### 5.3.4 Dissolved Oxygen and Nitrate as Terminal Electron Acceptors

During the oxic experiments (Experiments A and B, and the first 28–30 hours of Experiment C), oxygen concentrations decreased rapidly in all SOB inoculated microcosms, but not in the abiotic controls (Fig 5.2, Table D3). Although a greater concentration of oxygen was consumed by the heterotrophic genera *Delftia* and *Pseudomonas* without sulfur substrate (Fig D1, Table D3), this

observation supports the prediction that oxygen is used as terminal electron acceptor (TEA) for sulfur oxidation when available.

However, no obvious TEA was paired with thiosulfate oxidation under suboxic conditions. Although established under oxic conditions, the thiosulfate-amended microcosms in Experiment C became anoxic by ~ 30 h (Table D2, Fig D2). Additional tests to examine the oxygen supply via surface diffusion indicated that SOB microcosms were anoxic at all probe depths, and ingress of oxygen via surface diffusion was insubstantial over the course of the incubation period (0.75 μM/h oxygen ingress was detected in an abiotic, anoxic control system). During the period of suboxia, ([DO] < 1 μM) there was no statistically significant change in the concentrations of nitrogen species (nitrate, nitrite, ammonia; Table D2). Further, the only SOB with the capacity to reduce nitrate, *Thiomonas*, was found at very low relative abundances in the suboxic experiments (Fig 5.5). Both lines of evidence indicate that the low proton yield cannot be accounted for by a shift to thiosulfate oxidation using nitrate. Since no other oxidants, such as manganese or iron, were readily available in the medium (2.0 mM $MgSO_4$, 0.2 mM $NH_4Cl$, 1.4 mM $K_2HPO_4$, 8.3 mM $NaNO_3$, and trace elements), this suggests thiosulfate was metabolised by SOB in these microcosms with an atypical electron acceptor.

## 5.4 Discussion

### 5.4.1 Sulfur Reactions in the Oxic Tetrathionate-Amended Microcosms

The production of acid in the oxic microcosms amended with tetrathionate, indicates that latter stage $S_4I$ pathway reactions were active in *Halothiobacillus* and *Pandoraea* dominated SOB communities. These genera either oxidized tetrathionate (a) directly to sulfate or (b) indirectly to other polythionates, and perhaps even ZVS, some of which subsequently oxidized to sulfate. In these microcosms, the $\Delta H^+ : \Delta SO_4^{2-}$ yield was not low once buffering in the media was accounted for, so aligns with direct oxidation. However, the small concentrations of thiosulfate formed and consumed are evidence suggesting that cycling through higher order polythionate pools may have occurred.

Members of the genus *Halothiobacillus*, which grew to compose the majority of the tetrathionate-amended communities, are also observed to process tetrathionate in other contexts. When isolated strains of *H. neapolitanus* were cultured under oxic conditions, they thrived on both thiosulfate

or tetrathionate as energy sources (Wood, Woodall, and Kelly 2005). *H. kellyi*, isolated from hydrothermal vents in the Aegean sea, was also found to be capable of growth on thiosulfate and tetrathionate under oxic conditions (Sievert, Heidorn, and Kuever 2000).

However, known sulfur enzyme mechanisms are insufficient to explain the changes in sulfur speciation observed in these microcosms. Direct oxidation of tetrathionate to sulfate appears the most likely process. However, the enzymes thought to compose the latter half of the $S_4I$ pathway (equation 2) fall broadly into two mechanisms, neither of which is a simple direct oxidation. Some mechanisms, such as those proposed by Pyne et al. (SoxB and SoxCD), are believed to split tetrathionate into sulfate and ZVS (Pyne et al. 2018). Although SoxB is present in the SOB metagenomes, the mechanism does not explain the generation of thiosulfate during Experiments A and B. However, the majority of proposed mechanisms, such as those facilitated by the TetH enzyme, are thought to disproportionate tetrathionate into thiosulfate, sulfate and ZVS, possibly via a process that generates higher-order SOIs, such as trithionate [$S_3O_6^{2-}$, Table 1.5, (Kanao, Kamimura, and Sugio 2007; Beard et al. 2011; Rameez et al. 2020; J. Zhang et al. 2020; Cai et al. 2022)]. The TetH pathway is described in *Acidothiobacillus caldus* and *A. ferrooxidans* as a reaction that forms disulfane monosulfonic acid (DSMSA), which then spontaneous decomposes to thiosulfate and ZVS, as shown in equation 10 (De Jong et al. 1997; Kanao, Kamimura, and Sugio 2007; Beard et al. 2011; Y. Yu et al. 2014; R. Wang et al. 2019; Camacho, Jessen, et al. 2020b; Gwak et al. 2022; Dahl 2005):

$$\text{TetH: } S_4O_6^{2-} + H_2O \rightarrow SO_4^{2-} + S_2O_3^{2-} + S^0 + 2\ H^+ \quad (10)$$

While there is consensus that the reaction facilitated by the TetH enzyme results in the formation of sulfate, thiosulfate, and ZVS, Beard et al. proposed that the intermediary, DSMSA, is also capable of forming other polythionates ($S_6O_6^{2-}$, $S_5O_6^{2-}$) under both aerobic and anaerobic conditions, opening the door to polythionate cycling (Beard et al. 2011). Pentathionate has also occasionally been detected as a product of tetrathionate hydrolase, and may be a polythionate formed in these microcosms (Bugaytsova and Lindström 2004). *Thiomonas intermedia K12* oxidation of tetrathionate was previously shown to result in thiosulfate, sulfate, and trithionate (speculated to form from DSMSA following the hydrolysis of tetrathionate), suggesting that trithionate may have also formed in this experiment (Wentzien and Sand 2004). In these microcosms, only low concentrations of thiosulfate and $S^0$ were detected, reducing support for

the TetH mechanism. This suggests an alternate enzyme, yet to be identified, exists which facilitates direct tetrathionate oxidation.

### 5.4.2 Sulfur Reactions in the Oxic Thiosulfate-Amended Microcosms

Over the oxic period in Experiment C (<30 h, changes calculated from 0–24 hours), both the $\Delta H^+ : \Delta SO_4^{2-}$ yield and the $\Delta SO_4^{2-} : \Delta S\text{-}S_2O_3^{2-}$ ratio are within the theoretical range accounted for by the cSOx pathway was the sole sulfur oxidation reaction. Although the proton yield was lower than theoretical, this can be accounted for by phosphate buffering in the system. Parallel activation of the cSOx and $S_4I$ Part 1 pathways might also contribute to the low proton yield, as was previously proposed to explain the low $\Delta H^+ : \Delta SO_4^{2-}$ ratios observed in 500 L mesocosm experiments in 2020 (Chapter 4).

### 5.4.3 Sulfur Reactions in the Suboxic Thiosulfate-Amended Microcosms

Previous research identified the key role the genera *Halothiobacillus* and *Thiomonas* in producing acidity in mine wastewater systems via the cSOx pathway (K. Whaley-Martin et al. 2019) (Chapter 4). As a result of this study, *Pandoraea* should be added to this suite of cSOx SOB in mine wastewaters. The proton yield ($\Delta H^+ : \Delta SO_4^{2-}$) remained extremely low during the suboxic experimental duration, although it was slightly higher than during the oxic portion. Similarly, low $\Delta H^+ : \Delta SO_4^{2-}$ ratios have been observed previously for *Halothiobacillus* isolated from this wastewater systems, where the calculated ratio was 0–0.3 (K. Whaley-Martin et al. 2019), although phosphate buffering would also have been present in this media (1.1% (w/v) $K_2HPO_4$). While low proton yields might, again, be accounted for by phosphate buffering, the sulfur speciation data clearly indicates that the cSOx pathway was not the sole active mechanism for metabolism in these microcosms. Although 4.2 mM of thiosulfate was converted to sulfate over 118 h, and the remaining 7.5 mM was converted to unknown aqueous sulfur species based on the sulfur mass balance (a comparison of TotS at $t_0$ and $t_{end}$ indicates that S was not lost as $H_2S_{(g)}$). This indicates formation of unmeasured sulfur species, because the small concentration (<1.5 mM) of $S^0$ formed at the midpoint of the experiments was consumed by $t_{end}$.

Further, during the suboxic portion of the experiment (deltas calculated from 74–192 h), a lack of $e^-$ acceptors was observed as thiosulfate concentrations decreased by ~12 mM. During this period, no DO was detected at any probe depth, and surface diffusion would account for <1 μM/h.

Although nitrate was present at sufficient concentrations for thiosulfate oxidation, neither [$NO_3^-$] nor [$NO_2^-$] decreased to a degree that could account for their use as TEA, and the population of *Thiomonas* (the only genus with capacity to reduce $NO_3^-$) was negligible in these microcosms. In contrast, mine wastewater systems sometimes contain populations of *Thiobacillus*, whose use of nitrate as an electron acceptor has been previously demonstrated (Chapter 4; Whaley Martin et al, 2023).

Thiosulfate disproportionation, which might a potential mechanism for thiosulfate metabolism without an $e^-$ acceptor, is not supported by these experiments. Thiosulfate disproportionation according to equation 9 (Jackson and McInerney 2000) can be eliminated as a possible mechanism, as it would produce $HS^-/H_2S_{(g)}$ (1:1 ratio of $HS^-$ to $H_2S_{(g)}$ would be expected at pH 12; below this pH, $H_2S_{(g)}$ rapidly dominates, reaching 100% $H_2S_{(g)}$ by pH 5.5) and no known enzyme system can catalyze this reaction:

$$\text{No known enzyme: } S_2O_3^{2-} + H_2O \rightarrow SO_4^{2-} + HS^- + H^+ \qquad \Delta G^0 = -21.9 \text{ kJ/mol} \qquad (11)$$

Similarly, abiotic thiosulfate disproportionation is only spontaneous below pH 4, and therefore can be ruled out (Gwak et al. 2022). Finally, hydrolysis of thiosulfate via iSOx (contained within the cSOx genes), forms similar products to those formed via disproportionation (equation 13):

$$\text{iSOx (SoxAX, SoxYZ, SoxB): } S_2O_3^{2-} + H_2O \rightarrow S^0 + SO_4^{2-} + 2\ e^- + 2\ H^+ \qquad (12)$$

However, although the shift between cSOx and iSOx pathways has been observed in *Sulfurimonas* (S. Wang et al. 2021), there is no evidence of iSOx use by *Halothiobacillus*, *Thiomonas*, or *Pandoraea*. Further, high concentrations of the product $S^0$ were not observed in Experiment C, and if iSOx were employed, an $e^-$ acceptor would still be required.

The survival of SOB under suboxic conditions, indicated by the high proportion of *Halothiobacillus* and *Pandoraea* at $t_{end}$ in the treatments amended with thiosulfate (visual observations indicated increased cell density over the course of the experiment) is particularly intriguing, as the literature reports that these genera are strictly aerobic. Although strictly aerobic, *Halothiobacillus* has occasionally been found to oxidize sulfur under very low oxygen conditions (Magnuson et al. 2023).

Limited oxygen use by *Halothiobacillus* under suboxic conditions could be a potential explanation for the observations made in these experiments, particularly near the surface of the microcosms. An approximation of oxygen utilization rates by *Halothiobacillus*-dominated biofilms, based on biofilm oxygen penetration depths (Satoh et al. 2009) and oxygen utilization rates with sulfur oxidation observed in batch reactors (Jensen et al. 2011) suggest that biotic oxygen consumption might increase to 4 μM/h or a total of 0.7 mM over the anoxic portion of the experiment (Table D5). Activation of the $S_4I$ pathway P1 would be a plausible mechanism for reducing acidity generation, and it might be possible under microaerophilic conditions if SOB increased surface oxygen draw to ~1 mM over the anoxic potion of the experiment (equations 12–13). This would produce an experimental ratio of ~12 $\Delta S\text{-}S_2O_3^{2-}$ : 1 $\Delta O_2$, where the theoretical ratio is 8 $\Delta S\text{-}S_2O_3^{2-}$ : 1 $\Delta O_2$ (equations 13–14):

TsdA/$S_4I$ P1: $2\ S_2O_3^{2-} \rightarrow S_4O_6^{2-} + 2\ e^-$ (13)

Oxygen as a TEA: $2\ e^- + 2\ H^+ + ½\ O_2 \rightarrow H_2O$ (14)

Near the surface, *Halothiobacillus* in the thiosulfate-amended microcosms may be surviving on the low concentrations of oxygen in the water introduced through surface diffusion. However, even if low concentrations of oxygen were available at the surface of the microcosm, thiosulfate diffusion rates suggest that molecules near the bottom of the flask would not have time to come into contact with the surface layer (Table D6); therefore, an alternate $e^-$ acceptor must have been employed. In addition, activity of the first stage of the $S_4I$ pathway would not account for sulfate formation during this period. Manganese and iron, the $e^-$ acceptors whose reduction are next most favorable on the redox ladder, were not present in the media (see 5.2.1). With no other possible $e^-$ acceptor, polythionate reduction at the bottom of the 6 L microcosms may have been paired with thiosulfate oxidation to sulfate under suboxic conditions. Polythionates have been previously observed in SOB communities of *Halothiobacillus*, *Thiomonas*, and *Pandoraea*. Under anaerobic conditions, other studies observed sulfur, sulfite, and trithionate formation with thiosulfate oxidation in *Pandoraea*, as well as a small amount of trithionate formation with thiosulfate loss in *Halothiobacillus* (Anandham et al. 2008). *Thiomonas intermedia K12* (isolated from sewage) was observed to degrade tetrathionate to produce primarily pentathionate and small amounts of

hexathionate, thiosulfate, trithionate, and sulfate (Wentzien and Sand 2004). Sequencing mRNA may provide further insights into the sulfur enzymes active in the system.

### 5.4.4 Relevance to Mine Wastewater Systems

These microcosms demonstrate that proton yields resulting from thiosulfate oxidation by SOB fall far below those theoretically predicted. Tetrathionate oxidation produces nearly the $\Delta H^+$: $\Delta SO_4^{2-}$ theoretically predicted, but thiosulfate oxidation produces < 1/2. Given these ratios, is sulfur-driven acid generation a concern to mine wastewater systems?

Potential impacts can vary greatly considering typical SOI concentrations across four Canadian mine tailings reservoirs sampled in 2018: thiosulfate ($S–S_2O_3^{2-}$) < 0.003–0.8 mM, trithionate ($S–S_3O_6^{2-}$) < 0.03–0.1 mM, and tetrathionate ($S–S_4O_6^{2-}$) < 0.03–0.23 mM (K. Whaley-Martin et al. 2020). If 0.2 mM $S–S_2O_3^{2-}$ oxidation were to produce acid according to the ratio in observed in the anoxic microcosms (0.02:1 $H^+$/ $S–S_2O_3^{2-}$), this would produce 0.004 mM $H^+$, which would decrease the pH from 7 to 5.4. If the same concentration of tetrathionate (0.2 mM $S–S_4O_6^{2-}$) was to produce the acid ratio observed in the tetrathionate-amended microcosms ($\Delta H^+ : \Delta SO_4^{2-}$ [assumed from $S\text{-}S_4O_6^{2-}$] ~ 2.2:1), this would produce 0.44 mM $H^+$, which would decrease the pH from 7 to 3.4. However, buffering in the water would reduce these impacts, perhaps even neutralize them completely. With this range in potential outcomes from SOI concentrations observed at active mine sites, we need greater clarity as to which SOB-facilitated SOI reactions occur in these systems; this continues to be an important future research direction.

## 5.5 Conclusions

In mine wastewaters, the activities of sulfur pathways used by *Halothiobacillus, Thiomonas*, and *Pandoraea* are important, as they impact the ability to predict and prevent acidity generation in tailings impoundments. These experiments demonstrate that acidity generation will occur immediately with both tetrathionate oxidation under oxic conditions and with thiosulfate oxidation under oxic and anoxic conditions, yet at ratios lower than would theoretically be predicted. The low initial acid generation, in combination with gaps in the sulfur mass balance, indicate that S redox processes occur that are not currently linked to known sulfur enzyme systems. It is possible that polythionates are forming which add complexity to the tetrathionate oxidation, and further studies are needed to investigate which enzyme-facilitated reactions occur

within this polythionate pool. To date, research into this pool is limited as standards for these compounds ($S_3O_6^{2-}$, $S_4O_6^{2-}$, $S_5O_6^{2-}$) are not readily available and robust analytical techniques need to be developed. In addition, these SOB communities demonstrated an ability to oxidize thiosulfate under suboxic conditions with no apparent TEA, which is a phenomenon requiring further investigation.

These observations contrast with the previous observations that *Halothiobacillus*-dominated SOB communities amended with thiosulfate always produce acidity through cSOx pathway activation (K. Whaley-Martin et al. 2023). Therefore, the interplay between cSOx and $S_4I$ pathway in genera such as *Halothiobacillus* is an important consideration when predicting mine wastewater acidity. For applications in mine wastewater management, 16S rRNA gene sequences are a technique which can be immediately applied to screen for SOB communities. However, because of the presence of multiple pathways in several SOB genera, there is additional value in developing targeted screening for the activation of specific enzymes such as SoxCD, TsdA, TetH, and DsrC. Further research is also required to clarify the specifics of polythionate cycling in mine wastewater systems. Finally, the development of treatments to promote the use of the cSOx pathway by the SOB community would facilitate immediate acid generation, allowing onsite treatment.

# 6

# Conclusions

*"Look deep into nature, and then you will understand everything better."*
*~Albert Einstein*

## 6.1 Summary of Thesis Chapters

Pragmatically, this thesis seeks to address how our understanding of current sulfur-oxidizing bacteria (SOB) metabolisms affects the timing and magnitude of acidity generation in mine wastewater. The introductory chapter begins by identifying the problem of acid generation due to SOI oxidation in mine wastewater, and introducing recently identified SOB genera, such as *Halothiobacillus*, as likely playing a role in the process. I then explore the past 25 years of sulfur enzyme literature, describing the substeps of the cSOx, iSOx + rDSR and $S_4I$ pathways, as well as the disagreement in the literature over the final stages of the $S_4I$ pathway. Next, I describe how these pathways may thrive in different ecological niches due to responses to thermodynamic and kinetic drivers of pathway fitness. Finally, I outline three objectives for the research: surveying the effect a broad range of environmental parameters on SOB community composition, identifying which sulfur pathways are active in response to the most influential of these parameters, and finally exploring the gaps between sulfur speciation and known enzyme pathways.

In Chapter 3, I identified several SOB genera, abundant in the oxidation reservoir of a tailings wastewater management system, which fall broadly into two guilds. The SOB in Guild A processes thiosulfate through the cSOx and $S_4I$ pathways (*Halothiobacillus, Thiomonas* — cSOx and $S_4I$), while the SOB of Guild B processes thiosulfate via the iSOx + rDSR pathways (*Thiobacillus* — iSOx and rDSR). This builds on previous work which identified the acid generation role *Halothiobacillus* and *Thiomonas* likely play, as salt-tolerate genera (K. Whaley-Martin et al. 2019; Camacho, Jessen, et al. 2020). This study also identified several additional

SOB genera which likely play minor roles via the $S_4I$ pathway and unclassified enzymes (*Brevundimonas*, *Sediminibacterium*, *Acidovorax*).

Chapter 3 further demonstrated that the relative abundance of these SOB genera often responded to environmental parameters; evidence was found for responses to oxygen and sulfur substrate, tentative evidence for responses to nitrate and organic carbon, but no responses for light. The response to the terminal electron acceptor (TEA) gradient was the most pronounced, with Guild A (cSOx and $S_4I$ pathways) most abundant in oxic conditions, while Guild B (iSOx + rDSR pathway) was more abundant under anoxic conditions. Under anoxic conditions, the use of nitrate as the terminal electron acceptor produced little acidity. The acid generation response to sulfur substrate was also pronounced. Thiosulfate initially produced a much lower low initial proton yield than tetrathionate, from which it was inferred that the $S_4I$ pathway was active. Overall, the SOB communities influenced the geochemistry in the 500 L mesocosms, indicating that they are likely also influential at a landscape scale.

In Chapter 4, eight 500 L mesocosms were used to explore if the activities of these three sulfur oxidation pathways would also respond to various ecological niche spaces (defined by differences in oxygen, nitrate, thiosulfate, and tetrathionate). Indeed, each of the three known sulfur oxidation pathways were active in these mesocosms, in an expanded suite of SOB:

- *Halothiobacillus* and *Thiomonas* — cSOx and $S_4I$, Guild A
- *Thiovirga* and *Sulfurovum* — cSOx, Guild A
- *Sediminibacterium* — $S_4I$, Guild A
- *Acidovorax* — tetrathionate reduction, unclassified
- *Thiobacillus* — iSOx and rDSR, Guild B
- *Desulfurivibrio* — rDSR, Guild B

Further, sometimes two of these pathways were active in parallel. One of the key take-aways of this study was that the proton yield ($H^+$:$SO_4^{2-}$) was found to be much lower than theoretically predicted by assuming all thiosulfate would be oxidized to sulfate using oxygen. Both parallel pathway activity and the use of nitrate as an electron acceptor were posited as explanations for why the low proton yield.

In Chapter 5, I used high concentrations of SOB and SOI in laboratory microcosms to exaggerate the acid-generating phenomenon observed in the oxidation reservoir. In these microcosms, I again isolated *Halothiobacillus* and *Thiomonas* (cSOx and $S_4I$ Part 1 — Guild A), whose key roles has been previously identified. However, *Pandoraea* (cSOx — Guild A) was additionally found to belong to the suite of key SOB. Linking the sulfur metabolic pathways of these genera with the geochemical reactants/products revealed three main findings: (i) the measured proton yield ($\Delta H^+ : \Delta SO_4^{2-}$) was, again, much lower than theoretical for all sulfur oxidation reactions; (ii) although an enzyme mechanism is lacking, these SOB have the ability to oxidize tetrathionate to sulfate under oxic conditions; and (iii) *Halothiobacillus*- and *Pandoraea*-dominated communities (Guild A) metabolized thiosulfate without nitrate reduction or sufficient oxygen under suboxic conditions. These findings suggest that the $S_4I$ pathway is more widespread than previously thought, potentially active under suboxic as well as oxic conditions. Further, this study highlighted the critical role oxidation of tetrathionate, and potentially other polythionates, plays in acid generation in this system – emphasizing the need for improved analytical methods in order to explore the reaction pathways ($S_4I$ Part 2 and unclassified reactions) which have not been fully characterised. In the future, applying this knowledge shows how a fundamental understanding of sulfur metabolism can inform water management best practices for an active metal mine site in northern Canada.

## 6.2 Relevance to the Field of Ecology

Theoretically, the patterns that connect sulfur pathway activity with ecological niche space observed in these systems are underpinned by fundamental questions of ecology and evolution: (i) “Why does sulfur pathway expression increased dominance of certain genera in a SOB community in response to the conditions?” and (ii) “What is driving this apparent choice?” The answer to this second question might be that increase fitness results from energetic efficiency, taking the form of a cost/benefit trade-off between ATP spent and gained due to pathway choice in response to substrates and TEA. Yet this preliminary hypothesis requires more theoretical and experimental work to explore if it applies here, and in other systems.

This work confirms that both sulfur substrates (thiosulfate and tetrathionate) and electron acceptor (oxygen and nitrate) are key environmental factors defining ecological niche space partitioning of

SOB. The observation that SOB communities respond to environmental gradients can be used to begin to inform a conceptual diagnostic framework for the timing and magnitude of acid generation in mine wastewater (Fig 6.1).

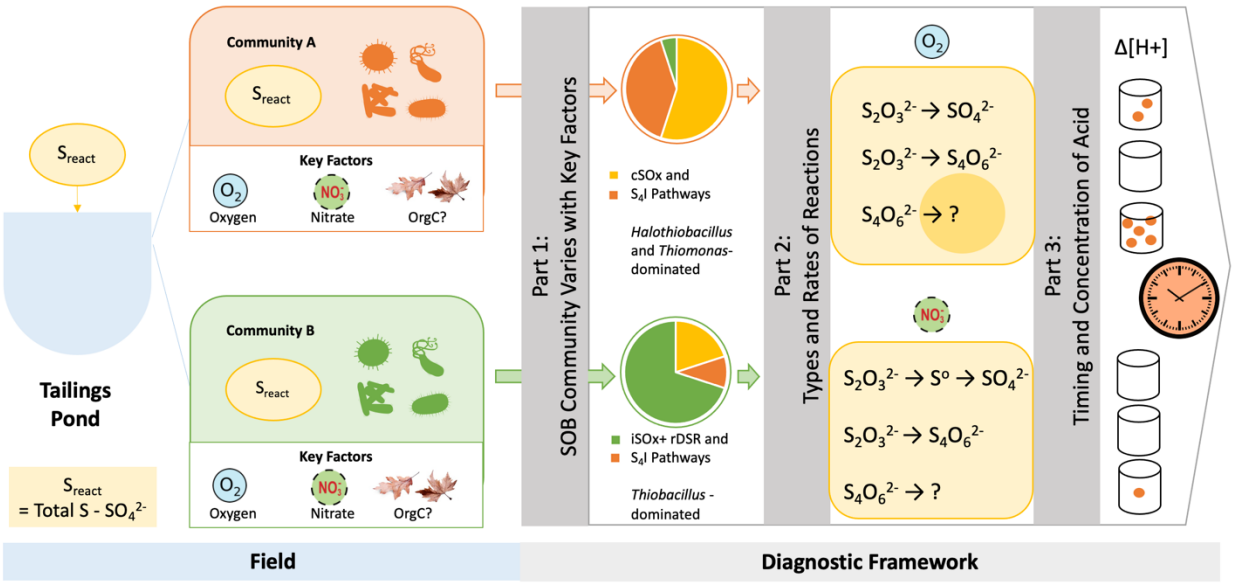


**Fig 6.1** Key findings inform a diagnostic framework for acid generation. The diagnostic framework can be used as a conceptual tool for determining the timing and magnitude of acid generation in mine wastewaters based on the presence of SOB communities.

This conceptual framework is also one of the first attempts to link genetic abundance and expression to geochemical changes at a macro scale. Recent work has succeeded in linking distinctions in geochemistry to differences in SOB and SRB communities; however, the processes facilitated by these microbes are not yet predictively linked to geochemical outcomes (M. Chen et al. 2024; Vigneron et al. 2021; Bell et al. 2020; Dick 2019). There have been a few recent studies which demonstrate that environmental niche partitioning occurs in SOB communities. Camacho et al. (2020) observed shifts in SOB communities in response to pH (Camacho, Jessen, et al. 2020) and Whaley Martin et al (2023) demonstrated oxygen-driven partitioning in the oxidation reservoir (K. J. Whaley-Martin et al. 2023). Despite simplifications of internal cell metabolisms, the power of the conceptual links made in these studies, and this framework, is that fundamental processes at the micro scale can be used to comprehend macro scale tailings systems.

Further elucidating the environmental parameters supporting varied SOB metabolisms could play a useful role in expanding this framework to predict geochemical outcomes, particularly acid generation, in more detail.

## 6.3 Implications of the Conceptual Framework

This conceptual framework (Fig 6.1) begins to clarify the causes of unpredictable SOI oxidation, subsequent acidity generation, and toxicity in mine wastewater systems. The framework addresses some knowledge gaps by linking SOB genera with sulfur metabolic processes and responses to environmental conditions. It demonstrates that metagenomic characterization can be used to predict which SOI oxidation reactions may occur, and that initial acidity yields ($\Delta H^+ : \Delta SO_4^{2-}$) due to thiosulfate oxidation are much lower than theoretically predicted. It also demonstrates that oxygen and nitrate concentrations, which vary with depth and season in most mine wastewater management systems (Whaley-Martin et al. 2019; Grettenberger, Havig, and Hamilton 2019; Miettinen et al. 2021), play a role in both pathway partitioning and proton yield. However, the framework also highlights gaps around the latter stage of the $S_4I$ pathway and the role of polythionate oxidation. Due to these gaps in understanding the enzyme mechanisms for latter stage $S_4I$ pathway processes, this framework identifies why the timing and magnitude of acid generation from SOI oxidation can only be partially predicted.

The development of this conceptual framework can inform environmental protection at mine sites in Canada, and abroad. In Canada, the ecological niche partitioning has recently been found to have cross-mine significance (Twible et al. 2024). Here, wastewater may experience changes in the depth of the oxic zone linked to seasons (due to winter ice cover), which now can be seen to drive a divide between cSOx + $S_4I$ and iSOx+ rDSR pathways (K. J. Whaley-Martin et al. 2023). Further, the previously overlooked role of the $S_4I$ pathway, explain why the onset of acid generation may be delayed by days or even weeks. With direct links to the onset and magnitude of acidity generation, the pathway–niche response is, therefore, a foundational framework that will allow the mining industry to predictively model and manage wastewater using 16S rRNA gene sequence characterization as a currently available tool to provide insights into process.

## 6.4 Future Research Directions

Although this thesis lays a groundwork from which to understand the role SOB play in thiosalt oxidation in mine wastewaters, it frames many future research questions. This research identifies the key role of all three universal sulfur oxidation pathways in determining if acidity-generating SOI intermediates are present in mine wastewater. It also highlights a gap between the sulfur enzymes currently identified in genera such as *Halothiobacillus*, and the polythionate cycling which might comprise the latter stage(s) of the $S_4I$ pathway. To make progress in this direction, improved analytical measurement techniques for ZVS, tetrathionate, and if possible other polythionates are necessary. Matching these improved chemical analyses with transcriptomic or protein characterization could shed light onto these unknown sulfur enzyme mechanisms.

Therefore, we propose that progress can be made in detecting sulfur pathway activity in mine wastewater. From this work in this thesis, 16S rRNA gene sequence characterization is a tool currently available, along with the three line of evidence table (Fig 4.3), which can approximate sulfur pathway presence in mine wastewaters. However, development of mRNA primers directly targeting genes from each of the three sulfur pathways (such as *soxCD, soxB, tsdA, tetH,* and *dsrC*) would provide higher resolution inferences. In addition, further experimentation could be directed towards exploring how environmental conditions impact not only pathway activity, but the rates of SOI oxidation. As these areas gain greater definition, this framework of sulfur metabolism understanding can begin to be integrated into mass balance water flow models such as MineMod™. This will allow mines to determine how likely the risk of SOI oxidation and acid generation might be in water downstream of active tailings impoundments, encouraging better stewardship of this essential resource.

# References


Aardt, M. Van, S. E. Duncan, J. E. Marcy, T. E. Long, and C. R. Hackney. 2001. "Effectiveness of Poly(Ethylene Terephthalate) and High-Density Polyethylene in Protection of Milk Flavor." *Journal of Dairy Science* 84 (6): 1341–47. https://doi.org/10.3168/jds.S0022-0302(01)70164-6.

Anandham, Rangasamy, Pandiyan Indiragandhi, Soon Wo Kwon, Tong Min Sa, Che Ok Jeon, Yong Ki Kim, and Hyeong Jin Jee. 2010. "*Pandoraea thiooxydans* sp. nov., a Facultatively Chemolithotrophic, Thiosulfate-Oxidizing Bacterium Isolated from Rhizosphere Soils of Sesame (*Sesamum indicum* L.)." *International Journal of Systematic and Evolutionary Microbiology* 60 (1): 21–26. https://doi.org/10.1099/ijs.0.012823-0.

Anandham, Rangasamy, Pandiyan Indiragandhi, Munusamy Madhaiyan, Kyoung Yul Ryu, Hyeong Jin Jee, and Tong Min Sa. 2008. "Chemolithoautotrophic Oxidation of Thiosulfate and Phylogenetic Distribution of Sulfur Oxidation Gene (SoxB) in Rhizobacteria Isolated from Crop Plants." *Research in Microbiology* 159 (9–10): 579–89. https://doi.org/10.1016/j.resmic.2008.08.007.

Anantharaman, Karthik, Bela Hausmann, Sean P Jungbluth, Rose S Kantor, Adi Lavy, Lesley A Warren, Michael S Rappé, et al. 2018. "Expanded Diversity of Microbial Groups That Shape the Dissimilatory Sulfur Cycle." *The ISME Journal* 12 (7): 1715–28. https://doi.org/10.1038/s41396-018-0078-0.

Anda, Valerie De, Icoquih Zapata-Peñasco, Augusto Cesar Poot-Hernandez, Luis E. Eguiarte, Bruno Contreras-Moreira, and Valeria Souza. 2017. "MEBS, a Software Platform to Evaluate Large (Meta)Genomic Collections According to Their Metabolic Machinery: Unraveling the Sulfur Cycle." *GigaScience* 6 (11). https://doi.org/10.1093/gigascience/gix096.

Arsène-Ploetze, Florence, Sandrine Koechler, Marie Marchal, Jean-Yves Coppée, Michael Chandler, Violaine Bonnefoy, Céline Brochier-Armanet, et al. 2010. "Structure, Function, and Evolution of the *Thiomonas spp.* Genome." Edited by Nancy A. Moran. *PLoS Genetics* 6 (2): e1000859. https://doi.org/10.1371/journal.pgen.1000859.

Balci, Nurgul, Bernhard Mayer, Wayne C. Shanks, and Kevin W. Mandernack. 2012. "Oxygen and Sulfur Isotope Systematics of Sulfate Produced during Abiotic and Bacterial Oxidation of Sphalerite and Elemental Sulfur." *Geochimica et Cosmochimica Acta* 77: 335–51. https://doi.org/10.1016/j.gca.2011.10.022.

Baquero, Fernando, Teresa M. Coque, Juan Carlos Galán, and Jose L. Martinez. 2021. "The Origin of Niches and Species in the Bacterial World." *Frontiers in Microbiology*. https://doi.org/10.3389/fmicb.2021.657986.

Barrows, John K., and Michael W. Van Dyke. 2023. "A CsoR Family Transcriptional Regulator, TTHA1953, Controls the Sulfur Oxidation Pathway in *Thermus thermophilus* HB8." *Journal of Biological Chemistry* 299 (6): 104759. https://doi.org/10.1016/j.jbc.2023.104759.

Beard, Simón, Alberto Paradela, Juan P. Albar, and Carlos A. Jerez. 2011a. "Growth of

*Acidithiobacillus ferrooxidans* ATCC 23270 in Thiosulfate under Oxygen-Limiting Conditions Generates Extracellular Sulfur Globules by Means of a Secreted Tetrathionate Hydrolase." *Frontiers in Microbiology* 2 (APR). https://doi.org/10.3389/fmicb.2011.00079.

Bell, Emma, Tiina Lamminmäki, Johannes Alneberg, Anders F. Andersson, Chen Qian, Weili Xiong, Robert L. Hettich, Manon Frutschi, and Rizlan Bernier-Latmani. 2020. "Active Sulfur Cycling in the Terrestrial Deep Subsurface." *ISME Journal*. https://doi.org/10.1038/s41396-020-0602-x.

Beller, Harry R., Patrick S.G. Chain, Tracy E. Letain, Anu Chakicherla, Frank W. Larimer, Paul M. Richardson, Matthew A. Coleman, Ann P. Wood, and Donovan P. Kelly. 2006. "The Genome Sequence of the Obligately Chemolithoautotrophic, Facultatively Anaerobic Bacterium *Thiobacillus denitrificans*." *Journal of Bacteriology* 188 (4): 1473–88. https://doi.org/10.1128/JB.188.4.1473-1488.2006.

Bernier, Luc, and Lesley A. Warren. 2007. "Geochemical Diversity in S Processes Mediated by Culture-Adapted and Environmental-Enrichments of *Acidithiobacillus spp*." *Geochimica et Cosmochimica Acta* 71 (23): 5684–97. https://doi.org/10.1016/j.gca.2007.08.010.

Brito, José A., Kevin Denkmann, Inês A.C. Pereira, Margarida Archer, and Christiane Dahl. 2015. "Thiosulfate Dehydrogenase (TsdA) from *Allochromatium vinosum*." *Journal of Biological Chemistry* 290 (14): 9222–38. https://doi.org/10.1074/jbc.M114.623397.

Bugaytsova, Zhanna, and E. Börje Lindström. 2004. "Localization, Purification and Properties of a Tetrathionate Hydrolase from *Acidithiobacillus caldus.*" *European Journal of Biochemistry* 271 (2): 272–80. https://doi.org/10.1046/j.1432-1033.2003.03926.x.

Buonvino, Silvia, Ilaria Arciero, and Sonia Melino. 2022. "Thiosulfate-Cyanide Sulfurtransferase a Mitochondrial Essential Enzyme: From Cell Metabolism to the Biotechnological Applications." *International Journal of Molecular Sciences* 23 (15): 8452. https://doi.org/10.3390/ijms23158452.

Cáceres, Miquel De, Pierre Legendre, Susan K. Wiser, and Lluís Brotons. 2012. "Using Species Combinations in Indicator Value Analyses." Edited by Robert B. O'Hara. *Methods in Ecology and Evolution* 3 (6): 973–82. https://doi.org/10.1111/j.2041-210X.2012.00246.x.

Cai, Ruining, Wanying He, Rui Liu, Jing Zhang, Xin Zhang, and Chaomin Sun. 2022. "Deep-Sea In Situ Insights into the Formation of Zero-Valent Sulfur Driven by a Bacterial Thiosulfate Oxidation Pathway." *MBio* 13 (4). https://doi.org/10.1128/mbio.00143-22.

Camacho, David, Rodolfo Frazao, Aurélien Fouillen, Antonio Nanci, B. Franz Lang, Simon C. Apte, Christian Baron, and Lesley A. Warren. 2020. "New Insights into *Acidithiobacillus thiooxidans* Sulfur Metabolism through Coupled Gene Expression, Solution Chemistry, Microscopy, and Spectroscopy Analyses." *Frontiers in Microbiology* 11 (March). https://doi.org/10.3389/fmicb.2020.00411.

Camacho, David, Gerdhard L Jessen, Jiro F Mori, Simon C Apte, Chad V Jarolimek, and Lesley A Warren. 2020. "Microbial Succession Signals the Initiation of Acidification in Mining Wastewaters." *Mine Water and the Environment* 39 (4): 669–83. https://doi.org/10.1007/s10230-020-00711-9.

Caporaso, J. Gregory, Christian L. Lauber, William A. Walters, Donna Berg-Lyons, James Huntley, Noah Fierer, Sarah M. Owens, et al. 2012. "Ultra-High-Throughput Microbial

Community Analysis on the Illumina HiSeq and MiSeq Platforms." *ISME Journal* 6 (8): 1621–24. https://doi.org/10.1038/ismej.2012.8.

Carlson, Hans K., Iain C. Clark, Steven J. Blazewicz, Anthony T. Iavarone, and John D. Coates. 2013. "Fe(II) Oxidation Is an Innate Capability of Nitrate-Reducing Bacteria That Involves Abiotic and Biotic Reactions." *Journal of Bacteriology* 195 (14): 3260–68. https://doi.org/10.1128/JB.00058-13.

Chen, Lin-xing, Min Hu, Li-nan Huang, Zheng-shuang Hua, Jia-liang Kuang, Sheng-jin Li, and Wen-sheng Shu. 2015. "Comparative Metagenomic and Metatranscriptomic Analyses of Microbial Communities in Acid Mine Drainage." *The ISME Journal* 9 (7): 1579–92. https://doi.org/10.1038/ismej.2014.245.

Chen, Molly, Daniel S Grégoire, Jeffrey G Bain, David W Blowes, and Laura A Hug. 2024. "Legacy Copper/Nickel Mine Tailings Potentially Harbor Novel Iron/Sulfur Cycling Microorganisms within Highly Variable Communities." Edited by John R. Spear. *Applied and Environmental Microbiology* 90 (6): 1–21. https://doi.org/10.1128/aem.00143-24.

Chen, X.-G., A.-L. Geng, R. Yan, W.D. Gould, Y.-L. Ng, and D.T. Liang. 2004. "Isolation and Characterization of Sulphur-Oxidizing *Thiomonas sp.* and Its Potential Application in Biological Deodorization." *Letters in Applied Microbiology* 39 (6): 495–503. https://doi.org/10.1111/j.1472-765X.2004.01615.x.

Christel, Stephan, Jimmy Fridlund, Antoine Buetti-Dinh, Moritz Buck, Elizabeth L. Watkin, and Mark Dopson. 2016. "RNA Transcript Sequencing Reveals Inorganic Sulfur Compound Oxidation Pathways in the Acidophile *Acidithiobacillus ferrivorans*." Edited by Rich Boden. *FEMS Microbiology Letters* 363 (7): fnw057. https://doi.org/10.1093/femsle/fnw057.

Chua, Kah-Ooi, Wah-Seng See-Too, Robson Ee, Yan-Lue Lim, Wai-Fong Yin, and Kok-Gan Chan. 2019. "In Silico Analysis Reveals Distribution of Quorum Sensing Genes and Consistent Presence of LuxR Solos in the *Pandoraea* Species." *Frontiers in Microbiology* 10 (August). https://doi.org/10.3389/fmicb.2019.01758.

Coles, V. J., M. R. Stukel, M. T. Brooks, A. Burd, B. C. Crump, M. A. Moran, J. H. Paul, et al. 2017. "Ocean Biogeochemistry Modeled with Emergent Trait-Based Genomics." *Science*. https://doi.org/10.1126/science.aan5712.

Cook, Alasdair M., Theo H. M. Smits, and Karin Denger. 2008. "Sulfonates and Organotrophic Sulfite Metabolism." In *Microbial Sulfur Metabolism*. https://doi.org/10.1007/978-3-540-72682-1_14.

Cron, Brandi R., Cody S. Sheik, Fotios Christos A. Kafantaris, Gregory K. Druschel, Jeffrey S. Seewald, Christopher R. German, Gregory J. Dick, John A. Breier, and Brandy M. Toner. 2020. "Dynamic Biogeochemistry of the Particulate Sulfur Pool in a Buoyant Deep-Sea Hydrothermal Plume." *ACS Earth and Space Chemistry* 4 (2): 168–82. https://doi.org/10.1021/acsearthspacechem.9b00214.

Dahl, Christiane. 2005. *Environmental Technologies to Treat Sulfur Pollution - Principles and Applications*. Edited by Piet N.L. Lens (Ed.). *Environmental Technologies to Treat Sulfur Pollution - Principles and Applications*. 2nd Editio. IWA Publishing. https://doi.org/10.2166/9781780403038.

Dahl, Christiane, Bettina Franz, Daniela Hensen, Anne Kesselheim, and Renate Zigann. 2013. "Sulfite Oxidation in the Purple Sulfur Bacterium *Allochromatium vinosum*: Identification of SoeABC as a Major Player and Relevance of SoxYZ in the Process." *Microbiology (United Kingdom)* 159 (PART 12): 2626–38. https://doi.org/10.1099/mic.0.071019-0.

Dam, Bomba, Sukhendu Mandal, Wriddhiman Ghosh, Sujoy K. Das Gupta, and Pradosh Roy. 2007. "The S4-Intermediate Pathway for the Oxidation of Thiosulfate by the Chemolithoautotroph *Tetrathiobacter kashmirensis* and Inhibition of Tetrathionate Oxidation by Sulfite." *Research in Microbiology* 158 (4): 330–38. https://doi.org/10.1016/j.resmic.2006.12.013.

Denef, Vincent J., Ryan S. Mueller, and Jillian F. Banfield. 2010. "AMD Biofilms: Using Model Communities to Study Microbial Evolution and Ecological Complexity in Nature." *ISME Journal* 4 (5): 599–610. https://doi.org/10.1038/ismej.2009.158.

Denkmann, Kevin, Fabian Grein, Renate Zigann, Anna Siemen, Johannes Bergmann, Sebastian van Helmont, Anne Nicolai, Inês A. C. Pereira, and Christiane Dahl. 2012. "Thiosulfate Dehydrogenase: A Widespread Unusual Acidophilic c -type Cytochrome." *Environmental Microbiology* 14 (10): 2673–88. https://doi.org/10.1111/j.1462-2920.2012.02820.x.

Dick, Gregory J. 2019. "The Microbiomes of Deep-Sea Hydrothermal Vents: Distributed Globally, Shaped Locally." *Nature Reviews Microbiology* 17 (5): 271–83. https://doi.org/10.1038/s41579-019-0160-2.

Du, Rui, Di Gao, Yiting Wang, Lijun Liu, Jingguang Cheng, Jiwen Liu, Xiao-Hua Zhang, and Min Yu. 2022. "Heterotrophic Sulfur Oxidation of *Halomonas titanicae* SOB56 and its Habitat Adaptation to the Hydrothermal Environment." *Frontiers in Microbiology* 13 (June). https://doi.org/10.3389/fmicb.2022.888833.

Eckley, C. S., T. P. Luxton, J. L. McKernan, J. Goetz, and J. Goulet. 2015. "Influence of Reservoir Water Level Fluctuations on Sediment Methylmercury Concentrations Downstream of the Historical Black Butte Mercury Mine, OR." *Applied Geochemistry* 61: 284–93. https://doi.org/10.1016/j.apgeochem.2015.06.011.

Friedrich, Cornelius G., Frank Bardischewsky, Dagmar Rother, Armin Quentmeier, and Jörg Fischer. 2005. "Prokaryotic Sulfur Oxidation." *Current Opinion in Microbiology*. https://doi.org/10.1016/j.mib.2005.04.005.

Friedrich, Cornelius G., Dagmar Rother, Frank Bardischewsky, Armin Quentmeier, and Jörg Fischer. 2001. "Oxidation of Reduced Inorganic Sulfur Compounds by Bacteria: Emergence of a Common Mechanism?" *Applied and Environmental Microbiology* 67 (7): 2873–82. https://doi.org/10.1128/AEM.67.7.2873-2882.2001.

Frigaard, Niels-Ulrik, and Christiane Dahl. 2008. "Sulfur Metabolism in Phototrophic Sulfur Bacteria." In , 103–200. https://doi.org/10.1016/S0065-2911(08)00002-7.

Fujishiro, Naoji, Junna Hatae, and Hiroshi Kawata. 1994. "A Program for Calculation of the Proton Activity Coefficient." *Computers in Biology and Medicine* 24 (3): 221–28. https://doi.org/10.1016/0010-4825(94)90018-3.

Gao, Shuang, Zhiling Li, Yanan Hou, Aijie Wang, Qian Liu, and Cong Huang. 2022. "Effects of Different Carbon Sources on the Efficiency of Sulfur-Oxidizing Denitrifying Microorganisms." *Environmental Research* 204 (PA): 111946.

https://doi.org/10.1016/j.envres.2021.111946.

Garcia, Catherine A, George I Hagstrom, Alyse A Larkin, Lucas J Ustick, Simon A Levin, Michael W Lomas, and Adam C Martiny. 2020. "Linking Regional Shifts in Microbial Genome Adaptation with Surface Ocean Biogeochemistry" 375 (1798). https://doi.org/http://dx.doi.org/10.1098/rstb.2019.0254.

Ghosh, Wriddhiman, and Bomba Dam. 2009. "Biochemistry and Molecular Biology of Lithotrophic Sulfur Oxidation by Taxonomically and Ecologically Diverse Bacteria and Archaea." *FEMS Microbiology Reviews* 33 (6): 999–1043. https://doi.org/10.1111/j.1574-6976.2009.00187.x.

Giovannelli, Donato, Matthew Chung, Justin Staley, Valentin Starovoytov, Nadine Le Bris, and Costantino Vetriani. 2016. "*Sulfurovum riftiae* sp. nov., a Mesophilic, Thiosulfate-Oxidizing, Nitrate-Reducing Chemolithoautotrophic Epsilonproteobacterium Isolated from the Tube of the Deep-Sea Hydrothermal Vent Polychaete *Riftia pachyptila*." *International Journal of Systematic and Evolutionary Microbiology* 66 (7): 2697–2701. https://doi.org/10.1099/ijsem.0.001106.

Götz, Florian, Petra Pjevac, Stephanie Markert, Jesse McNichol, Dörte Becher, Thomas Schweder, Marc Mussmann, and Stefan M. Sievert. 2019. "Transcriptomic and Proteomic Insight into the Mechanism of Cyclooctasulfur- versus Thiosulfate-Oxidation by the Chemolithoautotroph *Sulfurimonas denitrificans*." *Environmental Microbiology* 21 (1): 244–58. https://doi.org/10.1111/1462-2920.14452.

Govil, Tanvi, Navanietha K. Rathinam, David R. Salem, and Rajesh K. Sani. 2019. "Taxonomical Diversity of Extremophiles in the Deep Biosphere." In *Microbial Diversity in the Genomic Era*, 631–56. Elsevier. https://doi.org/10.1016/B978-0-12-814849-5.00035-6.

Gregersen, Lea H., Donald A. Bryant, and Niels Ulrik Frigaard. 2011. "Mechanisms and Evolution of Oxidative Sulfur Metabolism in Green Sulfur Bacteria." *Frontiers in Microbiology* 2 (MAY): 1–14. https://doi.org/10.3389/fmicb.2011.00116.

Grein, Fabian, Inês A. C. Pereira, and Christiane Dahl. 2010. "Biochemical Characterization of Individual Components of the *Allochromatium vinosum* DsrMKJOP Transmembrane Complex Aids Understanding of Complex Function In Vivo." *Journal of Bacteriology* 192 (24): 6369–77. https://doi.org/10.1128/JB.00849-10.

Grettenberger, Christen L., Jeff R. Havig, and Trinity L. Hamilton. 2020. "Metabolic Diversity and Co-occurrence of Multiple *Ferrovum* Species at an Acid Mine Drainage Site." *BMC Microbiology*, 1–14. https://doi.org/10.1101/751859.

Gu, Zuguang, Roland Eils, and Matthias Schlesner. 2016. "Complex Heatmaps Reveal Patterns and Correlations in Multidimensional Genomic Data." *Bioinformatics* 32 (18): 2847–49. https://doi.org/10.1093/bioinformatics/btw313.

Gwak, Joo Han, Samuel Imisi Awala, Ngoc Loi Nguyen, Woon Jong Yu, Hae Young Yang, Martin Von Bergen, Nico Jehmlich, et al. 2022. "Sulfur and Methane Oxidation by a Single Microorganism." *Proceedings of the National Academy of Sciences of the United States of America* 119 (32): 1–12. https://doi.org/10.1073/pnas.2114799119.

Haja, Dominik K., Chang-Hao Wu, Farris L. Poole, John Sugar, Samuel G. Williams, Anne K.

Jones, and Michael W. W. Adams. 2020. “Characterization of Thiosulfate Reductase from *Pyrobaculum aerophilum* Heterologously Produced in *Pyrococcus furiosus*.” *Extremophiles* 24 (1): 53–62. https://doi.org/10.1007/s00792-019-01112-9.

Hall, Nina Lansbury, and Talia Jeanneret. 2015. “Social Licence to Operate.” *Corporate Communications: An International Journal* 20 (2): 213–27. https://doi.org/10.1108/ccij-01-2014-0005.

Han, Yuchen, and Mirjam Perner. 2015. “The Globally Widespread Genus *sulfurimonas*: Versatile Energy Metabolisms and Adaptations to Redox Clines.” *Frontiers in Microbiology* 6 (SEP): 1–17. https://doi.org/10.3389/fmicb.2015.00989.

Hao, Tian wei, Peng yu Xiang, Hamish R. Mackey, Kun Chi, Hui Lu, Ho kwong Chui, Mark C.M. van Loosdrecht, and Guang Hao Chen. 2014. “A Review of Biological Sulfate Conversions in Wastewater Treatment.” *Water Research* 65: 1–21. https://doi.org/10.1016/j.watres.2014.06.043.

Harrold, Zoë R., Mark L. Skidmore, Trinity L. Hamilton, Libby Desch, Kirina Amada, Will Van Gelder, Kevin Glover, Eric E. Roden, and Eric S. Boyd. 2016. “Aerobic and Anaerobic Thiosulfate Oxidation by a Cold-Adapted, Subglacial Chemoautotroph.” *Applied and Environmental Microbiology* 82 (5): 1486–95. https://doi.org/10.1128/AEM.03398-15.

Heinzinger, N. K., S. Y. Fujimoto, M. A. Clark, M. S. Moreno, and E. L. Barrett. 1995. “Sequence Analysis of the Phs Operon in *Salmonella typhimurium* and the Contribution of Thiosulfate Reduction to Anaerobic Energy Metabolism.” *Journal of Bacteriology* 177 (10): 2813–20. https://doi.org/10.1128/jb.177.10.2813-2820.1995.

Hensel, Michael, Andrew P. Hinsley, Thomas Nikolaus, Gary Sawers, and Ben C. Berks. 1999. “The Genetic Basis of Tetrathionate Respiration in *Salmonella typhimurium*.” *Molecular Microbiology* 32 (2): 275–87. https://doi.org/10.1046/j.1365-2958.1999.01345.x.

Hensen, Daniela, Detlef Sperling, Hans G. Trüper, Daniel C. Brune, and Christiane Dahl. 2006. “Thiosulphate Oxidation in the Phototrophic Sulphur Bacterium *Allochromatium vinosum*.” *Molecular Microbiology* 62 (3): 794–810. https://doi.org/10.1111/j.1365-2958.2006.05408.x.

Herbert, Roger B., Maria Malmström, Gustav Ebenå, Ursula Salmon, Embaie Ferrow, and Matthias Fuchs. 2005. “Quantification of Abiotic Reaction Rates in Mine Tailings: Evaluation of Treatment Methods for Eliminating Iron- and Sulfur-Oxidizing Bacteria.” *Environmental Science and Technology*. https://doi.org/10.1021/es0400537.

Hinsley, Andrew P., and B. C. Berks. 2002. “Specificity of Respiratory Pathways Involved in the Reduction of Sulfur Compounds by *Salmonella enterica*.” *Microbiology* 148 (11): 3631–38. https://doi.org/10.1099/00221287-148-11-3631.

Hirschler, Aurélie, Christine Carapito, Loïc Maurer, Julie Zumsteg, Claire Villette, Dimitri Heintz, Christiane Dahl, et al. 2021. “Biodesulfurization Induces Reprogramming of Sulfur Metabolism in *Rhodococcus qingshengii* IGTS8: Proteomics and Untargeted Metabolomics.” *Microbiology Spectrum* 9 (2). https://doi.org/10.1128/spectrum.00692-21.

Hua, Z.-S., Y.-J. Han, L.-X. Chen, J. Liu, M. Hu, S.-J. Li, J.-L. Kuang, P.S. Chain, L.-N. Huang, and W.-S. Shu. 2015. “Ecological Roles of Dominant and Rare Prokaryotes in Acid Mine Drainage Revealed by Metagenomics and Metatranscriptomics.” *ISME Journal* 9 (6):

1280–94. https://doi.org/10.1038/ismej.2014.212.

Huang, Jiangxun, Qingguang Li, Pan Wu, Shilu Wang, Shangyi Gu, Mingwei Guo, and Yong Fu. 2022. “The Buffering of a Riverine Carbonate System under the Input of Acid Mine Drainage: Example from a Small Karst Watershed, Southwest China.” *Frontiers in Environmental Science* 10 (September): 1–11. https://doi.org/10.3389/fenvs.2022.1020452.

Inagaki, Fumio, Ken Takai, Kenneth H. Nealson, and Koki Horikoshi. 2004. “*Sulfurovum lithotrophicum* gen. nov., sp. nov., a Novel Sulfur-Oxidizing Chemolithoautotroph within the ε-Proteobacteria Isolated from Okinawa Trough Hydrothermal Sediments.” *International Journal of Systematic and Evolutionary Microbiology* 54 (5): 1477–82. https://doi.org/10.1099/ijs.0.03042-0.

Ito, Tsukasa, Kenichi Sugita, Isao Yumoto, Yoshinobu Nodasaka, and Satoshi Okabe. 2005. “*Thiovirga sulfuroxydans* gen. nov., sp. nov., a Chemolithoautotrophic Sulfur-Oxidizing Bacterium Isolated from a Microaerobic Waste-Water Biofilm.” *International Journal of Systematic and Evolutionary Microbiology* 55 (3): 1059–64. https://doi.org/10.1099/ijs.0.63467-0.

Jackson, B. E., and M. J. McInerney. 2000. “Thiosulfate Disproportionation by *Desulfotomaculum thermobenzoicum*.” *Applied and Environmental Microbiology* 66 (8): 3650–53. https://doi.org/10.1128/AEM.66.8.3650-3653.2000.

Jenner, Leon P., Julia M. Kurth, Sebastian Van Helmont, Katarzyna P. Sokol, Erwin Reisner, Christiane Dahl, Justin M. Bradley, Julea N. Butt, and Myles R. Cheesman. 2019. “Heme Ligation and Redox Chemistry in Two Bacterial Thiosulfate Dehydrogenase (TsdA) Enzymes.” *Journal of Biological Chemistry* 294 (47): 18002–14. https://doi.org/10.1074/jbc.RA119.010084.

Jensen, Henriette Stokbro, Piet N.L. Lens, Jeppe L. Nielsen, Kai Bester, Asbjørn Haaning Nielsen, Thorkild Hvitved-Jacobsen, and Jes Vollertsen. 2011. “Growth Kinetics of Hydrogen Sulfide Oxidizing Bacteria in Corroded Concrete from Sewers.” *Journal of Hazardous Materials* 189 (3): 685–91. https://doi.org/10.1016/j.jhazmat.2011.03.005.

Jiang, Guangming, Keshab Raj Sharma, Albert Guisasola, Jurg Keller, and Zhiguo Yuan. 2009. “Sulfur Transformation in Rising Main Sewers Receiving Nitrate Dosage.” *Water Research* 43 (17): 4430–40. https://doi.org/10.1016/j.watres.2009.07.001.

Jin, Qusheng, and Matthew F. Kirk. 2018. “pH as a Primary Control in Environmental Microbiology: 1. Thermodynamic Perspective.” *Frontiers in Environmental Science* 6 (MAY): 1–15. https://doi.org/10.3389/fenvs.2018.00021.

———. 2018b. “pH as a Primary Control in Environmental Microbiology: 2. Kinetic Perspective.” *Frontiers in Environmental Science* 6 (September): 1–16. https://doi.org/10.3389/fenvs.2018.00101.

Jong, Govardus A. H. De, Wim Hazeu, Piet Bos, and J. Gijs Kuenen. 1997a. “Isolation of the Tetrathionate Hydrolase from *Thiobacillus acidophilus*.” *European Journal of Biochemistry* 243 (3): 678–83. https://doi.org/10.1111/j.1432-1033.1997.00678.x.

Jong, Govardus A.H. De, Wim Hazeu, Piet Bos, and J. Gijs Kuenen. 1997b. “Polythionate Degradation by Tetrathionate Hydrolase of *Thiobacillus ferrooxidans*.” *Microbiology* 143 (2): 499–504. https://doi.org/10.1099/00221287-143-2-499.

Junkins, Emily N., Joseph B. McWhirter, Laura-Isobel McCall, and Bradley S. Stevenson. 2022. "Environmental Structure Impacts Microbial Composition and Secondary Metabolism." *ISME Communications* 2 (1): 15. https://doi.org/10.1038/s43705-022-00097-5.

Kanao, Tadayoshi, Kazuo Kamimura, and Tsuyoshi Sugio. 2007. "Identification of a Gene Encoding a Tetrathionate Hydrolase in *Acidithiobacillus ferrooxidans*." *Journal of Biotechnology* 132 (1): 16–22. https://doi.org/10.1016/j.jbiotec.2007.08.030.

Kang, Heeyoung, Haneul Kim, Beom Il Lee, Yochan Joung, and Kiseong Joh. 2014. "*Sediminibacterium goheungense* sp. nov., Isolated from a Freshwater Reservoir." *International Journal of Systematic and Evolutionary Microbiology* 64 (PART 4): 1328–33. https://doi.org/10.1099/ijs.0.055137-0.

Kappler, Ulrike, Cornelius G. Friedrich, Hans G. Trüper, and Christiane Dahl. 2001. "Evidence for Two Pathways of Thiosulfate Oxidation in *Starkeya novella* (Formerly *Thiobacillus novellus*)." *Archives of Microbiology* 175 (2): 102–11. https://doi.org/10.1007/s002030000241.

Kilmartin, James R., Megan J. Maher, Kuakarun Krusong, Christopher J. Noble, Graeme R. Hanson, Paul V. Bernhardt, Mark J. Riley, and Ulrike Kappler. 2011. "Insights into Structure and Function of the Active Site of SoxAX Cytochromes." *Journal of Biological Chemistry* 286 (28): 24872–81. https://doi.org/10.1074/jbc.M110.212183.

Kim, Yonghoon, Bobae Kim, Keunsoo Kang, and Tae Young Ahn. 2016. "*Sediminibacterium aquarii* sp. nov., Isolated from Sediment in a Fishbowl." *International Journal of Systematic and Evolutionary Microbiology* 66 (11): 4501–5. https://doi.org/10.1099/ijsem.0.001380.

Kirjavainen, V., N. Schreithofer, and K. Heiskanen. 2002. "Effect of Calcium and Thiosulfate Ions on Flotation Selectivity of Nickel-Copper Ores." *Minerals Engineering* 15 (1–2): 1–5. https://doi.org/10.1016/S0892-6875(01)00213-8.

Klatt, Judith M., and Lubos Polerecky. 2015. "Assessment of the Stoichiometry and Efficiency of $CO_2$ Fixation Coupled to Reduced Sulfur Oxidation." *Frontiers in Microbiology* 6 (May): 484. https://doi.org/10.3389/fmicb.2015.00484.

Kletzin, A. 1992. "Molecular Characterization of the Sor Gene, Which Encodes the Sulfur Oxygenase/Reductase of the Thermoacidophilic Archaeum *Desulfurolobus ambivalens*." *Journal of Bacteriology* 174 (18): 5854–59. https://doi.org/10.1128/jb.174.18.5854-5859.1992.

Koch, Tobias, and Christiane Dahl. 2018. "A Novel Bacterial Sulfur Oxidation Pathway Provides a New Link between the Cycles of Organic and Inorganic Sulfur Compounds." *ISME Journal* 12 (10): 2479–91. https://doi.org/10.1038/s41396-018-0209-7.

Kuyucak, Nural. 1998. "Mining, the Environment and the Treatment of Mine Effluents." *International Journal of Environment and Pollution* 10 (2): 315. https://doi.org/10.1504/IJEP.1998.005151.

Lahme, Sven, Cameron M. Callbeck, Lucy E. Eland, Anil Wipat, Dennis Enning, Ian M. Head, and Casey R.J. Hubert. 2020. "Comparison of Sulfide-Oxidizing *Sulfurimonas* Strains Reveals a New Mode of Thiosulfate Formation in Subsurface Environments." *Environmental Microbiology* 22 (5): 1784–1800. https://doi.org/10.1111/1462-2920.14894.

Lester, William W., Micheal S. Adams, and Andrew M. Farmer. 1988. “Effects of Light and Temperature on Photosynthesis of the Nuisance Alga Cladophora Glomerata (L.) Kutz from Green Bay, Lake Michigan.” *New Phytologist* 109 (1): 53–58. https://doi.org/10.1111/j.1469-8137.1988.tb00218.x.

Li, Jingjing, Fabienne Göbel, Hsun Yun Hsu, Julian Nikolaus Koch, Natalie Hager, Wanda Antonia Flegler, Tomohisa Sebastian Tanabe, and Christiane Dahl. 2024. “YeeE-like Bacterial SoxT Proteins Mediate Sulfur Import for Oxidation and Signal Transduction.” *Communications Biology* 7 (1): 1–12. https://doi.org/10.1038/s42003-024-07270-7.

Li, Jingjing, Kaya Törkel, Julian Koch, Tomohisa Sebastian Tanabe, Hsun Yun Hsu, and Christiane Dahl. 2023. “In the Alphaproteobacterium *Hyphomicrobium denitrificans* SoxR Serves a Sulfane Sulfur-Responsive Repressor of Sulfur Oxidation.” *Antioxidants* 12 (8). https://doi.org/10.3390/antiox12081620.

Li, Wenji, Meng Zhang, Da Kang, Wenda Chen, Tao Yu, Dongdong Xu, Zhuo Zeng, Yiyu Li, and Ping Zheng. 2020. “Mechanisms of Sulfur Selection and Sulfur Secretion in a Biological Sulfide Removal (BISURE) System.” *Environment International* 137 (January): 105549. https://doi.org/10.1016/j.envint.2020.105549.

Lindsay, Matthew B.J., Michael C. Moncur, Jeffrey G. Bain, John L. Jambor, Carol J. Ptacek, and David W. Blowes. 2015. “Geochemical and Mineralogical Aspects of Sulfide Mine Tailings.” *Applied Geochemistry* 57: 157–77. https://doi.org/10.1016/j.apgeochem.2015.01.009.

Liu, Felicia Y.L., Lauren E. Twible, Tara E. Colenbrander Nelson, Kelly Whaley-Martin, Yunyun Yan, James L.S. Arrey, and Lesley A. Warren. 2025. “Microbial Sulfur Cycling Determinants and Implications for Environmental Impacts.” *Chemosphere* 372 (January): 144084. https://doi.org/10.1016/j.chemosphere.2025.144084.

Lopes, Ana Rita, Diana Madureira, Ana Diaz, Sílvia Santos, Maria Cristina Vila, and Olga Cristina Nunes. 2020. “Characterisation of Bacterial Communities from an Active Mining Site and Assessment of Its Potential Metal Solubilising Activity.” *Journal of Environmental Chemical Engineering* 8 (6): 104495. https://doi.org/10.1016/j.jece.2020.104495.

Lu, W.-P., and D. P. Kelly. 1988. “Cellular Location and Partial Purification of the ‘Thiosulphate-Oxidizing Enzyme’ and ‘Trithionate Hydrolyase’ from *Thiobacillus tepidarius*.” *Microbiology* 134 (4): 877–85. https://doi.org/10.1099/00221287-134-4-877.

Luo, Jianfei, Xiaoqin Tan, Kexin Liu, and Weitie Lin. 2018. “Survey of Sulfur-Oxidizing Bacterial Community in the Pearl River Water Using SoxB, Sqr, and DsrA as Molecular Biomarkers.” *3 Biotech* 8 (1). https://doi.org/10.1007/s13205-017-1077-y.

Luther, George W., Alyssa J. Findlay, Daniel J. MacDonald, Shannon M. Owings, Thomas E. Hanson, Roxanne A. Beinart, and Peter R. Girguis. 2011. “Thermodynamics and Kinetics of Sulfide Oxidation by Oxygen: A Look at Inorganically Controlled Reactions and Biologically Mediated Processes in the Environment.” *Frontiers in Microbiology* 2. https://doi.org/10.3389/fmicb.2011.00062.

Lyratzakis, Alexandros, Jakob Meier-Credo, Julian D Langer, and Georgios Tsiotis. 2023. “Insights into the Sulfur Metabolism of *Chlorobaculum tepidum* by Label-free Quantitative

Proteomics." *Proteomics*, no. April 2022: 2200138. https://doi.org/10.1002/pmic.202200138.

Ma, Jie, Hui Liu, Chen Zhang, Kang Ding, Rong Chen, and Shan Liu. 2020. "Joint Response of Chemistry and Functional Microbial Community to Oxygenation of the Reductive Confined Aquifer." *Science of the Total Environment* 720. https://doi.org/10.1016/j.scitotenv.2020.137587.

Magnuson, Elisse, Ianina Altshuler, Nastasia J Freyria, Richard J Leveille, and Lyle G Whyte. 2023. "Sulfur-cycling Chemolithoautotrophic Microbial Community Dominates a Cold, Anoxic, Hypersaline Arctic Spring." *Microbiome*, 1–20. https://doi.org/10.1186/s40168-023-01628-5.

Martin, Marcel. 2011. "Cutadapt Removes Adapter Sequences from High-Throughput Sequencing Reads." *EMBnet.Journal* 17: 10–12.

Meier, Dimitri V., Petra Pjevac, Wolfgang Bach, Stephane Hourdez, Peter R. Girguis, Charles Vidoudez, Rudolf Amann, and Anke Meyerdierks. 2017. "Niche Partitioning of Diverse Sulfur-Oxidizing Bacteria at Hydrothermal Vents." *ISME Journal* 11 (7): 1545–58. https://doi.org/10.1038/ismej.2017.37.

Melton, Emily Denise, Dimitry Y. Sorokin, Lex Overmars, Olga Chertkov, Alicia Clum, Manoj Pillay, Natalia Ivanova, et al. 2016. "Complete Genome Sequence of *Desulfurivibrio alkaliphilus* strain AHT2T, a Haloalkaliphilic Sulfidogen from Egyptian Hypersaline Alkaline Lakes." *Standards in Genomic Sciences* 11 (1): 67. https://doi.org/10.1186/s40793-016-0184-4.

Meulenberg, Rogier, Jack T. Pronk, Johannes Frank, Wim Hazeu, Piet Bos, and J. Gijs Kuenen. 1992. "Purification and Partial Characterization of a Thermostable Trithionate Hydrolase from the Acidophilic Sulphur Oxidizer *Thiobacillus acidophilus*." *European Journal of Biochemistry* 209 (1): 367–74. https://doi.org/10.1111/j.1432-1033.1992.tb17298.x.

Meulenberg, Rogier, Jack T. Pronk, Wim Hazeu, Piet Bos, and J. Gijs Kuenen. 1992. "Oxidation of Reduced Sulphur Compounds by Intact Cells of *Thiobacillus acidophilus*." *Archives of Microbiology* 157 (2): 161–68. https://doi.org/10.1007/BF00245285.

Meyer, Birte, Johannes F. Imhoff, and Jan Kuever. 2007. "Molecular Analysis of the Distribution and Phylogeny of the SoxB Gene among Sulfur-Oxidizing Bacteria - Evolution of the Sox Sulfur Oxidation Enzyme System." *Environmental Microbiology* 9 (12): 2957–77. https://doi.org/10.1111/j.1462-2920.2007.01407.x.

Mhonde, Ngoni, Leena Pitkänen, Kirsten Corin, and Nóra Schreithofer. 2021. "The Solution Interaction of Tetrathionate Ions and Sodium Isobutyl Xanthate and Its Effect on the Flotation of Galena and Chalcopyrite." *Minerals* 11 (2): 204. https://doi.org/10.3390/min11020204.

Miettinen, Hanna, Malin Bomberg, Thi Minh Khanh Le, and Päivi Kinnunen. 2021. "Identification and Metabolism of Naturally Prevailing Microorganisms in Zinc and Copper Mineral Processing." *Minerals* 11 (2): 1–31. https://doi.org/10.3390/min11020156.

Miranda-Trevino, Jorge C., Michael Pappoe, Kelly Hawboldt, and Christina Bottaro. 2013. "The Importance of Thiosalts Speciation: Review of Analytical Methods, Kinetics, and Treatment." *Critical Reviews in Environmental Science and Technology* 43 (19): 2013–70.

https://doi.org/10.1080/10643389.2012.672047.

Mori, Koji, Kaoru Yamaguchi, and Satoshi Hanada. 2018. "*Sulfurovum denitrificans* sp. nov., an Obligately Chemolithoautotrophic Sulfur-Oxidizing Epsilonproteobacterium Isolated from a Hydrothermal Field." *International Journal of Systematic and Evolutionary Microbiology* 68 (7): 2183–87. https://doi.org/10.1099/ijsem.0.002803.

Müller, Fabian H., Tiago M. Bandeiras, Tim Urich, Miguel Teixeira, Cláudio M. Gomes, and Arnulf Kletzin. 2004. "Coupling of the Pathway of Sulphur Oxidation to Dioxygen Reduction: Characterization of a Novel Membrane-Bound Thiosulphate:Quinone Oxidoreductase." *Molecular Microbiology* 53 (4): 1147–60. https://doi.org/10.1111/j.1365-2958.2004.04193.x.

Murillo, Alejandro A., Salvador Ramírez-Flandes, Edward F. DeLong, and Osvaldo Ulloa. 2014. "Enhanced Metabolic Versatility of Planktonic Sulfur-Oxidizing γ-Proteobacteria in an Oxygen-Deficient Coastal Ecosystem." *Frontiers in Marine Science* 1 (JUL): 1–13. https://doi.org/10.3389/fmars.2014.00018.

Musuku, Benjamin, Diana Kasymova, Eija Saari, and Olli Dahl. 2023. "Influence of Water Quality on Sulphide Ore Oxidation and Speciation of Sulphur Anions during Autogenous Milling." *Minerals* 13 (2): 277. https://doi.org/10.3390/min13020277.

Nancucheo, Ivan, José A P Bitencourt, Prafulla K Sahoo, Joner Oliveira Alves, José O Siqueira, and Guilherme Oliveira. 2017. "Recent Developments for Remediating Acidic Mine Waters Using Sulfidogenic Bacteria." *BioMed Research International* 2017: 7256582. https://doi.org/10.1155/2017/7256582.

Opara, Chiamaka Belsonia, Nor Kamariah, Jeroen Spooren, Katrin Pollmann, and Sabine Kutschke. 2023. "Interesting Halophilic Sulphur-Oxidising Bacteria with Bioleaching Potential: Implications for Pollutant Mobilisation from Mine Waste." *Microorganisms* 11 (1): 222. https://doi.org/10.3390/microorganisms11010222.

Pakostova, Eva, D. Barrie Johnson, Zhongwen Bao, Peter M. MacKenzie, Carol J. Ptacek, and David W. Blowes. 2020. "Bacterial and Archaeal Diversity in Sulfide-Bearing Waste Rock at Faro Mine Complex, Yukon Territory, Canada." *Geomicrobiology Journal* 37 (6): 511–19. https://doi.org/10.1080/01490451.2020.1731020.

Pakostova, Eva, Mason McAlary, Stephanie Marshall, Samantha McGarry, Carol J. Ptacek, and David W. Blowes. 2022. "Microbiology of a Multi-Layer Biosolid/Desulfurized Tailings Cover on a Mill Tailings Impoundment." *Journal of Environmental Management* 302 (PA): 114030. https://doi.org/10.1016/j.jenvman.2021.114030.

Pantke, Claudia, Martin Obst, Karim Benzerara, Guillaume Morin, Georges Ona-Nguema, Urs Dippon, and Andreas Kappler. 2012. "Green Rust Formation during Fe(II) Oxidation by the Nitrate-Reducing *Acidovorax sp.* Strain BoFeN1." *Environmental Science & Technology* 46 (3): 1439–46. https://doi.org/10.1021/es2016457.

Paredes, Gabriela, Tobias Viehboeck, Raymond Lee, Marton Palatinszky, Michaela Mausz, Sigfried Reipert, Arno Schintlmeister, et al. 2020. "Anaerobic Sulfur Oxidation Underlies Adaptation of a Chemosynthetic Symbiont to Oxic-Anoxic Interfaces." *BioRxiv*, January, 2020.03.17.994798. https://doi.org/10.1101/2020.03.17.994798.

Peeters, Charlotte, Evelien De Canck, Margo Cnockaert, Evie De Brandt, Cindy Snauwaert,

Bart Verheyde, Eliza Depoorter, Theodore Spilker, John J. LiPuma, and Peter Vandamme. 2019. “Comparative Genomics of *Pandoraea*, a Genus Enriched in Xenobiotic Biodegradation and Metabolism.” *Frontiers in Microbiology* 10 (November): 1–21. https://doi.org/10.3389/fmicb.2019.02556.

Pereira, Inês A.Cardoso, Ana Raquel Ramos, Fabian Grein, Marta Coimbra Marques, Sofia Marques da Silva, and Sofia Santos Venceslau. 2011. “A Comparative Genomic Analysis of Energy Metabolism in Sulfate Reducing Bacteria and Archaea.” *Frontiers in Microbiology* 2 (APR). https://doi.org/10.3389/fmicb.2011.00069.

Pott, Andrea S., and Christiane Dahl. 1998. “Sirohaem Sulfite Reductase and Other Proteins Encoded by Genes at the Dsr Locus of *Chromatium vinosum* are Involved in the Oxidation of Intracellular Sulfur.” *Microbiology*. https://doi.org/10.1099/00221287-144-7-1881.

Prausnitz, John M., Rudiger N. Lichtenthaler, and Edmundo Gomes de Azevedo. 1978. *Molecular Thermodynamics of Fluid Phase Equilibria*. Edited by Bernard Goodwin. 3rd ed. Upper Saddle River, New Jersey.

Pronk, J.T., R Meulenberg, W Hazeu, P Bos, and J.G. Kuenen. 1990. “Oxidation of Reduced Inorganic Sulphur Compounds by *Acidophilic thiobacilli*.” *FEMS Microbiology Letters* 75 (2–3): 293–306. https://doi.org/10.1111/j.1574-6968.1990.tb04103.x.

Pyne, Prosenjit, Masrure Alam, Moidu Jameela Rameez, Subhrangshu Mandal, Abhijit Sar, Nibendu Mondal, Utsab Debnath, et al. 2018. “Homologs from Sulfur Oxidation (Sox) and Methanol Dehydrogenation (Xox) Enzyme Systems Collaborate to Give Rise to a Novel Pathway of Chemolithotrophic Tetrathionate Oxidation.” *Molecular Microbiology* 109 (2): 169–91. https://doi.org/10.1111/mmi.13972.

Rameez, Moidu Jameela, Prosenjit Pyne, Subhrangshu Mandal, Sumit Chatterjee, Masrure Alam, Sabyasachi Bhattacharya, Nibendu Mondal, Jagannath Sarkar, and Wriddhiman Ghosh. 2020. “Two Pathways for Thiosulfate Oxidation in the Alphaproteobacterial Chemolithotroph *Paracoccus thiocyanatus* SST.” *Microbiological Research* 320. https://doi.org/10.1016/j.micres.2019.126345.

Rangasamy, Anandham, Janahiraman Veeranan, Indira Gandhi Pandiyan, Wo Kwon Soon, Yook Chung Keun, Hyun Han Gwang, Ho Choi Joon, and Min Sa Tong. 2014. “Early Plant Growth Promotion of Maize by Various Sulfur Oxidizing Bacteria that uses Different Thiosulfate Oxidation Pathway.” *African Journal of Microbiology Research* 8 (1): 19–27. https://doi.org/10.5897/ajmr2013.5661.

Ray, W. Keith, Gang Zeng, M. Benjamin Potters, Aqil M. Mansuri, and Timothy J. Larson. 2000. “Characterization of a 12-Kilodalton Rhodanese Encoded by GlpE of *Escherichia coli* and its Interaction with Thioredoxin.” *Journal of Bacteriology* 182 (8): 2277–84. https://doi.org/10.1128/JB.182.8.2277-2284.2000.

Rethmeier, Jörg, Andreas Rabenstein, Monika Langer, and Ulrich Fischer. 1997. “Detection of Traces of Oxidized and Reduced Sulfur Compounds in Small Samples by Combination of Different High-Performance Liquid Chromatography Methods.” *Journal of Chromatography A* 760 (2): 295–302. https://doi.org/10.1016/S0021-9673(96)00809-6.

Rittmann, Bruce E, and Perry L. McCarty. 2001. “Environmental Biotechnology: Principles and Applications.” *Current Opinion in Biotechnology*. https://doi.org/10.1016/S0958-1669(96)80047-4.

Romero, R., P. Viedma, and D. Cotoras. 2024. “Biooxidation of Hydrogen Sulfide to Sulfur by Moderate Thermophilic Acidophilic Bacteria.” *Biodegradation* 35 (2): 195–208. https://doi.org/10.1007/s10532-023-10049-y.

Sahin, Nurettin, Akio Tani, Recep Kotan, Ivo Sedláček, Kazuhide Kimbara, and Abdurrahman U. Tamer. 2011. “*Pandoraea oxalativorans* sp. nov., *Pandoraea faecigallinarum* sp. nov. and *Pandoraea vervacti* sp. nov., Isolated from Oxalate-Enriched Culture.” *International Journal of Systematic and Evolutionary Microbiology* 61 (9): 2247–53. https://doi.org/10.1099/ijs.0.026138-0.

Sakurai, Hidehiro, Takuro Ogawa, Michiko Shiga, and Kazuhito Inoue. 2010. “Inorganic Sulfur Oxidizing System in Green Sulfur Bacteria.” *Photosynthesis Research* 104 (2–3): 163–76. https://doi.org/10.1007/s11120-010-9531-2.

Satoh, Hisashi, Mitsunori Odagiri, Tsukasa Ito, and Satoshi Okabe. 2009. “Microbial Community Structures and in Situ Sulfate-Reducing and Sulfur-Oxidizing Activities in Biofilms Developed on Mortar Specimens in a Corroded Sewer System.” *Water Research* 43 (18): 4729–39. https://doi.org/10.1016/j.watres.2009.07.035.

Sauvé, Véronique, Pietro Roversi, Kirstin J. Leath, Elspeth F. Garman, Robin Antrobus, Susan M. Lea, and Ben C. Berks. 2009. “Mechanism for the Hydrolysis of a Sulfur-Sulfur Bond Based on the Crystal Structure of the Thiosulfohydrolase SoxB.” *Journal of Biological Chemistry* 284 (32): 21707–18. https://doi.org/10.1074/jbc.M109.002709.

Schedel, Michael, and Hans G. Trüper. 1980. “Anaerobic Oxidation of Thiosulfate and Elemental Sulfur in *Thiobacillus denitrificans*.” *Archives of Microbiology* 124–124 (2–3): 205–10. https://doi.org/10.1007/BF00427728.

Schippers, Axel, Peter-georg Jozsa, and Wolfgang Sand. 1996. “Sulfur Chemistry in Bacterial Leaching of Pyrite.” *Applied and Environmental Microbiology* 62 (9): 3424–31. https://doi.org/10.1128/aem.62.9.3424-3431.1996.

Schmidt, J W, and K Conn. 1969. “Abatement of Pollution from Mine Wastewaters.” *Canadian Mining Journal* 90 (6): 54–60.

Schwarz, Alex, José Ignacio Suárez, Marcelo Aybar, Iván Nancucheo, Patricio Martínez, and Bruce E. Rittmann. 2020. “A Membrane-Biofilm System for Sulfate Conversion to Elemental Sulfur in Mining-Influenced Waters.” *Science of the Total Environment* 740. https://doi.org/10.1016/j.scitotenv.2020.140088.

Sievert, Stefan M., Thorsten Heidorn, and Jan Kuever. 2000. “*Halothiobacillus kellyi* sp. nov., a Mesophilic, Obligately Chemolithoautotrophic, Sulfur-Oxidizing Bacterium Isolated from a Shallow- Water Hydrothermal Vent in the Aegean Sea, and Emended Description of the Genus *Halothiobacillus*.” *International Journal of Systematic and Evolutionary Microbiology* 50 (3): 1229–37. https://doi.org/10.1099/00207713-50-3-1229.

Skousen, Jeff, Carl E. Zipper, Arthur Rose, Paul F. Ziemkiewicz, Robert Nairn, Louis M. McDonald, and Robert L. Kleinmann. 2017. “Review of Passive Systems for Acid Mine Drainage Treatment.” *Mine Water and the Environment* 36 (1): 133–53.

https://doi.org/10.1007/s10230-016-0417-1.

Smirnov, V. V., E. A. Kiprianova, and L. V. Babich. 2001. "Auxotrophy and Utilization of Oxidized and Reduced Mineral Sulfur Forms by *Brevundimonas diminuta* Strains." *Mikrobiolohichnyi Zhurnal (Kiev, Ukraine : 1993)* 63 (5): 27–33. http://www.ncbi.nlm.nih.gov/pubmed/11785417.

Song, Yali, Jianqiang Jia, Dongmei Liu, Lina Choi, Gejiao Wang, and Mingshun Li. 2017. "*Sediminibacterium roseum* sp. nov., Isolated from Sewage Sediment." *International Journal of Systematic and Evolutionary Microbiology* 67 (11): 4674–79. https://doi.org/10.1099/ijsem.0.002355.

Spallarossa, A., J. L. Donahue, T. J. Larson, M. Bolognesi, and D. Bordo. 2001. "*Escherichia coli* GlpE Is a Prototype Sulfurtransferase for the Single-Domain Rhodanese Homology Superfamily." *Structure* 9 (11): 1117–25. https://doi.org/10.1016/S0969-2126(01)00666-9.

Stockdreher, Yvonne, Sofia S. Venceslau, Michaele Josten, Hans-Georg Sahl, Inês A. C. Pereira, and Christiane Dahl. 2012. "Cytoplasmic Sulfurtransferases in the Purple Sulfur Bacterium *Allochromatium vinosum*: Evidence for Sulfur Transfer from DsrEFH to DsrC." Edited by John R. Battista. *PLoS ONE* 7 (7): e40785. https://doi.org/10.1371/journal.pone.0040785.

Stumm, Werner, and James J. Morgan. 1995. *Aquatic Chemistry: Chemical Equilibria and Rates in Natural Waters*. 3rd ed. New York : Wiley, C1996.

Sun, Xiaoxu, Tianle Kong, Fangbai Li, Max M. Häggblom, Max Kolton, Ling Lan, Maggie C.Y. Lau Vetter, et al. 2022. "*Desulfurivibrio spp.* Mediate Sulfur-Oxidation Coupled to Sb(V) Reduction, a Novel Biogeochemical Process." *ISME Journal* 16 (6): 1547–56. https://doi.org/10.1038/s41396-022-01201-2.

Suter, Elizabeth A., Maria G. Pachiadaki, Enrique Montes, Virginia P. Edgcomb, Mary I. Scranton, Craig D. Taylor, and Gordon T. Taylor. 2021. "Diverse Nitrogen Cycling Pathways across a Marine Oxygen Gradient Indicate Nitrogen Loss Coupled to Chemoautotrophic Activity." *Environmental Microbiology* 23 (6): 2747–64. https://doi.org/10.1111/1462-2920.15187.

Tanabe, Tomohisa Sebastian, and Christiane Dahl. 2022a. "HMS-S-S: A Tool for the Identification of Sulphur Metabolism-related Genes and Analysis of Operon Structures in Genome and Metagenome Assemblies." *Molecular Ecology Resources* 22 (7): 2758–74. https://doi.org/10.1111/1755-0998.13642.

———. 2023. "HMSS2: An Advanced Tool for the Analysis of Sulphur Metabolism, Including Organosulphur Compound Transformation, in Genome and Metagenome Assemblies." *Molecular Ecology Resources*, no. May (July): 1–16. https://doi.org/10.1111/1755-0998.13848.

Thorup, Casper, Andreas Schramm, Alyssa J. Findlay, Kai W. Finster, and Lars Schreiber. 2017. "Disguised as a Sulfate Reducer: Growth of the Deltaproteobacterium *Desulfurivibrio alkaliphilus* by Sulfide Oxidation with Nitrate." *MBio* 8 (4): 1–9. https://doi.org/10.1128/mBio.00671-17.

Twible, Lauren E., Kelly Whaley-Martin, Lin-Xing Chen, Tara Colenbrander Nelson, James L.S. Arrey, Chad V. Jarolimek, Josh J. King, et al. 2024. "pH and Thiosulfate Dependent

Microbial Sulfur Oxidation Strategies across Diverse Environments." *Frontiers in Microbiology* 15 (July). https://doi.org/10.3389/fmicb.2024.1426584.

Ullrich, Sophie R., Carolina González, Anja Poehlein, Judith S. Tischler, Rolf Daniel, Michael Schlömann, David S. Holmes, and Martin Mühling. 2016. "Gene Loss and Horizontal Gene Transfer Contributed to the Genome Evolution of the Extreme Acidophile '*Ferrovum*.'" *Frontiers in Microbiology* 7 (MAY): 1–23. https://doi.org/10.3389/fmicb.2016.00797.

Varga, Dénes, and Attila K. Horváth. 2007. "Kinetics and Mechanism of the Decomposition of Tetrathionate Ion in Alkaline Medium." *Inorganic Chemistry* 46 (18): 7654–61. https://doi.org/10.1021/ic700992u.

Venceslau, S. S., Y. Stockdreher, C. Dahl, and I. A.C. Pereira. 2014. "The 'Bacterial Heterodisulfide' DsrC Is a Key Protein in Dissimilatory Sulfur Metabolism." *Biochimica et Biophysica Acta - Bioenergetics* 1837 (7): 1148–64. https://doi.org/10.1016/j.bbabio.2014.03.007.

Verburg, Rens, Nico Bezuidenhout, Terrence Chatwin, and Keith Ferguson. 2009. "The Global Acid Rock Drainage Guide (GARD Guide)." *Mine Water and the Environment* 28 (4): 305. https://doi.org/10.1007/s10230-009-0078-4.

Vigneron, Adrien, Perrine Cruaud, Alexander I. Culley, Raoul Marie Couture, Connie Lovejoy, and Warwick F. Vincent. 2021. "Genomic Evidence for Sulfur Intermediates as New Biogeochemical Hubs in a Model Aquatic Microbial Ecosystem." *Microbiome* 9 (1): 1–14. https://doi.org/10.1186/s40168-021-00999-x.

Vliet, Daan M. van, F. A.Bastiaan von Meijenfeldt, Bas E. Dutilh, Laura Villanueva, Jaap S. Sinninghe Damsté, Alfons J.M. Stams, and Irene Sánchez-Andrea. 2021. "The Bacterial Sulfur Cycle in Expanding Dysoxic and Euxinic Marine Waters." *Environmental Microbiology* 23 (6): 2834–57. https://doi.org/10.1111/1462-2920.15265.

Wang, Junjie, Zhuowei Cheng, Jiade Wang, Dongzhi Chen, Jingkai Zhao, and Songkai Qiu. 2023. "Temperature and pH on Microbial Desulfurization of Sulfide Wastewater: From Removal Performance to Gene Regulation Mechanism." *SSRN Electronic Journal* 53 (December 2022): 103720. https://doi.org/10.2139/ssrn.4326619.

Wang, Rui, Jian Qiang Lin, Xiang Mei Liu, Xin Pang, Cheng Jia Zhang, Chun Long Yang, Xue Yan Gao, et al. 2019. "Sulfur Oxidation in the Acidophilic Autotrophic *Acidithiobacillus spp.*" *Frontiers in Microbiology* 10 (JAN): 1–20. https://doi.org/10.3389/fmicb.2018.03290.

Wang, Shasha, Lijing Jiang, Qitao Hu, Liang Cui, Bitong Zhu, Xiaoteng Fu, Qiliang Lai, Zongze Shao, and Suping Yang. 2021. "Characterization of *Sulfurimonas hydrogeniphila* sp. nov., a Novel Bacterium Predominant in Deep-Sea Hydrothermal Vents and Comparative Genomic Analyses of the Genus *Sulfurimonas*." *Frontiers in Microbiology* 12 (February): 1–20. https://doi.org/10.3389/fmicb.2021.626705.

Wang, Yulin, Yulin Zhang, Yu Hu, Lei Liu, Shuang Jiang Liu, and Tong Zhang. 2023. "Genome-Centric Metagenomics Reveals the Host-Driven Dynamics and Ecological Role of CPR Bacteria in an Activated Sludge System." *Microbiome* 11 (1): 1–17. https://doi.org/10.1186/s40168-023-01494-1.

Warren, L. A., K. L. I Norlund, and L. Bernier. 2008. “Microbial Thiosulphate Reaction Arrays: The Interactive Roles of Fe(III), $O_2$ and Microbial Strain on Disproportionation and Oxidation Pathways.” *Geobiology* 6 (5): 461–70. https://doi.org/10.1111/j.1472-4669.2008.00173.x.

Wasmund, Kenneth, Marc Mußmann, and Alexander Loy. 2017. “The Life Sulfuric: Microbial Ecology of Sulfur Cycling in Marine Sediments.” *Environmental Microbiology Reports* 9 (4): 323–44. https://doi.org/10.1111/1758-2229.12538.

Watanabe, Tomohiro, Hisaya Kojima, Kazuhiro Umezawa, Chiaki Hori, Taichi E. Takasuka, Yukako Kato, and Manabu Fukui. 2019. “Genomes of Neutrophilic Sulfur-Oxidizing Chemolithoautotrophs Representing 9 Proteobacterial Species from 8 Genera.” *Frontiers in Microbiology* 10 (February): 1–13. https://doi.org/10.3389/fmicb.2019.00316.

Watling, H. R., D. M. Collinson, S. Fjastad, A. H. Kaksonen, J. Li, C. Morris, F. A. Perrot, S. M. Rea, and D. W. Shiers. 2014. “Column Bioleaching of a Polymetallic Ore: Effects of pH and Temperature on Metal Extraction and Microbial Community Structure.” *Minerals Engineering* 58: 90–99. https://doi.org/10.1016/j.mineng.2014.01.022.

Wei, Cai, Dan Sun, Wenliang Yuan, Lei Li, Chaoxu Dai, Zuozhou Chen, Xiaomin Zeng, et al. 2023. “Metagenomics Revealing Molecular Profiles of Microbial Community Structure and Metabolic Capacity in Bamucuo Lake, Tibet.” *Environmental Research* 217 (September 2022): 114847. https://doi.org/10.1016/j.envres.2022.114847.

Welte, Cornelia, Swetlana Hafner, Christian Krätzer, Armin Quentmeier, Cornelius G. Friedrich, and Christiane Dahl. 2009. “Interaction between Sox Proteins of Two Physiologically Distinct Bacteria and a New Protein Involved in Thiosulfate Oxidation.” *FEBS Letters* 583 (8): 1281–86. https://doi.org/10.1016/j.febslet.2009.03.020.

Wentzien, S. W., and W. Sand. 2004. “Tetrathionate Disproportionation by *Thiomonas intermedia* K12.” *Engineering in Life Sciences* 4 (1): 25–30. https://doi.org/10.1002/elsc.200400007.

Whaley-Martin, Kelly, Lin-xing Chen, Tara Colenbrander Nelson, Jennifer Gordon, Rose Kantor, Lauren E Twible, Stephanie Marshall, et al. 2023. “$O_2$ Partitioning of Sulfur Oxidizing Bacteria Drives Acidity and Thiosulfate Distributions in Mining Waters.” *Nature Communications* 14 (1): 2006. https://doi.org/10.1038/s41467-023-37426-8.

Whaley-Martin, Kelly, Gerdhard L. Jessen, Tara Colenbrander-Nelson, Jiro F. Mori, Simon C. Apte, Chad Jarolimek, and Lesley A. Warren. 2019. “The Potential Role of *Halothiobacillus* spp. in Sulfur Oxidation and Acid Generation in Circum-Neutral Mine Tailings Reservoirs.” *Frontiers in Microbiology* 10 (MAR). https://doi.org/10.3389/fmicb.2019.00297.

Whaley-Martin, Kelly, Stephanie Marshall, Tara Colenbrander-Nelson, Lauren Twible, Chad V. Jarolimek, Josh J. King, Simon C. Apte, and Lesley A. Warren. 2020. “A Mass-Balance Tool for Monitoring Potential Dissolved Sulfur Oxidation Risks in Mining Impacted Waters.” *Mine Water and the Environment* 39: 291–307. https://doi.org/10.1007/s10230-020-00671-0.

Wood, Ann P., Claire A. Woodall, and Donovan P. Kelly. 2005. "*Halothiobacillus neapolitanus* Strain OSWA Isolated from 'The Old Sulphur Well' at Harrogate (Yorkshire, England)." *Systematic and Applied Microbiology* 28 (8): 746–48. https://doi.org/10.1016/j.syapm.2005.05.013.

Xie, Shaobin, Shasha Wang, Dengfeng Li, Zongze Shao, Qiliang Lai, Yejian Wang, Mingcong Wei, Xiqiu Han, and Lijing Jiang. 2019. "S*ulfurovum indicum* sp. nov., a Novel Hydrogen- and Sulfur-Oxidizing Chemolithoautotroph Isolated from a Deep-Sea Hydrothermal Plume in the Northwestern Indian Ocean." *International Journal of Systematic and Evolutionary Microbiology* 71 (3). https://doi.org/10.1099/ijsem.0.004748.

Xin, Yufeng, Yaxin Wang, Honglin Zhang, Yu Wu, Yongzhen Xia, Huanjie Li, and Xiaohua Qu. 2023. "*Cupriavidus pinatubonensis* JMP134 Alleviates Sulfane Sulfur Toxicity after the Loss of Sulfane Dehydrogenase through Oxidation by Persulfide Dioxygenase and Hydrogen Sulfide Release." *Metabolites* 13 (2). https://doi.org/10.3390/metabo13020218.

Xu, Shuangbin, Meijun Chen, Tingze Feng, Li Zhan, Lang Zhou, and Guangchuang Yu. 2021. "Use Ggbreak to Effectively Utilize Plotting Space to Deal With Large Datasets and Outliers." *Frontiers in Genetics* 12 (November). https://doi.org/10.3389/fgene.2021.774846.

Yong, Delicia, Robson Ee, Yan Lue Lim, Choo Yee Yu, Geik Yong Ang, Kah Yan How, Kok Keng Tee, Wai Fong Yin, and Kok Gan Chan. 2016. "Complete Genome Sequence of *Pandoraea thiooxydans* DSM 25325T, a Thiosulfate-Oxidizing Bacterium." *Journal of Biotechnology* 217: 51–52. https://doi.org/10.1016/j.jbiotec.2015.11.009.

Yu, Qingzi, Weining Sun, and Haichun Gao. 2021. "Thiosulfate Oxidation in Sulfur-reducing *Shewanella oneidensis* and Its Unexpected Influences on the Cytochrome c Content." *Environmental Microbiology* 23 (11): 7056–72. https://doi.org/10.1111/1462-2920.15807.

Yu, Yangyang, Xiangmei Liu, Huiyan Wang, Xiuting Li, and Jianqun Lin. 2014. "Construction and Characterization of TetH Overexpression and Knockout Strains of *Acidithiobacillus ferrooxidans*." *Journal of Bacteriology* 196 (12): 2255–64. https://doi.org/10.1128/JB.01472-13.

Yuan, Q., P. Wang, C. Wang, J. Chen, X. Wang, and S. Liu. 2021. "Indicator Species and Co-Occurrence Pattern of Sediment Bacterial Community in Relation to Alkaline Copper Mine Drainage Contamination." *Ecological Indicators,* 120. https://doi.org/DOI: 10.1016/j.ecolind.2020.106884.

Zakharyuk, A. G., Ya V. Ryzhmanova, A. N. Avtukh, and V. A. Shcherbakova. 2019. "Iron-Reducing Microbial Communities of the Lake Baikal Low-Temperature Bottom Sediments." *Microbiology (Russian Federation)* 88 (2): 156–63. https://doi.org/10.1134/S0026261719020139.

Zander, Ulrich, Annette Faust, Björn U. Klink, Daniele De Sanctis, Santosh Panjikar, Armin Quentmeier, Frank Bardischewsky, Cornelius G. Friedrich, and Axel J. Scheidig. 2011. "Structural Basis for the Oxidation of Protein-Bound Sulfur by the Sulfur Cycle Molybdohemo-Enzyme Sulfane Dehydrogenase SoxCD." *Journal of Biological Chemistry* 286 (10): 8349–60. https://doi.org/10.1074/jbc.M110.193631.

Zhang, Jing, Rui Liu, Shichuan Xi, Ruining Cai, Xin Zhang, and Chaomin Sun. 2020. “A Novel Bacterial Thiosulfate Oxidation Pathway Provides a New Clue about the Formation of Zero-Valent Sulfur in Deep Sea.” *ISME Journal* 14 (9): 2261–74. https://doi.org/10.1038/s41396-020-0684-5.

Zhang, Ruo-Chen, Xi-Jun Xu, Chuan Chen, Bo Shao, Xu Zhou, Yuan Yuan, Duu-Jong Lee, and Nan-Qi Ren. 2019. “Bioreactor Performance and Microbial Community Analysis of Autotrophic Denitrification under Micro-Aerobic Condition.” *Science of The Total Environment* 647 (January): 914–22. https://doi.org/10.1016/j.scitotenv.2018.07.389.

Zhou, Jizhong, and Daliang Ning. 2017. “Stochastic Community Assembly: Does It Matter in Microbial Ecology?” *Microbiology and Molecular Biology Reviews* 81 (4): 1–32. https://doi.org/10.1128/MMBR.00002-17.

Zhou, Lijie, Yongzhou Lai, Zhiyuan Shao, Yixin Jian, and Wei Qin Zhuang. 2023. “Keystone Bacteria in a Thiosulfate-Driven Autotrophic Denitrification Microbial Community.” *Chemical Engineering Journal* 470 (April): 144321. https://doi.org/10.1016/j.cej.2023.144321.

Zhou, Zhichao, Patricia Q. Tran, Elise S. Cowley, Elizabeth Trembath-Reichert, and Karthik Anantharaman. “Diversity and ecology of microbial sulfur metabolism.” *Nature Reviews Microbiology* 23 (Feburary): 122-140. https://doi.org/10.1038/s41579-024-01104-3.

# Appendix A: Gibbs Free Energy Calculations and Metagenomic Inference

**Table A1** Theoretical Calculations of ΔG Values for S Metabolic Pathways

| Sulfur Pathway | Sulfur Oxidation Half Reaction | $R_d$ $\Delta G^{o'}$ (kJ/e-) | TEA Reduction Half Reaction | $R_a$ $\Delta G^{o'}$ (kJ/e-) | Calculated Gibb's Free Energy of Reaction $\Delta G^{o'}$ (kJ/e-) |
|---|---|---|---|---|---|
| cSOx | $S_2O_3^{2-} + 5\ H_2O \rightarrow 2\ SO_4^{2-} + 10\ H^+ + 8\ e^-$ | 23.6 / 23.6 | $¼\ O_2 + H^+ + e^- \rightarrow H_20$ | -78.7 / -78.7 | -102.4 / -102.3 |
| iSOx | $S_2O_3^{2-} + H_2O \rightarrow SO_4^{2-} + S^0 + 2\ H^+ + 2\ e$- | - / 36.9 | $¼\ O_2 + H^+ + e^- \rightarrow H_20$ | -78.7 / -78.7 | - 115.6 / -115.6 |
| rDSR | $S^0 + 4\ H_2O \rightarrow SO_4^{2-} + 8\ H^+ + 6\ e$- | 19.2 / 19.2 | $¼\ O_2 + H^+ + e^- \rightarrow H_20$ | -78.7 / -78.7 | -104.9 / -97.9 |
| $S_4$I P1 | $2\ S_2O_3^{2-} \rightarrow S_4O_6^{2-} + 2\ e$- | -26.6 / - | $¼\ O_2 + H^+ + e^- \rightarrow H_20$ | -78.7 / -78.7 | -52.1 / -52.1 |
| $S_4$I P2 | $S_4O_6^{2-} + 10\ H_2O \rightarrow 4\ SO_4^{2-} + 20\ H^+ + 20\ e$- | 32.9 / - | $¼\ O_2 + H^+ + e^- \rightarrow H_20$ | -78.7 / -78.7 | -111.6 / -111.6 |
| cSOx | $S_2O_3^{2-} + 5\ H_2O \rightarrow 2\ SO_4^{2-} + 10\ H^+ + 8\ e^-$ | 23.6 / 23.6 | $1/8\ NO_3^- + 5/4\ H^+ + e^- \rightarrow 1/8\ NH_4^+ + 3/8\ H_2O$ | -32.1 / -35.1 | -52.7 / -58.7 |
| iSOx | $S_2O_3^{2-} + H_2O \rightarrow SO_4^{2-} + S^0 + 2\ H^+ + 2\ e$- | - / 36.9 | $1/8\ NO_3^- + 5/4\ H^+ + e^- \rightarrow 1/8\ NH_4^+ + 3/8\ H_2O$ | -32.1 / -35.1 | - 69.0 / -78.7 |
| rDSR | $S^0 + 4\ H_2O \rightarrow SO_4^{2-} + 8\ H^+ + 6\ e$- | 19.2 / 19.2 | $1/8\ NO_3^- + 5/4\ H^+ + e^- \rightarrow 1/8\ NH_4^+ + 3/8\ H_2O$ | -32.1 / -35.1 | -55.2 / -54.3 |
| $S_4$I P1 | $2\ S_2O_3^{2-} \rightarrow S_4O_6^{2-} + 2\ e$- | -26.6 / - | $1/8\ NO_3^- + 5/4\ H^+ + e^- \rightarrow 1/8\ NH_4^+ + 3/8\ H_2O$ | -32.1 / -35.1 | -2.4 / -8.5 |
| $S_4$I P2 | $S_4O_6^{2-} + 10\ H_2O \rightarrow 4\ SO_4^{2-} + 20\ H^+ + 20\ e$- | 32.9 / - | $1/8\ NO_3^- + 5/4\ H^+ + e^- \rightarrow 1/8\ NH_4^+ + 3/8\ H_2O$ | -32.1 / -35.1 | -65.0 / -68.0 |
| cSOx | $S_2O_3^{2-} + 5\ H_2O \rightarrow 2\ SO_4^{2-} + 10\ H^+ + 8\ e^-$ | 23.6 / 23.6 | $1/5\ NO_3^- + 6/5\ H^+ + e^- \rightarrow 1/10\ N_{2\ (g)} + 3/5\ H_2O$ | -62.4 / -72.2 | -83.2 / -95.78 |
| iSOx | $S_2O_3^{2-} + H_2O \rightarrow SO_4^{2-} + S^0 + 2\ H^+ + 2\ e$- | - / 36.9 | $1/5\ NO_3^- + 6/5\ H^+ + e^- \rightarrow 1/10\ N_{2\ (g)} + 3/5\ H_2O$ | -62.4 / -72.2 | - 99.3 / -78.7 |

| | | | | | |
|---|---|---|---|---|---|
| rDSR | $S^0 + 4\ H_2O \rightarrow SO_4^{2-} + 8\ H^+ + 6\ e^-$ | 19.2 / 19.2 | $1/5\ NO_3^- + 6/5\ H^+ + e^- \rightarrow 1/10\ N_{2\ (g)} + 3/5\ H_2O$ | -62.4 / -72.2 | -85.7 / -91.4 |
| $S_4I$ P1 | $2\ S_2O_3^{2-} \rightarrow S_4O_6^{2-} + 2\ e^-$ | -26.6 / - | $1/5\ NO_3^- + 6/5\ H^+ + e^- \rightarrow 1/10\ N_{2\ (g)} + 3/5\ H_2O$ | -62.4 / -72.2 | -33.0 / -45.6 |
| $S_4I$ P2 | $S_4O_6^{2-} + 10\ H_2O \rightarrow 4\ SO_4^{2-} + 20\ H^+ + 20\ e^-$ | 32.9 / - | $1/5\ NO_3^- + 6/5\ H^+ + e^- \rightarrow 1/10\ N_{2\ (g)} + 3/5\ H_2O$ | -62.4 / -72.2 | -92.5 / -105 |

*ΔG values are represented as "x / y". The "x" values were calculated for a saline black sea environment, similar to mine wastewater [pH=8, 283 K, 25‰ salinity and 298 K: ammonium, 0.64; monovalent anions, 0.58; divalent anions, 0.109; gases, 1.2, (van Vliet, von Meijenfeldt, Dutilh, Villanueva, Sinninghe Damsté, Stams, and Sánchez-Andrea 2021)]. The "y" values are those calculated using the $\Delta G^{o'}$ constants provided in Environmental Biotechnology: Principles and Applications (Rittmann and McCarty 2001).

The $\Delta G^{o'}$ constants, where not available for an e- donor pair were calculated according to:

$$\Delta G^\circ = \sum \Delta Gf^\circ(\text{products}) - \sum \Delta Gf^\circ\ (\text{reactants})$$

$$\Delta G^\circ / e^- = \Delta G^\circ / n$$

Where $\Delta G^\circ$ = Gibbs free energy change for the reaction (in J/mol or kJ/mol), and n = number of electrons transferred.

**Sample Calculation:**

Gibb's Free Energies of Formation: $SO_4^{2-}$ = -744.6 KJ/mol; $S_2O_3^{2-}$ = -513.4 KJ/mol; $S^o$ = 0 KJ/mol; $H_2O$ = -237.2 KJ/mol; $H^+$, pH 7 = -39.87 KJ/mol

Equation: $S_2O_3^{2-} + H_2O \rightarrow SO_4^{2-} + S^0 + 2\ H^+ + 2\ e^-$

Restated in standard form (per $e^-$ consumed): $\frac{1}{2}\ SO_4^{2-} + \frac{1}{2}\ S^0 + H^+ + e^- \rightarrow \frac{1}{2}\ S_2O_3^{2-} + \frac{1}{2}\ H_2O$

$$\Delta G^\circ = \sum \Delta Gf^\circ(\text{products}) - \sum \Delta Gf^\circ\ (\text{reactants})$$

$$= (0.5*-513.4 + 0.5*-237.2\ ) - (0.5*-744.6 + 0.5*0 + 1*-39.87)$$

$$= 36.87\ kJ/\ e^-$$

# Metagenomic Inference

For a complete list of metagenome-assembled genomes for sulfur oxidizing bacterial genera please see the following ggbase link: https://ggkbase.berkeley.edu/mine_tailing_impoundment_time_series/organisms; for gene lists by sample, click on individual samples and, select the genes tab, and then search the annotations section (ex. https://ggkbase.berkeley.edu/OR_07242016_13/organisms/359861)

**Rationale**

A process of metagenomic inference was used to predict the presence of sulfur oxidizing pathways (cSOx, iSOx, rDSR, and S4I) in the SOB identified in these mesocosm experiments via 16S rRNA gene sequencing.

**Study Site**

The study site from which the metagenomes were collected and sequenced (from 2014–2018) was an active tailings impoundment at a copper-nickel mine near Sudbury, Ontario, Canada.

**Samples Sequenced**

A series of 30 metagenomes were sequenced from the active tailings impoundment, listed in Appendix A Table 1.

**Methods for DNA Isolation, Library Prep and Sequencing**

"Construction of libraries (insert length ~500 bp) and sequencing by Illumina HiSeq 1500 with paired-end 150 bp sequencing kit, were performed at McMaster University's Metagenomics Facility at McMaster (Farncombe Metagenomics Facility, Mobix Lab services, and Surrette lab's Microbiome services). The assembled scaffolds with a minimum length of 1 kbp (hereafter "1k_scaffolds") were included for gene prediction and subsequent analyses. The protein-coding genes were predicted by Prodigal V2.6.392 from 1k_scaffolds. The predicted protein-coding genes were compared against the databases of Kyoto Encyclopedia of Genes and Genomes (KEGG)95, UniRef10096 and UniProt97 using Usearch (version v10.0.240_i86linux64)98 for annotation." (K. Whaley-Martin et al. 2023)

**Table A2** Metagenomic Samples Sequenced from the Mine Tailings Impoundment

| Sample # | Date | Depth (m) |
|---|---|---|
| 1 | Mar 2015 | 0.25 |
| 2 | Mar 2015 | 0.75 |
| 3 | Mar 2015 | 21 |
| 4 | May 2015 | 2.5 |
| 5 | May 2015 | 3.5 |
| 6 | Aug 2015 | 1.0 |
| 7 | Aug 2015 | 2.8 |
| 8 | Aug 2015 | 25.8 |
| 9 | Jul 2016 | 1.5 |
| 10 | Jul 2016 | 10 |

| Sample # | Date | Depth (m) |
|---|---|---|
| 11 | Jun 2017 | 2 |
| 12 | Jun 2017 | 10 |
| 13 | Jul 2017 | 0.5 |
| 14 | Jul 2017 | 2.0 |
| 15 | Jul 2017 | 10 |
| 16 | Aug 2017 | 0.5 |
| 17 | Aug 2017 | 2 |
| 18 | Aug 2017 | 10 |
| 19 | Sep 2017 | 10 |
| 20 | Nov 2017 | 0.5 |

| Sample # | Date | Depth (m) |
|---|---|---|
| 21 | Nov 2017 | 10 |
| 22 | May 2018 | 0.5 |
| 23 | May 2018 | 2.8 |
| 24 | May 2018 | 10 |
| 25 | Jul 2018 | 0.5 (site 1) |
| 26 | Jul 2018 | 0.5 (site 2) |
| 27 | Jul 2018 | 10 |
| 28 | Aug 2018 | 0.5 |
| 29 | Aug 2018 | 2.5 |
| 30 | Aug 2018 | 10 |

**For more information see:**

Whaley-Martin, K.J., Chen, LX., Nelson, T.C. et al. $O_2$ partitioning of sulfur oxidizing bacteria drives acidity and thiosulfate distributions in mining waters. Nat Commun 14, 2006 (2023).

# Appendix B: Supplemental Information for Chapter 3

**Table B1** Complete Geochemical Data from 500 L Mesocosms in 2019

| Exp | Treatment | Rep | Mesocosm | Depth (cm) | Day | pH (Bottom) | Temp (°C) | DO (mg/L) | DO (mM) | $NO_3^-$ (mM) | Std Dev $NO_3^-$ (mM) | $S\text{-}S_2O_3^{2-}$ (mM) | St Dev $S\text{-}S_2O_3^{2-}$ (mM) | $SO_4^{2-}$ (mM) | St Dev $SO_4^{2-}$ (mM) |
|---|---|---|---|---|---|---|---|---|---|---|---|---|---|---|---|
| (a) | Dark, Unstirred | R1 | M01 | 50 | 0 | - | 17.5 | 9.58 | 0.30 | 0.01 | 0.02 | 0.18 | 0.01 | - | - |
| (a) | Dark, Unstirred | R1 | M01 | 50 | 8 | 7.58 | 18.3 | 7.52 | 0.24 | - | - | 0.13 | 0.03 | - | - |
| (a) | Dark, Unstirred | R1 | M01 | 50 | 14 | 6.59 | 21.2 | 5.85 | 0.18 | 0.01 | 0.02 | 0.02 | 0.00 | - | - |
| (a) | Dark, Unstirred | R1 | M01 | 50 | 22 | 5.49 | 20.8 | 1.38 | 0.04 | 0.02 | 0.02 | nd | nd | - | - |
| (a) | Dark, Unstirred | R1 | M01 | 50 | 29 | 4.75 | 21.4 | 0.24 | 0.01 | 0.03 | 0.00 | nd | nd | - | - |
| (a) | Dark, Stirred | R1 | M02 | 50 | 0 | - | 23.4 | 8.06 | 0.25 | 0.02 | 0.02 | 0.16 | 0.00 | - | - |
| (a) | Dark, Stirred | R1 | M02 | 50 | 8 | 7.14 | 22.3 | 7.08 | 0.22 | - | - | 0.04 | 0.01 | - | - |
| (a) | Dark, Stirred | R1 | M02 | 50 | 14 | 6.28 | 23.2 | 6.95 | 0.22 | - | - | 0.04 | 0.03 | - | - |
| (a) | Dark, Stirred | R1 | M02 | 50 | 22 | 4.38 | 23.8 | 6.95 | 0.22 | - | - | nd | nd | - | - |
| (a) | Dark, Stirred | R1 | M02 | 50 | 29 | 4.26 | 22.9 | 7.14 | 0.22 | - | - | nd | nd | - | - |
| (a) | Dark, Unstirred | R2 | M03 | 50 | 0 | - | 30.1 | 7.84 | 0.25 | 0.00 | 0.00 | 0.17 | 0.01 | - | - |
| (a) | Dark, Unstirred | R2 | M03 | 50 | 8 | 7.58 | 17.6 | 7.05 | 0.22 | - | - | 0.11 | 0.01 | - | - |
| (a) | Dark, Unstirred | R2 | M03 | 50 | 14 | 6.83 | 19.1 | 4.84 | 0.15 | 0.00 | 0.00 | 0.08 | 0.01 | - | - |
| (a) | Dark, Unstirred | R2 | M03 | 50 | 22 | 6.40 | 19.7 | 3.95 | 0.12 | - | - | nd | nd | - | - |
| (a) | Dark, Unstirred | R2 | M03 | 50 | 29 | 6.09 | 20.4 | 2.92 | 0.09 | 0.05 | 0.00 | nd | nd | - | - |
| (a) | Dark, Stirred | R2 | M04 | 50 | 0 | - | - | 7.48 | 0.23 | 0.01 | 0.02 | 0.17 | 0.00 | - | - |
| (a) | Dark, Stirred | R2 | M04 | 50 | 8 | 7.18 | 21.7 | 7.04 | 0.22 | - | - | 0.08 | 0.01 | - | - |
| (a) | Dark, Stirred | R2 | M04 | 50 | 14 | 6.47 | 22.6 | 7.04 | 0.22 | - | - | 0.04 | 0.00 | - | - |
| (a) | Dark, Stirred | R2 | M04 | 50 | 22 | 5.23 | 23.0 | 6.66 | 0.21 | - | - | nd | nd | - | - |
| (a) | Dark, Stirred | R2 | M04 | 50 | 29 | 4.80 | 21.2 | 2.62 | 0.08 | 0.04 | 0.00 | nd | nd | - | - |

Note: Sulfite ($SO_3^{2-}$) was non-detectable throughout all experiments and timepoints; $Day_0$ DO data inferred from June 26th, 2019.

(-) indicates no value available; gap in data; nd = non-detect

**Table B1 cont.** Complete Geochemical Data from 500 L Mesocosms in 2019

| Exp | Treatment | Rep | Mesocosm | Depth (cm) | Day | pH (Bottom) | Temp (°C) | DO (mg/L) | DO (mM) | $NO_3^-$ (mM) | Std Dev $NO_3^-$ (mM) | $S\text{-}S_2O_3^{2-}$ (mM) | St Dev $S\text{-}S_2O_3^{2-}$ (mM) | $SO_4^{2-}$ (mM) | St Dev $SO_4^{2-}$ (mM) |
|---|---|---|---|---|---|---|---|---|---|---|---|---|---|---|---|
| (a) | Light, Unstirred | R1 | M05 | 50 | 0 | - | 29.7 | 7.63 | 0.24 | 0.01 | 0.01 | 0.18 | 0.01 | - | - |
| (a) | Light, Unstirred | R1 | M05 | 50 | 8 | 7.45 | 20.1 | 6.06 | 0.19 | - | - | 0.11 | 0.02 | - | - |
| (a) | Light, Unstirred | R1 | M05 | 50 | 14 | 6.18 | 21.4 | 1.41 | 0.04 | - | - | 0.06 | 0.00 | - | - |
| (a) | Light, Unstirred | R1 | M05 | 50 | 22 | 5.06 | 22.2 | 0.26 | 0.01 | - | - | nd | nd | - | - |
| (a) | Light, Unstirred | R1 | M05 | 50 | 29 | 4.48 | 22.3 | 0.17 | 0.01 | - | - | nd | nd | - | - |
| (a) | Light, Stirred | R1 | M06 | 50 | 0 | - | 18.0 | 9.22 | 0.29 | 0.00 | 0.00 | 0.17 | 0.01 | - | - |
| (a) | Light, Stirred | R1 | M06 | 50 | 8 | 7.20 | 24.1 | 7.08 | 0.22 | - | - | 0.09 | 0.01 | - | - |
| (a) | Light, Stirred | R1 | M06 | 50 | 14 | 6.62 | 24.9 | 7.22 | 0.23 | 0.03 | 0.00 | 0.06 | 0.00 | - | - |
| (a) | Light, Stirred | R1 | M06 | 50 | 22 | 5.74 | 25.0 | 7.22 | 0.23 | - | - | nd | nd | - | - |
| (a) | Light, Stirred | R1 | M06 | 50 | 29 | 4.31 | 22.0 | 2.64 | 0.08 | 0.04 | 0.00 | nd | nd | - | - |
| (a) | Light, Unstirred | R2 | M07 | 50 | 0 | - | 16.9 | 9.24 | 0.29 | 0.03 | 0.00 | 0.18 | 0.01 | - | - |
| (a) | Light, Unstirred | R2 | M07 | 50 | 8 | 7.30 | 21.0 | 6.68 | 0.21 | - | - | 0.19 | 0.05 | - | - |
| (a) | Light, Unstirred | R2 | M07 | 50 | 14 | 5.47 | 22.4 | 1.16 | 0.04 | - | - | 0.15 | 0.05 | - | - |
| (a) | Light, Unstirred | R2 | M07 | 50 | 22 | 4.00 | 23.0 | 0.33 | 0.01 | - | - | nd | nd | - | - |
| (a) | Light, Unstirred | R2 | M07 | 50 | 29 | 3.97 | 22.9 | 1.37 | 0.04 | 0.01 | 0.03 | nd | nd | - | - |
| (a) | Light, Stirred | R2 | M08 | 50 | 0 | - | - | 7.48 | 0.23 | 0.03 | 0.00 | 0.18 | 0.01 | - | - |
| (a) | Light, Stirred | R2 | M08 | 50 | 8 | 7.13 | 24.7 | 6.84 | 0.21 | - | - | 0.13 | 0.03 | - | - |
| (a) | Light, Stirred | R2 | M08 | 50 | 14 | 6.41 | 25.9 | 6.59 | 0.21 | - | - | 0.10 | 0.03 | - | - |
| (a) | Light, Stirred | R2 | M08 | 50 | 22 | 5.61 | 26.1 | 7.08 | 0.22 | - | - | nd | nd | - | - |
| (a) | Light, Stirred | R2 | M08 | 50 | 29 | 3.96 | 22.9 | 2.86 | 0.09 | 0.04 | 0.04 | nd | nd | - | - |

Note: Sulfite ($SO_3^{2-}$) was non-detectable throughout all experiments and timepoints; $Day_0$ DO data inferred from June 26th, 2019.

(-) indicates no value available; gap in data; nd = non-detect.

**Table B1 cont.** Complete Geochemical Data from 500 L Mesocosms in 2019

| Exp | Treatment | Rep | Mesocosm | Depth (cm) | Day | pH (Bottom) | Temp (°C) | DO (mg/L) | DO (mM) | $NO_3^-$ (mM) | Std Dev $NO_3^-$ (mM) | $S\text{-}S_2O_3^{2-}$ (mM) | St Dev $S\text{-}S_2O_3^{2-}$ (mM) | $SO_4^{2-}$ (mM) | St Dev $SO_4^{2-}$ (mM) |
|---|---|---|---|---|---|---|---|---|---|---|---|---|---|---|---|
| (b) | Control | R1 | M09 | 90 | -6 | 6.56 | 24.9 | 8.25 | 0.26 | - | - | - | - | - | - |
| (b) | Control | R1 | M09 | 90 | 0 | 3.91 | 22.6 | 4.73 | 0.15 | 0.11 | 0.00 | nd | nd | - | - |
| (b) | Control | R1 | M09 | 90 | 7 | 3.88 | 21.8 | 6.26 | 0.20 | - | - | - | - | - | - |
| (b) | Control | R1 | M09 | 90 | 9 | 3.85 | 21.5 | 6.95 | 0.22 | - | - | nd | nd | - | - |
| (b) | Control | R1 | M09 | 90 | 13 | 3.90 | 21.4 | 7.34 | 0.23 | 0.07 | 0.00 | nd | nd | 8.1 | 0.7 |
| (b) | Control | R1 | M09 | 90 | 20 | 3.94 | 20.5 | 7.81 | 0.24 | 0.07 | 0.00 | nd | nd | 8.1 | 0.0 |
| (b) | Control | R1 | M09 | 90 | 27 | 3.95 | 18.0 | 7.67 | 0.24 | 0.07 | 0.00 | nd | nd | 7.7 | 0.5 |
| (b) | Control | R2 | M10 | 90 | -6 | 6.16 | 23.7 | 8.38 | 0.26 | - | - | - | - | - | - |
| (b) | Control | R2 | M10 | 90 | 0 | 3.99 | 22.4 | 4.02 | 0.13 | 0.12 | 0.00 | nd | nd | - | - |
| (b) | Control | R2 | M10 | 90 | 7 | 3.98 | 21.4 | 5.93 | 0.19 | - | - | - | - | - | - |
| (b) | Control | R2 | M10 | 90 | 9 | 3.97 | 21.4 | 7.2 | 0.23 | - | - | nd | nd | - | - |
| (b) | Control | R2 | M10 | 90 | 13 | 4.06 | 21.4 | 7.2 | 0.23 | 0.07 | 0.00 | nd | nd | 8.8 | 0.2 |
| (b) | Control | R2 | M10 | 90 | 20 | 4.05 | 20.4 | 7.31 | 0.23 | 0.07 | 0.00 | nd | nd | 8.2 | 0.4 |
| (b) | Control | R2 | M10 | 90 | 27 | 4.03 | 17.8 | 7.75 | 0.24 | 0.07 | 0.00 | nd | nd | 8.0 | 0.3 |
| (b) | 2.0 mM $S\text{-}S_2O_3^{2-}$ | R1 | M11 | 90 | -6 | 5.99 | 23.0 | 8.68 | 0.27 | 0.12 | 0.00 | - | - | 8.2 | 0.1 |
| (b) | 2.0 mM $S\text{-}S_2O_3^{2-}$ | R1 | M11 | 90 | 0 | 4.38 | 23.2 | 4.39 | 0.14 | 0.12 | 0.00 | 2.23 | 0.04 | - | - |
| (b) | 2.0 mM $S\text{-}S_2O_3^{2-}$ | R1 | M11 | 90 | 7 | 5.76 | 21.9 | 0.03 | 0.00 | - | - | 0.33 | 0.28 | - | - |
| (b) | 2.0 mM $S\text{-}S_2O_3^{2-}$ | R1 | M11 | 90 | 9 | 5.84 | 21.6 | 1.56 | 0.05 | - | - | - | - | - | - |
| (b) | 2.0 mM $S\text{-}S_2O_3^{2-}$ | R1 | M11 | 90 | 13 | 6.09 | 22.2 | 2.73 | 0.09 | 0.08 | 0.00 | 0.17 | 0.03 | 9.4 | 0.9 |
| (b) | 2.0 mM $S\text{-}S_2O_3^{2-}$ | R1 | M11 | 90 | 20 | 5.37 | 20.2 | 0.78 | 0.02 | 0.07 | 0.00 | 0.08 | 0.00 | 8.6 | 0.1 |
| (b) | 2.0 mM $S\text{-}S_2O_3^{2-}$ | R1 | M11 | 90 | 27 | 4.39 | 17.3 | 4.11 | 0.13 | 0.07 | 0.00 | 1.12 | 0.15 | 8.9 | 0.0 |
| (b) | 2.0 mM $S\text{-}S_2O_3^{2-}$ | R2 | M12 | 90 | -6 | 6.36 | 25.2 | 7.82 | 0.24 | 0.21 | 0.01 | - | - | 8.1 | 0.2 |
| (b) | 2.0 mM $S\text{-}S_2O_3^{2-}$ | R2 | M12 | 90 | 0 | 4.15 | 22.6 | 4.92 | 0.15 | 0.12 | 0.00 | 1.76 | 0.16 | - | - |
| (b) | 2.0 mM $S\text{-}S_2O_3^{2-}$ | R2 | M12 | 90 | 7 | 5.90 | 21.2 | 0.39 | 0.01 | - | - | 0.84 | 0.22 | - | - |
| (b) | 2.0 mM $S\text{-}S_2O_3^{2-}$ | R2 | M12 | 90 | 9 | 5.86 | 21.0 | 1.8 | 0.06 | - | - | - | - | - | - |
| (b) | 2.0 mM $S\text{-}S_2O_3^{2-}$ | R2 | M12 | 90 | 13 | 6.40 | 21.1 | 0.82 | 0.03 | 0.08 | 0.00 | 0.17 | 0.24 | 9.7 | 1.5 |

**Table B1 cont**. Complete Geochemical Data from 500 L Mesocosms in 2019

| Exp | Treatment | Rep | Mesocosm | Depth (cm) | Day | pH (Bottom) | Temp (°C) | DO (mg/L) | DO (mM) | $NO_3^-$ (mM) | Std Dev $NO_3^-$ (mM) | S-$S_2O_3^{2-}$ (mM) | St Dev S-$S_2O_3^{2-}$ (mM) | $SO_4^{2-}$ (mM) | St Dev $SO_4^{2-}$ (mM) |
|---|---|---|---|---|---|---|---|---|---|---|---|---|---|---|---|
| (b) | 2.0 mM S-$S_2O_3^{2-}$ and 0.2 mM $NO_3^-$ | R1 | M13 | 90 | -6 | 6.53 | 22.5 | 8.5 | 0.27 | 0.22 | 0.00 | - | - | 8.4 | 0.1 |
| (b) | 2.0 mM S-$S_2O_3^{2-}$ and 0.2 mM $NO_3^-$ | R1 | M13 | 90 | 0 | 5.50 | 23.1 | 4.26 | 0.13 | 0.10 | 0.03 | 2.14 | 0.06 | - | - |
| (b) | 2.0 mM S-$S_2O_3^{2-}$ and 0.2 mM $NO_3^-$ | R1 | M13 | 90 | 7 | 6.28 | 21.9 | 1.09 | 0.03 | - | - | 1.04 | 0.37 | - | - |
| (b) | 2.0 mM S-$S_2O_3^{2-}$ and 0.2 mM $NO_3^-$ | R1 | M13 | 90 | 9 | 6.42 | 21.6 | 2.00 | 0.06 | - | - | 0.92 | 0.01 | - | - |
| (b) | 2.0 mM S-$S_2O_3^{2-}$ and 0.2 mM $NO_3^-$ | R1 | M13 | 90 | 13 | 6.67 | 21.8 | 1.93 | 0.06 | 0.36 | 0.00 | 0.61 | 0.05 | 7.3 | 0.3 |
| (b) | 2.0 mM S-$S_2O_3^{2-}$ and 0.2 mM $NO_3^-$ | R1 | M13 | 90 | 20 | 6.96 | 20.4 | 1.83 | 0.06 | 0.04 | 0.00 | nd | nd | 8.5 | 0.3 |
| (b) | 2.0 mM S-$S_2O_3^{2-}$ and 0.2 mM $NO_3^-$ | R1 | M13 | 90 | 27 | 5.96 | 17.7 | 2.77 | 0.09 | 0.04 | 0.00 | 0.84 | 0.02 | 8.6 | 0.1 |
| (b) | 2.0 mM S-$S_2O_3^{2-}$ and 0.2 mM $NO_3^-$ | R2 | M14 | 90 | -6 | 5.94 | 22.4 | 8.31 | 0.26 | 0.17 | 0.00 | - | - | 8.5 | 0.6 |
| (b) | 2.0 mM S-$S_2O_3^{2-}$ and 0.2 mM $NO_3^-$ | R2 | M14 | 90 | 0 | 4.28 | 23.8 | 4.42 | 0.14 | 0.12 | 0.00 | 1.68 | 0.02 | - | - |
| (b) | 2.0 mM S-$S_2O_3^{2-}$ and 0.2 mM $NO_3^-$ | R2 | M14 | 90 | 7 | 5.78 | 22.5 | 2.38 | 0.07 | - | - | 0.98 | 0.14 | - | - |
| (b) | 2.0 mM S-$S_2O_3^{2-}$ and 0.2 mM $NO_3^-$ | R2 | M14 | 90 | 9 | 5.99 | 21.8 | 3.87 | 0.12 | - | - | 1.03 | 0.01 | - | - |
| (b) | 2.0 mM S-$S_2O_3^{2-}$ and 0.2 mM $NO_3^-$ | R2 | M14 | 90 | 13 | 6.28 | 22.0 | 2.26 | 0.07 | 0.28 | 0.00 | 0.80 | 0.09 | 8.4 | 0.5 |
| (b) | 2.0 mM S-$S_2O_3^{2-}$ and 0.2 mM $NO_3^-$ | R2 | M14 | 90 | 20 | 7.46 | 20.7 | 2.89 | 0.09 | 0.04 | 0.00 | nd | nd | 8.6 | 0.2 |
| (b) | 2.0 mM S-$S_2O_3^{2-}$ and 0.2 mM $NO_3^-$ | R2 | M14 | 90 | 27 | 5.74 | 17.9 | 2.36 | 0.07 | 0.04 | 0.00 | nd | nd | 8.7 | 0.3 |
| (b) | 2.0 mM S-$S_2O_3^{2-}$ and OrgC | R1 | M15 | 90 | -6 | 6.51 | - | 6.19 | 0.19 | - | - | - | - | - | - |
| (b) | 2.0 mM S-$S_2O_3^{2-}$ and OrgC | R1 | M15 | 90 | 0 | 4.49 | 23.3 | 3.6 | 0.11 | 0.12 | 0.00 | 0.12 | 0.00 | - | - |
| (b) | 2.0 mM S-$S_2O_3^{2-}$ and OrgC | R1 | M15 | 90 | 7 | 5.79 | 21.5 | -0.02 | 0.00 | - | - | - | - | - | - |
| (b) | 2.0 mM S-$S_2O_3^{2-}$ and OrgC | R1 | M15 | 90 | 9 | 6.14 | 21.5 | 1.2 | 0.04 | - | - | 0.57 | 0.01 | - | - |
| (b) | 2.0 mM S-$S_2O_3^{2-}$ and OrgC | R1 | M15 | 90 | 13 | 6.07 | 21.3 | 1.23 | 0.04 | 0.05 | 0.03 | 0.05 | 0.00 | 9.1 | 0.2 |
| (b) | 2.0 mM S-$S_2O_3^{2-}$ and OrgC | R1 | M15 | 90 | 20 | 4.00 | 20.5 | 0.64 | 0.02 | 0.04 | 0.00 | nd | nd | 9.0 | 0.0 |
| (b) | 2.0 mM S-$S_2O_3^{2-}$ and OrgC | R1 | M15 | 90 | 27 | 3.59 | 18.0 | 0.13 | 0.00 | 0.08 | 0.00 | 1.09 | 0.09 | 9.0 | 0.7 |
| (b) | 2.0 mM S-$S_2O_3^{2-}$ and OrgC | R2 | M16 | 90 | -6 | 4.59 | - | 6.94 | 0.22 | - | - | - | - | - | - |
| (b) | 2.0 mM S-$S_2O_3^{2-}$ and OrgC | R2 | M16 | 90 | 0 | 5.69 | 22.9 | 3.7 | 0.12 | 0.10 | 0.03 | 3.07 | 0.03 | - | - |
| (b) | 2.0 mM S-$S_2O_3^{2-}$ and OrgC | R2 | M16 | 90 | 7 | 5.78 | 21.4 | 0.57 | 0.02 | - | - | 0.68 | 0.09 | - | - |
| (b) | 2.0 mM S-$S_2O_3^{2-}$ and OrgC | R2 | M16 | 90 | 9 | 5.78 | 21.4 | 1.91 | 0.06 | - | - | 0.67 | 0.01 | - | - |
| (b) | 2.0 mM S-$S_2O_3^{2-}$ and OrgC | R2 | M16 | 90 | 13 | 5.85 | 21.4 | 1.36 | 0.04 | - | - | 0.44 | 0.01 | 8.8 | 1.5 |
| (b) | 2.0 mM S-$S_2O_3^{2-}$ and OrgC | R2 | M16 | 90 | 20 | 4.45 | 20.1 | 1.25 | 0.04 | 0.04 | 0.00 | nd | nd | 8.8 | 0.1 |
| (b) | 2.0 mM S-$S_2O_3^{2-}$ and OrgC | R2 | M16 | 90 | 27 | 3.65 | 17.4 | 0.37 | 0.01 | 0.09 | 0.00 | 0.89 | 0.03 | 5.7 | 0.3 |

**Table B1 cont.** Complete Geochemical Data from 500 L Mesocosms in 2019

| Exp | Treatment | Mesocosm | Depth (cm) | Day | pH (Bottom) | S-$S_2O_3^{2-}$ (mM) | St Dev S-$S_2O_3^{2-}$ (mM) | $SO_4^{2-}$ (mM) | St Dev $SO_4^{2-}$ (mM) |
|---|---|---|---|---|---|---|---|---|---|
| (c) | SOB Community 1 + 2.0 mM S-$S_4O_6^{2-}$ | M17 | 90 | 0 | 7.2 | 0.05 | 0.00 | 9.0 | 0.66 |
| (c) | SOB Community 1 + 2.0 mM S-$S_4O_6^{2-}$ | M17 | 90 | 20 | 3.3 | nd | nd | 9.2 | 0.37 |
| (c) | Control: 2.0 mM S-$S_4O_6^{2-}$+ No SOB | M18 | 90 | 0 | 7.2 | 0.06 | 0.01 | 9.5 | 1.03 |
| (c) | Control: 2.0 mM S-$S_4O_6^{2-}$+ No SOB | M18 | 90 | 20 | 4.4 | nd | nd | 8.7 | 1.03 |
| (c) | SOB Community 1 + S-$S_2O_3^{2-}$ | M19 | 90 | 0 | 7.2 | 1.76 | 0.03 | 8.5 | 0.32 |
| (c) | SOB Community 1 + S-$S_2O_3^{2-}$ | M19 | 90 | 20 | 6.1 | 0.98 | 0.01 | 8.7 | 1.03 |
| (c) | Control: 2.0 mM S-S2O32- + No SOB | M20 | 90 | 0 | 7.2 | 1.74 | 0.12 | 9.0 | 0.36 |
| (c) | Control: 2.0 mM S-S2O32- + No SOB | M20 | 90 | 20 | 7.3 | 1.07 | 0.02 | 8.7 | 1.03 |
| (c) | SOB Community 2 + 2.0 mM S-$S_4O_6^{2-}$ | M21 | 90 | 0 | 7.2 | 0.03 | 0.00 | 9.6 | 1.03 |
| (c) | SOB Community 2 + 2.0 mM S-$S_4O_6^{2-}$ | M21 | 90 | 20 | 3.1 | nd | nd | 9.0 | 1.03 |
| (c) | SOB Community 3 + 2.0 mM S-$S_4O_6^{2-}$ | M22 | 90 | 0 | 7.2 | 0.02 | 0.00 | 8.9 | 0.28 |
| (c) | SOB Community 3 + 2.0 mM S-$S_4O_6^{2-}$ | M22 | 90 | 20 | 3.0 | nd | nd | 8.4 | 1.03 |
| (c) | SOB Community 2 + 2.0 mM S-$S_2O_3^{2-}$ | M23 | 90 | 20 | 5.4 | 1.03 | 0.01 | 8.3 | 0.28 |
| (c) | SOB Community 2 + 2.0 mM S-$S_2O_3^{2-}$ | M23* | 90 | 0 | 7.2 | 1.67 | 0.25 | 8.3 | 0.28 |
| (c) | SOB Community 3 + 2.0 mM S-$S_2O_3^{2-}$ | M23 | 90 | 20 | 5.4 | 1.03 | 0.01 | 8.1 | 0.23 |
| (c) | SOB Community 3 + 2.0 mM S-$S_2O_3^{2-}$ | M24 | 90 | 0 | 7.2 | 1.87 | 0.22 | 9.7 | 0.23 |
| (c) | SOB Community 2 + 2.0 mM S-$S_2O_3^{2-}$ | M24 | 90 | 20 | 6.2 | 1.12 | 0.01 | 9.5 | 0.30 |

* Thiosulfate concentration from 10 cm depth subbed in for missing data at $day_0$; Sulfate concentration error at $day_{end}$ estimated for Experiment C samples where none recorded.

Note: Sulfite ($SO_3^{2-}$) was not detected throughout all experiments and timepoints

(-) indicates no value available; gap in data

nd = non-detectable, below limit of detection; a conservative LOD for analysis were as follows: 0.04 mM S for thiosulfate, 0.013 mM S for sulfate. All sulfate values calculated using a 10x dilution technique.

**Table B2** Relative Abundance of SOB from 500 L Mesocosms in 2019

| Exp | Treatment | Rep | Mesocosm # | Day | *Halothiobacillus* | *Ferrovum* | *Thiomonas* | *Sediminibacterium* | *Brevundimonas* | *Acidovorax* | *Thiobacillus* |
|---|---|---|---|---|---|---|---|---|---|---|---|
| (a) | Dark, Unstirred | R1 | M01 | 2 | 0.00 | 0.00 | 0.00 | 42.48 | 0.00 | 17.79 | 0.00 |
| (a) | Dark, Stirred | R1 | M02 | 2 | 1.25 | 0.00 | 0.00 | 35.57 | 0.00 | 23.63 | 0.00 |
| (a) | Dark, Unstirred | R2 | M03 | 2 | 0.00 | 0.00 | 0.00 | 36.26 | 0.00 | 19.55 | 0.00 |
| (a) | Dark, Stirred | R2 | M04 | 2 | 1.61 | 0.00 | 0.00 | 40.49 | 0.00 | 16.92 | 0.00 |
| (a) | Light, Unstirred | R1 | M05 | 2 | 0.00 | 0.00 | 0.00 | 39.96 | 0.00 | 14.71 | 0.00 |
| (a) | Light, Unstirred | R2 | M07 | 2 | 0.00 | 0.00 | 0.00 | 33.60 | 0.00 | 10.15 | 0.00 |
| (a) | Light, Stirred | R2 | M08 | 2 | 1.48 | 0.00 | 0.00 | 32.93 | 0.00 | 17.61 | 0.00 |
| (a) | Dark, Unstirred | R1 | M01 | 29 | 3.18 | 0.00 | 0.00 | 0.00 | 17.51 | 0.00 | 0.00 |
| (a) | Dark, Stirred | R1 | M02 | 29 | 7.83 | 0.00 | 1.32 | 7.24 | 2.54 | 0.00 | 0.00 |
| (a) | Dark, Unstirred | R2 | M03 | 28 | 0.00 | 0.00 | 0.00 | 14.55 | 49.50 | 0.00 | 0.00 |
| (a) | Dark, Stirred | R2 | M04 | 29 | 0.00 | 0.00 | 0.00 | 0.00 | 1.74 | 0.00 | 0.00 |
| (a) | Light, Unstirred | R1 | M05 | 29 | 5.16 | 0.00 | 0.00 | 0.00 | 11.37 | 0.00 | 1.46 |
| (a) | Light, Stirred | R1 | M06 | 29 | 24.91 | 0.00 | 0.00 | 2.32 | 0.00 | 0.00 | 19.12 |
| (a) | Light, Unstirred | R2 | M07 | 29 | 0.00 | 0.00 | 0.00 | 0.00 | 0.00 | 0.00 | 0.00 |
| (a) | Light, Unstirred | R2 | M07 | 29 | 12.96 | 0.00 | 0.00 | 7.44 | 0.00 | 0.00 | 0.00 |
| (a) | Light, Stirred | R2 | M08 | 29 | 42.91 | 0.00 | 2.46 | 0.00 | 0.00 | 0.00 | 6.58 |

**Table B2 cont.** Relative Abundance of SOB from 500 L Mesocosms in 2019

| Exp | Treatment | Rep | Mesocosm # | Day | *Halothiobacillus* | *Ferrovum* | *Thiomonas* | *Sediminibacterium* | *Brevundimonas* | *Acidovorax* | *Thiobacillus* |
|---|---|---|---|---|---|---|---|---|---|---|---|
| (b) | All Tank Fill | R1 | M09-M16 | -6 | 44.34 | 15.10 | 10.02 | 0.00 | 0.00 | 7.99 | 0.00 |
| (b) | Control | R1 | M09 | 0 | 2.57 | 44.83 | 8.87 | 0.00 | 0.00 | 0.00 | 0.00 |
| (b) | Control | R1 | M09 | 14 | 0.00 | 2.56 | 1.87 | 0.00 | 0.00 | 0.00 | 0.00 |
| (b) | Control | R1 | M09 | 26 | 0.00 | 14.01 | 4.36 | 0.00 | 0.00 | 0.00 | 0.00 |
| (b) | Control | R2 | M10 | 0 | 2.58 | 15.04 | 2.47 | 0.00 | 1.57 | 0.00 | 0.00 |
| (b) | Control | R2 | M10 | 20 | 0.00 | 16.54 | 13.49 | 0.00 | 0.00 | 0.00 | 0.00 |
| (b) | Control | R2 | M10 | 26 | 0.00 | 14.95 | 3.61 | 0.00 | 0.00 | 0.00 | 0.00 |
| (b) | 2.0 mM S-$S_2O_3^{2-}$ | R1 | M11 | 0 | 1.33 | 2.53 | 0.00 | 0.00 | 1.45 | 0.00 | 0.00 |
| (b) | 2.0 mM S-$S_2O_3^{2-}$ | R1 | M11 | 14 | 16.28 | 16.28 | 6.98 | 0.00 | 0.00 | 0.00 | 0.00 |
| (b) | 2.0 mM S-$S_2O_3^{2-}$ | R1 | M11 | 26 | 1.35 | 1.68 | 5.27 | 0.00 | 0.00 | 0.00 | 0.00 |
| (b) | 2.0 mM S-$S_2O_3^{2-}$ | R1 | M12 | 0 | 0.00 | 0.00 | 0.00 | 0.00 | 1.73 | 0.00 | 0.00 |
| (b) | 2.0 mM S-$S_2O_3^{2-}$ | R2 | M12 | 20 | 5.80 | 0.00 | 14.05 | 0.00 | 5.57 | 0.00 | 0.00 |
| (b) | 2.0 mM S-$S_2O_3^{2-}$ | R2 | M12 | 26 | 2.26 | 0.00 | 21.59 | 0.00 | 3.31 | 0.00 | 0.00 |

For workflow from raw 16S gene sequencing data with OTUs listed, see the folder “Chapter 3 Supplementary 16S rRNA data (curation steps)” at the following link: http://128.100.14.155:8088/share.cgi?ssid=204a2ab4254d4911874cd20953dfb1ed.

**Table B2 cont.** Relative Abundance of SOB from 500 L Mesocosms in 2019

| Exp | Treatment | Rep | Mesocosm # | Day | *Halothiobacillus* | *Ferrovum* | *Thiomonas* | *Sedimini-bacterium* | *Brevundimonas* | *Acidovorax* | *Thiobacillus* |
|---|---|---|---|---|---|---|---|---|---|---|---|
| (b) | All Tank Fill | R1 | M09-M16 | -6 | 44.34 | 15.10 | 10.02 | 0.00 | 0.00 | 7.99 | 0.00 |
| (b) | 2.0 mM S-$S_2O_3^{2-}$ and 0.2 mM $NO_3^-$ | R1 | M13 | 0 | 0.00 | 0.00 | 0.00 | 0.00 | 1.99 | 0.00 | 0.00 |
| (b) | 2.0 mM S-$S_2O_3^{2-}$ and 0.2 mM $NO_3^-$ | R1 | M13 | 13 | 0.00 | 0.00 | 0.00 | 0.00 | 2.71 | 0.00 | 0.00 |
| (b) | 2.0 mM S-$S_2O_3^{2-}$ and 0.2 mM $NO_3^-$ | R1 | M13 | 26 | 0.00 | 0.00 | 3.80 | 0.00 | 12.85 | 0.00 | 2.04 |
| (b) | 2.0 mM S-$S_2O_3^{2-}$ and OrgC | R1 | M15 | 0 | 29.28 | 22.03 | 10.47 | 0.00 | 0.00 | 0.00 | 0.00 |
| (b) | 2.0 mM S-$S_2O_3^{2-}$ and OrgC | R1 | M15 | 14 | 0.00 | 0.00 | 0.00 | 0.00 | 0.00 | 0.00 | 0.00 |
| (b) | 2.0 mM S-$S_2O_3^{2-}$ and OrgC | R1 | M15 | 26 | 5.42 | 5.04 | 24.64 | 0.00 | 0.00 | 0.00 | 0.00 |
| (b) | 2.0 mM S-$S_2O_3^{2-}$ and 0.2 mM $NO_3^-$ | R2 | M14 | 0 | 1.51 | 1.51 | 0.00 | 0.00 | 0.00 | 0.00 | 0.00 |
| (b) | 2.0 mM S-$S_2O_3^{2-}$ and 0.2 mM $NO_3^-$ | R2 | M14 | 20 | 4.92 | 2.58 | 3.25 | 0.00 | 0.00 | 0.00 | 0.00 |
| (b) | 2.0 mM S-$S_2O_3^{2-}$ and 0.2 mM $NO_3^-$ | R2 | M14 | 26 | 1.68 | 0.00 | 3.43 | 0.00 | 1.06 | 0.00 | 0.00 |
| (b) | 2.0 mM S-$S_2O_3^{2-}$ and OrgC | R2 | M16 | 0 | 6.69 | 3.10 | 1.06 | 0.00 | 1.79 | 0.00 | 0.00 |
| (b) | 2.0 mM S-$S_2O_3^{2-}$ and OrgC | R2 | M16 | 20 | 3.04 | 3.45 | 29.73 | 0.00 | 0.00 | 0.00 | 0.00 |
| (b) | 2.0 mM S-$S_2O_3^{2-}$ and OrgC | R2 | M16 | 26 | 11.03 | 4.99 | 40.23 | 0.00 | 0.00 | 0.00 | 0.00 |

For workflow from raw 16S gene sequencing data with OTUs listed, see "Chapter 3 Supplementary 16S rRNA data (curation steps)" at the following link: http://128.100.14.155:8088/share.cgi?ssid=204a2ab4254d4911874cd20953dfb1ed.

**Table B2 cont.** Relative Abundance of SOB from 500 L Mesocosms in 2019

| Exp | Treatment | Mesocosm # | Day | *Halothiobacillus* | *Ferrovum* | *Thiomonas* | *Sediminibacterium* | *Brevundimonas* | *Acidovorax* | *Thiobacillus* |
|---|---|---|---|---|---|---|---|---|---|---|
| (c) | SOB Community 1 + 2.0 mM S-$S_4O_6^{2-}$ | M17 | 0 | 24.83 | 0.00 | 0.00 | 3.46 | 0.00 | 10.25 | 6.43 |
| (c) | SOB Community 1 + 2.0 mM S-$S_4O_6^{2-}$ | M17 | 21 | 10.90 | 0.00 | 0.00 | 0.00 | 0.00 | 16.19 | 1.75 |
| (c) | Control: 2.0 mM S-$S_4O_6^{2-}$+ No SOB | M18 | 0 | 1.26 | 0.00 | 0.00 | 0.00 | 0.00 | 1.26 | 2.72 |
| (c) | Control: 2.0 mM S-$S_4O_6^{2-}$+ No SOB | M18 | 21 | 1.97 | 0.00 | 0.00 | 0.00 | 0.00 | 24.24 | 1.35 |
| (c) | SOB Community 1 + S-$S_2O_3^{2-}$ | M19 | 0 | 18.39 | 0.00 | 0.00 | 2.94 | 0.00 | 13.91 | 8.49 |
| (c) | SOB Community 1 + S-$S_2O_3^{2-}$ | M19 | 21 | 3.56 | 0.00 | 0.00 | 0.00 | 0.00 | 30.34 | 2.05 |
| (c) | Control: 2.0 mM S-S2O32- + No SOB | M20 | 0 | 9.34 | 0.00 | 0.00 | 5.90 | 0.00 | 7.40 | 9.75 |
| (c) | Control: 2.0 mM S-S2O32- + No SOB | M20 | 21 | 1.17 | 0.00 | 0.00 | 3.90 | 1.99 | 4.35 | 1.30 |
| (c) | SOB Community 2 + 2.0 mM S-$S_4O_6^{2-}$ | M21 | 0 | 15.46 | 0.00 | 0.00 | 2.39 | 0.00 | 9.97 | 5.78 |
| (c) | SOB Community 2 + 2.0 mM S-$S_4O_6^{2-}$ | M21 | 21 | 5.50 | 0.00 | 0.00 | 0.00 | 2.07 | 0.00 | 0.00 |
| (c) | SOB Community 3 + 2.0 mM S-$S_4O_6^{2-}$ | M22 | 0 | 17.99 | 0.00 | 0.00 | 2.74 | 0.00 | 14.83 | 6.74 |
| (c) | SOB Community 3 + 2.0 mM S-$S_4O_6^{2-}$ | M22 | 20 | 10.75 | 0.00 | 0.00 | 0.00 | 0.00 | 2.74 | 0.00 |
| (c) | SOB Community 2 + 2.0 mM S-$S_2O_3^{2-}$ | M23 | 0 | 22.21 | 0.00 | 0.00 | 4.01 | 0.00 | 9.90 | 5.15 |
| (c) | SOB Community 2 + 2.0 mM S-$S_2O_3^{2-}$ | M23 | 20 | 5.15 | 0.00 | 0.00 | 0.00 | 0.00 | 12.47 | 1.06 |
| (c) | SOB Community 3 + 2.0 mM S-$S_2O_3^{2-}$ | M24 | 0 | 4.14 | 0.00 | 0.00 | 0.00 | 0.00 | 3.37 | 0.00 |
| (c) | SOB Community 3 + 2.0 mM S-$S_2O_3^{2-}$ | M24 | 22 | 1.13 | 0.00 | 0.00 | 0.00 | 0.00 | 3.76 | 0.00 |

For workflow from raw 16S gene sequencing data with OTUs listed, see "Chapter 3 Supplementary 16S rRNA data (curation steps)" at the following link: http://128.100.14.155:8088/share.cgi?ssid=204a2ab4254d4911874cd20953dfb1ed.

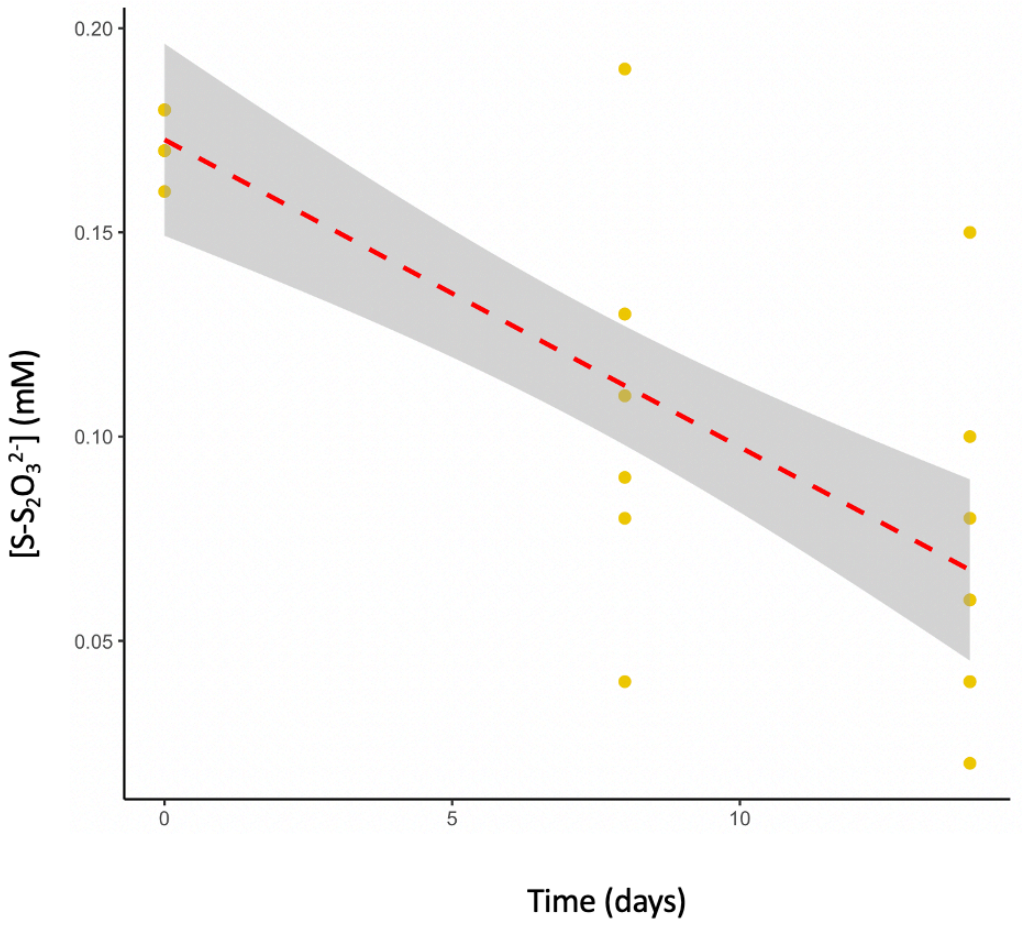


**Fig B1** For Experiment a, the thiosulfate concentrations decreased linearly across the eight mesocosms, at a mean rate of -0.0075 ± 0.0025 mM S per day, and a 95 % confidence interval of (-0.01005071, -0.004999968).

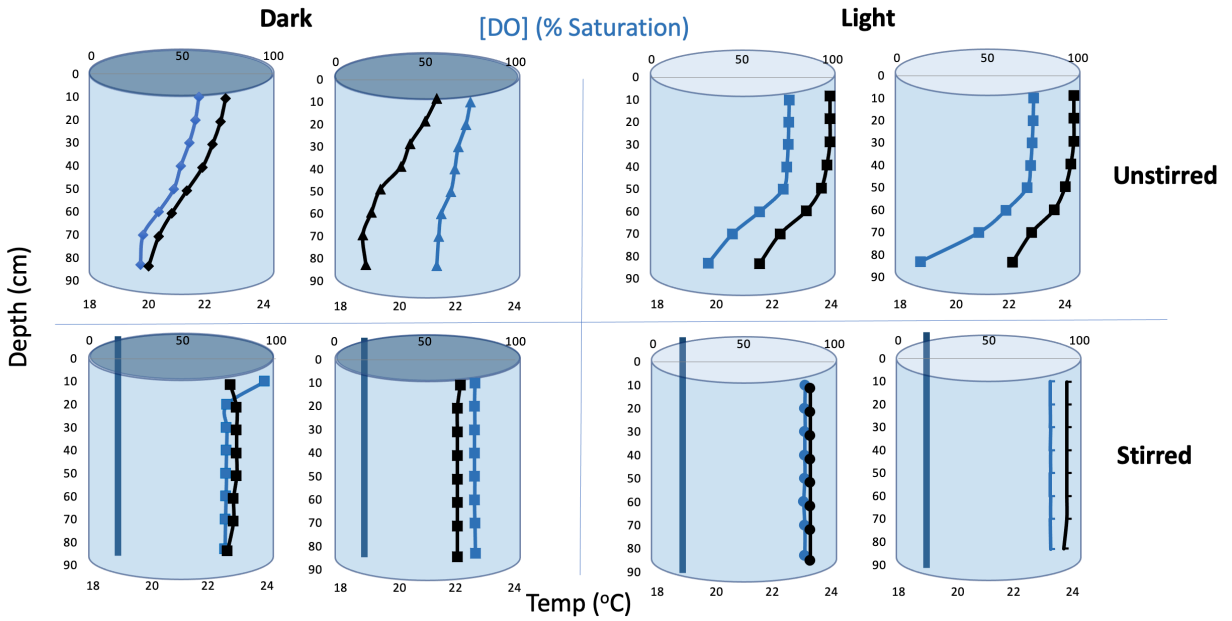


(a)

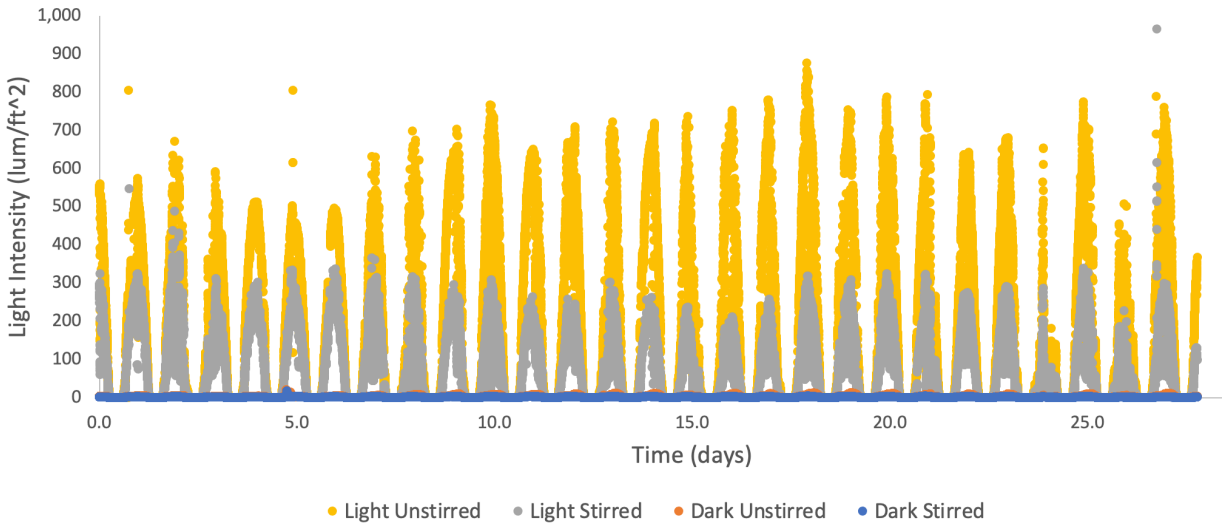


(b)

**Fig B2** Dissolved light and oxygen concentrations in the Experiment a. The (a) temperature and dissolved oxygen profiles on day$_{14}$ and (b) light intensity at the bottom of the mesocosms across all timepoints. Note: fluctuations between zero and maximum values occurred according do daily cycle of sunrise/sunset.

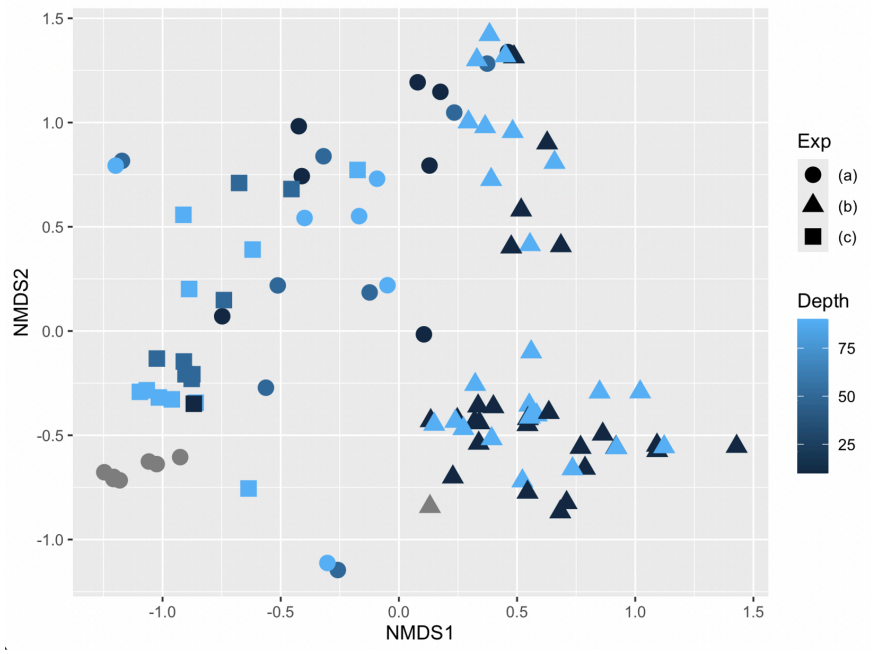


(a)

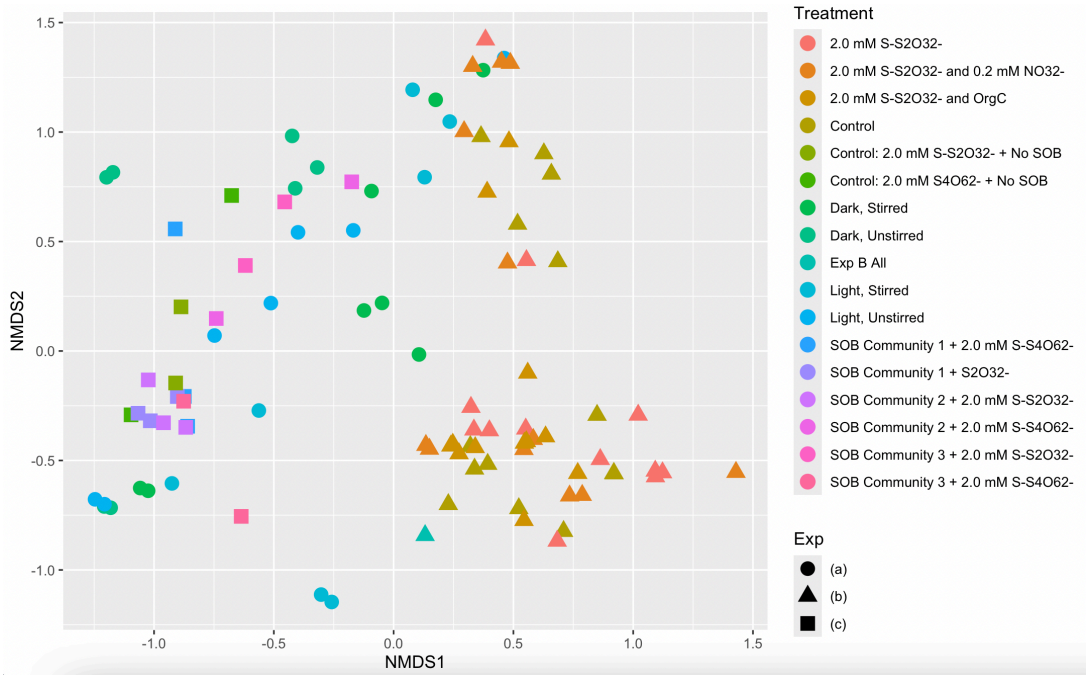


(b)

**Fig B3** Non-metric dimensional scaling of 16S rRNA gene–sequenced communities in experiments a, b, and c (which represent all bacteria detected, not only sulfur-oxidizing bacteria) shows some clustering by experiment (shape), but no recognizable patterns by (a) depth or (b) treatment.

# Appendix C: Supplemental Information for Chapter 4

**Table C1** Potential Enzyme-Facilitated Sulfur Reactions from Current Literature with Nitrate as Terminal Electron Acceptor*

| Pathway | S Gene | Sulfur Substrate Half Reaction | Nitrate to Ammonium as TEA Half Reaction | $\Delta H^+/S$ |
|---|---|---|---|---|
| **$H_2S$ Oxi.** | *fccAB/ sqr* | $H_2S \rightarrow S^0 + 2\ H^+ + 2\ e^-$ | $2\ e^- + \frac{1}{4}\ NO_3^- + 10/4\ H^+ \rightarrow \frac{1}{4}\ NH_4^+ + \frac{3}{4}\ H_2O$ | **-0.5** |
| **Overall** | | **$H_2S + \frac{1}{4}\ NO_3^- + \frac{1}{2}\ H^+ \rightarrow S^0 + \frac{1}{4}\ NH_4^+ + H_2O$** | | **-0.5** |
| **SOx** | *soxAX, soxYZ* | $S_2O_3^{2-}$ + SoxYZ-$S^-$ $\rightarrow$ SoxYZ-S-S-$SO_3^-$ + 2 $e^-$ | $2\ e^- + \frac{1}{4}\ NO_3^- + 10/4\ H^+ \rightarrow \frac{1}{4}\ NH_4^+ + \frac{3}{4}\ H_2O$ | **-1.25** |
| | *soxB* | SoxYZ-$S_3O_3^-$ + $H_2O$ $\rightarrow$ $SO_4^{2-}$ + 2 $H^+$ + SoxYZ-S-$S^-$ | | **1** |
| | *soxCD* | SoxYZ-S-$S^-$ + 3 $H_2O$ $\rightarrow$ SoxYZ-S-$SO_3^-$ + 6 $H^+$ + 6 $e^-$ | $6\ e^- + 3/4\ NO_3^- + 30/4\ H^+ \rightarrow \frac{3}{4}\ NH_4^+ + 9/4\ H_2O$ | **-0.75** |
| | *soxB* | SoxYZ-S-$SO_3^-$ + $H_2O$ $\rightarrow$ $SO_4^{2-}$ + 2 $H^+$ + SoxYZ-$S^-$ | | **1** |
| **SOx Overall** | *soxAXBCDYZ* | **$S_2O_3^{2-} + 2\ H_2O + NO_3^- \rightarrow 2\ SO_4^{2-} + NH_4^+$** | | **0** |
| **iSOx** | *soxAX, soxYZ* | $S_2O_3^{2-}$ +SoxYZ-$S^-$ $\rightarrow$ SoxYZ-S-S-$SO_3^-$ + 2 $e^-$ | $2\ e^- + \frac{1}{4}\ NO_3^- + 10/4\ H^+ \rightarrow \frac{1}{4}\ NH_4^+ + \frac{3}{4}\ H_2O$ | **-1.25** |
| | *soxB* | SoxYZ-$S_3O_3^-$ + $H_2O$ $\rightarrow$ $SO_4^{2-}$ + 2 $H^+$ + SoxYZ-S-$S^-$ | | **1** |
| **iSOx Overall** | *soxAXZYB* | **$S_2O_3^{2-} + \frac{1}{4}\ NO_3^- + \frac{1}{4}\ H_2O + \frac{1}{2}\ H^+ \rightarrow SO_4^{2-} + S^0 + \frac{1}{4}\ NH_4^+$** | | **-0.25** |
| **rDSR** | *?* | DsrEFH-SH $\rightarrow$ DsrEFH-S-SH | | |
| | *dsrC, dsrEFH* | DsrEFH-S-SH + DsrC(-SH)$_2$ $\rightarrow$ DsrC(-SH -SS) + $H^+$ + DsrEFH-SH | | **1** |
| | *dsrAB* | DsrC(-SH -SS) + 3 $H_2O$ $\rightarrow$ $SO_3^{2-}$ + DsrC(-$S_2$) + 7 $H^+$ + 6 $e^-$ | 4 $e^-$ + 1/2 $NO_3^-$ + 5 $H^+$ $\rightarrow$ 1/2 $NH_4^+$ + 3/2 $H_2O$ | **0** |
| | *dsrMKJOP* | DsrC($S_2$) + 2 $H^+$ + 2 $e^-$ $\rightarrow$ DsrC(-SH)$_2$ | | |
| | *aprAB, aprM* | $SO_3^{2-}$ + AMP $\rightarrow$ APS + $e^-$ | e- + 1/8 $NO_3^-$ + 10/8 $H^+$ $\rightarrow$ 1/8 $NH_4^+$ + 3/8 $H_2O$ | **-1.25** |
| | *sat* | APS + $H_2O$ $\rightarrow$ $SO_4^{2-}$ + $e^-$ + 2 $H^+$ | e- + 1/8 $NO_3^-$ + 10/8 $H^+$ $\rightarrow$ 1/8 $NH_4^+$ + 3/8 $H_2O$ | **0.75** |
| **rDSR Overall** | *dsrABCEFHMKJOP, aprABM, sat* | $S^0 + \frac{3}{4}\ NO_3^- + 7/4\ H_2O \rightarrow SO_4^{2-} + 0.5\ H^+ + \frac{3}{4}\ NH_4^+$ | | **0.5** |
| **iSOx + rDSR** | | **$S_2O_3^{2-} + 2\ H_2O + NO_3^- \rightarrow 2\ SO_4^{2-} + NH_4^+$** | | **0** |
| **$S_4I$ – Part 1** | *doxDA/tsdA* | 2 $S_2O_3^{2-}$ $\rightarrow$ $S_4O_6^{2-}$ + 2 $e^-$ | $2\ e^- + \frac{1}{4}\ NO_3^- + 10/4\ H^+ \rightarrow \frac{1}{4}\ NH_4^+ + \frac{3}{4}\ H_2O$ | **0.625** |
| **Part 1 Overall** | | $2\ S_2O_3^{2-} + \frac{1}{4}\ NO_3^- + 10/4\ H^+ \rightarrow S_4O_6^{2-} + \frac{1}{4}\ NH_4^+ + \frac{3}{4}\ H_2O$ | | **-0.625** |
| **$S_4I$ – Part 2?** | *otr/ttrABC* | $S_4O_6^{2-}$ + 2 $e^-$ $\rightarrow$ 2 $S_2O_3^{2-}$ | | |
| | *tsr* | $S_2O_3^{2-}$ $\rightarrow$ $SO_3^{2-}$ + $S^0$ | | |
| | *tetH* | $S_4O_6^{2-}$ + $H_2O$ $\rightarrow$ $SO_4^{2-}$ + $S_2O_3^{2-}$ + 2 $H^+$ | | |
| | *soeABC/sorAB* | $SO_3^{2-}$ + $H_2O$ $\rightarrow$ $SO_4^{2-}$ + 2 $H^+$ + 2 $e^-$ | 2 $e^-$ + 1/4 $NO_3^-$ + 10/4 $H^+$ $\rightarrow$ 1/4 $NH_4^+$ + 3/4 $H_2O$ | |
| | *soxB* | $S_4O_6^{2-}$ + 2 $H_2O$ $\rightarrow$ 2 $SO_4^{2-}$ + 4 $H^+$ + 2 $S^0$ | | |
| **Part 2 Overall** | | $4\ S_4O_6^{2-} + 7\ NO_3^- + 19\ H_2O \rightarrow 16\ SO_4^{2-} + 7\ NH_4^+ + 10\ H^+$ | | **0.625** |
| **$S_4I$ Overall** | | **$S_2O_3^{2-} + 2\ H_2O + NO_3^- \rightarrow 2\ SO_4^{2-} + NH_4^+$** | | **0** |

*Based on a review of current literature (see Table 1.3, above).

? indicates a gap in the literature.

**Table C1 cont.** Potential Enzyme-Facilitated Sulfur Reactions from Current Literature with Nitrate as Terminal Electron Acceptor*

| Pathway | S Gene | Sulfur Substrate Half Reaction | Nitrate to Nitrogen as TEA Half Reaction | $\Delta H^+/S$ |
|---|---|---|---|---|
| **$H_2S$ Oxi.** | *fccAB/ sqr* | $H_2S \rightarrow S^0 + 2\ H^+ + 2\ e^-$ | $2\ e^- + 2/5\ NO_3^- + 12/5\ H^+ \rightarrow 1/5\ N_2 + 6/5\ H_2O$ | **-2** |
| **Overall** | | **$H_2S + 2/5\ NO_3^- + 2\ H^+ \rightarrow S^0 + 1/5\ N_2 + 6/5\ H_2O$** | | **-2** |
| **SOx** | *soxAX, soxYZ* | $S_2O_3^{2-}$ + SoxYZ-$S^-$ $\rightarrow$ SoxYZ-S-S-$SO_3^-$ + 2 $e^-$ | $2\ e^- + 2/5\ NO_3^- + 12/5\ H^+ \rightarrow 1/5\ N_2 + 6/5\ H_2O$ | **-1.2** |
| | *soxB* | SoxYZ-$S_3O_3^-$ + $H_2O$ $\rightarrow$ $SO_4^{2-}$ + 2 $H^+$ + SoxYZ-S-$S^-$ | | **1** |
| | *soxCD* | SoxYZ-S-$S^-$ + 3 $H_2O$ $\rightarrow$ SoxYZ-S-$SO_3^-$ + 6 $H^+$ + 6 $e^-$ | $6\ e^- + 6/5\ NO_3^- + 36/5\ H^+ \rightarrow 3/5\ N_2 + 18/5\ H_2O$ | **-0.6** |
| | *soxB* | SoxYZ-S-$SO_3^-$ + $H_2O$ $\rightarrow$ $SO_4^{2-}$ + 2 $H^+$ + SoxYZ-$S^-$ | | **1** |
| **SOx Overall** | *soxAXBCDYZ* | **$S_2O_3^{2-} + 1/5\ H_2O + 8/5\ NO_3^- \rightarrow 2\ SO_4^{2-} + 4/5\ N_2 + 2/5\ H^+$** | | **0.2** |
| **iSOx** | *soxAX, soxYZ* | $S_2O_3^{2-}$ +SoxYZ-$S^-$ $\rightarrow$ SoxYZ-S-S-$SO_3^-$ + 2 $e^-$ | $2\ e^- + 2/5\ NO_3^- + 12/5\ H^+ \rightarrow 1/5\ N_2 + 6/5\ H_2O$ | **-1.2** |
| | *soxB* | SoxYZ-$S_3O_3^-$ + $H_2O$ $\rightarrow$ $SO_4^{2-}$ + 2 $H^+$ + SoxYZ-S-$S^-$ | | **1** |
| **iSOx Overall** | *soxAXZYB* | **$S_2O_3^{2-} + 2/5\ NO_3^- + 2/5\ H^+ \rightarrow SO_4^{2-} + S^0 + 1/5\ N_2 + 1/5\ H_2O$** | | **-0.2** |
| **rDSR** | *?* | DsrEFH-SH $\rightarrow$ DsrEFH-S-SH | | |
| | *dsrC, dsrEFH* | DsrEFH-S-SH + DsrC(-SH)$_2$ $\rightarrow$ DsrC(-SH -SS) + $H^+$ + DsrEFH-SH | | **1** |
| | *dsrAB* | DsrC(-SH -SS) + 3 $H_2O$ $\rightarrow$ $SO_3^{2-}$ + DsrC(-$S_2$) + 7 $H^+$ + 6 $e^-$ | $4\ e^- + 4/5\ NO_3^- + 24/5\ H^+ \rightarrow 2/5\ N_2 + 12/5\ H_2O$ | **0.2** |
| | *dsrMKJOP* | DsrC($S_2$) + 2 $H^+$ + 2 $e^-$ $\rightarrow$ DsrC(-SH)$_2$ | | |
| | *aprAB, aprM* | $SO_3^{2-}$ + AMP $\rightarrow$ APS + $e^-$ | $e^- + 1/5\ NO_3^- + 6/5\ H^+ \rightarrow 1/10\ N_2 + 3/5\ H_2O$ | **-1.2** |
| | *sat* | APS + $H_2O$ $\rightarrow$ $SO_4^{2-}$ + $e^-$ + 2 $H^+$ | $e^- + 1/5\ NO_3^- + 6/5\ H^+ \rightarrow 1/10\ N_2 + 3/5\ H_2O$ | **0.8** |
| **rDSR Overall** | *dsrABCEFHMKJOP, aprABM, sat* | $S^0 + 6/5\ NO_3^- + 2/5\ H_2O \rightarrow SO_4^{2-} + 3/5\ N_2 + 4/5\ H^+$ | | **0.8** |
| **iSOx + rDSR** | | **$S_2O_3^{2-} + 8/5\ NO_3^- + 1/5\ H_2O \rightarrow 2\ SO_4^{2-} + 4/5\ N_2 + 2/5\ H^+$** | | **0.4** |
| **$S_4I$ – Part 1** | *doxDA/tsdA* | 2 $S_2O_3^{2-}$ $\rightarrow$ $S_4O_6^{2-}$ + 2 $e^-$ | $2\ e^- + 2/5\ NO_3^- + 12/5\ H^+ \rightarrow 1/5\ N_2 + 6/5\ H_2O$ | **-0.6** |
| **Part 1 Overall** | | **$2\ S_2O_3^{2-} + 2/5\ NO_3^- + 12/5\ H^+ \rightarrow S_4O_6^{2-} + 1/5\ N_2 + 6/5\ H_2O$** | | **-0.6** |
| **$S_4I$ – Part 2?** | *otr/ttrABC* | $S_4O_6^{2-}$ + 2 $e^-$ $\rightarrow$ 2 $S_2O_3^{2-}$ | | |
| | *tsr* | $S_2O_3^{2-}$ $\rightarrow$ $SO_3^{2-}$ + $S^0$ | | |
| | *tetH* | $S_4O_6^{2-}$ + $H_2O$ $\rightarrow$ $SO_4^{2-}$ + $S_2O_3^{2-}$ + 2 $H^+$ | | |
| | *soeABC/sorAB* | $SO_3^{2-}$ + $H_2O$ $\rightarrow$ $SO_4^{2-}$ + 2 $H^+$ + 2 $e^-$ | $2\ e^- + 2/5\ NO_3^- + 12/5\ H^+ \rightarrow 1/5\ N_2 + 6/5\ H_2O$ | |
| | *soxB* | $S_4O_6^{2-}$ + 2 $H_2O$ $\rightarrow$ 2 $SO_4^{2-}$ + 4 $H^+$ + 2 $S^0$ | | |
| **Part 2 Overall** | | $S_4O_6^{2-} + 14/5\ NO_3^- + 8/5\ H_2O \rightarrow 4\ SO_4^{2-} + 7/5\ N_2 + 16/5\ H^+$ | | **0.8** |
| **$S_4I$ Overall** | | **$2\ S_2O_3^{2-} + 16/5\ NO_3^- + 2/5\ H_2O \rightarrow 4\ SO_4^{2-} + 8/5\ N_2 + 4/5\ H^+$** | | **0.2** |

*Based on a review of current literature (see Table 1.3, above).

? indicates a gap in the literature.

**Table C2** Summary of Geochemical Data for the Mesocosm Experiment

| Treatment | Code | Day | pH (bottom) | pH (top) | Temp °C | D.O (mM) | D.O (mg/L) | $NO_3^-$ (mM) | Std. Dev $NO_3^-$ (mM) | $NH_4^+$ (mM) | Std. Dev $NH_4^+$ (mM) |
|---|---|---|---|---|---|---|---|---|---|---|---|
| $T_{12}S_{4(2.0)}$ | $E_1$ | 0 | 6.52 | 6.64 | 14 | 0.07 | 2.24 | 0.04 | 0.00 | 0.15 | 0.02 |
| | | 1.25 | 6.09 | 5.86 | - | 0.00 | 0.00 | 0.05 | 0.00 | 0.16 | 0.02 |
| | | 16 | 5.52 | 5.71 | 11.9 | 0.10 | 3.20 | 0.06 | 0.04 | 0.21 | 0.02 |
| | | 28 | 5.19 | 5.52 | 9.9 | 0.04 | 1.28 | 0.35 | 0.22 | 0.43 | 0.13 |
| $T_{12}S_{4(2.0)}N_{2.0}$ | $E_2$ | 0 | 6.27 | 6.18 | 13.5 | 0.15 | 4.80 | 0.04 | 0.00 | 0.25 | 0.01 |
| | | 1.25 | 5.90 | 5.80 | - | 0.06 | 1.92 | 1.48 | 0.00 | 0.25 | 0.05 |
| | | 16 | 5.84 | 5.77 | 11.3 | 0.08 | 2.56 | 1.31 | 0.05 | 0.25 | 0.03 |
| | | 28 | 5.63 | 5.60 | 9.8 | 0.11 | 3.52 | 2.18 | 0.21 | 0.47 | - |
| $T_{12}S_{2(2.0)}$ | $E_3$ | 0 | 7.43 | 6.26 | 14 | 0.03 | 0.96 | 0.06 | 0.02 | 0.09 | 0.02 |
| | | 1.25 | 7.66 | 6.24 | - | 0.00 | 0.00 | 0.05 | 0.01 | 0.06 | 0.02 |
| | | 16 | 6.0* | 6.04 | 11.9 | 0.07 | 2.24 | 0.09 | 0.02 | 0.16 | 0.05 |
| | | 28 | 6.1* | 6.16 | 10.4 | 0.00 | 0.00 | 0.71 | 0.74 | 0.34 | 0.22 |
| $T_{12}S_{2(2.0)}N_{2.0}$ | $E_4$ | 0 | 5.65 | 6.08 | 13.4 | 0.03 | 0.96 | 0.06 | 0.00 | 0.17 | 0.01 |
| | | 1.25 | 5.22 | 5.50 | - | 0.00 | 0.00 | 1.39 | 0.04 | 0.14 | 0.03 |
| | | 16 | 5.61 | 6.43 | 11.3 | 0.18 | 5.76 | 1.37 | 0.12 | 0.21 | 0.02 |
| | | 28 | 6.52 | 7.40 | 9.6 | 0.19 | 6.08 | 1.49 | 0.12 | 0.25 | 0.03 |

Notes: Sulfur amendments were made at day 1.25 of the experiment; Added 2.0 mM thiosulfate and tetrathionate as sulfur

(-) indicates no data available; nitrite and sulfite in all treatments < LOD of 0.1 mM; DO is dissolved oxygen content. [HS−] not measured or often detected.

*pH data from mesocosm bottom waters (50 cm depth from surface) is not available, so approximated with pH data from top of mesocosm E3 (10 cm depth from surface of the water in the mesocosm). Values from the bottom of the mesocosm were used for ΔH+ calculations throughout the manuscript.

**Table C2** cont. Summary of Geochemical Data for the Mesocosm Experiment

| Treatment | Code | Day | $SO_4^{2-}$ (mM) | St Dev $SO_4^{2-}$ (mM) | S-$S_2O_3^{2-}$ (mM) | St Dev S-$S_2O_3^{2-}$ (mM) | $S^0$ (mM) | St Dev $S^0$ (mM) | S-$S_4O_6^{2-}$ (mM) | Std Dev S-$S_4O_6^{2-}$ (mM) | Total S (mM) | St Dev Total S (mM) |
|---|---|---|---|---|---|---|---|---|---|---|---|---|
| $T_{12}S_{4(2.0)}$ | $E_1$ | 0 | 7.44 | - | - | - | 0.18 | - | - | - | - | - |
| | | 1.25 | 7.96 | 0.08 | 1.79 | 0.03 | - | - | 0.56 | 0.13 | 10.9 | 0.52 |
| | | 16 | 8.84 | 0.05 | 1.63 | 0.00 | 0.23 | 0.05 | 0.17 | 0.01 | 11.5 | 0.98 |
| | | 28 | 9.31 | 0.82 | 1.24 | 0.01 | 0.20 | 0.03 | - | - | 12.5 | 0.54 |
| $T_{12}S_{4(2.0)}N_{2.0}$ | $E_2$ | 0 | 7.78 | 0.09 | - | - | 0.00 | - | - | - | - | - |
| | | 1.25 | 8.33 | 0.29 | 0.47 | 0.00 | - | - | 0.20 | 0.00 | 9.1 | 0.27 |
| | | 16 | 8.97 | 0.08 | 0.32 | 0.00 | 0.15 | 0.11 | 0.22 | 0.02 | 11.2 | 0.25 |
| | | 28 | 9.35 | 0.54 | 0.15 | 0.01 | 0.02 | 0.01 | - | - | 10.4 | 1.16 |
| $T_{12}S_{2(2.0)}$ | $E_3$ | 0 | 9.29 | 0.40 | - | - | 0.18 | - | - | - | - | - |
| | | 1.25 | 9.43 | 0.28 | 2.96 | 0.03 | - | - | 0.19 | 0.12 | 12.7 | 0.36 |
| | | 16 | 10.64 | 0.07 | 1.96 | 0.02 | 0.30 | 0.21 | 0.13 | - | 13.3 | 0.58 |
| | | 28 | 10.45 | 0.48 | 1.21 | 0.01 | 0.48 | 0.81 | - | - | 13.5 | 0.34 |
| $T_{12}S_{2(2.0)}N_{2.0}$ | $E_4$ | 0 | 7.80 | 0.09 | - | - | 0.00 | - | - | - | - | - |
| | | 1.25 | 8.31 | 0.07 | 1.46 | 0.02 | - | - | 0.19 | 0.00 | 9.2 | 1.18 |
| | | 16 | 10.75 | 2.13 | 0.91 | 0.01 | 0.08 | 0.04 | 0.17 | 0.06 | 9.7 | 1.36 |
| | | 28 | 9.67 | 0.21 | 0.40 | 0.00 | 0.06 | 0.01 | 0.22 | 0.02 | 12.1 | 2.05 |

Notes: Sulfur amendments were made at day 1.25 of the experiment; Added 2.0 mM thiosulfate and tetrathionate as sulfur

(-) indicates no data available; nitrite and sulfite in all treatments < LOD of 0.1 mM; DO is dissolved oxygen content.

[$HS^-$] not measured or often detected in the tailings impoundment.

*pH data from mesocosm bottom waters (50 cm depth from surface of the water in the mesocosm) is not available, so approximated with pH data from top of mesocosm $E_3$ (10 cm depth from surface of the water in the mesocosm).

**Table C2 cont**. Summary of Geochemical Data for the Mesocosm Experiment

| Treatment | Code | Day | pH (bottom) | pH (top) | Temp °C | D.O (mM) | D.O (mg/L) | $NO_3^-$ (mM) | Std. Dev $NO_3^-$ (mM) | $NH_4^+$ (mM) | Std. Dev $NH_4^+$ (mM) |
|---|---|---|---|---|---|---|---|---|---|---|---|
| $S_{2(2.0)}$ | $E_5$ | 0 | 6.09 | - | 14.4 | 0.13 | 4.16 | 0.05 | 0.01 | 0.10 | - |
| | | 1.25 | 6.46 | - | - | 0.03 | 0.96 | 0.07 | 0.01 | 0.04 | 0.01 |
| | | 16 | 5.75 | - | 12.2 | 0.09 | 2.88 | 0.15 | 0.07 | 0.21 | 0.02 |
| | | 28 | 5.78 | - | 10.7 | 0.00 | 0.00 | 0.40 | 0.20 | 0.22 | 0.03 |
| $S_{2(2.0)}N_{2.0}$ | $E_6$ | 0 | 4.02 | 4.01 | 13.6 | 0.27 | 8.64 | 0.08 | 0.01 | 0.21 | - |
| | | 1.25 | 5.10 | 4.13 | - | 0.23 | 7.36 | 1.77 | 0.09 | 0.17 | 0.06 |
| | | 16 | 6.63 | 8.12 | 11.3 | 0.24 | 7.68 | 1.82 | 0.34 | 0.39 | 0.18 |
| | | 28 | 7.12 | 8.25 | 9.6 | 0.24 | 7.68 | 2.07 | - | 0.31 | 0.09 |
| $T_{12}$ | $E_7$ | 0 | 6.52 | 6.40 | 14.3 | 0.28 | 8.96 | 0.07 | 0.01 | 0.19 | 0.00 |
| | | 1.25 | 6.71 | 6.91 | - | 0.04 | 1.28 | 0.07 | 0.00 | 0.21 | 0.00 |
| | | 16 | 6.75 | 6.96 | 11.4 | 0.19 | 6.08 | 0.22 | 0.10 | 0.27 | 0.06 |
| | | 28 | 6.73 | 7.20 | 9.8 | 0.14 | 4.48 | 0.10 | - | 0.22 | - |
| $T_{12}N_{2.0}$ | $E_8$ | 0 | 7.01 | 6.91 | 13.7 | 0.29 | 9.28 | 1.74 | 0.01 | 0.19 | 0.03 |
| | | 1.25 | 7.32 | 7.68 | - | 0.02 | 0.64 | 1.75 | 0.04 | 0.21 | 0.02 |
| | | 16 | 6.52 | 7.25 | 10.9 | 0.13 | 4.16 | 2.00 | 0.24 | 0.27 | 0.02 |
| | | 28 | 6.06 | 6.45 | 9.4 | 0.04 | 1.28 | 1.54 | 0.11 | 0.23 | 0.06 |

Notes: Sulfur amendments were made at $day_{1.25}$ of the experiment; Added 2.0 mM thiosulfate and tetrathionate as sulfur

(-) indicates no data available; nitrite and sulfite in all treatments < LOD of 0.1 mM; DO is dissolved oxygen content. [$HS^-$] not measured or often detected in the Ox Res.

*pH data from mesocosm bottom waters (50 cm depth from surface of the water in the mesocosm) is not available, so approximated with pH data from top of mesocosm $E_3$ (10 cm depth from surface of the water in the mesocosm). Values from the bottom of the mesocosm were used for $\Delta H^+$ calculations throughout the manuscript.

**Table C2 cont**. Summary of Geochemical Data for the Mesocosm Experiment

| Treatment | Code | Day | $SO_4^{2-}$ (mM) | St Dev $SO_4^{2-}$ (mM) | S-$S_2O_3^{2-}$ (mM) | St Dev S-$S_2O_3^{2-}$ (mM) | $S^0$ (mM) | St Dev $S^0$ (mM) | S-$S_4O_6^{2-}$ (mM) | Std Dev S-$S_4O_6^{2-}$ (mM) | Total S (mM) | St Dev Total S (mM) |
|---|---|---|---|---|---|---|---|---|---|---|---|---|
| $S_{2(2.0)}$ | $E_5$ | 0 | - | - | - | - | 0.08 | - | - | - | - | - |
| | | 1.25 | 7.66 | 0.09 | 2.53 | 0.04 | - | - | 0.34 | 0.26 | 12.4 | 0.89 |
| | | 16 | 9.44 | 0.27 | 1.64 | 0.01 | 0.12 | 0.02 | 0.60 | - | 12.9 | 0.77 |
| | | 28 | 8.42 | 0.46 | 0.86 | 0.01 | 0.12 | 0.02 | - | - | 12.5 | 1.06 |
| $S_{2(2.0)}N_{2.0}$ | $E_6$ | 0 | - | - | - | - | 0.00 | - | - | - | - | - |
| | | 1.25 | 6.95 | 1.18 | 1.39 | 0.06 | - | - | 0.09 | 0.02 | 9.4 | 1.63 |
| | | 16 | 7.96 | 0.10 | 0.71 | 0.01 | 0.02 | 0.04 | 0.13 | - | 8.7 | 0.38 |
| | | 28 | 7.45 | 0.27 | 0.45 | 0.01 | 0.03 | 0.01 | 0.20 | - | 14.3 | 0.47 |
| $T_{12}$ | $E_7$ | 0 | 7.12 | 0.11 | - | - | 0.00 | - | - | - | - | - |
| | | 1.25 | 7.83 | 0.38 | 0.46 | 0.00 | - | - | 0.09 | 0.02 | 8.4 | 0.12 |
| | | 16 | 8.30 | 0.06 | 0.24 | 0.00 | 0.01 | 0.01 | 0.10 | - | 10.4 | 0.32 |
| | | 28 | 7.80 | 0.08 | 0.12 | 0.01 | 0.03 | 0.00 | 0.10 | - | 8.1 | 0.55 |
| $T_{12}N_{2.0}$ | $E_8$ | 0 | 7.54 | 0.35 | - | - | 0.00 | - | - | - | - | - |
| | | 1.25 | 8.38 | 0.18 | 0.49 | 0.01 | - | - | 0.08 | 0.02 | 8.2 | 0.23 |
| | | 16 | 8.64 | 0.30 | 0.06 | 0.03 | 0.03 | 0.01 | 0.09 | 0.02 | 8.2 | 0.22 |
| | | 28 | 7.92 | 0.14 | 0.00 | 0.01 | 0.00 | - | 0.10 | - | 8.7 | 1.38 |

Notes: Sulfur amendments were made at $day_{1.25}$ of the experiment; Added 2.0 mM thiosulfate and tetrathionate as sulfur

(-) indicates no data available; nitrite and sulfite in all treatments < LOD of 0.1 mM; DO is dissolved oxygen content. [$HS^-$] not measured or often detected in the Ox Res.

*pH data from mesocosm bottom waters (50 cm depth from surface of the water in the mesocosm) is not available, so approximated with pH data from top of mesocosm $E_3$ (10 cm depth from surface of the water in the mesocosm).

**Table C3** Effect of Oxygen and Nitrate on Rates of Thiosulfate Loss in Mesocosms

| Mesocosm | Treatment | k ($day^{-1}$) | $S_2O_3^{2-}$ half-life (days) |
|---|---|---|---|
| $E_1T_{12}S_{4(2.0)}$ | 12 L Tailings + 2.0 mM $S_4O_6^{2-}$ | 0.01 | 69.3 |
| $E_3T_{12}S_{2(2.0)}$ | 12 L Tailings + 2.0 mM $S_2O_3^{2-}$ | 0.03 | 23.1 |
| $E_7T_{12}$ | 12 L Tailings | 0.05 | 13.9 |
| $E_5S_{2(2.0)}$ | 2.0 mM $S_2O_3^{2-}$ | 0.04 | 17.3 |
| $E_2T_{12}S_{4(2.0)}N_{2.0}$ | 12 L Tailings + 2.0 mM $S_4O_6^{2-}$ + 2.0 mM $NO_3^-$ | 0.04 | 17.3 |
| $E_4T_{12}S_{2(2.0)}N_{2.0}$ | 12 L Tailings + 2.0 mM $S_2O_3^{2-}$ + 2.0 mM $NO_3^-$ | 0.05 | 13.9 |
| $E_8T_{12}N_{2.0}$ | 12 L Tailings + 2.0 mM $NO_3^-$- | 0.14 | 4.95 |
| $E_6S_{2(2.0)}N_{2.0}$ | 2.0 mM $S_2O_3^{2-}$ + 2.0 mM $NO_3^-$ | 0.04 | 17.3 |

**Table C4** Frequency of MAGs of Sulfur-Oxidizing Bacteria Containing One or More Copy/ies of each S Gene

| | Potential $S_4I$ | | | | S Red | | | SOx | | | | | | rDSR | | | | | | | | | | | | | S Uptake |
|---|---|---|---|---|---|---|---|---|---|---|---|---|---|---|---|---|---|---|---|---|---|---|---|---|---|---|---|
| | *tsdA* | *tetH** | *sdo* | *sor* | *ttrA* | *ttrB* | *ttrC* | *soxA* | *soxB* | *soxC* | *soxX* | *soxY* | *soxZ* | *dsrC* | *dsrA* | *dsrB* | *dsrE* | *dsrF* | *dsrH* | *dsrC* | *dsrMK JOP* | *aprA* | *aprB* | *sat* | *qmoA* | *qmoB* | *qmoC* | *sqr* |
| ***Halothio-bacillus spp.*** | 1.0 | 0.0 | 0.8 | 0.8 | 0.0 | 0.0 | 0.1 | 1.0 | 1.0 | 1.0 | 1.0 | 0.9 | 0.9 | 0.0 | 0.0 | 0.0 | 0.0 | 0.0 | 0.0 | 0.0 | 0.0 | 0.0 | 0.0 | 0.0 | 0.0 | 0.0 | 1.0 |
| ***Thiomonas spp.*** | 1.0 | 0.0 | 1.0 | 0.0 | 0.3 | 0.0 | 0.0 | 1.0 | 1.0 | 1.0 | 1.0 | 1.0 | 1.0 | 0.0 | 0.0 | 0.0 | 0.0 | 0.0 | 0.0 | 0.0 | 0.0 | 0.0 | 0.0 | 0.0 | 0.0 | 0.0 | 1.0 |
| ***Thiobacillus spp.*** | 0.7 | 0.4 | 1.0 | 0.1 | 0.3 | 0.3 | 0.3 | 1.0 | 0.9 | 0.0 | 1.0 | 0.8 | 0.9 | 1.0 | 1.0 | 0.9 | 0.9 | 0.9 | 1.0 | 0.9 | 0.9 | 0.9 | 0.9 | 1.0 | 0.9 | 0.9 | 1.0 | 1.0 |
| ***Sedimini-bacterium spp.*** | 0.9 | 0.0 | 1.0 | 0.0 | 0.0 | 0.0 | 0.0 | 0.0 | 0.0 | 0.0 | 0.0 | 0.0 | 0.0 | 0.2 | 0.0 | 0.0 | 0.0 | 0.0 | 0.0 | 0.2 | 0.0 | 0.0 | 0.0 | 0.0 | 0.0 | 0.0 | 0.5 | 0.4 |
| ***Thiovirga spp.*** | 0.0 | 0.0 | 1.0 | 0.0 | 0.0 | 0.0 | 0.0 | 1.0 | 1.0 | 1.0 | 1.0 | 1.0 | 1.0 | 0.0 | 0.0 | 0.0 | 0.0 | 0.0 | 0.0 | 0.0 | 0.0 | 0.0 | 0.0 | 0.0 | 0.0 | 0.0 | 0.0 | 1.0 |
| ***Acidovorax spp.*** | 0.0 | 0.0 | 0.9 | 0.0 | 0.8 | 0.8 | 0.8 | 0.0 | 0.0 | 0.1 | 0.0 | 0.0 | 0.0 | 0.1 | 0.1 | 0.1 | 0.1 | 0.1 | 0.1 | 0.0 | 0.1 | 0.0 | 0.0 | 0.0 | 0.0 | 0.0 | 0.0 | 0.9 |
| ***Sulfurovum spp.*** | 0.0 | - | 0.0 | 0.0 | 0.0 | 0.0 | 0.0 | 0.2 | 0.2 | 0.2 | 0.1 | 0.2 | 0.2 | 0.0 | 0.0 | 0.0 | 0.0 | 0.0 | 0.0 | 0.0 | 0.0 | 0.0 | 0.0 | 0.0 | 0.0 | 0.0 | 0.0 | 0.2 |
| ***Desulfurivibrio spp.**** | - | - | - | - | - | - | - | - | - | - | - | - | - | 1.0 | 1.0 | 1.0 | 1.0 | 1.0 | 1.0 | 1.0 | 1.0 | 1.0 | 1.0 | 1.0 | 1.0 | 1.0 | 1.0 | 1.0 |

*Values for the frequency of the tetH in *Thiobacillus* metagenomes found in the Oxidation Reservoir calculated manually from annotated genomes for a core list of 137 metagenomes covering 8 most common SOB genera.

***Desulfurivibrio* sulfur genes identified in published metagenomes, not from site samples: *Desulfurivibrio alkaliphilus* (Vigneron et al. 2021; Bell et al. 2020; Dick 2019); *Desulfurivibrio alkaliphilus strain AHT2T* - (Thorup et al. 2017); and *Desulfurivibrio spp.* (Melton et al. 2016). Genes identified in all three functioned as in the reverse direction (rDSR) suggesting sulfur oxidization occurs in this genus, sometimes paired with Sb reduction (Sun et al. 2022). Note Oxidation Reservoir samples were selected to align with Nature Comm publication – LW & LT - personal communication. (-) indicates no data available, or gene not identified in the literature.

**Table C5a** Relative Abundance of Genera as Proportions of Sulfur Metabolizing Community

| Mesocosm | Treatment | Day | Genus as Fraction of Total Sulfur Community (%) | | | | | | | |
|---|---|---|---|---|---|---|---|---|---|---|
| | | | *Halothiobacillus* | *Thiomonas* | *Thiovirga* | *Sulfurovum* | *Thiobacillus* | *Sediminibacterium* | *Acidovorax* | *Desulfurivibrio* |
| $E_1$ | $T_{12}S_{4(2.0)}$ | 0 | 28.9 | 28.1 | 14.0 | 0.0 | 0.0 | 0.0 | 0.0 | 28.9 |
| | | 14 | 0.0 | 3.6 | 86.0 | 10.4 | 0.0 | 0.0 | 0.0 | 0.0 |
| | | 24 | 0.7 | 2.3 | 1.4 | 1.4 | 7.6 | 0.0 | 0.9 | 85.6 |
| $E_2$ | $T_{12}S_{4(2.0)}N_{2.0}$ | 0 | 7.2 | 86.4 | 0.1 | 0.0 | 0.9 | 0.0 | 0.0 | 5.4 |
| | | 14 | 10.0 | 0.0 | 15.0 | 0.0 | 75.0 | 0.0 | 0.0 | 0.0 |
| | | 24 | - | - | - | - | - | - | - | - |
| $E_3$ | $T_{12}S_{2(2.0)}$ | 0 | 0.0 | 6.2 | 0.0 | 0.0 | 6.7 | 0.0 | 0.0 | 87.1 |
| | | 14 | - | - | - | - | - | - | - | - |
| | | 24 | - | - | - | - | - | - | - | - |
| $E_4$ | $T_{12}S_{2(2.0)}N_{2.0}$ | 0 | 6.4 | 81.7 | 0.0 | 0.0 | 4.3 | 1.6 | 0.0 | 6.0 |
| | | 14 | 0.0 | 0.0 | 100.0 | 0.0 | 0.0 | 0.0 | 0.0 | 0.0 |
| | | 24 | 0.9 | 2.9 | 5.2 | 0.6 | 85.4 | 0.8 | 1.4 | 2.8 |
| $E_5$ | $S_{2(2.0)}$ | 0 | 0.6 | 99.4 | 0.0 | 0.0 | 0.0 | 0.0 | 0.0 | 0.0 |
| | | 14 | 0.9 | 97.4 | 0.2 | 0.0 | 1.1 | 0.0 | 0.5 | 0.0 |
| | | 24 | 0.7 | 98.8 | 0.0 | 0.0 | 0.2 | 0.0 | 0.2 | 0.0 |
| $E_6$ | $S_{2(2.0)}N_{2.0}$ | 0 | 0.0 | 100.0 | 0.0 | 0.0 | 0.0 | 0.0 | 0.0 | 0.0 |
| | | 14 | 0.0 | 60.0 | 0.0 | 0.0 | 0.0 | 42.0 | 0.0 | 0.0 |
| | | 24 | 0.0 | 62.5 | 0.0 | 0.0 | 0.0 | 12.5 | 25.0 | 0.0 |
| $E_7$ | $T_{12}$ | 0 | 0.0 | 100.0 | 0.0 | 0.0 | 0.0 | 0.0 | 0.0 | 0.0 |
| | | 14 | 0.0 | 0.0 | 69.3 | 24.1 | 0.0 | 0.0 | 6.3 | 0.3 |
| | | 24 | 0.0 | 1.3 | 11.5 | 6.4 | 0.0 | 0.0 | 80.8 | 0.0 |
| $E_8$ | $T_{12}N_{2.0}$ | 0 | 0.0 | 52.3 | 0.0 | 0.0 | 0.0 | 47.7 | 0.0 | 0.0 |
| | | 14 | 0.0 | 0.0 | 28.3 | 3.8 | 0.6 | 0.0 | 67.3 | 0.0 |
| | | 24 | 0.0 | 1.5 | 5.9 | 0.0 | 4.4 | 0.0 | 88.2 | 0.0 |

For workflow from raw 16S gene sequencing data with operational taxonomic units (OTUs) listed, see "Chapter 4 Supplementary 16S rRNA data (curation steps)" at the following link: http://128.100.14.155:8088/share.cgi?ssid=204a2ab4254d4911874cd20953dfb1ed.

**Table C5b** Relative Abundance of Sulfur-Oxidizing Bacteria as a Proportion of Total Microbial Community.

| Mesocosm | Treatment | Day | Genus as Fraction of Total Sulfur Community (%) | | | | | | | |
|---|---|---|---|---|---|---|---|---|---|---|
| | | | *Halothiobacillus* | *Thiomonas* | *Thiovirga* | *Sulfurovum* | *Thiobacillus* | *Sediminibacterium* | *Acidovorax* | *Desulfurivibrio* |
| $E_1$ | $T_{12}S_{4(2.0)}$ | 0 | 0.35 | 0.34 | 0.17 | 0.00 | 0.00 | 0.00 | 0.00 | 0.35 |
| | | 14 | 0.00 | 0.39 | 9.42 | 1.14 | 0.00 | 0.00 | 0.00 | 0.00 |
| | | 24 | 0.04 | 0.13 | 0.08 | 0.08 | 0.42 | 0.00 | 0.05 | 4.76 |
| $E_2$ | $T_{12}S_{4(2.0)}N_{2.0}$ | 0 | 0.82 | 9.87 | 0.01 | 0.00 | 0.1 | 0.00 | 0.00 | 0.62 |
| | | 14 | 0.02 | 0.00 | 0.03 | 0.00 | 0.15 | 0.00 | 0.00 | 0.00 |
| | | 24 | - | - | - | - | - | - | - | - |
| $E_3$ | $T_{12}S_{2(2.0)}$ | 0 | 0.00 | 0.24 | 0.00 | 0.00 | 0.26 | 0.00 | 0.00 | 3.38 |
| | | 14 | - | - | - | - | - | - | - | - |
| | | 24 | - | - | - | - | - | - | - | - |
| $E_4$ | $T_{12}S_{2(2.0)}N_{2.0}$ | 0 | 0.15 | 1.91 | 0.00 | 0.00 | 0.1 | 0.04 | 0.00 | 0.14 |
| | | 14 | 0.00 | 0.00 | 0.61 | 0.00 | 0.00 | 0.00 | 0.00 | 0.00 |
| | | 24 | 0.08 | 0.27 | 0.48 | 0.06 | 7.93 | 0.07 | 0.13 | 0.26 |
| $E_5$ | $S_{2(2.0)}$ | 0 | 0.13 | 21.80 | 0.00 | 0.00 | 0.00 | 0.01 | 0.00 | 0.00 |
| | | 14 | 0.05 | 5.54 | 0.01 | 0.00 | 0.06 | 0.00 | 0.03 | 0.00 |
| | | 24 | 0.03 | 4.21 | 0.00 | 0.00 | 0.01 | 0.00 | 0.01 | 0.00 |
| $E_6$ | $S_{2(2.0)}N_{2.0}$ | 0 | 0.00 | 0.35 | 0.00 | 0.00 | 0.00 | 0.00 | 0.00 | 0.00 |
| | | 14 | 0.00 | 0.03 | 0.00 | 0.00 | 0.00 | 0.02 | 0.00 | 0.00 |
| | | 24 | 0.00 | 0.05 | 0.00 | 0.00 | 0.00 | 0.01 | 0.02 | 0.00 |
| $E_7$ | $T_{12}$ | 0 | 0.00 | 0.45 | 0.00 | 0.00 | 0.00 | 0.00 | 0.00 | 0.00 |
| | | 14 | 0.00 | 0.00 | 2.53 | 0.88 | 0.00 | 0.00 | 0.23 | 0.01 |
| | | 24 | 0.00 | 0.01 | 0.09 | 0.05 | 0.00 | 0.00 | 0.63 | 0.00 |
| $E_8$ | $T_{12}N_{2.0}$ | 0 | 0.00 | 0.09 | 0.00 | 0.00 | 0.00 | 0.08 | 0.00 | 0.00 |
| | | 14 | 0.00 | 0.00 | 0.98 | 0.13 | 0.02 | 0.00 | 2.33 | 0.00 |
| | | 24 | 0.00 | 0.01 | 0.04 | 0.00 | 0.03 | 0.00 | 0.60 | 0.00 |

For workflow from raw 16S gene sequencing data with operational taxonomic units (OTUs) listed, see "Chapter 4 Supplementary 16S rRNA data (curation steps)" at the following link: http://128.100.14.155:8088/share.cgi?ssid=204a2ab4254d4911874cd20953dfb1ed.

**Table C6** Actual vs. Theoretical Proton Yield in Experimental Mesocosms*

| | | | | | Theoretical ΔH+ According to Varied Proportions Processed by Each Pathway | | | | | | | |
|---|---|---|---|---|---|---|---|---|---|---|---|---|
| | | | | | Case 1 | Case 2 | Case 3 | Case 4 | Case 5 | Case 6 | Case 7 | Case 8 |
| | | Proportion of Thiosulfate by Pathway | % SOx | | 100 | 0 | 0 | 0 | 1 | 34 | 17 | 16 |
| | | | % $S_4I$ | | 0 | 100 | 0 | 1 | 0 | 66 | 33 | 34 |
| | | | % ½ SOx | | 0 | 0 | 100 | 99 | 99 | 0 | 50 | 50 |
| **Meso-cosm** | **Day** | **pH** | **S-$S_2O_3^{2-}$ (mM)** | **Actual ΔH+ (mM)** | **Case 1 ΔH+ (μM)** | **Case 2 ΔH+ (μM)** | **Case 3 ΔH+ (μM)** | **Case 4 ΔH+ (μM)** | **Case 5 ΔH+ (μM)** | **Case 6 ΔH+ (μM)** | **Case 7 ΔH+ (μM)** | **Case 8 ΔH+ (μM)** |
| $E_1$ | 0.00 | 6.52 | | | | | | | | | | |
| | 1.25 | 6.09 | 1.79 | | | | | | | | | |
| | 28.0 | 5.19 | 1.24 | 6.2 | 550.0 | -275.0 | 0.0 | -2.8 | 5.5 | 5.5 | 2.8 | -5.5 |
| $E_2$ | 0.00 | 6.27 | | | | | | | | | | |
| | 1.25 | 5.90 | 0.47 | | | | | | | | | |
| | 28.0 | 5.63 | 0.15 | 1.8 | 320.0 | -160.0 | 0.0 | -1.6 | 3.2 | 3.2 | 1.6 | -3.2 |
| $E_3$ | 0.00 | 7.43 | | | | | | | | | | |
| | 1.25 | 7.66 | 2.96 | | | | | | | | | |
| | 28.0 | 6.10 | 1.21 | 0.8 | 1750.0 | -875.0 | 0.0 | -8.8 | 17.5 | 17.5 | 8.8 | -17.5 |
| $E_4$ | 0.00 | 5.65 | | | | | | | | | | |
| | 1.25 | 5.22 | 1.46 | | | | | | | | | |
| | 28.0 | 6.52 | 0.4 | -1.9 | 1060.0 | -530.0 | 0.0 | -5.3 | 10.6 | 10.6 | 5.3 | -10.6 |
| $E_5$ | 0.00 | 6.09 | | | | | | | | | | |
| | 1.25 | 6.46 | 2.53 | | | | | | | | | |
| | 28.0 | 5.78 | 0.86 | 0.8 | 1670.0 | -835.0 | 0.0 | -8.4 | 16.7 | 16.7 | 8.4 | -16.7 |
| $E_6$ | 0.00 | 4.02 | | | | | | | | | | |
| | 1.25 | 5.10 | 1.39 | | | | | | | | | |
| | 28.0 | 7.12 | 0.45 | -95.4 | 940.0 | -470.0 | 0.0 | -4.7 | 9.4 | 9.4 | 4.7 | -9.4 |
| $E_7$ | 0.00 | 6.52 | | | | | | | | | | |
| | 1.25 | 6.71 | 0.46 | | | | | | | | | |
| | 28.0 | 6.73 | 0.12 | -0.1 | 340.0 | -170.0 | 0.0 | -1.7 | 3.4 | 3.4 | 1.7 | -3.4 |
| $E_8$ | 0.00 | 7.01 | | | | | | | | | | |
| | 1.25 | 7.32 | 0.49 | | | | | | | | | |
| | 28.0 | 6.06 | 0.00 | 0.8 | 490.0 | -245.0 | 0.0 | -2. | 4.9 | 4.9 | 2.5 | -4.9 |

*Proton yield in eight scenarios were explored, each consisting of a different proportions of thiosulfate oxidation through cSOx (1 $H^+$: -1 S-$S_2O_3^{2-}$), $S_4I$ P1 (- 0.5 $H^+$: -1 S-$S_2O_3^{2-}$) and iSOx pathways (O $H^+$: -1 S-$S_2O_3^{2-}$). The theoretical proton yield was calculated according to ∑ -[$S_2O_3^{2-}$]*% cSOx yield/100 + -[$S_2O_3^{2-}$]*% $S_4I$ yield/100 + -[$S_2O_3^{2-}$]*% iSOx yield/100). For simplicity, consistent fractions were assumed over the 28 days of the experiment. Theoretical scenarios (orange) best fitting actual detected delta H+ (green) are highlighted.

Note: this was a preliminary attempt at modelling: the effects of S4I part 2, rDSR, tetrathionate reduction pathways were not included at this stage, but could further influence the proton yield, as would the reduction of $NO_3^-$ as a terminal electron acceptor.

**Table C7** Capacity of Sulfur-Oxidizing Bacteria to use Oxygen and/or Nitrate as Terminal Electron Acceptor from the Literature

| Genus & species | Aerobic ($O_2$ only) | Anaerobic ($NO_3^-$ only) | Both $O_2$ or $NO_3^-$ | Reference |
|---|---|---|---|---|
| *Thiobacillus denitrificans* | | | yes | (Sun et al. 2022) |
| *Thiobacillus acidophilus* | | | yes | (Ghosh and Dam 2009) |
| *Thiobacillus denitrificans* ATCC 25259 | | | yes | (Jong et al. 1997) |
| *Halothiobacillus neapolitanus* | strictly aerobic | | | (Beller et al. 2006) |
| *Halothiobacillus kellyi* | aerobic | no | | (Wood, Woodall, and Kelly 2005) |
| *Thiomonas sp.* | aerobic | | | (Sievert, Heidorn, and Kuever 2000) |
| *Thiomonas sp.* | aerobic | | Partial* | (X.-G. Chen et al. 2004) |
| *Sediminibacterium aquarii sp. nov* | strictly aerobic | | | (Arsène-Ploetze et al. 2010) |
| *Sediminibacterium ginsengisoli* DCY13T | strictly aerobic | | | (Kim et al. 2016) |
| *Sediminibacterium aquarii* | aerobic | | | (Kang et al. 2014) |
| *Thiovirga sulfuroxydans* | aerobic | not observed | | (Song et al. 2017) |
| *Acidovorax sp.* Strain BoFeN1 | | nitrate-dependent iron oxidation | | (Ito et al. 2005) |
| *Acidovorax ebreus* | | As above | | (Pantke et al. 2012) |
| *Sulfurovum spp.* | | | yes | (Carlson et al. 2013) |
| *Sulfurovum denitrificans* | | | yes | (Meier et al. 2017) |
| *Sulfurovum lithotrophicum* | | | yes | (Mori, Yamaguchi, and Hanada 2018) |
| *Sulfurovum indicum* | | | yes | (Inagaki et al. 2004) |
| *Sulfurovum riftiae* | | yes | | (Xie et al. 2019) |
| *Desulfurivibrio alkaliphilus* | | yes | | (Giovannelli et al. 2016) |
| *Desulfurivibrio spp.* | | yes (and Sb reduction) | | (Thorup et al. 2017) |

*****a few genes from nitrate and nitrite reduction present, but not a complete pathway

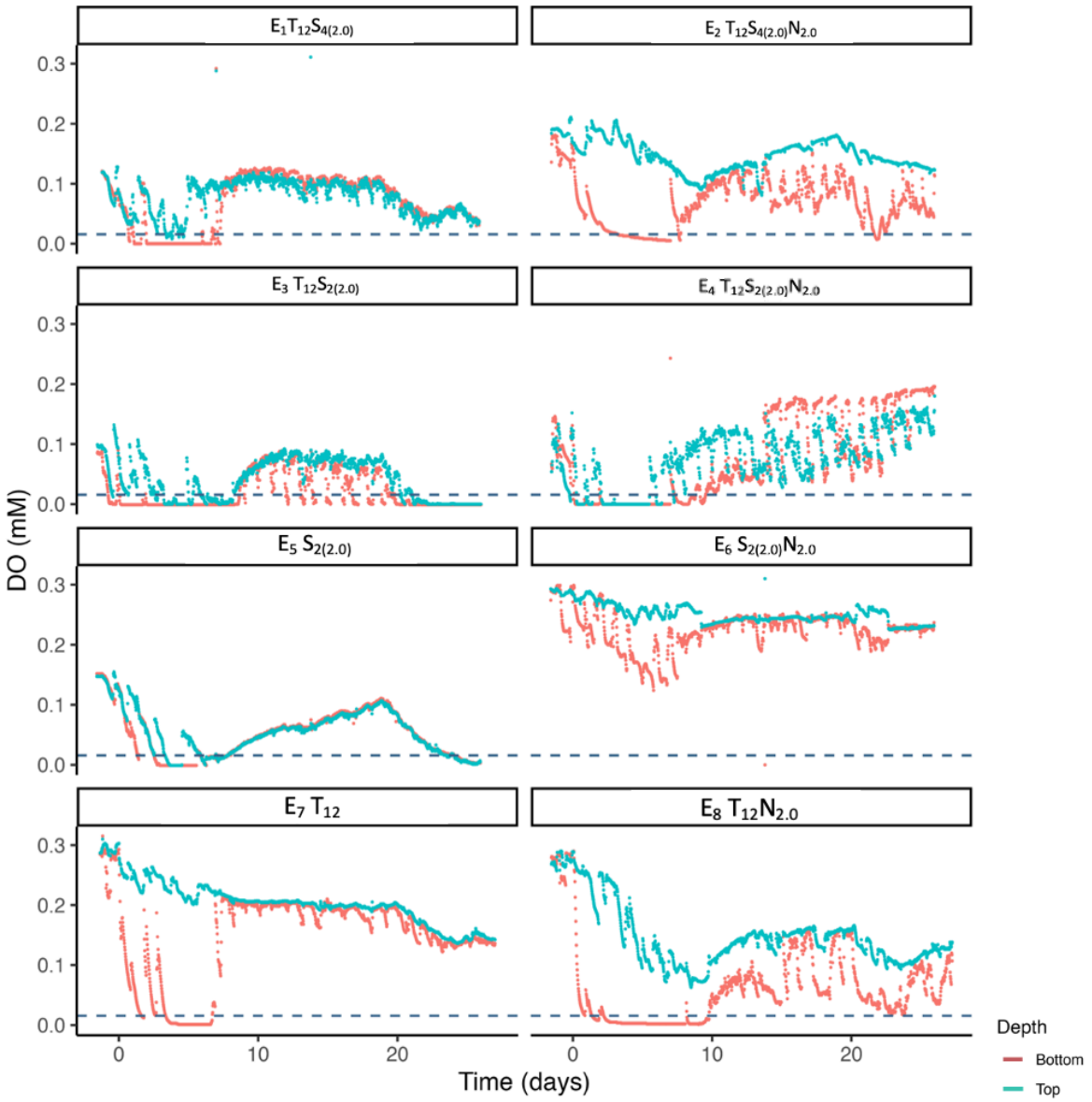


**Fig C1** Dissolved oxygen (DO) concentrations observed in mesocosms $E_1$–$E_8$ across the 28 days of the experiment at top (10 cm depth, blue points) and bottom (50 cm depth, red points). The dashed blue line (--) indicates the proposed oxygen concentration (0.5 mg/L; or 0.0156 mM) below which bacterial communities switch from exclusive use of oxygen to parallel use of both oxygen and nitrate, or nitrate only.

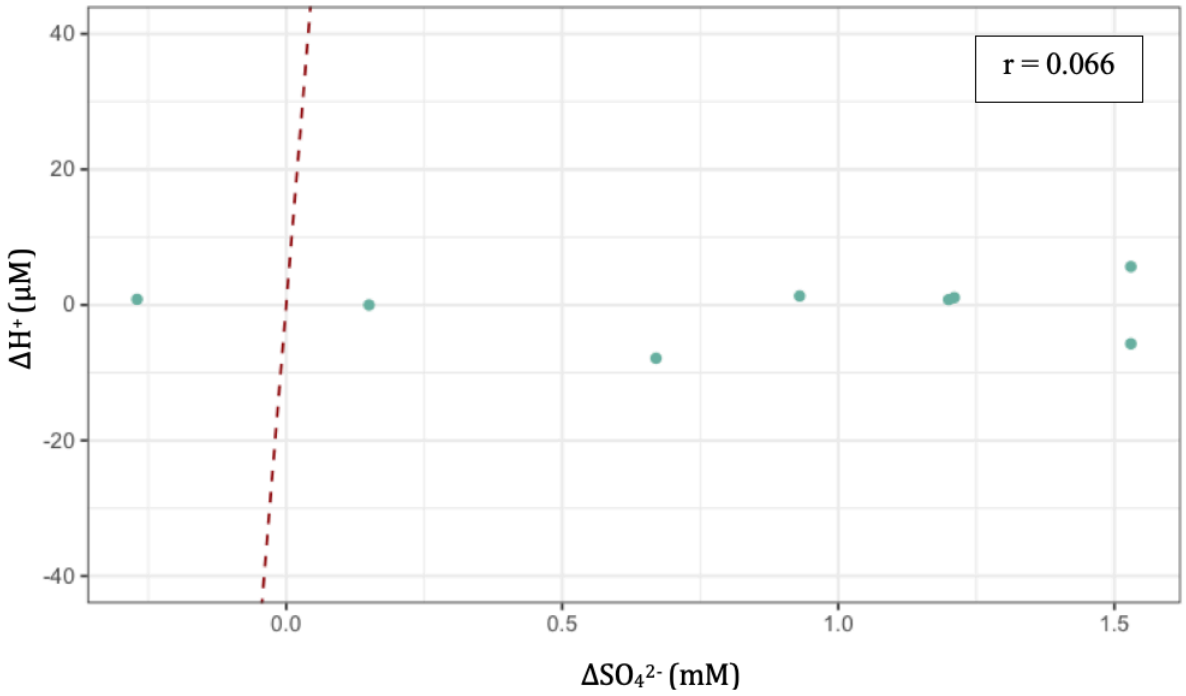


**Fig C2** Relationship between $\Delta H^+$ and $\Delta SO_4^{2-}$ across all mesocosms (between $day_{1.25}$, when amendment added, and $day_{28}$, Pearson r = 0.066, P = 0.88). Note: oxidation of thiosulfate via the complete SOx pathway would result in a 1:1 relationship between the two variables (red dashed line). Except for $E_8$, where sulfate decreased, the actual proton yields were much lower than this 1:1 ratio from sulfate concentrations would predict.

# Appendix D: Supplemental Information for Chapter 5

**Table D1** Review of Studies in Sulfur Enzyme Literature for Mining Wastewaters

| System Studied | 16S rRNA SOB | Metagenomes/ mRNA SOB | Geochemistry Products/ reactants | Geochemistry: Mass Balance | Reference |
|---|---|---|---|---|---|
| Mine Wastewater | 1 | 1 | 1 | 1 | (Sun et al. 2022) |
| – field | 1 | 1 | 1 | 1 | (Twible et al. 2024) |
| | 1 | 1 | 1 | 0 | (K. Whaley-Martin et al. 2023) |
| Mine Wastewater | 1 | 0 | 1 | 1 | (Miettinen et al. 2021) |
| – field & lab mixed communities | 1 | 1 | 1 | 0 | (K. Whaley-Martin et al. 2019) |
| | 1 | 1 | 1 | 0 | (Camacho, Jessen, et al. 2020a) |
| Mine Wastewater | 0 | 0 | 1 | 0 | (Sun et al. 2022) |
| – lab mixed communities | 0 | 1 | 1 | 1 | (Opara et al. 2023) |
| Mine Wastewater | 1 | 0 | 1 | 0 | (Camacho, Frazao, et al. 2020b) |
| – bioreactors/bioleaching | 1 | Targeted genes | 1 | 0 | (Watling et al. 2014) |
| | 1 | 0 | 1 | 1 | (W. Li et al. 2020) |
| | 1 | 0 | 1 | 0 | (Schwarz et al. 2020) |
| | 0 | TetH | 1 | 0 | (Romero, Viedma, and Cotoras 2024) |
| | 1 | 0 | 1 | 0 | (Bugaytsova and Lindström 2004) |
| Industrial Wastewater – lab grown mixed communities | 1 | 1 | 1 | 0 | (X.-G. Chen et al. 2004) |
| Mine Wastewater – SRB | 0 | 0 | 1 | 0 | (J. Wang et al. 2023) |
| | 1 | 1 | 1 | 0 | (Eckley et al. 2015) |

1 = Data present

0 = Data absent

**Table D1 cont.** Review of Studies in Sulfur Enzyme Literature for Mining Wastewaters Cont.

| System Studied | 16S rRNA SOB | Metagenomes/ mRNA SOB | Geochemistry Products/ reactants | Geochemistry: Mass Balance | Reference |
|---|---|---|---|---|---|
| Laboratory SOB Isolates | 1 | 1 | 0 | 0 | (Sun et al. 2022) |
| | 1 | 0 | 1 | 0 | (Chua et al. 2019) |
| | 0 | 1 | 1 | 0 | (Anandham et al. 2010) |
| | 1 | 0 | 1 | 0 | (Peeters et al. 2019) |
| | 1 | SoxB only | 1 | 1 | (Sahin et al. 2011) |
| | 1 | 0 | 1 | 0 | (Anandham et al. 2008) |
| | 1 | 0 | 1 | 0 | (Wood, Woodall, and Kelly 2005) |
| | 1 | 0 | 1 | 0 | (Sievert, Heidorn, and Kuever 2000) |
| | 1 | 1 | 0 | 0 | (X.-G. Chen et al. 2004) |
| | 0 | 0 | 1 | 1 | (Arsène-Ploetze et al. 2010) |
| | 0 | functional genes | 0 | 0 | (Wentzien and Sand 2004) |
| Lit Reviews | 1 | 1 | 0 | 0 | (Kappler et al. 2001) |
| | 1 | 1 | 0 | 0 | (Anantharaman et al. 2018b) |
| | 1 | no raw data | no raw data | 0 | (van Vliet, von Meijenfeldt, Dutilh, Villanueva, Sinninghe Damsté, Stams, and Sánchez-Andrea 2021) |
| | no raw data | no raw data | no raw data | no raw data | (Han and Perner 2015) |
| | 1 | 1 | 0 | 0 | (Hao et al. 2014) |
| | 1 | 1 | 0 | 0 | (Friedrich et al. 2001b) |
| | 1 | 1 | 0 | 0 | (Watanabe et al. 2019) |
| | no raw data | no raw data | no raw data | 0 | (Wasmund, Mußmann, and Loy 2017b) |
| | 1 | 1 | 1 | 0 | (Ghosh and Dam 2009) |

1 = Data present

0 = Data absent

**Table D2** Complete Geochemical Data for the 16 Microcosms

| Treatment | Code | Hours | $HS^-$ (mM) | Std Dev $HS^-$ (mM) | $S^0$ (mM) | Percent Difference $S^0$ (mM)** | $S\text{-}S_2O_3^{2-}$ (mM) | St Dev $S\text{-}S_2O_3^{2-}$ (mM) | $S\text{-}S_4O_6^{2-}$ (mM) | $SO_3^{2-}$ (mM) | St Dev $SO_3^{2-}$ (mM) | $SO_4^{2-}$ (mM) | St Dev $SO_4^{2-}$ (mM) | Total S (mM)*** | St Dev Total S (mM)**** |
|---|---|---|---|---|---|---|---|---|---|---|---|---|---|---|---|
| Abiotic Control (No SOI) | M1 | 0 | nd | 0.00 | 0.14 | NA | 0.00 | 0.00 | - | nd | 0.00 | 1.54 | 0.20 | 2.10 | nd |
| | | 8.5 | nd | 0.00 | nd | NA | 0.00 | 0.00 | - | nd | 0.00 | 1.54 | 0.23 | - | - |
| | | 24 | nd | 0.00 | nd | NA | 0.00 | 0.00 | + | nd | 0.00 | 1.79 | 0.26 | - | - |
| | | 51 | nd | 0.00 | nd | NA | 0.00 | 0.00 | - | nd | 0.00 | 1.70 | 0.17 | - | - |
| | | 74 | nd | 0.00 | nd | NA | 0.00 | 0.00 | + | nd | 0.00 | 1.93 | 0.07 | 2.10 | nd |
| Abiotic Control + Tetra | M2 | 0 | nd | 0.00 | 0.01 | NA | 0.00 | 0.00 | + | nd | 0.00 | 1.11 | 0.26 | 9.40 | nd |
| | | 8.5 | nd | 0.00 | nd | NA | 0.00 | 0.00 | + | nd | 0.00 | 1.56 | 0.15 | - | - |
| | | 24 | nd | 0.00 | nd | NA | 0.00 | 0.00 | + | nd | 0.00 | 1.65 | 0.47 | - | - |
| | | 51 | nd | 0.00 | nd | NA | 0.00 | 0.00 | + | nd | 0.00 | 1.77 | 0.10 | - | - |
| | | 74 | nd | 0.00 | nd | NA | 0.00 | 0.00 | + | nd | 0.00 | 1.74 | 0.08 | 9.00 | nd |
| 2 m SOB (No SOI) R1 | M3 | 0 | nd | 0.00 | 0.01 | NA | 0.00 | 0.00 | - | nd | 0.00 | 1.88 | 0.36 | 2.20 | nd |
| | | 8.5 | nd | 0.00 | nd | NA | 0.00 | 0.00 | - | nd | 0.00 | 1.58 | 0.51 | - | - |
| | | 24 | nd | 0.00 | nd | NA | 0.00 | 0.00 | - | nd | 0.00 | 1.84 | 0.21 | - | - |
| | | 51 | nd | 0.00 | nd | NA | 0.00 | 0.00 | - | 0.02 | 0.00 | 1.88 | 0.12 | - | - |
| | | 74 | nd | 0.00 | nd | NA | 0.00 | 0.00 | - | 0.02 | 0.00 | 2.08 | 0.09 | 2.30 | nd |
| 2 m SOB (No SOI) R2 | M4 | 0 | nd | 0.00 | nd | NA | 0.00 | 0.00 | - | nd | 0.00 | 1.53 | 0.11 | 2.00 | nd |
| | | 8.5 | nd | 0.00 | nd | NA | 0.00 | 0.00 | - | nd | 0.00 | 1.88 | 0.09 | - | - |
| | | 24 | nd | 0.00 | nd | NA | 0.00 | 0.00 | - | nd | 0.00 | 1.42 | 0.37 | - | - |
| | | 51 | nd | 0.00 | nd | NA | 0.00 | 0.00 | - | nd | 0.00 | 1.75 | 0.22 | - | - |
| | | 74 | nd | 0.00 | nd | NA | 0.00 | 0.00 | - | nd | 0.00 | 1.86 | 0.10 | 2.00 | nd |

**Table D2 cont.** Complete Geochemical Data for the 16 Microcosms

| Treatment | Code | Hours | $HS^-$ (mM) | Std Dev $HS^-$ (mM) | $S^0$ (mM) | Percent Difference $S^0$ (mM)** | $S\text{-}S_2O_3^{2-}$ (mM) | St Dev $S\text{-}S_2O_3^{2-}$ (mM) | $S\text{-}S_4O_6^{2-}$ (mM) | $SO_3^{2-}$ (mM) | St Dev $SO_3^{2-}$ (mM) | $SO_4^{2-}$ (mM) | St Dev $SO_4^{2-}$ (mM) | Total S (mM)*** | St Dev Total S (mM)**** |
|---|---|---|---|---|---|---|---|---|---|---|---|---|---|---|---|
| 2 m SOB + Tetra R1 | M5 | 0 | nd | 0.00 | nd | NA | 0.00 | 0.00 | + | nd | 0.00 | 1.33 | 0.24 | 9.70 | nd |
| | | 8.5 | nd | 0.00 | nd | NA | 0.00 | 0.00 | + | nd | 0.00 | 1.85 | 0.15 | - | - |
| | | 24 | nd | 0.00 | nd | NA | 0.19 | 0.00 | + | nd | 0.00 | 1.76 | 0.26 | - | - |
| | | 51 | nd | 0.00 | 0.07 | NA | 0.24 | 0.01 | + | 0.02 | 0.00 | 2.45 | 0.21 | - | - |
| | | 74 | nd | 0.00 | nd | NA | 0.00 | 0.00 | + | nd | 0.00 | 3.00 | 0.06 | 9.70 | nd |
| 2 m SOB + Tetra R2 | M6 | 0 | nd | 0.00 | nd | NA | 0.00 | 0.00 | + | nd | 0.00 | 1.97 | 0.15 | 10.00 | nd |
| | | 8.5 | nd | 0.00 | nd | NA | 0.00 | 0.00 | + | nd | 0.00 | 2.59 | 1.14 | - | - |
| | | 24 | nd | 0.00 | nd | NA | 0.18 | 0.00 | + | nd | 0.00 | 1.71 | 0.30 | - | - |
| | | 51 | nd | 0.00 | 0.02 | NA | 0.23 | 0.01 | + | 0.02 | 0.00 | 2.65 | 0.21 | - | - |
| | | 74 | nd | 0.00 | nd | NA | 0.00 | 0.00 | + | 0.02 | 0.00 | 3.41 | 0.13 | 10.10 | nd |
| 10 m SOB (No SOI) R1 | M7 | 0 | nd | 0.00 | nd | NA | 0.00 | 0.00 | - | 0.00 | 0.00 | 1.61 | 0.26 | 1.73 | 0.03 |
| | | 21.5 | nd | 0.00 | nd | NA | 0.00 | 0.00 | - | 0.00 | 0.00 | 1.82 | 0.26 | - | - |
| | | 44.5 | nd | 0.00 | nd | NA | 0.00 | 0.00 | - | 0.00 | 0.00 | 1.89 | 0.43 | - | - |
| | | 50.5 | nd | 0.00 | nd | NA | 0.00 | 0.00 | - | 0.00 | 0.00 | 2.03 | 0.11 | - | - |
| | | 70.5 | nd | 0.00 | nd | NA | 0.00 | 0.00 | - | 0.00 | 0.00 | 1.79 | 0.20 | 2.35 | 0.03 |
| 10 m SOB (No SOI) R2 | M8 | 0 | nd | 0.00 | nd | NA | 0.00 | 0.00 | - | 0.00 | 0.00 | 1.69 | 0.37 | 2.33 | 0.04 |
| | | 21.5 | nd | 0.00 | nd | NA | 0.00 | 0.00 | - | 0.00 | 0.00 | 1.61 | 0.41 | - | - |
| | | 44.5 | nd | 0.00 | nd | NA | 0.00 | 0.00 | - | 0.00 | 0.00 | 1.91 | 0.43 | + | + |
| | | 50.5 | nd | 0.00 | nd | NA | 0.00 | 0.00 | - | 0.00 | 0.00 | 1.72 | 0.35 | - | - |
| | | 70.5 | nd | 0.00 | nd | NA | 0.00 | 0.00 | - | 0.00 | 0.00 | 1.56 | 0.15 | 2.24 | 0.03 |

**Table D2 cont.** Complete Geochemical Data for the 16 Microcosms

| Treatment | Code | Hours | $HS^-$ (mM) | Std Dev $HS^-$ (mM) | $S^0$ (mM) | Percent Difference $S^0$ (mM)** | $S\text{-}S_2O_3^{2-}$ (mM) | St Dev $S\text{-}S_2O_3^{2-}$ (mM) | $S\text{-}S_4O_6^{2-}$ (mM) | $SO_3^{2-}$ (mM) | St Dev $SO_3^{2-}$ (mM) | $SO_4^{2-}$ (mM) | St Dev $SO_4^{2-}$ (mM) | Total S (mM)*** | St Dev Total S (mM)**** |
|---|---|---|---|---|---|---|---|---|---|---|---|---|---|---|---|
| 10 m SOB + Tetra R1 | M9 | 0 | nd | 0.00 | nd | NA | 0.00 | 0.00 | + | 0.00 | 0.00 | 1.76 | 0.29 | 10.15 | 0.06 |
| | | 21.5 | nd | 0.00 | nd | NA | 0.18 | 0.01 | + | 0.00 | 0.00 | 3.08 | 0.38 | - | - |
| | | 44.5 | nd | 0.00 | nd | NA | 0.43 | 0.02 | + | 0.00 | 0.00 | 1.79 | 0.23 | - | - |
| | | 50.5 | nd | 0.00 | nd | NA | 0.11 | 0.00 | + | 0.00 | 0.00 | 2.37 | 0.87 | - | - |
| | | 70.5 | nd | 0.00 | nd | NA | 0.00 | 0.00 | + | 0.00 | 0.00 | 3.03 | 0.68 | 9.96 | 0.06 |
| 10 m SOB + Tetra R2 | M10 | 0 | nd | 0.00 | nd | NA | 0.00 | 0.00 | + | 0.00 | 0.00 | 1.56 | 0.04 | 10.20 | 0.04 |
| | | 21.5 | nd | 0.00 | nd | NA | 0.18 | 0.01 | + | 0.00 | 0.00 | 1.62 | 0.12 | - | - |
| | | 44.5 | nd | 0.00 | nd | NA | 0.13 | 0.00 | + | 0.00 | 0.00 | 2.23 | 0.45 | - | - |
| | | 50.5 | nd | 0.00 | nd | NA | nd | 0.00 | + | 0.00 | 0.00 | 2.69 | 0.34 | - | - |
| | | 70.5 | nd | 0.00 | nd | NA | 0.00 | 0.00 | + | 0.00 | 0.00 | 2.56 | 0.09 | 10.37 | 0.06 |
| 2 m SOB + Thio R1 | M11 | 0 | | | 0.07 | 193 | 13.42* | 0.08 | + | 0.00 | 0.00 | 1.56 | 0.16 | 13.5 | 0.2 |
| | | 24 | nd | 0.00 | 0.09 | 169 | 13.20 | 0.16 | + | 0.00 | 0.00 | 2.51 | 0.13 | | - |
| | | 74 | - | - | 0.16 | 151 | 12.55 | 0.06 | + | 0.00 | 0.00 | 2.76 | 0.31 | | - |
| | | 144 | nd | 0.00 | 0.26 | 16 | 7.29 | 0.21 | + | 0.00 | 0.00 | 4.90 | 1.32 | | - |
| | | 192 | - | - | 0.02 | 23 | 0.89 | 0.02 | + | 0.00 | 0.00 | 6.91 | 1.05 | 14.5 | 0.2 |
| 2 m SOB + Thio R2 | M12 | 0 | nd | 0.00 | 0.01 | 180 | 14.21 | 1.51 | + | 0.00 | 0.00 | 1.74 | 0.44 | 12.9 | 0.2 |
| | | 24 | - | - | 0.02 | 13 | 13.21 | 0.07 | + | 0.00 | 0.00 | 2.37 | 0.02 | | - |
| | | 74 | nd | 0.00 | 0.25 | 147 | 12.83 | 0.30 | + | 0.00 | 0.00 | 2.80 | 0.24 | | - |
| | | 144 | - | - | 0.19 | 59 | 9.17 | 0.79 | + | 0.00 | 0.00 | 3.59 | 1.42 | | - |
| | | 192 | - | - | 0.24 | 15 | 4.24 | 0.76 | + | 0.00 | 0.00 | 6.16 | 0.57 | 14.3 | 0.2 |

**Table D2 cont.** Complete Geochemical Data for the 16 Microcosms

| Treatment | Code | Hours | $HS^-$ (mM) | Std Dev $HS^-$ (mM) | $S^0$ (mM) | Percent Difference $S^0$ (mM)** | $S\text{-}S_2O_3^{2-}$ (mM) | St Dev $S\text{-}S_2O_3^{2-}$ (mM) | $S\text{-}S_4O_6^{2-}$ (mM) | $SO_3^{2-}$ (mM) | St Dev $SO_3^{2-}$ (mM) | $SO_4^{2-}$ (mM) | St Dev $SO_4^{2-}$ (mM) | Total S (mM)*** | St Dev Total S (mM)**** |
|---|---|---|---|---|---|---|---|---|---|---|---|---|---|---|---|
| 10 m SOB + Thio R1 | M13 | 0 | nd | 0.00 | 0.05 | 172 | 13.51 | 0.04 | + | 0.00 | 0.00 | 1.78 | 0.26 | 11.7 | 0.2 |
| | | 24 | - | - | 0.13 | 131 | 13.26 | 0.40 | + | 0.00 | 0.00 | 2.33 | 0.06 | | - |
| | | 74 | - | - | 0.16 | 81 | 12.35 | 0.22 | + | 0.00 | 0.00 | 3.00 | 0.09 | | - |
| | | 144 | - | - | 1.50 | 161 | 8.38 | 0.43 | + | 0.00 | 0.00 | 4.50 | 0.20 | | - |
| | | 192 | - | - | 0.07 | 113 | 1.93 | 0.12 | + | 0.00 | 0.00 | 5.73 | 0.82 | 14.2 | 0.2 |
| 10 m SOB + Thio R2 | M14 | 0 | nd | 0.00 | 0.06 | 191 | 13.46 | 0.15 | + | 0.00 | 0.00 | 1.81 | 0.17 | 12.4 | 0.1 |
| | | 24 | - | - | 0.20 | 144 | 13.07 | 0.21 | + | 0.00 | 0.00 | 2.38 | 0.15 | | - |
| | | 74 | - | - | 0.20 | 183 | 12.39 | 0.31 | + | 0.00 | 0.00 | 3.04 | 0.14 | | - |
| | | 144 | - | - | 0.28 | 30 | 7.57 | 0.26 | + | 0.00 | 0.00 | 5.67 | 0.08 | | - |
| | | 192 | nd | 0.00 | 0.15 | 150 | 0.30 | 0.02 | + | 0.00 | 0.00 | 8.89 | 0.81 | 14.5 | 0.2 |
| Abiotic Control + Thio R1 | M15 | 0 | - | - | 0.03 | 189 | 12.46 | 0.13 | + | 0.00 | 0.00 | 1.45 | 0.50 | 11.2 | 0.1 |
| | | 24 | - | - | 0.01 | 200 | 11.65 | 0.33 | + | 0.00 | 0.00 | 1.91 | 0.08 | | - |
| | | 74 | - | - | 0.12 | 200 | 11.57 | 0.09 | + | 0.00 | 0.00 | 1.81 | 0.13 | | - |
| | | 144 | - | - | 0.04 | 200 | 11.66 | 0.21 | + | 0.00 | 0.00 | 1.64 | 0.28 | | - |
| | | 192 | - | - | 0.03 | 34 | 12.09 | 1.02 | + | 0.00 | 0.00 | 1.83 | 0.10 | 13.3 | 0.2 |
| Abiotic Control + Thio R2 | M16 | 0 | - | - | 0.01 | 127 | 11.68 | 0.05 | + | 0.00 | 0.00 | 1.51 | 0.42 | 11.2 | 0.2 |
| | | 24 | - | - | 0.03 | 124 | 11.65 | 0.33 | + | 0.00 | 0.00 | 1.91 | 0.08 | | - |
| | | 74 | - | - | 0.03 | 200 | 11.57 | 0.09 | + | 0.00 | 0.00 | 1.81 | 0.13 | | - |
| | | 144 | - | - | 0.04 | 200 | 11.66 | 0.21 | + | 0.00 | 0.00 | 1.64 | 0.28 | | - |
| | | 192 | - | - | 0.11 | 200 | 12.09 | 1.02 | + | 0.00 | 0.00 | 1.83 | 0.10 | 10.8 | 0.2 |

**Table D2 cont.** Complete Geochemical Data for the 16 Microcosms

| Treatment | Code | Hours | pH | D.O (mg/L) | D.O (mM) | $NO_3^-$ (mM) | Std. Dev $NO_3^-$ (mM) | $NH_4^+$ (mM) | Std. Dev $NH_4^+$ (mM) |
|---|---|---|---|---|---|---|---|---|---|
| Abiotic Control (No SOI) | M1 | 0 | 7.73 | 9.03 | 0.28 | | | | |
| | | 8.5 | 7.56 | - | - | | | | |
| | | 24 | 7.67 | - | - | | | | |
| | | 51 | 7.73 | - | - | | | | |
| | | 74 | 7.00 | 6.35 | 0.20 | | | | |
| Abiotic Control + Tetra | M2 | 0 | 7.84 | 8.59 | 0.27 | | | | |
| | | 8.5 | 7.56 | - | - | | | | |
| | | 24 | 7.39 | - | - | | | | |
| | | 51 | 7.73 | - | - | | | | |
| | | 74 | 7.00 | 7.35 | 0.23 | | | | |
| 2 m SOB (No SOI) R1 | M3 | 0 | 7.68 | 8.62 | 0.27 | | | | |
| | | 8.5 | 7.57 | - | - | | | | |
| | | 24 | 7.86 | - | - | | | | |
| | | 51 | 7.34 | - | - | | | | |
| | | 74 | - | 1.98 | 0.06 | | | | |
| 2 m SOB (No SOI) R2 | M4 | 0 | 7.91 | 9.00 | 0.28 | | | | |
| | | 8.5 | 7.94 | - | - | | | | |
| | | 24 | 7.86 | - | - | | | | |
| | | 51 | 7.56 | - | - | | | | |
| | | 74 | 7.00 | 1.37 | 0.04 | | | | |

Note: 0.00 values used even when value slightly below 0 recorded; (-) indicates no value recorded; * data not reported due to probe drift
Note: manufacture error on HOBO DO data loggers is given as ±0.2 mg/L , or < ±0.01 mM

**Table D2 cont.** Complete Geochemical Data for the 16 Microcosms

| Treatment | Code | Hours | pH | D.O (mg/L) | D.O (mM) | $NO_3^-$ (mM) | Std. Dev $NO_3^-$ (mM) | $NH_4^+$ (mM) | Std. Dev $NH_4^+$ (mM) |
|---|---|---|---|---|---|---|---|---|---|
| 2 m SOB + Tetra R1 | M5 | 0 | 7.91 | 8.27 | 0.26 | | | | |
| | | 8.5 | 7.79 | - | - | | | | |
| | | 24 | 7.42 | - | - | | | | |
| | | 51 | 6.27 | - | - | | | | |
| | | 74 | 3.29 | 2.49 | 0.08 | | | | |
| 2 m SOB + Tetra R2 | M6 | 0 | 7.92 | 8.49 | 0.27 | | | | |
| | | 8.5 | 7.80 | - | - | | | | |
| | | 24 | 7.58 | - | - | | | | |
| | | 51 | 6.31 | - | - | | | | |
| | | 74 | 3.29 | 2.78 | 0.09 | | | | |
| 10 m SOB (No SOI) R1 | M7 | 0 | 7.93 | 7.94 | 0.25 | | | | |
| | | 21.5 | 7.78 | - | - | | | | |
| | | 44.5 | 7.61 | - | - | | | | |
| | | 50.5 | 7.42 | - | - | | | | |
| | | 70.5 | - | 2.53 | 0.08 | | | | |
| 10 m SOB (No SOI) R2 | M8 | 0 | 7.92 | 8.24 | 0.26 | | | | |
| | | 21.5 | 7.81 | - | - | | | | |
| | | 44.5 | 7.53 | - | - | | | | |
| | | 50.5 | 7.28 | - | - | | | | |
| | | 70.5 | - | 1.90 | 0.06 | | | | |

Note: 0.00 values used even when value slightly below 0 recorded; (-) indicates no value recorded; * data not reported due to probe drift
Note: manufacture error on HOBO DO data loggers is given as ±0.2 mg/L, or < ±0.01 mM

**Table D2 cont.** Complete Geochemical Data for the 16 Microcosms

| Treatment | Code | Hours | pH | D.O (mg/L) | D.O (mM) | $NO_3^-$ (mM) | Std. Dev $NO_3^-$ (mM) | $NH_4^+$ (mM) | Std. Dev $NH_4^+$ (mM) |
|---|---|---|---|---|---|---|---|---|---|
| 10 m SOB + Tetra R1 | M9 | 0 | 7.92 | 8.09 | 0.25 | | | | |
| | | 8.5 | 7.21 | - | - | | | | |
| | | 24 | 4.83 | - | - | | | | |
| | | 51 | 3.97 | - | - | | | | |
| | | 74 | - | 3.29 | 0.10 | | | | |
| 10 m SOB + Tetra R2 | M10 | 0 | - | 8.52 | 0.27 | | | | |
| | | 8.5 | 6.98 | - | - | | | | |
| | | 24 | 4.34 | - | - | | | | |
| | | 51 | 3.74 | - | - | | | | |
| | | 74 | - | 3.05 | 0.10 | | | | |
| 2 m SOB + Thio R1 | M11 | 0 | 8.11 | 8.93 | 0.28 | 6.09 | 0.52 | 0.02 | 0.01 |
| | | 21.5 | 7.70 | 3.93 | 0.12 | 8.85 | 0.39 | 0.05 | 0.00 |
| | | 44.5 | 6.80 | 0.00 | 0.00 | 7.55 | 0.77 | 0.02 | 0.00 |
| | | 50.5 | 5.17 | 0.00 | 0.00 | 7.07 | 1.61 | 0.07 | 0.00 |
| | | 70.5 | 4.98 | 0.00 | 0.00 | 7.19 | 0.89 | - | - |
| 2 m SOB + Thio R2 | M12 | 0 | 8.24* | 8.94 | 0.28 | 6.63 | 1.74 | 0.04 | 0.00 |
| | | 21.5 | 8.4* | 3.36 | 0.11 | 8.28 | 0.13 | 0.06 | 0.00 |
| | | 44.5 | 7.77* | 0.00 | 0.00 | 7.78 | 0.50 | 0.08 | 0.04 |
| | | 50.5 | 6.54* | 0.00 | 0.00 | 6.04 | 2.04 | 0.10 | 0.02 |
| | | 70.5 | 6.42* | 0.00 | 0.00 | 7.46 | 0.67 | - | - |

Note: 0.00 values used even when value slightly below 0 recorded; (-) indicates no value recorded; * data not reported due to probe drift
Note: manufacture error on HOBO DO data loggers is given as ±0.2 mg/L, or < ±0.01 mM

**Table D2 cont.** Complete Geochemical Data for the 16 Microcosms

| Treatment | Code | Hours | pH | D.O (mg/L) | D.O (mM) | $NO_3^-$ (mM) | Std. Dev $NO_3^-$ (mM) | $NH_4^+$ (mM) | Std. Dev $NH_4^+$ (mM) |
|---|---|---|---|---|---|---|---|---|---|
| 10 m SOB + Thio R1 | M13 | 0 | 7.42 | 8.94 | 0.28 | 6.87 | 0.86 | 0.10 | 0.08 |
| | | 24 | 7.29 | 4.66 | 0.15 | 8.24 | 0.24 | 0.06 | 0.00 |
| | | 74 | 6.88 | 0.00 | 0.00 | 8.12 | 0.24 | 0.06 | 0.03 |
| | | 144 | 6.20 | 0.00 | 0.00 | 7.56 | 0.22 | 0.10 | 0.09 |
| | | 192 | 6.17 | 0.00 | 0.00 | 6.44 | 0.91 | - | - |
| 10 m SOB + Thio R2 | M14 | 0 | 7.81 | 8.86 | 0.28 | 7.46 | 1.13 | 0.06 | 0.00 |
| | | 24 | 7.61 | 3.70 | 0.12 | 8.22 | 0.51 | 0.06 | 0.00 |
| | | 74 | 7.80 | 0.00 | 0.00 | 8.05 | 0.42 | 0.06 | 0.02 |
| | | 144 | 5.58 | 0.00 | 0.00 | 8.24 | 0.12 | 0.09 | 0.01 |
| | | 192 | 4.90 | 0.00 | 0.00 | 8.94 | - | - | - |
| Abiotic Control + Thio R1 | M15 | 0 | 7.72 | 8.91 | 0.28 | 5.76 | 1.86 | 0.05 | 0.00 |
| | | 24 | 7.82 | 6.42 | 0.20 | 7.48 | 0.23 | 0.06 | 0.01 |
| | | 74 | 7.80 | 6.31 | 0.20 | 6.37 | 1.13 | 0.05 | 0.02 |
| | | 144 | 7.56 | 4.67 | 0.15 | 6.41 | 0.13 | 0.05 | 0.02 |
| | | 192 | 7.80 | 0.00 | 0.00 | 6.52 | 1.26 | - | - |
| Abiotic Control + Thio R2 | M16 | 0 | 7.68 | 8.83 | 0.28 | 5.97 | 1.51 | 0.06 | 0.00 |
| | | 24 | 7.75 | 7.83 | 0.24 | 7.48 | 0.30 | 0.06 | 0.01 |
| | | 74 | 7.56 | 8.13 | 0.25 | 6.91 | 0.48 | 0.05 | 0.00 |
| | | 144 | 7.22 | 3.48 | 0.11 | 6.35 | 0.98 | 0.05 | 0.00 |
| | | 192 | 6.98 | 0.00 | 0.00 | 7.00 | 0.37 | - | - |

Note: 0.00 values used even when value slightly below 0 recorded; (-) indicates no value recorded; * data not reported due to probe drift
Note: manufacture error on HOBO DO data loggers is given as ±0.2 mg/L, or < ±0.01 mM

**Table D3** Relative Abundance of Bacteria Genera in the 16 Mesocosms

| Microcosm | Treatment | Time | Exp | *Acinetobacter* | *Allorhizobium-Neorhizobium-Pararhizobium-Rhizobium* | *Brucella* | *Delftia* | *Halothiobacillus* | *Massilia* | *Pandoraea* | *Pseudomonas* | *Sphingobium* | *Stenotrophomonas* | *Thiomonas* | *Xanthobacter* |
|---|---|---|---|---|---|---|---|---|---|---|---|---|---|---|---|
| All | 2 m SOB + Tetra | $t_0$ | a | 0.13 | 0.00 | 0.00 | 85.64 | 0.52 | 0.00 | 11.69 | 1.16 | 0.01 | 0.03 | 0.75 | 0.00 |
| M3 | 2 m SOB (No SOI) R1 | $t_{end}$ | a | 0.01 | 0.00 | 0.00 | 90.13 | 0.54 | 0.01 | 8.76 | 0.17 | 0.00 | 0.01 | 0.32 | 0.00 |
| M4 | 2 m SOB (No SOI) R 2 | $t_{end}$ | a | 0.00 | 0.00 | 0.00 | 0.07 | 78.08 | 0.00 | 20.73 | 0.37 | 0.08 | 0.02 | 0.32 | 0.32 |
| M5 | 2 m SOB + Tetra R1 | $t_{end}$ | a | 0.01 | 0.00 | 0.00 | 0.03 | 90.11 | 0.00 | 8.79 | 0.16 | 0.05 | 0.02 | 0.52 | 0.31 |
| M6 | 2 m SOB + Tetra R2 | $t_{end}$ | a | 0.00 | 0.00 | 0.00 | 0.00 | 99.30 | 0.00 | 0.11 | 0.00 | 0.00 | 0.00 | 0.49 | 0.09 |
| All | 10 m SOB + Tetra | $t_0$ | b | 0.00 | 0.05 | 0.00 | 0.13 | 0.41 | 0.00 | 73.99 | 19.74 | 4.97 | 0.05 | 0.14 | 0.46 |
| M7 | 10 m SOB (No SOI) R1 | $t_{end}$ | b | 0.00 | 0.03 | 0.00 | 29.09 | 0.55 | 0.00 | 12.26 | 55.09 | 1.84 | 0.78 | 0.13 | 0.06 |
| M8 | 10 m SOB (No SOI) R2 | $t_{end}$ | b | 0.04 | 0.01 | 0.00 | 2.54 | 89.07 | 0.00 | 3.44 | 0.29 | 0.04 | 0.06 | 4.17 | 0.00 |
| M9 | 10 m SOB + Tetra R1 | $t_{end}$ | b | 0.03 | 0.00 | 0.00 | 0.42 | 91.78 | 0.00 | 3.28 | 0.25 | 0.04 | 0.24 | 3.77 | 0.00 |
| M10 | 10 m SOB + Tetra R2 | $t_{end}$ | b | 0.00 | 0.00 | 0.00 | 0.00 | 89.69 | 0.00 | 1.65 | 0.06 | 0.00 | 0.00 | 8.59 | 0.00 |
| M11/ M12 | 2 m SOB + Thio | $t_0$ | c | 0.04 | 0.00 | 0.00 | 0.00 | 96.67 | 0.00 | 0.15 | 0.02 | 0.00 | 0.00 | 2.14 | 0.97 |
| M13/ M14 | 10 m SOB + Thio | $t_0$ | c | 0.16 | 0.00 | 0.00 | 0.00 | 94.17 | 0.00 | 0.15 | 0.05 | 0.00 | 0.01 | 3.06 | 1.48 |
| M11 | 2 m SOB + Thio R1 | $t_{end}$ | c | 0.04 | 2.08 | 0.01 | 0.00 | 59.99 | 0.00 | 32.64 | 3.86 | 0.22 | 0.22 | 0.37 | 0.54 |
| M12 | 2 m SOB + Thio R2 | $t_{end}$ | c | 0.00 | 0.00 | 0.77 | 0.00 | 94.97 | 0.00 | 2.97 | 0.01 | 0.00 | 0.23 | 0.70 | 0.32 |
| M13 | 10 m SOB + Thio R1 | $t_{end}$ | c | 0.00 | 0.43 | 2.14 | 0.00 | 2.99 | 0.00 | 3.53 | 88.18 | 0.07 | 2.37 | 0.03 | 0.20 |
| M14 | 10 m SOB + Thio R2 | $t_{end}$ | c | 0.00 | 0.00 | 0.00 | 0.00 | 87.93 | 0.00 | 11.50 | 0.01 | 0.00 | 0.04 | 0.12 | 0.34 |

For workflow from raw 16S gene sequencing data with OTUs listed, see "Chapter 4 Supplementary 16S rRNA data (curation steps)" at the following link: http://128.100.14.155:8088/share.cgi?ssid=204a2ab4254d4911874cd20953dfb1ed.

**Table D4** Frequency of MAGs of Sulfur-Oxidizing Bacteria Containing One or More Copy/ies of each S Gene

| | Potential $S_4I$ | | | | | | | SOx | | | | | | rDSR | | | | | | | | | | | S Uptake |
|---|---|---|---|---|---|---|---|---|---|---|---|---|---|---|---|---|---|---|---|---|---|---|---|---|---|
| | ***tsdA*** | ***doxDA*** | ***sdo*** | ***TST*** | ***sor*** | ***SUOX*** | ***ttrABC*** | ***soxA*** | ***soxB*** | ***soxC*** | ***soxX*** | ***soxY*** | ***soxZ*** | ***dsrC*** | ***dsrA*** | ***dsrB*** | ***dsrE*** | ***dsrF*** | ***dsrH*** | ***dsrC*** | ***dsrMKJOP*** | ***aprAB*** | ***sat*** | ***qmoABC*** | ***sqr*** |
| *Halothiobacillus*[1] (Ox Res 10 m) | 1 | 0 | 1 | 1 | 1 | NA | 0 | 1 | 1 | 1 | 1 | 1 | 1 | 0 | 0 | 0 | 0 | 0 | 0 | 0 | 0 | 0 | 0 | 0 | 1 |
| *Halothiobacillus* (Ox Res 2 m) | 1 | 0 | 1 | 1 | 0 | NA | 0 | 1 | 1 | 1 | 1 | 1 | 1 | 0 | 0 | 0 | 0 | 0 | 0 | 0 | 0 | 0 | 0 | 0 | 1 |
| *Thiomonas* (Ox Res Average) | 1 | 0 | 1 | 1 | 0 | NA | 0 | 1 | 1 | 1 | 1 | 1 | 1 | 0 | 0 | 0 | 0 | 0 | 0 | 0 | 0 | 0 | 0 | 0 | 1 |
| *Pandoraea* (Lit review[2]) | - | - | - | 1 | - | 1 | - | 1 | 1 | - | 1 | 1 | 1 | - | - | - | - | - | - | - | - | - | - | - | 1 |
| *Pandoraea* (Flin Flon*) | 0 | 0 | 1 | 1 | 0 | NA | 0 | 1 | 1 | 1 | 1 | 1 | 1 | 0 | 0 | 0 | 0 | 0 | 0 | 0 | 0 | 0 | 0 | 0 | 1 |

NA – data not available from analysis

[1]The following genes were not detected in *Halothiobacillus:* cysA, cysC, cysD, cysl, cysP, cysW, cycU, psrA, psrB, phsA, sudA, sudB, hdrB1, hdrA1, hdrB2, hdrC2, asrA_asrB, asrC, sir, sreC and fsr; hdrA2 detected in *Thiomonas* but not *Halothiobacillus*; cysJ detected in *Halothiobacillus* but not *Thiomonas.*

[2] *Pandoraea* lit review based on a comparison of over 68 metagenomes (R. Wang et al. 2019). *Pandoraea* metagenomes also contain: cysA, cysD, cysE, cysJ , cysN, cysP, cysU dmdC, dmdD, ssuA, ssuB, ssuC, ssuD, ssuE, metX, metZ, tauB, tauC (Peeters et al. 2019; Rangasamy et al. 2014; Anandham et al. 2010, 2008; Yong et al. 2016).

Note: *Halothiobacillus* spp. metagenome assembled genomes for the initial communities used in these experiments (2017 2m and 10 m) also contain the ability to reduce nitrite to ammonia (*nirB*), but lack the capacity to reduce nitrate to nitrite (*narGHIJ* / *napAB*) (Peeters et al. 2019). *Thiomonas* spp. metagenomes have the capacity to reduce nitrate (*narGHIJ*) but not nitrite (*nirBSK*) (K. J. Whaley-Martin et al. 2023). Of the 68 *Pandoraea* genomes in the literature review, > 96% have the ability to reduce nitrite to ammonia (*nirB*), but only 25 % contain one of the genes required to reduce nitrate to nitrite ((*narG*), (K. J. Whaley-Martin et al. 2023)).

**Table D5** Calculation of Approximate Oxygen Utilization Rate (OUR) in Suboxic Microcosms

**Depth of Oxygen Penetration in SOB biofilms with *Halothiobacillus***

Microbial community structures and in situ sulfate-reducing and sulfur-oxidizing activities in biofilms developed on mortar specimens in a corroded sewer system

10.1016/j.watres.2009.07.035

| | | |
|---|---|---|
| Depth of Oxygen penetration (approx.) | 1000 | um |
| | 1 | mm |

**Approximate OUR**

Growth kinetics of hydrogen sulfide oxidizing bacteria in corroded concrete from sewers

10.1016/j.jhazmat.2011.03.005

**Range of oxygen utilization rates in an unstirred batch reactor (250 mg flask)**

| | | |
|---|---|---|
| OUR min | 0 | g m^-3 hr^-1 |
| OUR max | 14 | g m^-3 hr^-1 |
| OUR mid (estimated) | 10 | g m^-3 hr^-1 |
| **Surface area of media** | pi*r^2 - flask @ 6 L depth - pi*r^2 DO probe | |
| At t=0 (6 L depth) | 98 | cm^2 |
| At t=end (2 L depth) | 374 | cm^2 |
| **Volume of oxygen exposed media** | 374 | mm*cm*cm |
| | 3.74E-05 | m^3 |
| OUR * area mean (g m^-3 hr^-1*m^3) | 3.74E-04 | g/hr |
| OUR * area max | 5.24E-04 | g/hr |
| Molar Mass of O2 | 32 | g/mol |
| **Moles of Oxygen mean** | 1.17E-05 | mol/hr |
| | 1.17E+01 | umol/hr |
| **Mol of Oxygen max** | 1.64E-05 | mol/hr |
| | 1.64E+01 | umol/hr |
| **Volume of media in flask (mean)** | 4 | L |
| Mean OUR | 2.9 | uM/hr |
| Max OUR | 4.1 | uM/hr |
| **Duration of Suboxic Portion of Exp c** | 162 | hr |
| **Max Oxygen Consumption** | 0.66 | mM |

**Table D6** Calculation of Approx. Thiosulfate Diffusion Distance in Suboxic Microcosms

| | | | |
|---|---|---|---|
| **Volume of media in flask** | | | |
| Vmax | | 2000 | cm^3 |
| Vmean | | 4000 | cm^3 |
| Vmin | | 6000 | cm^3 |
| | | | |
| **Flask as a Cone** | **The Volume of Frustum of Cone=1/3 πH (R2 +Rr+r2 )** | | |
| radius (bottom, R) | | 12 | cm |
| radius (surface of water, r)max | | 6 | cm |
| radius (surface of water, r)mean | | 8 | cm |
| radius (surface of water, r)min | | 10 | cm |
| Solve for H (depth) | V/(1/3*pi*(R^2+Rr+r^2)) | | |
| | | | |
| **Depth of media in flask** | | | |
| dmax | | 23 | cm |
| dmean | | 13 | cm |
| **dmin** | | **5** | **cm** |
| | | | |
| **The Stokes-Einstein Law** | **$t=x^2/2D$** (Peeters et al. 2019) | | |
| | | | |
| **Symbol** | **Variable** | | **Units** |
| t | Time | | s |
| D | diffusion coefficient of a solute in a free solution | | cm^2/s |
| x | mean distance traveled by diffusing solute with time | | cm |
| | | | |
| t = time anoxic | | 162 | hrs |
| Conversion s/hour | | 3600 | s/hr |
| t = time anoxic | | 583200 | s |
| | | | |
| **The Stokes-Einstein Law** | **$x^2=2*t*D$** | | |
| Solve for x, using Dmean | 1.00E-05 | | cm^2/s |
| x | | 3.4 | cm |
| D (for sulfate at 25 degrees) | | 1.07E-05 | cm^2/s |
| x | | 3.5 | cm |
| **D chlorine (fast, small anion)** | | **2.03E-05** | **cm^2/s** |
| **x** | | **4.9** | **cm** |
| D glucose (slow, large molecule) | | 5.00E-06 | cm^2/s |
| x | | 0.19 | cm |

$$x_{max} = d_{min}$$

Therefore, the highest diffusion distance for thiosulfate ($x_{max}$) was only equal to the depth of the media after the final sampling ($d_{min}$). Prior to final sampling, diffusion would be insufficient to allow contact between the thiosulfate and the dissolved oxygen at the surface of the microcosms.

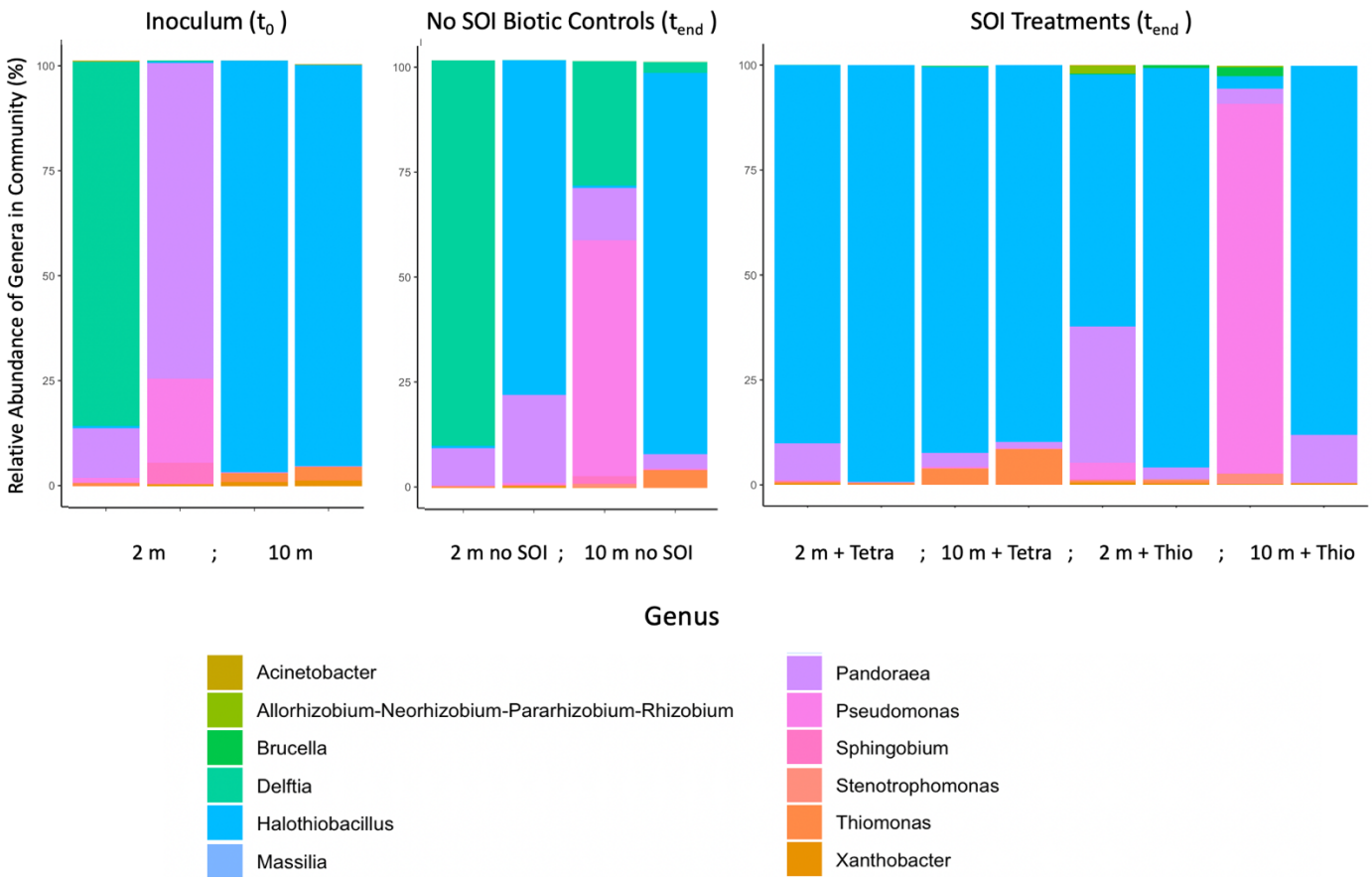


**Fig D1** 16S rRNA gene sequencing of microbial communities indicates that the initial microbial communities from 2 m and 10 m ($T_0$) were dominated by the sulfur-oxidizing genera *Halothiobacillus* and *Pandoraea*, and these two genera remained dominant in the SOB and S substrate-amended microcosms (SOI Treatments Tend: $M_5$, $M_6$, $M_9$, $M_{10}$, and $M_{11}$–$M_{14}$), while the heterotrophs *Delftia* and *Pseudomonas* grew in abundance in the microcosm that did not receive S amendments (No SOI Biotic Controls $T_{end}$: $M_3$, $M_4$, $M_7$, and $M_8$).

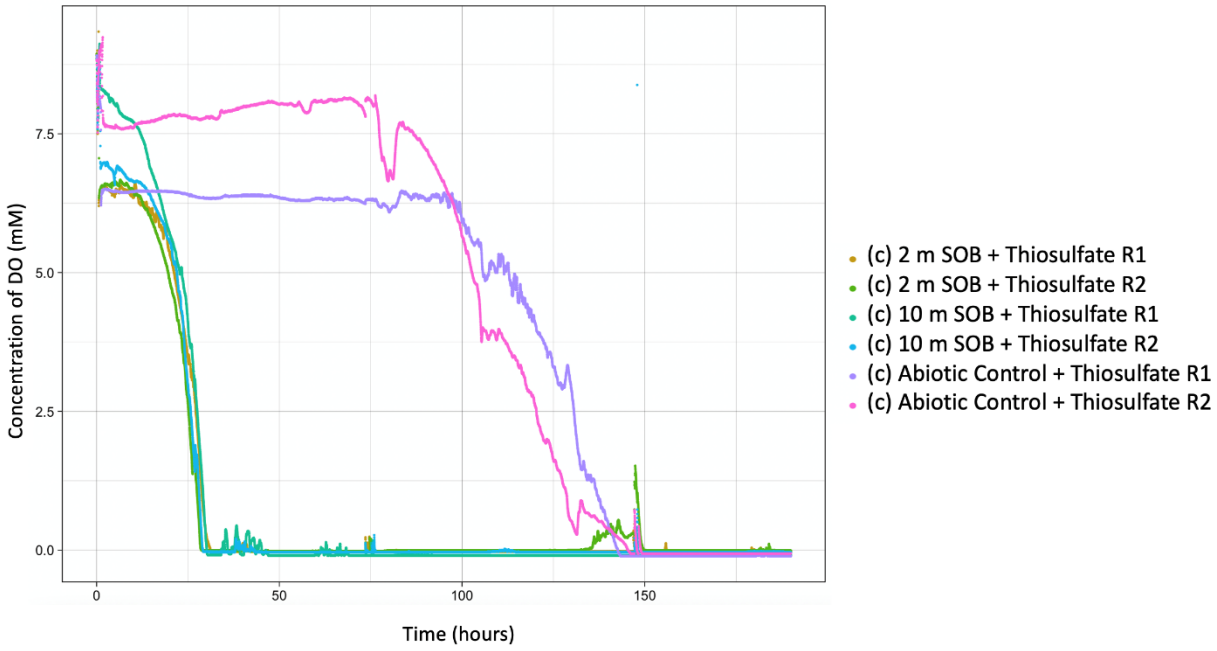


**Fig D2** Dissolved oxygen (DO) concentrations in Experiment C demonstrate that the microcosms became suboxic at ~30 hours and maintained suboxic conditions through the remaining 170 hours of the experiment. Probe measurements from 1 cm below the surface of the microcosm also indicated suboxia. (Oxygen loss in the abiotic controls at 100 hours likely indicates contamination of samples with non-sulfur-oxidizing bacteria [SOB] from the atmosphere midway through the experiment.)